University of Nottingham
UK | CHINA | MALAYSIA

Life cycle assessment and techno-economic analysis of sustainable ethanol production from industrial tail gas

Lingyun Zhang

This thesis is submitted to the

University of Nottingham

for the degree of Doctor of Philosophy

Faculty of Science and Engineering

Department of Chemical and Environmental Engineering

June 2024

Acknowledgements

This challenging PhD journey is finally coming to an end, filled with difficulties and opportunities that made me stronger and braver. I would like to thank all the people who have helped me along the way.

Firstly, I am deeply thankful to my supervisors: Prof. Cheng Heng Pang, Prof. Wei Wei, Dr. Kien Woh Kow and Prof. Edward Lester. During my PhD studies, you gave me great support and care, along with professional academic guidance and research skills. All of these will be invaluable assets in my future life. I am also profoundly grateful to my internal assessor, Dr. Mengxia Xu, and external assessor, Dr. Jia Li, for their thoughtful and thorough review of my work. Your constructive feedback has been pivotal in shaping the quality of my PhD thesis, and I am deeply appreciative of their efforts. I would also like to extend my gratitude to my other teachers and classmates I have met. Thanks for your encouragement and companionship throughout this journey.

I should not forget to thank my parents, Wanshui Zhang and Hongfang Fu, and my brother (Lingwei Zhang). I never felt fearful to challenge myself because I knew that whether I succeeded or failed,

they would always be trustworthy and the most solid backup for me. I will love you all until my last breath.

Lastly, I thank myself for never giving up, for persisting, and for working hard throughout this PhD journey.

Abstract

Conversion of low-value tail gas from industries into ethanol (TG-ethanol) is a promising cutting-edge route for value-added utilisation of tail gas. However, a systematic and objective understanding of the environmental impact and economic benefits is still lacking, and a comparison with traditional ethanol production technologies is urgently needed to justify its future competence. This thesis performed a life cycle assessment (LCA) and techno-economic analysis (TEA) of this “waste-to-value” technology and its upgraded process, as well as the upstream and downstream industries. First, the life cycle environmental impacts of Linz-Donawitz Gas from the steel industry into ethanol (LDG-ethanol) were evaluated and compared with other ethanol pathways. LDG-ethanol exhibited 22–25% lower comprehensive environmental impact than Corn-ethanol and Coal-ethanol. Sensitivity analysis highlighted electricity as a key factor, reducing electricity consumption and introducing green power can mitigate the environmental impact by 15–68%. While some technologies have been demonstrated for commercial deployment, new technological concepts keep emerging to improve the life cycle and techno-economic performance. In this investigation, a novel ethanol production technology integrating TG-ethanol with electro-

catalytic CO_2 reduction (TGEE-ethanol) was first proposed. Different integration scenarios using steel, iron alloy, and calcium carbide tail gas were modularly modelled, followed by LCA and TEA via Monte Carlo simulation. Results suggested TGEE-ethanol could increase ethanol capacity 1.3 – 2.9 times with a carbon efficiency of 36 – 82%, and carbon footprint of 1.77 – 3.93 t CO_2eq/t ethanol, with 32 – 63% higher carbon reduction potential than TG-ethanol. Minimum ethanol selling price is estimated at 428 – 962 $/t ethanol, lower than the ethanol market price (900 – 1080 $/t). In addition, the upstream and downstream should be investigated to identify the environmental and economic benefits of such low-carbon technologies. The results show that upstream (steeling-LDG-ethanol) industries showed potential carbon reductions of 5.3 – 5.6 $MtCO_2$ and economic benefits of $2.97 – 3.49 billion by 2060. Downstream (TGEE-ethanol-jet fuel) industries exhibited lower carbon footprints for TGEE-ethanol from iron alloy (IEJ, 65 g CO_2eq/MJ) and calcium carbide (CEJ, 74 g CO_2eq/MJ) than fossil jet fuel (90 g CO_2eq/MJ), while costs are higher. Carbon taxes of $10, $50, and $100 could reduce costs by 3 – 32%, achieving cost parity with fossil fuels 2 – 10 years earlier than previously estimated around 2050. Therefore, a comprehensive analysis suggests that the TGEE process is a more

economically and environmentally benign next-generation technology for producing ethanol from industrial tail gas. Overall, this study could provide guidance for future planning and strategies for the ethanol industry and may be inspiring to help heavy industries seek new technologies to reuse CO/CO_2-containing waste gases.

Keywords: ethanol, industrial tail gas, life cycle assessment, techno-economic, Monte Carlo simulation

Achievements

Journal Papers

1. Lingyun Zhang, Qun Shen, Kien-Woh Kow, Wei Chen, Tao Wu, Edward Lester, Cheng Heng Pang, Wei Wei, et al. Potential solution to the sustainable ethanol production from industrial tail gas: An integrated life cycle and techno-economic analysis*, Chem. Eng. J.,* 2024 (487), 150493. (CAS Q1, SciVal 1%, IF: 13.3)
2. Lingyun Zhang, Jumoke Oladejo, Ayotunde Dawodu, et al. Sustainable Jet Fuel from Municipal Solid Waste–Investigation of Carbon Negativity and Affordability Claims, *Resour. Conserve. Recycl.,* 2024 (210), 107819. (CAS Q1, SciVal 1%, IF: 11.2)
3. Lingyun Zhang, Qun Shen, Cheng Heng Pang, Kien-Woh Kow, Edward Lester, Tao Wu, Nannan Sun, Wei Wei, et al, Life cycle assessment of bio-fermentation ethanol production and its influence in China's steeling industry. *J. Clean. Prod.,* 2023 (397), 136492. (CAS Q1, SciVal 1%, IF: 9.7)
4. Lingyun Zhang, Wei Chen, Kien-Woh Kow, Cheng Heng Pang, Nannan Sun, Wei Wei, et al. Frontiers of CO_2 Capture and

Utilization (CCU) Towards Carbon Neutrality. *Adv. Atmos. Sci.,* 2022, 39 (8), 1252-1270. (CAS Q2, IF: 6.5)

5. Lingyun Zhang, Nannan Sun, Tao Wu, Wei Wei, Cheng Heng Pang, et al. The integration of hydrogenation and carbon capture utilisation and storage technology: A potential low-carbon approach to chemical synthesis in China. *Int J Energy Res.,* 2021 (45), 19789-19818. (CAS Q2, IF: 4.3)

Attended Conferences

- UNNC 6th Annual FoSE PGR Showcase. Poster presentation. Lingyun Zhang, Cheng Heng Pang, Kien-Woh Kow, Wei Wei, Edward Lester, et al. “Life cycle assessment and techno-economic analysis of sustainable ethanol production from industrial tail gas”. 13 June 2024, Ningbo, China.
- Partner Day and 2nd DTP Symposium. In-person, poster presentation. Lingyun Zhang, Cheng Heng Pang, Kien-Woh Kow, Wei Wei, Edward Lester, et al. “Life cycle environmental assessment and techno-economic analysis of green & low-carbon ethanol pathways”. 13 April 2024, Ningbo, China.

- The First Wisdom Lake PGR Development Conference & the 2023 XJTLU Postgraduate Research Symposium. In-person, oral presentation. Lingyun Zhang, Cheng Heng Pang, Kien-Woh Kow, Wei Wei, Edward Lester, et al. “Life cycle environmental assessment and techno-economic analysis of green & low-carbon ethanol pathways”. 13 - 15 December 2023, Suzhou, China.
- 5th International conference on “Renewable energy, resources and sustainable technologies”. In-person, oral presentation. Lingyun Zhang, Cheng Heng Pang, Kien-Woh Kow, Wei Wei, Edward Lester, et al. “Life cycle assessment and techno-economic analysis of ethanol production via industrial tail gas”. 13 - 14 November 2023, Paris, France.
- The UK Carbon Capture and Storage Research Community (UKCCSRC) Knowledge Exchange Conference. In-person, oral presentation. Lingyun Zhang, Cheng Heng Pang, Kien-Woh Kow, Wei Wei, Edward Lester, et al. “Life cycle assessment and ethanol industry system construction under zero carbon background”. 6 – 7 September 2023, Sheffield, UK.

- 2023 International Conference on Resource Sustainability (icRS 2023). In-person, oral presentation. Lingyun Zhang, Cheng Heng Pang, Kien-Woh Kow, Wei Wei, Edward Lester, et al. “Life cycle assessment and techno-economic of low-carbon and green ethanol production technology”. 7 – 9 August 2023, Surrey, UK.
- The UK Carbon Capture and Storage Research Community (UKCCSRC) Spring 2023 conference. In-person, poster presentation. Lingyun Zhang, Cheng Heng Pang, Kien-Woh Kow, Wei Wei, Edward Lester, et al. “Life cycle-based techno-economic and environmental assessment of green ethanol production by low-value tail gas”. 28 – 29 March 2023, Cardiff, UK.
- UNNC 4th Annual FoSE PGR Showcase. Poster presentation. Lingyun Zhang, Cheng Heng Pang, Kien-Woh Kow, Wei Wei, Edward Lester, et al. “Life cycle environmental impact of ethanol production by bio-fermentation from steel industry tail gas”. 10 June 2022, Ningbo, China.
- icRs Sustainable Urbanisation 2020 conference. In-person, oral presentation. Lingyun Zhang, Cheng Heng Pang, Kien-Woh Kow,

Wei Wei, et al. “CCUS technology and hydrogen industry integrated development”. 13 – 15 December 2020, Ningbo, China.

- UNNC 6th PGR Conference. In-person, oral presentation. Lingyun Zhang, Cheng Heng Pang, Kien-Woh Kow, Wei Wei, et al. “The research on the low-carbon development of the coal chemical industry”. 19 November 2020, Ningbo, China.

Contents

List of Figures

List of Tables

Nomenclature

Name	Abbreviation
AD	Anderson-Darling
ADP	Abiotic Resource Depletion Potential
ADP-e	Abiotic depletion elements
ADP-f	Abiotic depletion fossils
AP	Acidification potential
ASTM	American Society for Testing Materials
ATJ	Alcohol-to-jet fuel
BAS	The baseline scenario
BASS	BAS-Steel
BASI	BAS-Iron alloy
BASC	BAS-Calcium carbide
BF-BOF	Furnace-Basic Oxygen Furnace
BMS	Biomass separation unit
CDF	Cumulative distribution function
CE	Carbon efficiency

CEJ	Calcium carbide tail gas-based ethanol to jet fuel pathways
CF	Carbon footprints
CML	Corner-Middle-Layer-Method
CO_2eq	Carbon dioxide equivalents
CP	Comprehensive performance index
CWS	Cycle water system
DCF	Discounted Cash Flow
DME	Dimethyl ether
DIS	Distillation dehydration unit
DDGS	Distiller’s dried grains with soluble
E10	Gasoline blend with 10% ethanol to form ethanol gasoline
ECR	Electro-catalytic CO_2 reduction
ED	Energy demand
EE	Energy efficiency
EF	Emission factor
EI	Comprehensive environmental impact
EOFP	Zone formation potential for ecosystems
EP	Eutrophication potential
EPA	Environmental Protection Agency
ETJ	Ethanol-to-jet fuel
EU	European Union

EW	Entropy weight
FAETP	Freshwater aquatic ecotoxicity potential
FEP	Freshwater eutrophication potential
FETP	Freshwater ecotoxicity potential
FFP	Fossil fuel potential
FMT	Fermentation process
FRT	Fermentation unit
F-T	Fischer-Tropsch
GHG	Greenhouse gas
GREET	Greenhouse Gases Regulated Emissions, and Energy use in Transportation
GSH	Glutathione
GWP	Global Warming Potential
HEFA	Hydroprocessed esters and fatty acids
HOFP	Zone formation potential for humans
HP	Hydropower
HTP	Human Toxicity Potential
HTPc	Human toxicity potential for cancer
HTPnc	Human toxicity potential for non-cancer
IATA	International Air Transportation Association
IEA	International Energy Agency
IEJ	
IPCC	Intergovernmental Panel on Climate Change

IRP	Ionizing radiation potential
IRR	Internal rate of return
ISO	International Organization for Standardization
LCA	Life cycle assessment
LCCs	Lignin-carbohydrate complexes
LCI	Life Cycle Inventory
LCIA	Life Cycle Impact Assessment
LDG	Linz Danowitz gas
LDG-ethanol	Ethanol from Linz Danowitz gas
LEE	LDG-ethanol energy efficient
LEEGH	LDG-ethanol-energy efficient + hydropower
LEEGP	LDG-ethanol-energy efficient + photovoltaic power
LEEGW	LDG-ethanol-energy efficient + wind power
LEGH	LDG-ethanol-hydropower
LEGP	LDG-ethanol-photovoltaic power
LEGW	LDG-ethanol-wind power
LOP	Land occupation potential
MA	Methyl acetate
MAETP	Marine aquatic ecotoxicity potential
MEP	Marine eutrophication potential
MESP	Minimum ethanol selling price
METP	Marine ecotoxicity potential
Mt	Million tons

MSP	Minimum selling price
MTBE	Methyl tert-butyl ether
NCF	Net life cycle carbon footprints
NPV	Net present value
ODP	Ozone depletion potential
PDF	Probability density function
PE	Product energy
PMFP	Particulate matter formation potential
POCP	Photochemical ozone creation potential
POE	ECR coupled with the fermented waste gas post-combustion
PRE	ECR coupled with the fermented waste gas pre-combustion
PRT	Pre-treatment unit
PV	Photovoltaic power
RFA	Renewable Fuels Association
SAF	Sustainable aviation fuel
SEJ	Steel tail gas-based ethanol to jet fuel pathways
SIP	Synthetic iso-paraffin
SOP	Surplus ore potential
TAP	Terrestrial acidification potential
TEA	Techno-economic analysis
TED	Total energy demand

TETP	Terrestrial ecotoxicity potential
TGC	Tail-gas combustion unit
TGEE	TG-ethanol coupled with ECR technology
TG-ethanol	Tail gas-based ethanol
TGT	Tail-gas treatment
TPC	Total production costs
US	United States
WCP	Water consumption potential
WP	Wind power
WWT	Wastewater treatment unit

CHAPTER 1. Introduction

1.1 Background

Ethanol, as an indispensable bulk chemical, has been extensively used in the chemical, medical, agricultural, and food industries. Moreover, in recent decades, ethanol has been increasingly recognized as a promising solution for sustainable transportation fuel. Whether as a bulk chemical or as a transportation fuel, ethanol plays a crucial role in the global transition toward net-zero emissions. For instance, as a transport fuel, a total of 66 countries and regions around the world have promoted the use of ethanol to partially replace gasoline by blending with 10% ethanol to form ethanol gasoline (E10) [1]. This has led to a rapid year-on-year increase in global demand for fuel ethanol. According to the International Energy Agency (IEA) [2], ethanol production, primarily derived from biomass fermentation, reached a record high of 100 million tons per year in 2021. The United States and Brazil accounted for approximately 83% of global production, while China contributed only 3% [2]. In 2021, China consumed 140 million tons of gasoline, implying a demand for 140 million tons of fuel ethanol [3], assuming a 10% blending ratio. This indicates a market gap of 11 million tons per year for fuel

ethanol in China [4]. Additionally, the demand for ethanol as a chemical and for downstream applications, such as ethanol-derived aviation fuel, household chemicals, and additives in textile products, is gradually increasing [5]. Given the limited production capacity of existing ethanol pathways, China faces significant challenges in developing alternative ethanol production methods to ensure energy security while achieving net-zero targets [1, 6]. This study focuses on producing ethanol from renewable and waste resources, developing a combined life cycle and techno-economic assessment framework to better understand the full life cycle environmental impacts, techno-economic performance, and changes through 2060 for renewable ethanol production. The following paragraphs introduce an overview of tail gas ethanol technology and the necessity of understanding its sustainability issues from a life cycle perspective: industrial tail gas-ethanol technology, life cycle and techno-economic assessment methods, the role of electricity in ethanol production, and intensified technologies for improving carbon efficiency.

Industrial tail gas-ethanol technology. The first commercialised steel tail gas-ethanol (TG-ethanol) technology project from the steel industry in China was chosen as the evaluation object [7]. This project, which began operations in Hebei in 2018, has an annual ethanol

production capacity of 0.045 million tons. In this project, high-concentration CO from steel plant-produced Linz-Donawitz Gas (LDG) is converted into high-value products (such as ethanol, biomass, butanol, and biogas) through state-of-the-art gas bio-fermentation technology. This transformation of low-value industrial gases into high-value organic carbon products represents a significant breakthrough in waste-to-wealth biotechnology. Ethanol, the primary product, has been successfully utilized as a fuel in China, while protein biomass, a major byproduct, has emerged as a new feed alternative to expensive imported fishmeal. This technology opens a new pathway for producing fuel ethanol using non-grain, non-biomass, and non-fossil energy sources. The advancement of this technology is primarily reflected in three aspects [8]: 1) Mild reaction conditions and simple process equipment: The technology enables the one-step conversion of CO to ethanol under ambient temperature and pressure, offering high safety and reliability. This represents a revolutionary shift from inorganic to organic carbon; 2) A wide range of raw material sources: Industrial tail gases from various industries, including steel, calcium carbide, ferroalloy, phosphorus chemical, and petrochemical sectors, can be used as feedstock for ethanol production; 3) Low feedstock cost, high fermentation efficiency

and substantial cost advantages. However, there is a lack of systematic and objective understanding of the environmental impact benefits. It is crucial to compare this technology with traditional ethanol production methods to demonstrate its future competitiveness. This study emphasises the need for a comprehensive evaluation of the environmental impacts and benefits of LDG-ethanol technology, comparing it to conventional ethanol production processes to establish its viability and potential advantages in the context of sustainable development and net-zero emissions goals.

Life cycle and techno-economic assessment (LCA & TEA). The combination of Life Cycle Assessment (LCA) and Techno-Economic Analysis (TEA) provides a comprehensive approach to simultaneously consider the environmental and economic aspects of tail gas ethanol production. Through LCA, a comprehensive understanding of the various environmental impacts associated with the production, use, and disposal of tail gas ethanol can be obtained, including energy consumption, emissions, and resource utilization [9, 10]. At the same time, TEA can assess the technical efficiency, cost-effectiveness, and market competitiveness of the production process, aiding decision-makers in determining the optimal production strategies [11]. In

conducting LCA, various influencing factors need to be considered, such as raw material sourcing, energy consumption, production processes, product transportation, and waste management [12-14]. Such comprehensive analysis can help formulate more sustainable production strategies, promoting efficient resource utilization and environmental protection [15-18]. Meanwhile, TEA can provide an in-depth analysis of the technical implementation and economic viability of the production process to determine production costs, return on investment, and market outlook [19-21]. By integrating the results of LCA and TEA, decision-makers can gain a more holistic understanding of the feasibility and impacts of tail gas ethanol production, thereby formulating appropriate policies and strategies. This approach not only guides businesses but also supports decision-making for government agencies and environmental organizations, promoting the development of sustainable energy production and utilization [22-25]. Hence, the combination of LCA and TEA is of significant importance in the assessment and promotion of emerging technologies such as tail gas ethanol.

The role of electricity in ethanol production. Given its numerous advantages, TG-ethanol technology is expected to popularise rapidly. In the coming years, the power sector, as a major energy supplier, will play

a crucial role in this process, not only during the production phase of tail gas ethanol but also in the production processes of its raw materials (such as extraction, transportation, and manufacturing) and the final use stage, which is known to be energy intensive. Consequently, the greenhouse gas (GHG) emissions associated with these activities are likely driven by energy inputs, electricity in particular, which accounts for a large share of GHG emissions in the life cycle of ethanol production [26]. This implies that decarbonizing the power sector will substantially contribute to reducing GHG emissions throughout the life cycle of ethanol production. The electricity mix varies greatly from region to region, and while the global average carbon intensity of electricity generation provides an overall estimate, it is critical to understand more fully the impact of the carbon intensity of electricity in a particular region or country. Such understanding helps policymakers recognize the importance of electricity in battery systems and consider regional grid structures and future decarbonization in their decisions [27]. The geographic variation in electricity structures (i.e., regional grid structures) and temporal variations (i.e., future decarbonization trajectories) will significantly affect the GHG emissions in the production processes of raw materials [28], chemicals, and ethanol. This study investigates the

sensitivity of GHG emissions associated with various production elements and units in the ethanol production process to differences in electricity sustainability. It further analyses the GHG reduction potential that could be achieved with the expected decarbonization of the power sector by 2060. This study analyses the impact of electricity decarbonization on the life cycle GHG emissions of ethanol production, highlighting the critical roles of regional electricity structures and future decarbonization.

Intensified technologies for improving carbon efficiency. Electro-catalytic CO_2 reduction (ECR) to CO via an electrochemical way is considered a promising way [29] to realise CO_2 utilisation and is popularly studied [30]. Wherein the development of high-performance catalytic materials [31] for the efficient conversion of CO_2 to CO is the core of this technological process [32]. In recent work, Chen *et al*. found that hierarchical micro/nanostructured silver hollow fibre electrodes exhibited excellent catalytic performance in ECR reactions under mild conditions (atmospheric pressure and room temperature) [33]. Meanwhile, in their experiment, the ECR processes can be powered directly with low-grade renewable energy, such as Photovoltaic (PV) down to 3V [34], rather than other high-voltage power. All these merits

make ECR a viable option to be integrated into the TG-ethanol process [35]. That is, the tail gas CO_2 emitted from TG-ethanol can be converted into CO through ECR technology, and CO will be recycled to synthesize ethanol. This concept aims to further optimise the environmental benefits of TG-ethanol by modelling the process with engineering software, using mass and carbon balances to obtain input-output data, and ultimately assessing its life cycle environmental impact and techno-economic viability. This research aims to provide stakeholders with valuable insights for developing more efficient and eco-friendly technologies and policies.

1.2 Aims and Objectives

In order to address the aforementioned research gaps, this thesis aims to investigate the life cycle environmental impacts and techno-economic performance of producing sustainable ethanol from industrial tail gas to identify environmental hotspots (i.e., activities and materials with the largest overall contributions) and explore the reduction potential throughout their life cycle, emphasizing the economic benefits, break-even points and driving factors, as well as the impact on upstream and downstream industries.

The framework aims to address the following research questions:

1. What is the life cycle environmental impact of TG-ethanol throughout the cradle-to-gate production process, and how do they compare to biomass-based and fossil fuel-based ethanol? What are the contributions of each production unit, energy and material consumption to the environmental impact?
2. What is the potential for reducing the environmental impacts of the three ethanol production pathways through the application of different renewable electricity sources?
3. What are the two process feasibility of TG-ethanol production intensified by electro-catalytic CO_2 technology (TGEE)? What are the technical performance indicators of the optimal process and the analysis of carbon flow?
4. What are the results of the life cycle carbon footprint and economic performance of TGEE technology? What is the more reliable probability range of sensitivity analysis and Monte Carlo simulation to evaluate the LCA and TEA results of TGEE technology?
5. What are the impacts of TG-ethanol technology on upstream and downstream industries, and what are the projected carbon

reduction potentials and techno-economic benefits in these industries by 2060?

These research questions are addressed by investigating the main contributions to the life cycle environmental impacts of TG-ethanol, the driving factors of various environmental indicators, and possible optimisation scenarios and reduction measures. Focusing on the analysis of the TGEE process from industrial tail gas as feedstock in energy-intensive industries and the carbon reduction potential is intensified by electro-catalytic CO_2 reduction electrocatalysis. the carbon emission reduction impacts of green electricity on tail gas ethanol technology are explored. Furthermore, the impact of green electricity on carbon reduction of TG-ethanol and its competing routes is explored. Finally, the research perspective is further expanded to forecast and evaluate the carbon reduction potential and economic benefits of TG-ethanol technology in upstream and downstream industries by 2060.

The thesis has four objectives:

i. Develop a life cycle environmental impact analysis model to comprehensively evaluate the environmental performance of the TG-ethanol route and its competing routes, assessing the contribution of activities and energy material consumption.

ii. Identify typical sensitivities of environmental impacts using sensitivity analysis and set up optimisation scenarios to explore the maximum carbon reduction potential of TG-ethanol.

iii. Simulate the TGEE process under different scenarios through Aspen Plus modelling, determine the optimal TGEE process through key indicator analysis, and analyse its environmental sustainability and techno-economic feasibility based on LCA and TEA performance of the Monte Carlo method.

iv. Evaluate the environmental impact and techno-economic performance of TG-ethanol technology on upstream steel production and downstream aviation fuel, predicting its carbon reduction potential and economic benefits in the steel and aviation industries by 2060.

1.3 Outline of thesis

This thesis consists of 7 chapters, structured around the aforementioned research objectives. The framework of the dissertation is illustrated in **Figure 1**.

Chapter 1 introduces the overall theme of the thesis, including a description of the aims and objectives, as well as research questions.

Chapter 2 contains a literature review of the current status of the ethanol industry and ethanol production technologies, and the existing life cycle and techno-economic evaluation of ethanol production.

Chapter 3 outlines the general steps for assessing the life cycle environmental impacts of ethanol production from industrial tail gas, including model construction and commonly used indicators for LCA & TEA study, the methods for uncertainty analysis, and the selection of key mathematical distributions.

Chapter 4 presents a life cycle environmental impact assessment of ethanol production from Linz-Donawitz Gas (LDG) in the iron and steel industry via bio-fermentation technology, selects 11 typical environmental indicators to compare the environmental performance of this technology and its two competing technologies, examines carbon balance, energy balance and sensitivity factor, as well as explore the environmental impact reduction potential of green electricity on the three technologies.

Chapter 5 designs a coupling technology in which electro-catalytic CO_2 reduction technology as a process intensification technology to intensify the TG-ethanol process (TGEE) under different scenarios and evaluate the integrated LCA and TEA performance of TGEE technology. Three

typical industrial tail gases, sourced from steel, iron alloy, and calcium carbide production, serve as feedstocks for the TGEE process in the case study. Using Aspen Plus software to simulate this process and key indicators analysis to identify the optimal TGEE-ethanol process, and then life cycle and techno-economic analysis based on Monte Carlo simulation was employed to demonstrate the environmental sustainability and techno-economic viability.

Chapter 6 analyses the impact of renewable ethanol production from tail gas ethanol on upstream and downstream industries, with the upstream industry focusing on the iron and steel industry, which is significant in scale and economic importance, and the downstream industry selecting the renewable aviation fuel from this sustainable ethanol production technology, which has gained significant attention and shows great prospects in recent years.

Chapter 7 discusses the overall conclusions and key findings of the research.

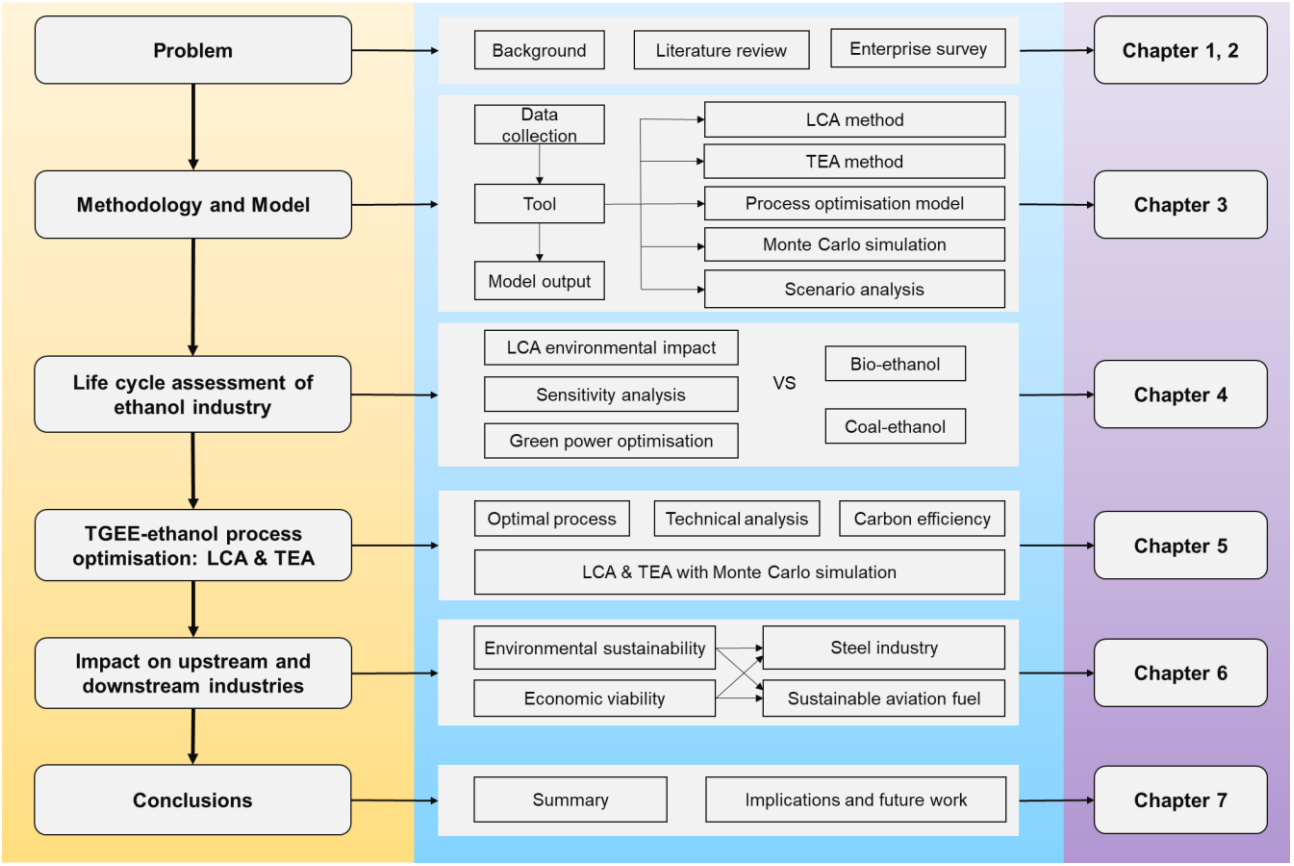

Figure 1. The framework of this thesis.

CHAPTER 2. Literature review

2.1 Introduction

This chapter provides background information on state-of-the-art ethanol production technologies, literature reviews related to ethanol production from coal-based and biomass-based, life cycle assessment (LCA), techno-economic analysis (TEA) and current research gaps.

2.2 Ethanol production state of the art

2.2.1 Ethanol industry

Ethanol is widely used in the chemical, pharmaceuticals, food and fuel industries as an essential bulk chemical and energy substitute. Meanwhile, fuel ethanol can effectively reduce PM2.5 and CO in vehicle exhausts as a good octane blending component and gasoline oxygenator [1]. The use of fuel ethanol as the power source of vehicles can supplement fossil fuel resources, reduce dependence on petroleum resources and reduce greenhouse gas and pollutant emissions. In addition, fuel ethanol can also be added to gasoline as an antiknock agent. Compared with gasoline without Methyl tert-butyl ether (MTBE) [36], fuel ethanol can help gasoline burn completely and significantly

reduce CO, hydrocarbons, PM 2.5, and other air pollutants. Currently, the threat of climate change is a present and growing danger, and it is urgent to promote sustainable energy consumption solutions that are economically variable and ecologically friendly. Transitioning from fossil fuels toward fuel ethanol and biofuels can effectively reduce carbon emissions and mitigate climate change, which countries worldwide have widely recognised [37-40].

According to the Renewable Fuels Association (RFA) statistics, global ethanol production has maintained a slight growth trend since 2015. However, Global ethanol production fell to 26 billion gallons in 2020 because of the COVID-19 pandemic [4]. The United States (US) remained the largest producer, accounting for over half of global output [41]. In China, the fuel ethanol capacity from 2007 to 2022 is shown in **Figure 2**. China's fuel ethanol production has also grown from 1.45 Mt in 2007 to 2.70 Mt in 2022, with an average annual growth rate of 4.84% [26]. China has proposed to promote the use of ethanol gasoline for vehicles nationwide by 2020. It is foreseeable that China's fuel ethanol market faces a large demand gap; compared with the United States and Brazil [39], China's ethanol demand will still have a significant growth rate in the future.

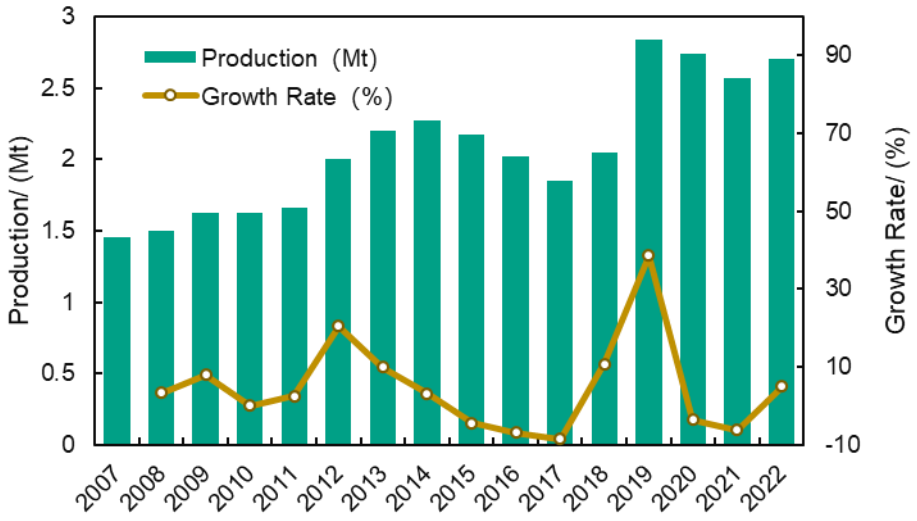

Figure 2. China fuel ethanol capacity from 2007-2022 (cited from [26]).

The regional distribution of ethanol production capacity in China is shown in **Figure 3**. The main capacity-contributing regions come from the northern region, with a total capacity of 6.51 Mt/yr, accounting for 83% of the total national capacity, and the remaining capacity comes from the southern regions with a total of 1.34 Mt/yr. Overall, the primary provinces with fuel ethanol production capacity are Henan, Jilin, Heilongjiang, Shaanxi, Inner Mongolia, Anhui, etc [26].

Currently, fuel ethanol companies in China mainly use corn and wheat as raw materials [42], and the development of fuel ethanol is facing a vast bottleneck amidst the international food crisis and soaring global food prices. China has also banned new grain-ethanol projects for food security, focusing on developing non-edible ethanol and working

towards the industrialisation of cellulose [43]. Therefore, the production of cellulosic fuel ethanol from other non-grains such as cassava and straw and the production of fuel ethanol from industrial exhaust gas will have more significant development in the future [44-46]. **Table 1** shows an overview of fuel ethanol projects in China. According to statistics, there are currently 20 operational fuel ethanol projects with a total capacity of 3.86 Mt/year and 17 projects under construction with a total capacity of 3.99 Mt/year.

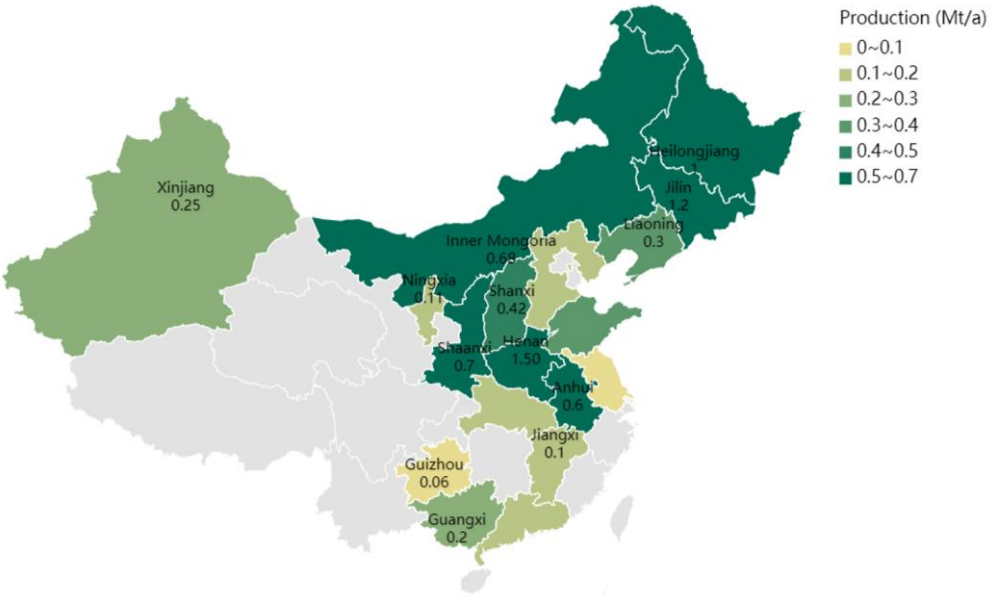

Figure 3. Regional distribution of ethanol capacity in China.

Table 1. Fuel ethanol projects in China.

Enterprise	Location	Capacity (Mt/year)	Status	Feedstock	Remark
Henan Tianguan Group Co., Ltd.	Henan	0.7	Operational	Corn, wheat	Supply area: Henan, Hubei, Hebei
Jilin Fuel Alcohol Co., Ltd.	Jilin	0.6	Operational	Corn, wheat	Supply area: Jilin, Liaoning
China Oil & Foodstuffs Corporation (COFCO) Biochemical (Anhui) Co., Ltd.	Anhui	60	Operational	Corn, wheat	Supply area: Anhui, Shandong, Jiangsu
COFCO Biochemical (Zhaodong) Co., Ltd.	Heilongjiang	40	Operational	Corn, wheat	Supply area: Heilongjiang
COFCO Bioenergy (Guangxi) Co., Ltd.	Guangxi	20	Operational	Cassava, Sweet sorghum stalks	Supply area: Guangxi
Heilongjiang wanlirunda biotechnology Co. Ltd.	Heilongjiang	30	Operational	Corn	/
Shandong Longlive Bio-technology Co., Ltd	Shandong	5	Operational	Corn cob waste	/
SDIC Guangdong Bioenergy Co., Ltd	Guangdong	15	Operational	Cassava, Sweet sorghum stalks	/
Shandong Vern Biochemical Co., Ltd	Shandong	12	Operational	Cassava	/
Inner Mongolia ZTE energy Co., Ltd	Inner Mongolia	3	Operational	Cassava, Sweet sorghum stalks	/
Liaoyuan Kyoho biochemical technology Co., Ltd	Jilin	5	Operational	Sweet sorghum stalks	/
Shaanxi Yanchang Petroleum	Shaanxi	10	Operational	Coal-based syngas	Product purity > 99.7%
Tangshan Zhongrong Technology Co., Ltd.	Hebei	10	Operational	Coke-oven gas	/
Shaanxi Xinghua Co., Ltd.	Shaanxi	10	Operational	Coal-based syngas	/
Henan Shunda Chemical Co., Ltd.	Henan	20	Operational	Acetic acid	Esterification and hydrogenation of acetic acid to ethanol
Jinan Shengquan Group Share Holding Co., Ltd.	Shandong	2	Operational	Cellulose	/
Shandong Zensun biology Co., Ltd.	Shandong	2	Operational	Corn straw	/
Beijing Shougang LangzaTech New Energy&Technology Co., Ltd. (Hebei)	Hebei	4.5	Operational	Tail-gas in the steel industry	DDGS-5000 t

Beijing Shougang LangzaTech New Energy&Technology Co., Ltd. (Ningxia)	Ningxia	4.5	Operational	Ferroalloy industrial exhaust gas	/
Jiangsu Sopo Chemical Co. Ltd.	Jiangsu	3	Operational	Coal-based syngas	/
Biotechnology in Inner Mongolia Co. Ltd.	Inner Mongolia	30	Plan	Corn	DDGS-270000 t
Jilin Boda biological chemicals Co. Ltd.	Jilin	25	Plan	Corn	DDGS-230000 t; Fusel oil-747 t
SDIC biological Tieling fuel ethanol project	Liaoning	30	Plan	Corn	DDGS-276300 t; Corn oil-20000 t
SDIC biological Hailun fuel ethanol project	Heilongjiang	30	Plan	Corn	DDGS-258000 t
Shandong Longlive cellulosic ethanol project	Shandong	10	Plan	Corn cob waste	Cellulosic ethanol production by biological enzyme
Jilin Tiancheng fuel ethanol project	Jilin	30	Plan	/	/
Hubei Tianguan fuel ethanol	Hubei	10	Plan	Cassava	/
Jiangxi Yufan fuel ethanol project	Jiangsu	10	Plan	Cassava	/
Inner Mongolia Lishen fuel ethanol project	Inner Mongolia	35	Plan	Corn	Feedstock consumption: Corn-9240000 t, straw-350000 t
Yanchang Xinghua syngas-ethanol project	Shaanxi	50	Plan	Coal-based syngas	Coal is carbonylated with dimethyl ether to produce ethanol
Shanxi Yangmei Fengxi Chemical Co. Ltd.	Shanxi	40	Plan	Coke-oven gas	100 Mt/a methanol, 0.4 Mt/a ethanol
Yima Coal industry project	Hunan	40	Plan	Coal	/
Lu’an group fuel ethanol project	/	2	Plan	Industrial tail-gas	Special microorganism of Jupeng biochemical
Ze New Energy Technology Ltd Ningxia waterfront	Ningxia	6	Plan	Metallurgical exhaust gas	DDGS-6600 t
Kanazawa New Energy Technology Limited, Guizhou Province	Guizhou	6	Plan	Metallurgical exhaust gas	DDGS-6600 t
Henan Shunda Chemical acetate-ethanol project	Henan	20	Plan	Acetic acid	/
Xinjiang Tianye Co. Ltd.	Xinjiang	25	Plan	Syngas	/

2.2.2 Ethanol production pathways

According to the different production raw materials, the production process of ethanol is mainly divided into three categories: petroleum-based ethylene hydration method, coal-based syngas to ethanol and biomass to ethanol, as shown in **Figure 4**. The ethylene hydration method uses petroleum as the primary raw material and is suitable for countries with rich petroleum resources [47], such as the United States and Russia. In recent years, due to the breakthrough of coal-based syngas to ethanol technology and the low cost, it has a good development prospect under the advantage of abundant coal resources in China [48]. However, the biomass-to-ethanol method is the current mainstream technology in China due to energy crises and reducing carbon emissions.

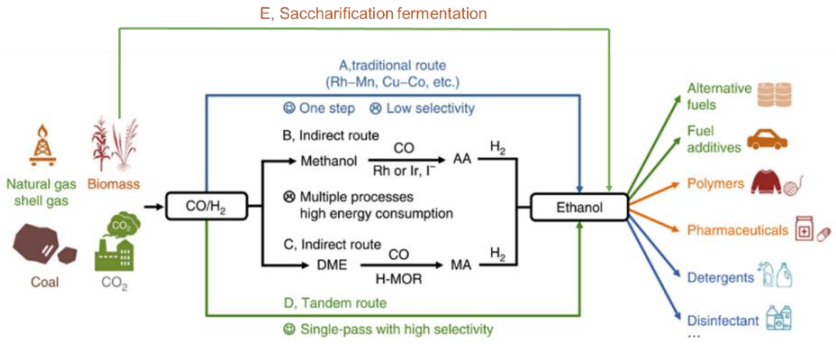

Figure 4. The diagram of different ethanol production technology (cited from [49]).

2.2.2.1 Coal-based syngas to ethanol

The technology of coal-based syngas to ethanol can be divided into direct and indirect methods [50]. The direct method means that ethanol can be produced directly from the syngas by bio-fermentation or direct catalysis; the indirect method means that the coal-based syngas is used as the raw material to obtain ethanol after the conversion of intermediate products, including the acetic acid hydrogenation method, the acetic esterification hydrogenation method, and dimethyl ether carbonylation, etc.

Syngas to ethanol by direct synthesis

The synthesis of ethanol from coal-based syngas (a mixture of hydrogen and carbon dioxide) is an important route in China based on its abundant coal resources. However, the production of ethanol from coal-based syngas currently has the problems of low selectivity, many technological processes and high energy consumption. Ethanol production from syngas by direct synthesis mainly depends on the catalytic effect of the catalyst and the adaptability and tolerance of the catalyst are the key indicators. Researchers are committed to developing efficient catalysts to improve the conversion rate of carbon monoxide and the selectivity of ethanol [49]. The current catalysts to

produce ethanol from syngas to ethanol can be divided into the following categories: (1) Cu-based catalysts, (2) Rh-based catalysts, (3) modified Fischer-Tropsch catalysts, (4) Mo-based catalysts and (5) two-component or multi-component catalysts, such as Rh-Mn, Rh-Fe, Cu-Co, Cu-Fe catalysts. Almost all of the above catalysts have limited CO conversion rates, and the ethanol selectivity is less than 60% [49].

Ethanol can be produced via CO hydrogenation (**equation (1)**), this reaction is thermodynamically favourable and highly exothermic. The equilibrium composition includes ethanol, methanol, water, carbon monoxide and hydrogen, the products of ethanol and water decrease with increasing temperature, while the reactants of CO and H_2 increase [51]. Thermodynamics suggests that CO hydrogenation should be carried out below ~300℃.

$$2CO + 4H_2 \rightarrow CH_3CH_2OH + H_2O \quad (1)$$

$$\Delta H_r^\circ = -253.6\ kJ/mol$$

$$\Delta G_r^\circ = -221.1\ kJ/mol$$

Although methanol is thermodynamically less favourable than ethanol, it is usually one of the main products of the reaction but must be kinetically limited. Ethanol can also be produced by homogenisation

of methanol (**equation (2)**). The reaction involves the reductive carbonylation of methanol to form the C-C bond on the redox catalyst to form ethanol.

$$CH_3OH + CO + 2H_2 \rightarrow C_2H_5OH + H2O \quad (2)$$

$$\Delta H_r^\circ = -165.1\ kJ/mol$$

$$\Delta G_r^\circ = -97.0\ kJ/mol$$

Both of the above reactions are associated with side effects that produce many products, such as methanol, isopropyl, alcohol, n-propyl alcohol, n-butyl alcohol, isobutyl alcohol, acetone, acetaldehyde, isobutane, n-butane, hexane, methane, CO_2, ethane, propadiene, propylene, and propane.

As for the commercialised project of coal-based syngas to ethanol, the world's first operated factory located in Shaanxi province of China in 2017, with an annual capacity of 0.1 Mt. **Figure 5** illustrates the process diagram for this world's first coal-based syngas to the ethanol plant [48], the process includes two main steps: (1) coal as raw materials, through coal gasification, water-gas shift, shift gas to methanol, purification, pressure swing adsorption, etc; (2) methanol, hydrogen and carbon monoxide co-reacted to obtain ethanol and its by-products.

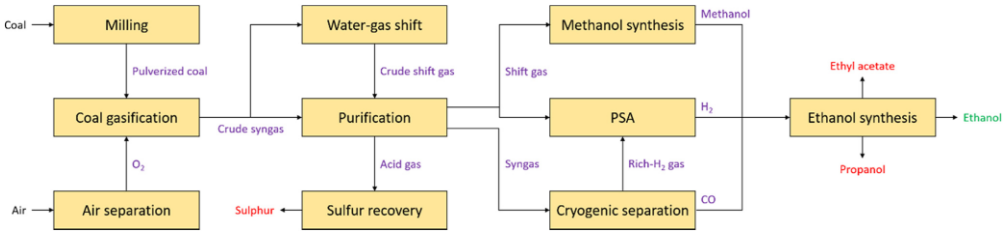

Figure 5. The process diagram of coal-based syngas ethanol (cited from [47]).

Hydrogenation of ethyl acetate to ethanol

The direct hydrogenation of acetic acid to ethanol means that under the action of a catalyst, acetic acid molecules are first separated into carboxylic acid or acetyl intermediates, and then further hydrogenated to form acetaldehyde or acetic acid. The main advantages of the acetic acid direct hydrogenation method are that it can digest the remaining acetic acid production capacity, has a short process flow, low energy consumption, and high ethanol product yield [52]. However, acetic acid hydrogenation catalysts are mostly precious metal catalysts, which are expensive and difficult to recycle. In addition, due to the corrosive nature of acetic acid, pipeline design investment is high and the overall cost is high. Hydrogenation of ethyl acetate to ethanol is the primary process of syngas to ethanol in China, the diagram is shown in **Figure 6**.

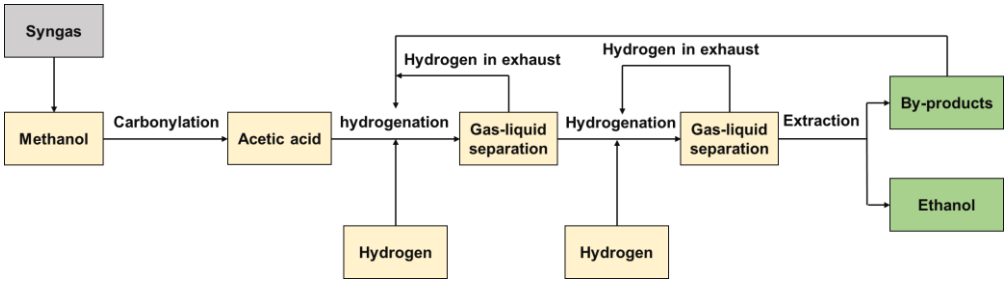

Figure 6. Diagram of Hydrogenation of ethyl acetate to ethanol.

Equation (3)-(7) represent the reaction formula of hydrogenation of ethyl acetate to ethanol. Temperature changes will affect the entire reaction process [53]. In the low-temperature region, the equilibrium conversion of acetic acid is high, and with the increase in reaction temperature, the conversion of acetic acid gradually decreases. As one of the reactants, ethanol has the same conversion rate and selectivity, while the selectivity of the by-product ethyl acetate increases with the temperature increases. Therefore, the development of efficient and stable catalysts is crucial for achieving high selectivity and yield of ethanol in acetic acid hydrogenation technology applications.

$$CH_3COOH + 2H_2 \rightarrow CH_3CH_2OH + H_2O \quad (3)$$

$$CH_3COOH + C_2H_5OH \rightarrow CH_3COOC_2H_5 + H_2O \quad (4)$$

$$CH_3COOH + H_2 \rightarrow CH_3CHO + H_2O \quad (5)$$

$$CH_3CH_2OH + H_2 \rightarrow CH_3CH_3 + H_2O \quad (6)$$

$$CH_3COOC_2H_5 + 2H_2 \rightarrow 2CH_3CH_2OH \quad (7)$$

The development of acetic acid hydrogenation to ethanol technology has garnered significant attention and efforts from both domestic and international enterprises and research institutions, resulting in notable achievements. In 2012, Shanghai Pujing successfully conducted a 600 t/a scale acetic acid hydrogenation pilot project in Shunda, Henan, achieving acetic acid conversion and ethanol selectivity exceeding 99% and 92%, respectively, with an ethanol space-time yield of 850 g/(kg cat • h) facilitated by noble metal catalysis [54]. In 2013, Celanese Corporation utilized its independently developed TCX technology and existing acetyl facilities to establish a 275 kt/a scale acetic acid hydrogenation to ethanol plant in Nanjing Chemical Industrial Park [55]. In 2016, Sinopec Group collaborated with American enterprises to optimize the demonstration plant for acetic acid hydrogenation to ethanol, achieving significant success [56].

Despite these remarkable advancements, several challenges persist. Issues such as incomplete chemical reactions or slow reaction rates limit product selectivity and carbon monoxide conversion rates. Additionally, further enhancement and optimization of catalyst properties are required.

In response to these challenges, Dalian Institute of Chemical Physics and Sinopec Group collaborated to construct a 30,000-ton acetic acid hydrogenation to ethanol project, which commenced successful operation in May 2016. The industrial demonstration unit produced anhydrous ethanol with a purity of up to 99.6%, surpassing the national standards for industrial ethanol in China [57]. This signifies a significant breakthrough in the industrial production of acetic acid hydrogenation to ethanol technology.

Acetate esterification and hydrogenation to ethanol

Acetate esterification and hydrogenation to ethanol include two processes: the methyl ester route and the ethyl ester route [58]. The main processes include the esterification of acetate to generate methyl acetate or ethyl acetate, the hydrogenation of acetate to generate crude alcohol, and the crude alcohol is distilled and separated to obtain fuel ethanol.

I. Acetic Acid-Methyl acetate- ethanol

Acetic acid is esterified with methanol to produce methyl acetate, and the separated and purified methyl acetate is hydrogenated under the action of a catalyst to produce methanol, ethanol and other products.

After the separation of products, methanol can be returned to the esterification process for recycling, and ethanol can be obtained by distillation [59]. The diagram is shown in **Figure 7**, and the reaction formula is as follows **equation (8)-(10)**:

Esterification reaction：$CH_3COOH + CH_3OH \rightarrow CH_3COOCH_3 + H_2O$ (8)

Hydrogenation reaction：$CH_3COOCH_3 + 2H_2 \rightarrow CH_3OH + C_2H_5OH$ (9)

$$CH_3COOH + 2H_2 \rightarrow C_2H_5OH + H_2O \quad (10)$$

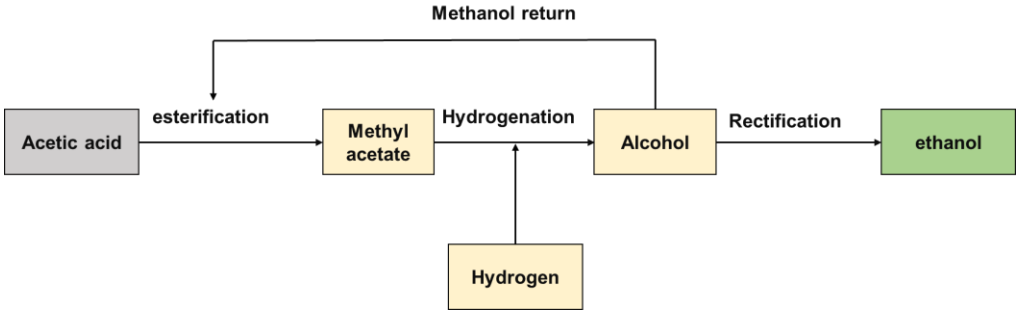

Figure 7. Acetate esterification and hydrogenation to ethanol (Methyl acetate route).

II. Acetic acid- Acetic ether- ethanol

Acetic acid and ethanol are mixed in a certain proportion and then reacted under the action of a catalyst to form ethyl acetate, which is distilled and separated to obtain about 92–93% of the crude ester, and then refined and separated from the water after preheating into the hydrogenation process [60]. Hydrogen is pressurized into the

hydrogenation process, mixed with ethyl acetate and vaporized in the hydrogenation reactor, under the action of the catalyst, ethyl acetate reacts with hydrogen to form ethanol, which is shown in **Figure 8**. After the dehydrogenation of crude ethanol, part of it is returned to the esterification process as raw material, and part of it is obtained from ethanol product after de-esterification, dehydration and de-weighting. The reaction is as follows **equation (11)-(13)**:

Esterification reaction: $CH_3COOH + C_2H_5OH \rightarrow CH_3COOC_2H_5 + H_2O$ (11)

Hydrogenation reaction: $CH_3COOC_2H_5 + 2H_2 \rightarrow 2C_2H_5OH$ (12)

$$CH_3COOH + 2H_2 \rightarrow C_2H_5OH \quad (13)$$

During the hydrogenation of ethyl acetate, a small amount of side reactions occurs. The main reactions are as follows **equation (14)-(17)**:

Form ethane reaction: $C_2H_5OH + H_2 \rightarrow C_2H_6 + H_2O$ (14)

Form ether reaction: $2C_2H_5OH + H_2 \rightarrow C_2H_5OC_2H_5 + H_2O$ (15)

Form acetaldehyde reaction：$CH_3COOC_2H_5 + H_2 \rightarrow CH_3CHO + C_2H_5OH$ (16)

$$C_2H_5OH \rightarrow CH_3CHO + H_2 \quad (17)$$

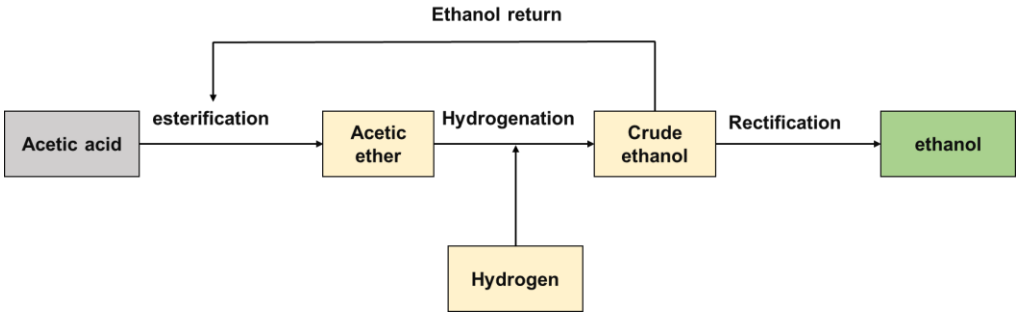

Figure 8. Acetate esterification and hydrogenation to ethanol (Acetic ether route).

Acetic acid esterification hydrogenation to ethanol process is considerable challenges, the generation of acetic acid ester mainly depends on the occurrence of the esterification reaction, and then the acetic acid ester is combined with the catalyst to complete the hydrogenation to ethanol process [8]. Compared to the hydrogenation of acetic acid directly to ethanol, the process of acetic acid esterification hydrogenation to ethanol is more robust but entails a more complex procedure. Its main advantage lies in its strong corrosion resistance, which can significantly mitigate energy consumption during separation. However, the process entails a lengthier route, with half of the product requiring recycling to the front end of the esterification cycle for reuse. Moreover, the utilization of acetic acid feedstock necessitates a high level of pipeline design and entails substantial initial investment. Henan Shunda Chemical's 200000 tons/year acetic acid esterification and

hydrogenation to ethanol plant was completed and put into operation in 2015, with a total investment of about 640.85 million yuan, of which 587.4 million yuan was invested in construction [61]. The construction includes the hydrogenation process, compression process, hydrogenation process, refining process, utility, etc.

Currently, research efforts in the acetate hydrogenation to ethanol process focus on enhancing corrosion resistance and continuously improving energy consumption in separation processes. Natthanon *et al*. [58] reported a two-step reaction of cellulose and acetic acid fermentation and hydrogenation to produce ethanol process. Cellulose is hydrolysed by the hot compress method to produce cellulose derivatives, which are then fermented to obtain acetic acid. Acetic acid was first esterified to produce ethyl acetate, and ethyl acetate was produced as ethanol under the action of Cu-Zn catalysts, and only a small amount of methane and ethane by-products were produced at the reaction temperature of 210–270^{o}C [58].

Dimethyl ether to ethanol

The process of carbonylation of dimethyl ether to ethanol mainly involves the dehydration reaction of methanol to generate dimethyl ether,

the carbonylation reaction of dimethyl ether and carbon monoxide to generate a methyl acetate mixture, and finally hydrogenation reaction again to get ethanol [62], the main process shown in **Figure 9**. Compared with the acetic acid feedstock process, this process has lower catalyst requirements, does not require the use of higher-cost precious metal catalysts better corrosion-resistant reaction kettles, and has lower production costs. The by-products of methanol and methyl acetate also have certain economic value, and the reaction is as **equation (18)-(20):**

Carbonylation：$\mathrm{CH_3OCH_3} + CO \rightarrow CH_3COOCH_3$ (18)

Hydrogenation： $CH_3COOCH_3 + 2H_2 \rightarrow CH_3OH + C_2H_5OH$ (19)

$$CH_3OCH_3 + CO + 2H_2 \rightarrow C_2H_5OH + CH_3OH \quad (20)$$

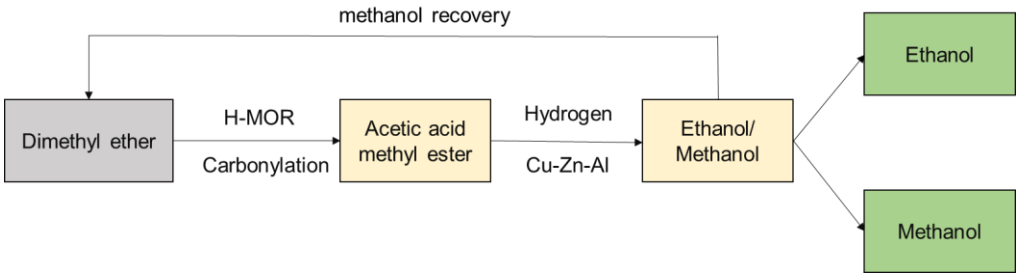

Figure 9. Acetate esterification and hydrogenation to ethanol (Acetic ether route).

In recent years, the process of producing ethanol from dimethyl ether (DME) has gained traction, primarily involving the carbonylation of DME

to methyl acetate (MA) on zeolite and subsequent hydrogenation of MA on copper catalysts to ethanol [63]. The carbonylation reaction on molecular sieves represents a crucial step in this process, garnering increased attention due to its high reaction efficiency and broad industrial prospects. Efforts have been focused on enhancing the activity and stability of zeolites. Transition metal-modified zeolites often yield more active and potentially more stable carbonylation catalysts. Simultaneously, reducing the crystal size of zeolites and adjusting their morphology has been shown to significantly enhance diffusion efficiency, thereby improving catalytic stability. Overall, the development of active and stable carbonylation catalysts for DME largely hinges on appropriately controlling acid site distribution and adjusting zeolite size and shape [62].

Qinghong Wei *et al*. [64] reported a simplified reaction pathway for ethanol synthesis from DME and syngas. Using DME and syngas as feedstocks and employing a relay combination catalyst of Cu/HZSM35 (magnesium-modified zeolite) and Cu-Zn-Al, efficient ethanol synthesis was achieved in a dual-catalyst bed reactor. The reaction exhibited high activity under conditions of 220^{o}C and 1.5 MPa, with a DME conversion rate of 27.1% and ethanol selectivity reaching 46.7%. Xingang Li *et al*.

[65] demonstrated DME carbonylation to methyl acetate under the action of H-MOR (hierarchical Mordenite), followed by hydrogenation of methyl acetate to ethanol on a Cu/ZnO dual-bed catalyst reactor. At 220^{o}C, the DME rate conversion reached 100%, with methanol and ethanol yields of 46.3% and 42.2%, respectively.

Ce Du *et al*. [66] synthesized a highly ordered Cu-MOR@SiO_2 core-shell microcapsule catalyst using surface-expandable sol-gel technology. This microcapsule catalyst exhibited a high DME carbonylation conversion rate of 83.8% and ethanol selectivity of 48.7%. Traditional Cu-MOR catalysts suffer from sintering of Cu particles during preparation and reaction, affecting catalyst recyclability as regeneration requires heat treatment. Additionally, catalyst deactivation affects DME conversion, leading to higher selectivity towards methanol as a byproduct in dual-bed reactions. Therefore, the development of ordered mesoporous core-shell structures can improve DME carbonylation rates. The novel microcapsule catalyst developed in this work has a functional core encapsulated by a homogeneous water-permeable shell, which effectively improves the sintering and agglomeration of the functional core, with a Cu-MOR@SiO_2 core-shell catalyst on the top and Cu-Zn-Al catalyst at the bottom, which in essence does not add new active sites

but only helps to fully expose the unutilized sites make the catalyst exhibit high activity, high product yield, durability, and can be recycled.

2.2.2.2 Biomass to ethanol

Biomass fermentation methods can be divided into three main categories according to the different raw materials: grain ethanol (G1 generation) with wheat, rice, and corn as raw materials; non-grain ethanol (G1.5 generation) with sweet sorghum, cassava and sugar cane as raw materials; and cellulosic ethanol (G2 generation) with straw and other crop waste as raw materials. The main processes in the fermentation of biomass to ethanol are raw materials – conversion – sugar – microbial fermentation – ethanol mash – extraction – ethanol [67]. **Figure 10** illustrates the biomass-to-ethanol process diagram. Microorganisms are the dominant players in this process. The ethanol conversion capacity of microorganisms is a key criterion for selecting strains in the ethanol production process and providing the best process conditions can the production potential of strains to be fully exerted.

In fact, global ethanol production is mainly based on biological routes, by taking corn, wheat cassava, sugarcane, and sorghum as feedstocks [68]. However, there are major concerns over bio-ethanol production due

to the enormous amount of arable land required to grow the crops to meet the rapidly growing ethanol demand, as well as the great impact on forest biodiversity [69].

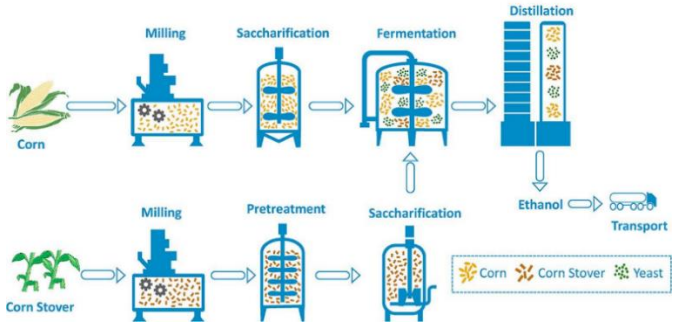

Figure 10. The process diagram of biomass to ethanol (cited from[70]).

Grain-ethanol (G1)

Grain ethanol belongs to the first generation (G1) of bioethanol and occupies the majority of China's fuel ethanol market [71]. Compared with other starchy raw materials, corn is one of the grains with the longest value chain and the most abundant product series [72]. The production process of Corn-ethanol is simple, with relatively low energy consumption and less equipment investment [73]. As a renewable resource, Corn-produced fuel ethanol is environmentally friendly. In 2019, China's ethanol production is expected to reach 7.96 million tons, with Corn-ethanol accounting for as much as 79%, reaching 6.32 million tons [74]. However, the grain ethanol industry faces the risk of competing

with the people for food, and the potential for grain development is limited amid concerns about food and energy security [75]. In the future, technologies for producing ethanol from non-grain materials will see greater development.

The diagram (**Figure 11**) and equation below represent the main process of producing ethanol from corn. First, corn is ground into flour for pretreatment, then the corn flour is mixed with water and enzymes, the starch in the corn is liquefied through a liquidation process to obtain the distiller's dried grains with soluble (DDGS) , after liquidation, the mash undergoes a saccharification process that converts the remaining starch into fermentable sugars [76], then the saccharification mash is added to yeast for fermentation, the yeast consumes the sugars in the saccharification mash and converts them into ethanol and CO_2. The fermentation process usually takes between 48 to 72 hours to complete. At the end of the fermentation, the ethanol is separated from the remaining solids and water through a distillation process, heated, condensed and collected to obtain the ethanol product [77]. The reaction is as follows **equation (21)-(23)**:

Total reaction for Corn-ethanol

$$(C_6H_{10}O_5)_n + nH_2O \rightarrow 2C_2H_5OH + 2CO_2 \quad (21)$$

- Saccharification

$$(C_6H_{10}O_5)_n + nH_2O \rightarrow nC_6H_{12}O_6 \quad (22)$$

- Fermentation

$$C_6H_{12}O_6 \rightarrow 2C_2H_5OH + 2CO_2 \quad (23)$$

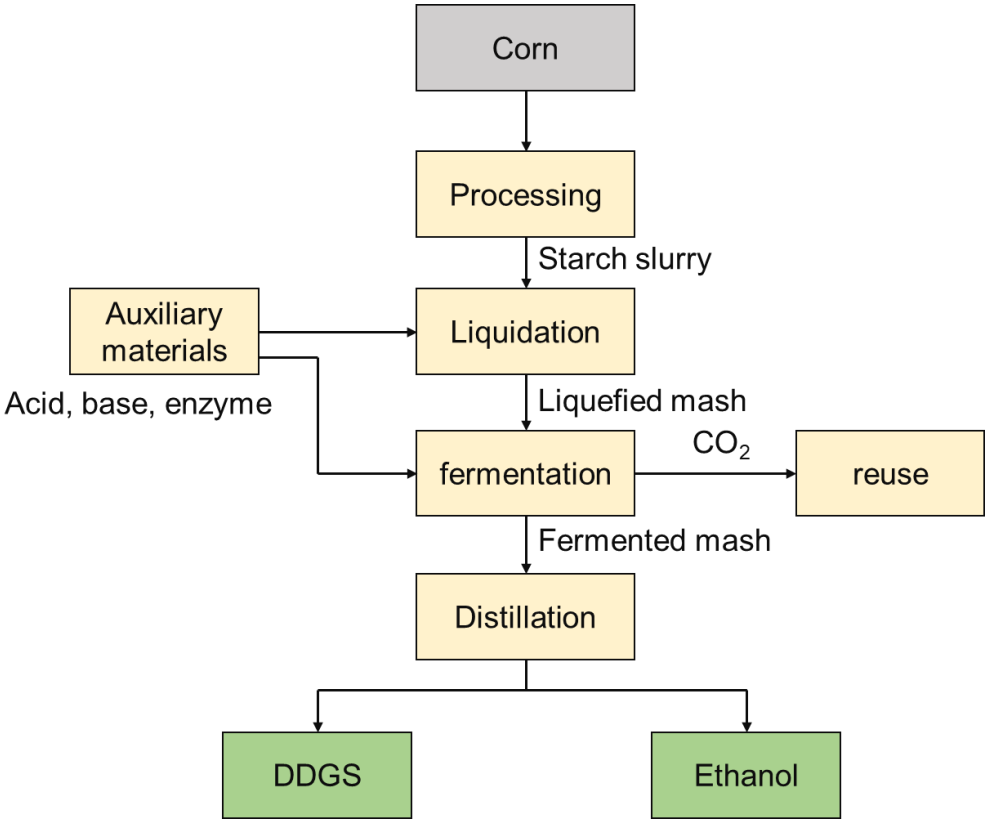

Figure 11. The process diagram of Corn-ethanol.

Corn ethanol is currently the most mature technology, and the production of corn ethanol is also increasing, but its disadvantages in competing for food are becoming increasingly urgent, as it is essential to increase the unit ethanol yield of corn. Pietro Sica *et al.* [78] evaluated the effect of adding sugarcane juice to corn ethanol production. The

results showed that the fermentation efficiency increased by 4.8% after the combination of corn and sugarcane juice. The benefits of adding sugarcane juice to Corn-ethanol are as follows: 1) Sugar provided by sugarcane juice can reduce the amount of corn used in Corn-ethanol production by 50%; 2) It can replace the water in the corn dilution process, which requires 2–3 L of water per kilogram of corn for dilution; 3) Improve fermentation efficiency by providing nutrients that stimulate the growth of the yeasts.

Chinmay Kurambhatt *et al.* [79] investigated the use of corn fractionation in the dry milling process to increase the number of by-products, improve their quality and value, provide feedstock for cellulosic ethanol production, and potentially improve the profitability of the dry milling process. The objective of the study was to develop process simulation models of eight different wet and dry corn fractionation technologies for the recovery of germ and pericarp fibres and/or endosperm fibres and to evaluate their techno-economic feasibility for commercial use. To improve the front-end fractionation technology of the dry grinding process, the investment cost for wet fractionation is approximately $9285–9738, and the investment cost for dry fractionation is $8335–8491. The cost of dry fractionation is lower than

the conventional process, and the return rate on both wet and dry fractionation is higher than the conventional process.

Jan Lewandrowski *et al.* [80] studied the greenhouse gas emission reduction effect of Corn-ethanol. In 2010, the U.S. Environmental Protection Agency (EPA) released a life cycle analysis of greenhouse gas (GHG) emissions associated with the production and combustion of Corn-ethanol. The EPA projected that by 2022, Corn-ethanol produced at a new refinery will have 21% lower emissions than gasoline with the equivalent energy. By 2018, the authors conducted a real-world assessment of Corn-ethanol emissions using available data, which showed that Corn-ethanol's actual GHG emissions were 39–43% lower than gasoline and additionally projected that Corn-ethanol's GHG emissions would be 47–77% lower than gasoline emissions by 2022. Many countries are developing or revising renewable energy policies. Typically, biofuel alternatives to gasoline are required to reduce GHG emissions by more than 21%.

Non-grain-ethanol (G1.5)

Non-grain ethanol (G1.5) is based on sugar-based crops as feedstocks, mainly including cassava, sugarcane, sugar beets and sweet sorghum, as well as sugarcane molasses and sugar beet

molasses and other sugar mill wastes [81]. The fermentable sugars present in these sugar-based feedstocks are mainly glucose, fructose and sucrose. Compared to G1 starch-based crops, fermentable sugars in sugar-based crops can be directly fermented and converted to ethanol by yeast or other fermenting microorganisms without other processing [82, 83].

The feedstock for G1.5 bioethanol is squeezed under hot water spray conditions to obtain crude sugar juice, which is collected by inputting lime (e.g., Ca $(OH)_2$) to purify and neutralize organic acids. The lime is filtered and clarified, and the removed portion is made into a filter cake [84]. The concentrated syrup is then supplemented with ammonium sulphate or other nitrogen sources, sterilized, and the pH and sugar concentration adjusted. Ammonium sulphate or other nitrogen sources are added to the concentrated syrup for sterilization, pH adjustment, and sugar concentration adjustment. The syrup is then sent to the fermentation unit where it is fermented by microorganisms (preferably yeast). Sugar-based biomass fermentation is often carried out in single-concentration or double-concentration continuous fermentation, and the fermented mature mash is separated by centrifugation and sent to the distillation and dehydration unit to obtain fuel ethanol [85]. The by-

products and residues generated during the production process can be used for different purposes: bagasse from the sugar juice purification process can be used to generate electricity in the plant, and the filter cake can be used as an eco-friendly fertilizer for agricultural production, the by-product distillers grains can be used as animal feed or fertilizer.

Sarocha Pradyawong *et al.* [86] compared the bioethanol production from cassava starch with corn using a conventional and raw starch glutathione (GSH) hydrolysing process. The result shows that the final ethanol concentration with cassava starch for the GSH process was 2.8% higher than that for the conventional process. During the conventional process, cassava starch yielded the highest fermentation rates of dent corn, waxy corn, high amylose corn and cassava starch. Overall, the fermentation profile of cassava starch was like corn in terms of ethanol production and formation of glycerol. Therefore, cassava starch is a high-potential feedstock for bioethanol production due to its excellent fermentation performance, high yield of carbohydrates per unit of land, and growth on marginal lands with minimal agrochemical requirements [86].

Cellulosic-ethanol (G2)

Cellulosic biomass will be the main technology for ethanol production in the future. Cellulose has the advantages of abundant raw materials, wide sources, low costs, etc. Agricultural straw (corn straw, wheat straw) is a commonly used raw material for cellulosic ethanol [45], so the development of cellulose raw materials for ethanol production technology can also be realized on the full use of waste biomass, in line with the requirements of green environmental protection [87]. The process flow diagram of cellulosic ethanol is shown in **Figure 12**. Firstly, the structure of cellulose is destroyed by the pretreatment process, because its main components include cellulose, hemicellulose, and lignin, which are intertwined to form lignin-carbohydrate complexes (LCCs) [88]. LCCs are difficult to degrade, and pretreatment separates the cellulosic components from the hemicellulose and lignin to allow for enzymatic degradation to release glucose for ethanol fermentation. The current pretreatment technology is mainly based on a combination of physical and chemical, including steam blasting, liquid phase hot water pretreatment, acid pretreatment, etc [89]. Secondly, cellulose is hydrolysed into glucose through hydrolysis technology, which requires the participation of catalysts, and the commonly used catalysts are inorganic acid and cellulase, which form the acid hydrolysis and enzyme

hydrolysis processes, respectively [90]. Then, glucose is metabolized into crude ethanol through a fermentation reaction, followed by distillation, rectification, dehydration, separation, purification process, etc., to finally obtain ethanol products [91].

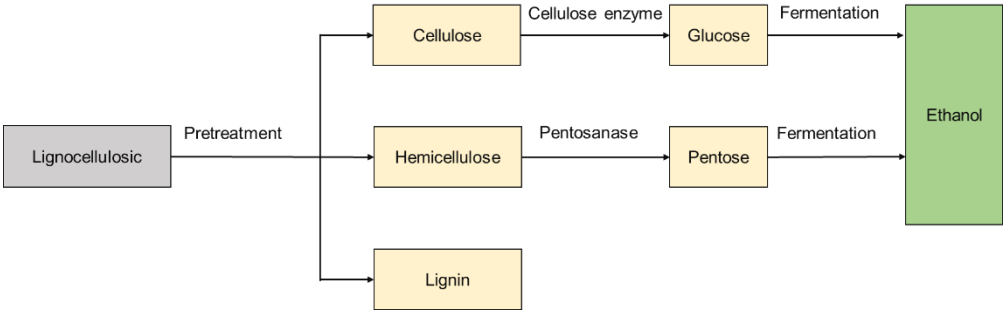

Figure 12. The process diagram of cellulosic ethanol.

Cellulosic ethanol technology efficiently utilizes the energy in cellulose, reduces the cost of biofuel production, effectively handles cellulose waste, and resolves the conflicts between people, food, and land caused by the previous use of food crops to produce biofuels [92]. Ethanol as a fuel additive can reduce harmful gas emissions, with its high octane rating and flame propagation speed improving energy efficiency. However, commercial-scale production of cellulose ethanol faces challenges such as low efficiency, low activity, high cost, high usage, and low hydrolysis efficiency of cellulase enzymes [93]. In addition, the high difficulty and cost of pretreatment processes result in overall production costs being higher. Cellulosic ethanol as one of the

solutions to transportation fuel supply and environmental challenges is still not economically competitive with ethanol produced from sugar- and starch-based feedstocks or petroleum-based transportation fuels, making cost reduction a priority task. Liu Chenguang *et al*. [94] proposed that researchers should consider the multidisciplinary nature of cellulosic ethanol production, gain an in-depth understanding of the physiological and metabolic reactions of microbial strains under industrial production conditions, conduct robust design, and perform unit integration and system optimization to save money. cost. Energy and water consumption. This could be the ultimate solution for the entire process of cellulosic ethanol production, making it economically competitive.

Since lignocellulose is pretreated and the biomass is not efficient at high solids loading, the ethanol titer obtained from cellulosic ethanol production is also much lower, with approximately 50% of the titer obtained from grain-ethanol fermentation [95]. This shortcoming increases the energy consumption for recovering ethanol through distillation and subsequently releases a large amount of residue that needs to be treated. Sitong Chen *et al*. [70] conducted a project to produce ethanol by mixing corn stover and corn. Corn stover was pretreated with dilute alkali and dilute acid, and then the pretreated corn

stover was saccharified, hydrolyzed and mixed with corn for fermentation to produce ethanol. The results showed that the alkali-pretreated corn stover and corn yielded 92.30 g/L ethanol at a mixing ratio of 10%. Using the fed-feed strategy, the ethanol titer was further increased to 96.43 g/L. In addition, the dilute acid pretreated corn stover blended with corn resulted in an ethanol titer of 104.9 g/L with an ethanol yield of 80.47% and a high yield of 2.19 g/L/h. This work demonstrated that the co-production of Corn-ethanol and cellulosic ethanol may be a transition strategy for the large-scale production of cellulosic ethanol.

2.2.2.3 Summary

Overall, the main differences between coal-based ethanol and biomass ethanol lie in three aspects: raw material sources, production processes, environmental and techno-economic impacts, as shown in **Table 2**. Coal-ethanol and biomass-based ethanol differ significantly in their production processes and environmental impacts. While coal-based ethanol relies on finite fossil fuel resources and involves carbon-intensive processes like coal gasification, biomass-based ethanol utilizes renewable organic materials and employs more environmentally friendly biochemical processes such as enzymatic hydrolysis and

fermentation. Consequently, biomass-based ethanol presents a more sustainable and ecologically sound alternative to coal-based ethanol, with lower carbon emissions and reduced environmental impact.

In recent years, there have been significant technological advancements in ethanol production processes both domestically and internationally. The main tasks are focused on increasing unit output and reducing production costs, with more emphasis on simplifying the production process. Corn-ethanol, is the mainstream process, such as non-cooking hydrolysis technology, cell immobilization technology, development of recombinant microorganisms, fermentation under high solids loading conditions, solid-state fermentation technology, and integration of different processes. Regarding the design of production processes, Shi *et al.* [96] studied the efficiency of fuel ethanol production using six maize varieties and found that the highest fuel ethanol yields were achieved by the “milling, fermentation, ester transfer” route. Enzyme research is also a hot topic for optimizing Corn-ethanol production technology [97], mainly focused on improving the pH range suitability of amylase. The optimal pH range for traditional amylase is 5.4–6.0, while the pH value of the corn slurry produced by existing processes is approximately 4.9, requiring the addition of a suitable

amount of liquid alkali to raise the pH value to adapt to the normal pH value for amylase activity. After liquefaction, sulfuric acid needs to be added to adjust the pH value of the liquefied slurry to 4.5 to suit the conditions for the action of glucoamylase. Adding auxiliary materials to adjust the pH value several times during the production process not only increases the cost of production but also increases the content of salt in the by-products. The development of yeast primarily focuses on reducing the amount of glucoamylase used and developing heat-resistant yeast strains. For instance, Mirko *et al.* [98] obtained high-temperature resistant strains through genetic engineering in laboratory experiments.

The challenges of cellulosic-ethanol production focus on two aspects: 1) breaking through the barrier effect of lignin on cellulose hydrolysis, and 2) developing efficient and low-cost biocatalysts. Technologically, in the pretreatment stage, it is necessary to analyze inhibitory effects and mass transfer efficiency from the perspective of raw materials. Suitable microbial flora can be found and genetically modified to produce more enzymes to enhance the effect of biological pretreatment. Liu *et al.* [99] achieved simultaneous saccharification and fermentation under high solid load conditions by steam explosion pretreatment. The final ethanol yield reached 85.6% by reducing the corn stover granularity in two steps

and washing to reduce the effect of inhibitors. In the hydrolysis and fermentation stage, efficient metabolically engineered yeast strains can be genetically engineered to tolerate various inhibitors and make full use of the difficult sugars in the enzymatic hydrolysate to produce high concentrations of ethanol, so as to construct a more reasonable enzymatic fermentation process. It has been found that the use of spermidine as an inducer to change the expression level of the key gene SPE3 in the synthesis pathway can improve the tolerance of acetic acid in yeast strains. In addition, since xylose and arabinose coexist in the hydrolysate after cellulose saccharification, yeast strains capable of absorbing and converting both sugars represent a significant breakthrough in promoting second-generation ethanol production technology. Rational metabolic pathways of strains can be designed using synthetic biology, and the limitations of existing metabolic pathways can be circumvented by using heterologous or recombinant enzyme systems. This approach helps address issues such as asynchronous xylose and arabinose fermentation and low pentose conversion efficiency.

Table 2. Comparison of ethanol production routes.

Technology		Feedstock	Process	Catalyst	Feature
Coal-based syngas to ethanol	Syngas to ethanol by direct synthesis	Coal	Direct synthesis	Rh-based catalysts	Low yield and selectivity, High energy consumption, Many side reactions.
	Hydrogenation of ethyl acetate to ethanol	Coal	Indirect synthesis	Noble metal catalyst	Short process flow, Low energy consumption, High yield.
	Acetate esterification and hydrogenation to ethanol	Coal	Indirect synthesis	Cu-based catalysts	Long process
	Dimethyl ether to ethanol	Coal	Indirect synthesis	Molecular sieve catalyst or Cu-based catalyst	Mature technology, Low cost, Low energy consumption,
Biomass to ethanol	Grain ethanol (G1)	Corn, wheat, paddy	Bio-fermentation	Enzyme	Mature technology, Feedstock limitation.
	Non-grain ethanol (G1.5)	Cassava, sugarcane, sweet sorghum	Bio-fermentation	Enzyme	Feedstock limitation
	Cellulosic ethanol (G2)	Corn stover, lignocellulosic	Bio-fermentation	Enzyme	Abundant feedstock, High energy consumption, High production cost.

2.3 LCA and TEA studies

Over the past decade, life cycle assessment (LCA) and techno-economic assessment (TEA) studies have been widely performed to evaluate the production of ethanol from biomass to ethanol, but studies on ethanol from other feedstocks have been rather limited, as shown in **Table 3**. All of these studies use environmental and economic indicators to compare the performance of different ethanol pathways from various biomass feedstocks, depending on the processes applied and/or final products employed. However, research on ethanol production from non-biomass feedstocks, such as renewable tail gas to ethanol by bio-fermentation remains relatively limited, necessitating further exploration and analysis.

A few studies have utilized LCA and TEA to compare the performance of ethanol production from various biomass feedstocks [16, 48] [17] [18] [100] [40]. The primary sources of raw materials are China and the United States, and the feedstocks include corn, wheat, cassava, corncob, sweet sorghum and corn stover. These studies primarily employed databases such as Greenhouse Gases Regulated Emissions, and Energy use in Transportation (GREET), SimaPro, and BIOFIT. LCA indicators focus on comprehensive environmental impact metrics,

including global warming potential (GWP), acidification potential (AP), eutrophication potential (EP), human toxicity potential (HTP), abiotic depletion elements (ADP-e), abiotic depletion fossils (ADP-f), photochemical ozone creation potential (POCP), freshwater aquatic ecotoxicity potential (FAETP), marine aquatic ecotoxicity potential (MAETP), terrestrial ecotoxicity potential (TETP), land use, and water footprint. Based on the above indicators, relevant studies have determined and compared the pros and cons of different ethanol routes [18, 48]. For example, Yu *et al.* [16, 17] comprehensively investigated the life cycle energy consumption and environmental impact of wheat-ethanol, Corn-ethanol and cassava- ethanol, the results show that three routes are all positive in net energy values, but the Corn-ethanol route has less CO_2 emissions than the other two, which is in line with other literatures' results [18, 40, 42, 101]. Regional characteristic in ethanol production is also highlighted to investigate. For example, *Wang et al.* [100] assessed embodied GHG in US and China fuel ethanol trade and their results showed that the emissions of ethanol imported from the US are lower than Corn-ethanol and cassava-based ethanol, but higher than corn stover-based and corncob-based in China. However, in other results, the emission of Corn-ethanol in the US is higher than corn-

ethanol, but lower than corncob-based in China [42, 43, 101]. The inconsistent results indicate that the LCA results are dependent on the specific situation and scientific conclusions could be obtained by specific analysis to specific problems. Additionally, the Coal-ethanol route as a new industrialization technology in the past two years, assessment and comparison have also been actively followed up to provide support for its development. For example, Li *et al.* [48] used the SimaPro model to assess the life cycle environmental impact of coal-based routes and compared it with biomass-derived ethanol (Corn-ethanol, corn stover-ethanol). In their study, the importance of the coal-based route is emphasized, not only offering a new downstream chain in the coal industry but also diversifying the sources of fuel ethanol away from biomass. However, the coal-based route faces a substantial challenge associated with its significant environmental impact, especially with its high greenhouse gas emissions, which should be paid attention to.

In terms of TEA, the studies primarily consider economic indicators such as net present value (NPV), minimum selling price (MSP), and internal rate of return (IRR). Additionally, related studies have explored the impact of energy consumption on these metrics. These comprehensive assessments provide valuable insights into the

environmental and economic performance of ethanol production from various biomass feedstocks, aiding in the optimization of ethanol production pathways and promoting sustainable development. Vasilakou *et al.* [102] conducted a techno-economic assessment to identify the most promising pretreatment technology for a G2 ethanol production plant in the EU. This study employed Aspen Plus for process simulation and incorporated corn stover availability data from 13 EU countries, and a comparative techno-economic assessment was performed to determine the MSP. The lowest MESP was found to be 0.39 EUR/L in Hungary and 0.43 EUR/L in Romania. These lower costs are due to the cheaper biomass, lower tax rates, lower wages, and higher corn stover yields in Eastern European countries. Smith *et al.* [103] evaluated the sustainability of the US biofuel industry, providing countrywide and county-level results with high geospatial resolution. Specifically, carbon emissions from biofuels were reduced by 42 MMt CO_2eq in 2017, at an additional cost of $6.2 billion, compared to conventional diesel and gasoline.

Out of the comparison between different feedstock studies, most studies focus on LCA & TEA of single feedstocks. The primary feedstocks studied include corn, sugarcane, cellulosic, cassava and

corn stover. These feedstocks exhibit distinct regional characteristics: corn is primarily sourced from the US and China, sugarcane from Brazil and India, cellulosic biomass from the US, China, and India, and cassava from China and Thailand. Typical databases used in these studies include GREET, Ecoinvent, GaBi, SimaPro, etc. LCA studies cover a variety of environmental impact indicators, but some focus specifically on global warming potential (GWP). Overall, the carbon footprint of G1 grain ethanol ranges from 14.6 to 214 g CO_2eq/MJ ethanol. Yang *et al.* [101] and Zhang *et al.* [104] examined that the GWP of grain ethanol in China ranges from -17 to 214 g CO_2eq/MJ ethanol, which is over 31% lower than the carbon intensity of domestically produced coal-based ethanol. The GWP of US Corn-ethanol ranges from 14.6 to 65.3 g CO_2eq/MJ ethanol [42], which is 13-49% lower than that of gasoline, with corn cultivation contributing 26%, ethanol production 58%, and land use change being a minor contributor (7%) [38, 103]. Additionally, Gerrior *et al*. [105] designed a novel closed-loop Corn-ethanol biorefinery in Canada. LCA results indicated that this biorefinery could reduce the environmental burdens from 38.5 to 26.4 g CO_2eq/MJ ethanol, attributed to reduced energy consumption and environmental credits from co-products. However, TEA results show that the overall operating costs

increased by 13% due to the high material costs associated with co-product recovery.

Literature available on G1.5 non-grain ethanol indicates that the GWP of G1.5 non-grain ethanol ranges from 3.36 to 256 g CO_2eq/MJ ethanol, with significant variations in the carbon footprint of ethanol produced from different feedstocks in various countries. These differences can be attributed to the distinct inventories considered and regional variations in biomass cultivation practices. In particular, the Chinese government is promoting non-grain fuel ethanol to ensure energy security, food security and environmental improvement. Jiao *et al.*[106] and Leng *et al*. [107] studied the carbon footprint of cassava ethanol in China ranging from 54 to 63 g CO_2eq/MJ ethanol. From an environmental perspective, cassava-ethanol has better global warming potential and photochemical ozone generation potential than gasoline. Monte Carlo simulations revealed that cassava yield, nitrogen fertilizer use, and steam use are key variables affecting the energy efficiency and environmental performance of cassava ethanol. Hiloidhari *et al.* [108] examined the carbon footprint of Indian sugarcane-ethanol under different allocation methods, reporting approximately 25 g CO_2eq/MJ ethanol for mass allocation, 22 g CO_2eq/MJ ethanol for energy allocation,

and 14 g CO_2eq/MJ ethanol for economic allocation. This underscores the importance of justifying the choice of allocation method in LCA studies, as it significantly influences the results. Pablo *et al.* [109] utilized simulation programs and mathematical tools to evaluate sugarcane-ethanol production via conventional, biochemical, and thermochemical pathways in Brazil. The carbon footprints of three pathways range from 131–256 g CO_2eq/MJ ethanol, with the biochemical pathway demonstrating the highest energy efficiency and the lowest overall CO_2 emissions (131.45 g CO_2eq/MJ ethanol). Following China and India, Thailand is emerging as a significant market for fuel ethanol in Asia. Currently, ethanol production in Thailand primarily involves the fermentation and distillation of cane molasses, cassava and cane juice as considered potential feedstocks. Nguyen *et al.* [110, 111] investigated the carbon footprints of cane molasses-ethanol and cassava-ethanol are 145 g CO_2eq/MJ and 133 g CO_2eq/MJ, respectively. The results show that the use of cassava-ethanol blended fuel reduces certain environmental loads over its entire life cycle compared to conventional gasoline, specifically by 6.1% for fossil energy use and 6.0% for global warming potential.

Cellulosic ethanol is widely recognized to have significant

environmental advantages over petroleum fuels and grain ethanol, particularly in reducing GHG emissions during transportation. Most of the conservative scenarios estimate GHG emissions of around 45 – 60 g CO_2eq/MJ ethanol [112-116], with feedstock cultivation, harvesting, grinding and transportation dominating the overall carbon footprint. Colin *et al* [113] investigated the GHG intensity of corn stover-based ethanol of 50.3 g CO_2eq/MJ ethanol, and 56.1 g CO_2eq/MJ ethanol of switchgrass-based ethanol using Intergovernmental Panel on Climate Change (IPCC) 100-year GWPs. If the coproduct credits were considered, a significant reduction in life cycle GHG intensity, resulted in intensities of 21 – 31 g CO_2eq/MJ ethanol. Both corn stover and switchgrass feedstock pathways have the potential to yield life cycle GHG reductions compared to petroleum gasoline of 40 – 50%, or by more than 70% when coproducts are considered. Olofsson *et al.* [117] designed a method to integrate enzyme production into the lignocellulosic ethanol production process. LCA results indicate that the greenhouse gas emissions of lignocellulosic ethanol from the new process are reduced by 13 – 88% compared to ethanol produced using purchased enzymes.

Table 3. Comparison of LCA results for ethanol production from different studies.

Feedstock	Studies	Region	Database	Indicators	Source
Wheat, Corn, Cassava	LCA&TEA	China	BIOFIT & GREET	NPV, NCF, EROEI, LCE	[16]
Wheat, Corn, Cassava	LCA	China	GREET	LCE	[17]
Corn, Cassava, Corncob	LCA	China	SimaPro	Environmental indicators*	[118]
Corn, Sweet sorghum, Cassava	LCA&TEA	China	NS*	Environmental indicators Economic indicators Energy indicators Resource-land use, water footprint Social-employment rate.	[119]
Corn, Corn stover, Coal	LCA&TEA	China	SimaPro	Environmental indicators, NPV, NCF, DPP, IRR	[48]
Corn, Cassava, Sweet sorghum	LCA	China	NS	WTP energy consumption, NEV, NER. WTW GHG emissions, NGRV, NGRR	[18]
Corn, Cassava, Sweet sorghum, Corn stover, Corncob	LCA	US-China	GREET	WTP GHG emissions	[100]
Wheat, corn, cassava	LCA	China	BIOFIT, GREET	TECff, NEV	[40]
Corn	LCA	China	eBalance	Environmental indicators	[101]
Corn	LCA	US	GaBi	GWP	[42]
Corn	LCA	US	GREET	Carbon intensity, GHG emissions, LUC	[38]
Corn	LCA&TEA	US	Ecoinvent	GHG, MFSP, WDP, EUT, RE, ALOP	[103]
Corn	LCA&TEA	Canada	Ecoinvent	GWP, land use, fossil resource, water use, capital costs	[105]
Corn	LCA	Argentina	SimaPro, GREET	Environmental indicators	[120]
Wheat	LCA	Sweden	IPCC	GHG	[121]
Sugarcane	LCA	India	NS	Energy, carbon, water footprints, EROI	[108]
Sugarcane	LCA&TEA	Brazil	IPCC 100	GWP	[109]
Sugarcane	LCA&TEA	Brazil	LCA	GWP, NPV, IRR, MARR,	[22]
Sugarcane	Social LCA	Brazil	Social Hotspot Database (SHDB)	Total cost, Direct cost, Indirect cost	[122]
Sugarcane	LCA	Argentina	Ecoinvent	AP, GWP, EP, PHO, DAR, ODP, FWEAT, TET	[123]
Sugarcane	LCA	India & Brazil	Ecoinvent, IEA	GHG, Non-renewable energy use (NREU), water use, human health (HH), ecosystem quality (EQ)	[124]
Cane molasses	LCA	Thailand	TEI, IPCC	Energy use, GWP, AP, NP, POCP, Land use	[110]

Cassava	LCA	Thailand	GREET, IPCC, TEI, IEA	Energy use, GWP, Acidification, Nutrient enrichment, POCP, Land use	[111]
Cassava	LCA	China	GREET	GHG, water use, energy efficiency	[106]
Cassava	LCA	China	Chinese life cycle database (CLCD)	GWP, AP, POFP, RI, energy demand	[107]
Cellulosic	LCA	US	GaBi	GWP	[113]
Cellulosic	TEA	China	NS	Price	[6]
Cellulosic	LCA&TEA	Process simulation	NREL	CAPEX, OPEX, GWP,	[114]
Lignocellulosic	LCA&TEA	Indian	Ecoinvent	Capital investment, MFSP, NPV, IRR, Environmental indicators	[115]
lignocellulosic	LCA&TEA	Process simulation	EU renewable energy directive (RED)	FCI, MESP, GWP, energy balance	[117]
lignocellulosic	LCA	India	Open LCA 16.1	GWP	[116]
lignocellulosic	TEA	EU	Process model	FCI, MESP	[102]
Corn stover	LCA	US	GREET, GaBi	Environmental indicators	[125]
Cornstalk	LCA&TEA	Process simulation	CLCD	ADP, AP, COD, EP, GWP, TPI	[126]
Corncob	LCA&TEA	China	GaBi	GHG, energy intensity, capital cost	[43]
Bio-oil	LCA&TEA	China	Ecoinvent	GWP, IRR, MSP, TCI	[127]
Pinus patula	LCA&TEA	Process simulation	SimaPro, Ecoinvent	NPV, Payback period, Environmental indicators	[128]
Rice-straw	LCA&TEA	Process simulation	NS	GHG, energy consumption, cost	[37]
Sawdust	LCA	Canada	IPCC	Energy consumption, CO_2 emission, production cost	[129]
Hemp hurds	LCA	Spain	NS	GWP, photochemical oxidants formation (PO), acidification potential (AP), eutrophication potential (EP) and fossil fuel extraction (FF).	[130]
Seaweeds	LCA&TEA	US	SimaPro	Environmental indicators, energy efficiency, MSP	[131]
Redcedar	LCA	US	SimaPro	GHG emissions, Non-renewable energy use, Land occupation, water use	[132]

2.4 LCA software and databases

The emergence of LCA software and databases has facilitated the collection and exchange of LCA data. The software tools are composed of four main parts: 1) an interface for users to model product systems; 2) a life cycle unit process database; 3) an impact assessment database that supports a variety of impact assessment methods; and 4) a calculator that combines the databases based on the product system modelling in the user interface. Table 4 summarises the widely used LCA research tools at home and overseas: GaBi, SimaPro, efootprint, GREET and OpenLCA. These software are all based on the LCA analysis framework and process of ISO 14040 to establish calculation models, and each of the five LCA software has its own characteristics, which are suitable for different scenarios and needs. GaBi is more suitable for industries with high requirements for accuracy and reliability, such as the chemical industry, electronics, etc. SimaPro is suitable for large enterprises and research institutes to conduct complex LCA studies. efootprint is more suitable for the calculation of the carbon footprint requirements of various industries; GREET is more suitable for the CO_2 emissions in the phases of automotive raw material acquisition, component manufacturing, automotive assembly, disposal, and

recycling, etc.; and OpenLCA is favored by the open source community and small and medium-sized enterprises because of its openness and sharing.

When using these LCA software, users need to choose the appropriate tool according to their actual needs. It is also necessary to pay attention to the accuracy and reliability of the data to ensure the validity of the assessment results. In addition, with the continuous advancement of environmental protection technology and the introduction of new environmental policies, these LCA software are constantly being updated and improved. Users need to pay attention to the latest version and updated content of the software in order to better use these tools to reduce carbon emissions and achieve sustainable development.

Table 4. LCA software and databases

Software	Server	Database	Method	Characteristics
GaBi	PEInternational, Germany	GaBi databases, ELCD, Ecoinvent, MLC	CML, Eco-indicator, Ecological, EDIP, Impact	1. Suitable for industries with high accuracy and reliability requirements; 2. Powerful modeling and analysis capabilities; 3. Functional modularization, flexible and adjustable modelling; 4. Hierarchical combination of processes with a clear life cycle flow structure.
SimpaPro	PRé Sustainability, Netherlands	SimaPro databases, Ecoinvent, ESU-ETH	Eco-indicator, CML, EPS, EDIP, Impact	1. Suitable for large corporations and research organisations conducting complex life cycle assessments; 2. Richness of data sources; 3. Clear data hierarchy; 4. Strong visualisation; 5. Various evaluation methods.
efootprint	IKE, China	Ecoinvent, ELCD, CLCD	LCIA characterization, normalization and weighted calculation	1. The world's only online LCA/Carbon Footprint system with large-scale application; 2. The first publicly released LCA/Carbon Footprint database in China; 3. Not only LCA/Carbon Footprint accounting software, but also a supply chain management system.
GREET	Argonne National Laboratory, US	Energy databases	WTT, TTW	1. Spreadsheet-based evaluation model; 2. Primarily used for LCA calculations in energy; 3. Dataset focused on energy fuels.
OpenLCA	GreenDelta, Open source	Open-source Simulation Tool	Open LCA-Impact Assessment	1. Open source and free software for Sustainability and Life Cycle Assessments; 2. Best-in-class import and export capabilities; 3. User-friendly; user interface in a variety of languages;

2.5 Literature summary and research gaps

Nowadays, ethanol can be readily produced via biological processes or fossil energy conversion [68] but is predominantly produced from bio-fermentation using corn, sugarcane, cassava, and cellulosic as feedstock [69]. However, there are major concerns over bio-ethanol production due to the enormous amount of arable land required to grow the crops to meet the rapidly growing ethanol demand, as well as competing with people for food and the great impact on forest biodiversity [39]. Cellulosic ethanol represents the most advanced G2 bioethanol technology, which could made from low-value agricultural co-products or wastes (corn stover, wheat straw, sugarcane bagasse, wood, or grass). Great efforts have been made to develop efficient biocatalysts, simplifying processes, reducing carbon emissions, and enhancing efficiency. However, this technology is still on the industrialization road. Besides, fossil fuel-based ethanol technologies, such as ethylene hydration and coal-to-ethanol conversion, are well developed [47, 48], but their massive fossil energy consumption and high carbon emission are his Achilles heel. Given the limitation of the current two main ethanol technologies (fossil fuel-based and biomass-based routes), the

development of alternative ethanol technologies has received tremendous interest.

Recently, the bio-fermentation conversion for low-valued industrial tail gas (containing CO and H_2 gases) to ethanol (TG-ethanol) has been reported as a promising route. It is glad to see that a bio-fermentation ethanol plant with Linz-Donawitz Gas (LDG) from the steel industry as feedstock was successfully established in China [7]. This “waste-to-value” conversion technology possesses several promising advantages, such as milder conditions, simpler operation, lower cost and less energy consumption. However, a systematic and objective understanding of the environmental impact, economic benefits and market shares is still lacking, and a comparison with traditional ethanol production technologies is urgently needed to justify its future competence. This thesis aims to investigate the integrated LCA and TEA performance of this TG-ethanol technology, evaluating its environmental impact and economic benefits and compare with its competitors. Additionally, it proposes a process intensification model to further optimize its environmental and economic impacts. The relevance of the research questions and the identified research gaps are summarized in Section 1.2.

CHAPTER 3. Methodology

3.1 Introduction

This chapter presents a methodology framework for the evaluation of the life cycle assessment and techno-economic analysis of sustainable ethanol production from industrial tail gas. Life cycle assessment methodology introduces the main steps and guidance of some key sub-methods, such as system boundary definition, allocation method selection, impact categories classification, etc. Techno-economic analysis method describes the evaluation model of technical and economic indicators, which is used to evaluate the energy and resource utilisation efficiency and economic benefits of the technology, providing scientific reference for investors to make correct decisions. Monte Carlo simulation summarizes the general steps used to assess the uncertainty of the objective model and the commonly used probability distributions to represent the types of datasets. The methodology introduction in this chapter aims to comprehensively and systematically analysis the optimal technology process from the perspective of environmental, technical, and economy, and then put forward scientific suggestions for the improvement of studied processes. It should be

noted that the detailed method and data inventory will be discussed in individual chapters.

3.2 Life cycle assessment (LCA)

Life cycle assessment (LCA) refers to the compilation and evaluation of the inputs and outputs and the potential environmental impacts of a product system throughout its life cycle [133]. Principles of LCA mainly include life cycle perspective, environmental focus, relative approach and functional unit, iterative approach, transparency, and comprehensiveness [134]. LCA considers the entire life cycle of a product, from raw material extraction and acquisition, through energy and material production and manufacturing, to use and end-of-life treatment and final disposal. Through such a systematic overview and perspective, the shifting of a potential environmental burden between life cycle stages or individual processes can be identified and possibly avoided [135]. LCA addresses the environmental aspects and impacts of a product system. Economic and social aspects and impacts are typically outside the scope of the LCA. In general, LCA can assist in identifying opportunities to improve the environmental performance of products at various stages in their life cycle, and then provide advice to

decision-makers in industry, government, or non-government organizations for the purpose of strategic planning, process optimization and indicator priority selection etc [136].

LCA studies comprise four phases. These are:

- the goal and scope definition

- life cycle inventory analysis (LCI)

- life cycle impact assessment (LCIA)

- life cycle interpretation

The relationship between the phases is illustrated in **Figure 13**.

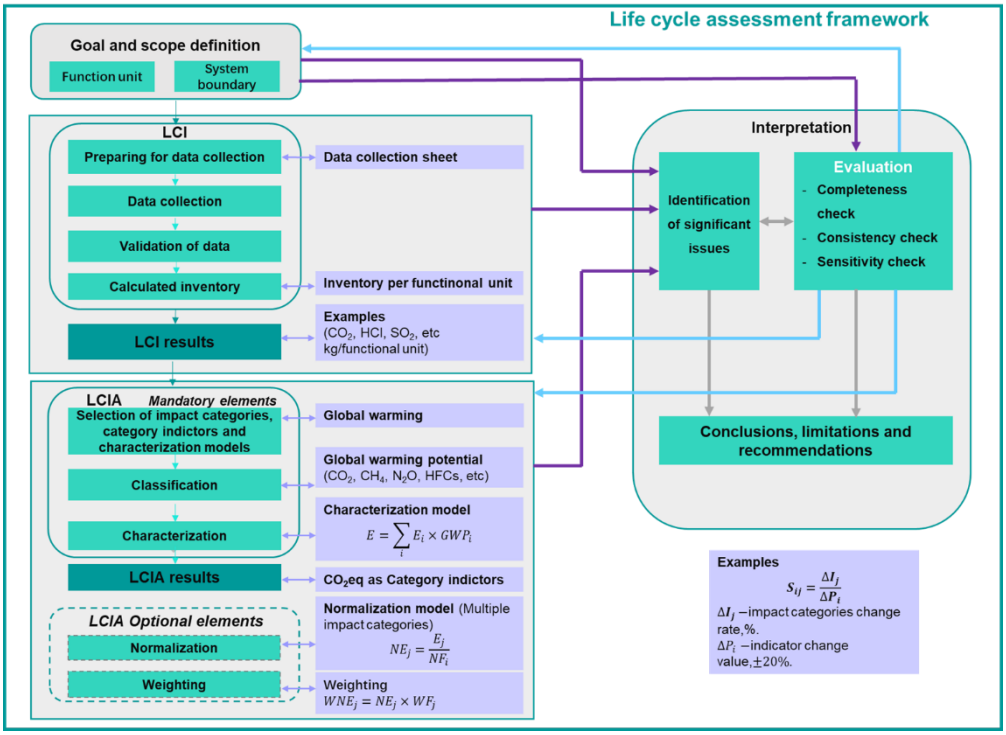

Figure 13. LCA methodology framework.

1) Goal and scope definition

The determination of the goal and scope is the first and crucial step in carrying out LCA research, and the following contents should be determined: goal, scope, functional unit, system boundary, data quality requirements and allocation method.

When formulating the aim of the study, it is important to have clear what are the impacts of the study on reality and state whether the study is to support decision-making at the micro or macro level. For example, we conducted an LCA carbon footprint study of a product to clarify the carbon footprint of the product throughout its life cycle, to determine whether it is a low-carbon product, whether the technology used is a low-carbon technology or a zero-carbon technology, and to filter out low carbon raw material routes by comparing the carbon footprint of products with different raw material routes [137]. The scope definition should describe the product system to be studied, including product type, specification, raw materials, technology, etc. The functional unit is a quantitative description of product functions, which provides a reference for the normalisation of product input and output data, and ensures that the established data list is accurate, effective, and measurable [138]. For example, the production of 1 ton of Corn-ethanol is a functional unit of an LCA study. Data quality requirements [139] should clarify the time-

related coverage, geographical coverage, technology coverage, data source, etc.

The system boundary determines which unit processes shall be included within the LCA. Generally, it is helpful to describe the system boundary using a process flowchart showing the unit processes and their inter-relationships. A “cradle-to-grave” system boundary is shown in **Figure 14 (a)**, five general life cycle stages, including the material acquisition & pre-processing, production, distribution & storage, use and end of life. Except for this complete life cycle (cradle-to-grave), “cradle-to-gate” (**Figure** 14 (b)) is a partial life cycle inventory including all emissions and removals from material acquisition through to when the intermediate product leaves the reporting company’s gate (typically immediately following its production) and excluding final product use and end-of-life [140]. For intermediate products, if the function of the corresponding final product is known, companies should complete a cradle-to-grave inventory. If the function of the final product for which the intermediate product is an input is not known, a cradle-to-gate boundary is defined. If a cradle-to-gate boundary is defined, companies shall disclose this in the inventory report.

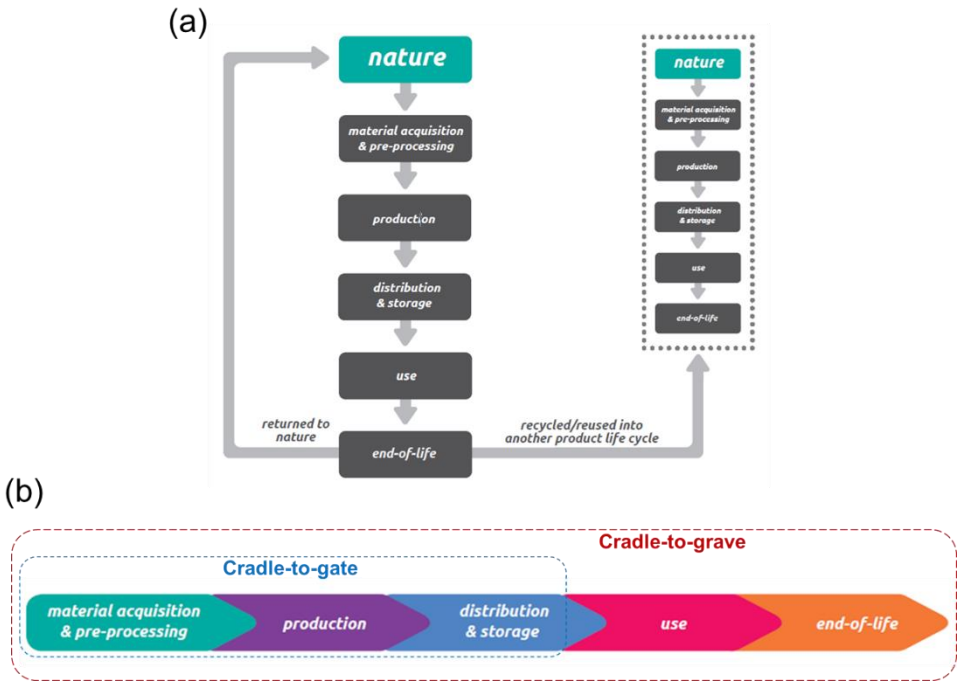

Figure 14. The system boundary of a product life cycle, (a) "cradle-to-grave", (b) the difference between "cradle-to-grave" and "cradle-to-gate" (cited from [141]).

In most product life cycles, there is at least one common process that has multiple valuable products as inputs or outputs (**Figure 15**), and it is not possible to collect data at an individual input or output level. In these cases, the total emissions or removals of a common process need to be divided between multiple inputs and outputs. This division, called allocation, is an important and sometimes challenging element of the product inventory process. Accurately allocating emissions or removals from the products under study is critical to maintaining the quality of GHG inventories. Generally, there are some allocation methods, starting with

physical allocation, which refers to allocating the inputs and emissions of the system based on an underlying physical relationship between the quantity of a product or co-product and the quantity of emissions generated, such as mass allocation or energy allocation [142]. Economic allocation is based on the market value of each when they exit the common process. According to ISO14044 [143], if allocation is unavoidable, it should first be considered based on the potential physical relationship between the studied product and co-products. When a physical relationship alone cannot be established or used as a basis for allocation, economic allocation or another allocation method that reflects other relationships between the studied systems should be considered.

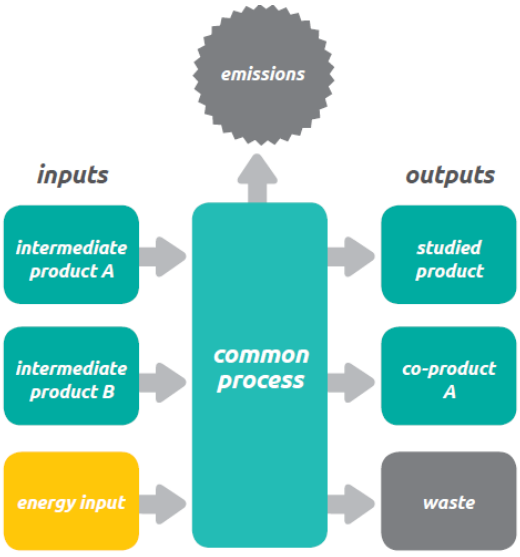

Figure 15. Common processes that require allocation (cited from [141]).

2) Life cycle inventory analysis (LCI)

LCI phase involves the compilation and quantification of inputs and outputs for a product throughout its life cycle. Inventory analysis mainly includes four steps: data collection preparation, data collection, data accounting and validation, and data aggregation and summary [144]. The input data are mainly raw materials, auxiliary materials, resources and energy consumption, and the output data are products, by-products, atmospheric emissions, wastewater, solid waste, etc. Data sources are mainly: literature data, field survey data and electronic databases.

3) Life cycle impact assessment (LCIA)

LCIA phase is aimed at understanding and evaluating the magnitude and significance of the potential environmental impacts for a product system throughout the life cycle of the product. The LCIA process is divided into four stages: classification of impact categories, characterisation (quantification of environmental impact categories), normalisation (unified unit), and weighting (assigning weights) [135]. Among them, classification and characterisation are mandatory elements of LCIA, while normalisation and weighting are optional elements.

The classification of impact categories is to assign the LCI inventory into different environmental impact categories. The midpoint impact

types such as Global Warming Potential (GWP), Acidification Potential (AP), Abiotic Resource Depletion Potential (ADP), Eutrophication Potential (EP), Ozone Layer Depletion Potential (ODP), Photochemical Ozone Creation Potential (POCP), etc. The end-point impact types are generally summarized into three categories: Human Health, Ecosystem, and Resource consumption [145].

Characterisation is the quantification process of different types of environmental impacts. Under each environmental impact type, the consumption and emissions of different substances have different magnitudes of environmental impact. So, characterisation involves the conversion of LCI results to common units and the aggregation of the converted results within the same impact category [134].

Normalisation is the conversion of all environmental impact categories into a unified unit using a baseline value, realising a comparison of the impact size of different environmental impact types in a product system.

Weighting is the process of converting normalised indicator results of different impact categories by using weighting factors. Since weighting steps are based on value choices rather than scientifically based, different individuals or organizations may have different preferences,

resulting in different weighting results [146]. Therefore, it is necessary to do a sensitivity analysis of the weighted results.

4) Life cycle interpretation

Life cycle interpretation is the phase of LCA in which the findings of either the inventory analysis or the impact assessment are evaluated with the defined goal and scope to reach conclusions and recommendations. It mainly includes the following elements: identification of significant issues by synthesising the results of inventory analysis and impact assessment, evaluation (completeness, sensitivity, and consistency check), drawing conclusions, identifying limitations, and making recommendations [136]. The main outputs of the interpretation phase are: identifying the key points that cause environmental impacts in the product life cycle, formulating improvement measures; analysing the internal and external material and energy exchanges of the product as a quantitative basis for product environmental performance analysis; identifying the contribution of each life cycle stage of the total environmental impact load, optimize the environmental performance of products and processes; determine key performance indicators through quantitative analysis types, and provide decision support for producers to optimize life cycle management [147].

3.3 Techno-economic analysis (TEA)

Techno-Economic Analysis (TEA) is a method to evaluate the technical and economic performance of an industrial process, product or system [148]. TEA combine engineering and process operation factors via a suitable model to examine the economics of the process and determine the viability of the process. To conduct an accurate and comprehensive TEA, a significant understanding of the process assessed is required: to allow for the development of an accurate mass and energy balance for the process in terms of the overall process and on a per-unit level [149], and the diagram is shown in **Figure 16**. When applying technical and economic analysis, a more complete system of indicators is generally used, including qualitative and quantitative indicators. Qualitative indicators are those that cannot be expressed in numerical or monetary terms, while quantitative indicators are those that can be calculated and expressed in numerical or monetary terms [150].

The primary elements of the techno-economic analysis in this study can be divided into two categories: technical and economic. On the technical side, it mainly includes the analysis of technical maturity, process flow analysis, energy efficiency, raw materials consumption and utility demand. The economic side mainly includes investment and cost

estimation, with typical indicators such as internal rate of return (IRR), net present value (NPV), minimum selling price (MSP), etc [151]. In practice, the technical index such as yield, energy efficiency and carbon efficiency can be obtained based on the mass and energy balance of the operating process or simulated process. Then, these technical parameters will be used as inputs for the economic analysis to build cost-income models, including capital costs model, operating costs model and revenue model to estimate the economic index.

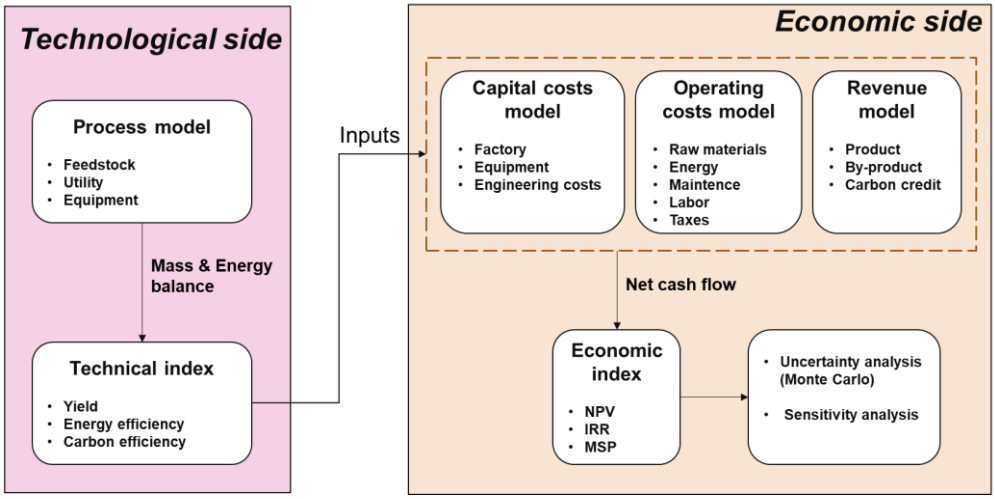

Figure 16. The illustration of the TEA method.

Energy efficiency (EE) is the energy of the product (PE) divided by the total energy demand (TED), as shown in **equation (24)**. The product energy is the sum of the energy of the main and by-products, while the total energy consumption includes the energy input of raw materials, and

the energy demand of fossil fuels and utilities (water, electricity and steam). The calculated energy efficiency is the energy input-output ratio per unit of product, and the energy demand is converted to a uniform unit MJ/kg in this study.

$$EE = \frac{PE}{TED} = \frac{\sum PE_a + PE_b + \cdots PE_i}{\sum ED_{fossil} + ED_{utility,a} + \cdots ED_{utility,i}} \quad (24)$$

Where the PE_a to PE_i refers to the product ath to ith, $ED_{utility,a}$ to $ED_{utility,i}$ refers to the utility ath to ith.

Carbon efficiency (CE) is the carbon mass of the product (CP) divided by the carbon mass of the feedstocks (CF), as shown in **equation (25)**. The numerator is the sum of the carbon mass of the main and by-products, and the denominator is the sum of the carbon mass of the feedstocks.

$$CE = \frac{CP}{CF} \quad (25)$$

Economic performance evaluation mainly includes investment expense, cost expense and product income. The total investment of a construction project mainly refers to the funds required to provide production equipment and facilities, including factory construction, equipment, pipelines, instruments, taxes and other expenses [152]. The cost mainly includes fixed operating costs and variable operating costs. Fixed operating costs refer to operating and maintenance costs,

depreciation costs, administrative costs, labour costs, distribution and selling costs, etc. Variable operating costs mainly include feedstock costs and utility costs [153]. The cost of feedstocks and utilities is taken from the market average in 2022, with the RMB and USD exchange rate of 7. Depreciation expenses are depreciated in line with 20 years, with a residual value of 5%, and the sum of various tax rates is 13% [154]. Product revenue refers to the total revenue of main products and by-products, obtained by the annual product yield and market prices. The economic assessment is evaluated according to the assumptions in **Table 5**.

Table5. Assumptions for the economic analysis.

Types	Items		Remarks
Investment	1	Factory construction	Enterprise and simulation data
	2	Equipment	Enterprise and simulation data
	3	Taxes	13%
Capital costs	4	1+2+3	
Fixed operating costs	5	Depreciation expenses	Straight-line depreciation, 20 years lifetime, residual value of 5%
	6	Operating and maintenance costs	Items 4*2%
	7	Administrative costs	Items 12*2%
	8	Labour costs	Items 12*4%
	9	Distribution and selling costs	Items 4*2%
Variable operating costs	10	Feedstock costs	Market price and simulation data
	11	Utility costs	Market price and simulation data
Total production costs (TPC)	12	4+5+6+7+8+9+10	
Revenue	13	Products	Market price
	14	By-products	Market price

3.4 Monte Carlo simulation

Monte Carlo simulation is a type of computational algorithm that uses repeated random sampling to obtain the likelihood of a range of outcomes occurring [155]. Monte Carlo Simulation can assess the impact of risk in many real-life scenarios, such as artificial intelligence, stock prices, price projection, project management, and pricing. Monte Carlo also provides a number of advantages over predictive models with fixed inputs, such as the ability to perform sensitivity analysis or calculate the correlation of inputs [156]. Sensitivity analysis allows decision-makers to understand the impact of individual inputs on a given outcome, while correlation analysis allows them to understand the relationships between any input variables.

Monte Carlo simulation is a numerical simulation method based on probabilistic statistics or random numbers, which establishes a probabilistic model of the research object, generates various probabilistic distributions of random variables, and estimates the numerical characteristics of the model using statistical methods, so as to obtain an approximate solution to the actual problem. In this paper, Monte Carlo simulation method is applied to estimate the possible range of values of life cycle carbon footprint, NPV and MSP, with a view to

providing researchers and stakeholders with more scientific and reliable results for reference. The following are the advantages and disadvantages of the Monte Carlo simulation method:

Advantages

1. High accuracy: Monte Carlo simulation approximates the real situation through a large number of repeated tests, and the numerical results obtained are relatively accurate, especially when dealing with complex systems or high-dimensional problems.

2. Wide range of applications: Monte Carlo simulation can simulate a variety of probability distributions and random processes, which is applicable to various types of problems, such as physics, chemistry, economics, finance, etc.

3. Strong interpretability: the results of Monte Carlo simulation are usually based on observable and understandable data and processes, so the results have good interpretability.

4. High flexibility: Monte Carlo simulation can be freely set according to the actual demand for model parameters, stochastic processes, etc., which is convenient for adjusting simulation conditions and result analysis.

5. Parallel calculation: Monte Carlo simulation can accelerate the calculation process and improve the calculation efficiency through parallel calculation.

Disadvantages

1. Large computational volume: Monte Carlo simulation requires a large number of repeated experiments to obtain accurate results, which is large in calculation amount and may lead to long calculation time for large-scale problems.

2. Sensitive to randomness: the results of Monte Carlo simulation are affected by the quality of random number generation, if the quality of random numbers is not high, it may lead to a large error in the results.

3. Need a suitable model: Monte Carlo simulation requires the establishment of a suitable mathematical model, which is more difficult to model complex problems, and model errors may affect the final results.

4. Sensitive to parameters: Monte Carlo simulation is sensitive to the selection of model parameters. Different parameters may lead to completely different results, so the parameters need to be adjusted carefully.

5. High computer performance requirements: Monte Carlo simulation requires a large amount of computing resources, including

high-performance computers, parallel computing software, etc., which may be difficult to implement in environments with limited resources. Monte Carlo simulation is based on the assumption that all the model parameters with uncertainties and input/output variables are random variables, and the procedures of this method are shown in **Figure 17**.

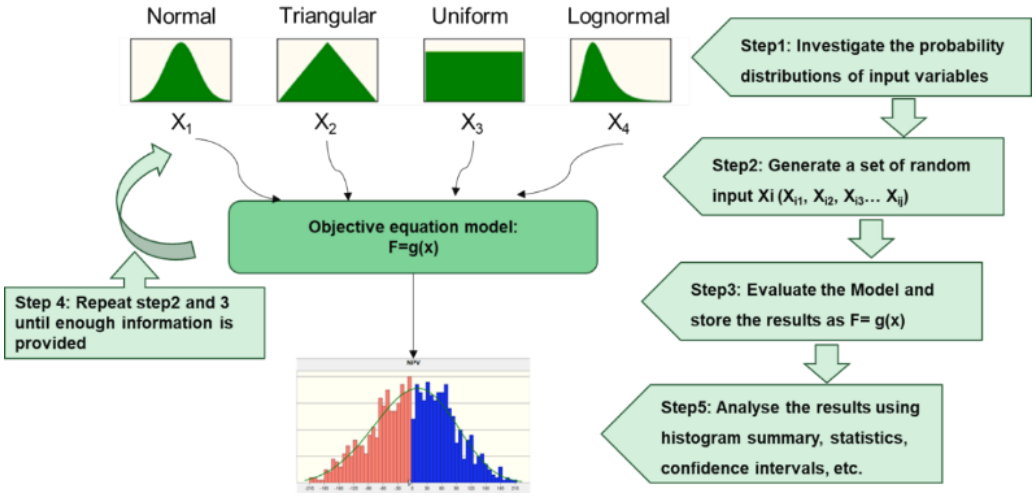

Figure 17. Procedures of Monte Carlo simulation.

(1) Describe and construct the probability process. i.e., to investigate and select the probability distribution of the input variables, commonly used probability distributions are normal distribution, triangular distribution, uniform distribution and lognormal distribution. The probability distribution of the input parameter represents a reasonable operating definition of the uncertain parameter [157]. Most of the probability distributions used in our research are constructed based on

statistical analysis of data collected by surveying the corresponding production process and market cost of the input parameters [158]. Normal distribution (Gaussian distribution) is a commonly used probability distribution in statistical areas to describe the continuous random variables, which was widely used to represent the dataset of product market price, human height, weight, salary, etc. A triangular distribution is based on knowledge of the minimum and maximum and an inspired guess as to what the modal value might be [159]. When there is very limited sample data of an uncertain parameter, the triangular distribution is used. These two distributions are very useful distribution for modelling processes where the relationship between variables is known but data is scarce and will be widely used in this study.

(2) For computer-generated random variables with known probability distributions, setting the number of iterations can lead to the corresponding sample size, and the generated variable dataset serves as the input to the objective function model.

(3) Generate simulation results based on the objective function model, and the model results are preliminarily evaluated whether the solution to the required problem is obtained. Also, some verification work can be carried out at this stage.

(4) Repeat steps 2 and 3 until enough information is provided, repeat the model-solving process, and summarize and verify the model results.

(5) Use statistical, summary and other methods to sort out the results, and use histograms, typical curves such as probability density function (PDF), and cumulative distribution function (CDF) to represent the results [160].

CHAPTER 4. Life cycle assessment of LDG-ethanol pathways

Part of this Chapter's work has been published in "Lingyun Zhang, Qun Shen, Cheng Heng Pang, Kien-Woh Kow, Edward Lester, Tao Wu, Nannan Sun, Wei Wei, et al, Life cycle assessment of bio-fermentation ethanol production and its influence in China's steeling industry. *J. Clean. Prod.,* 2023 (397), 136492."

4.1 Overview

In recent years, a bio-fermentation ethanol plant with Linz-Donawitz Gas (LDG) from the steeling industry as feedstock was successfully established in China [104]. It is glad to see that bio-fermentation conversion for low-valued industrial tail gas (containing CO and H_2 gases) to ethanol is reported as a promising route. This "waste-to-value" conversion technology possesses several promising advantages, such as milder conditions, simpler operation, lower cost and less energy consumption. However, a systematic and objective understanding of the environmental impact benefits is still lacking. In this chapter, the environmental footprint of the bio-fermentation ethanol from Linz-Donawitz Gas (LDG-ethanol) technology is systematically evaluated and

compared with traditional ethanol production routes under different scenarios (**Figure 18**). A life cycle assessment (LCA) framework is employed with the combination of the entropy weight (EW) method to aggregate the individual indicators to a comprehensive environmental impact (EI) to facilitate trade-offs and decisions. The assessment results show that the LDG-ethanol route is the most environmentally benign option, whose environmental impact value is 22 – 25% lower than that of the Corn-ethanol and Coal-ethanol routes. More importantly, electricity is the key determining factor, the environmental footprint of LDG-ethanol can be further decreased by 15 – 68% by lowering electricity consumption and introducing green power. As grid decarbonization gradually, such interesting characteristics endowed LDG-ethanol with enormous potential to achieve the decarbonization goal.

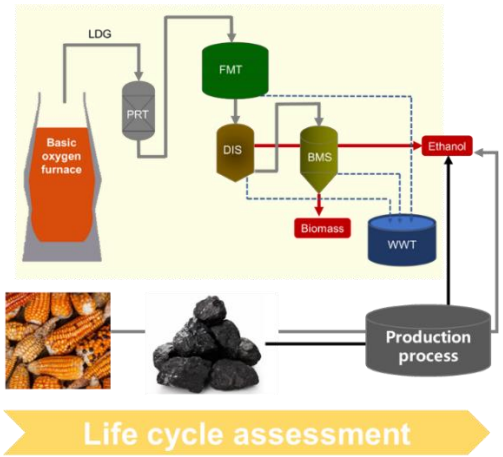

Figure 18. Graphical abstract of this chapter.

LDG-ethanol technology is an integrated technology for industrial tail gas bioconversion, which uses industrial tail gas as raw material and establishes the research model of “strain selection - bio-intelligence - pilot scale-up - industrial application” to realise the industrial system reshaping of industrial tail gas bio-conversion integrated technology. This technology realizes the high-value and low-carbon utilization of industrial tail gas for the first time and uses industrial tail gas as raw material to produce ethanol and microbial protein, opening up a new way of high-value utilization of industrial tail gas. It is a useful exploration to ensure the supply of fuel ethanol, which is conducive to promoting the development of the industrial gas circular economy, promoting regional economic development and industrial structure adjustment, and realizing the sustainability of raw materials, sustainable operations and sustainable supply.

Currently, LDG-ethanol technology has now been industrially applied in the steel and iron alloy fields. In May 2018, the world’s first steel industry tail gas fermentation method ethanol industrialization project (Hebei Shoulang) was completed in Shougang Jingtang Institute in Caofeidian, Hebei Province, with an annual production capacity of 45,000 tons of fuel ethanol and 5,000 tons of protein powder, and has

achieved continuous stable and long-term operation. In May 2021, the world's first set of iron alloy industrial tail gas fermentation ethanol industrial projects was completed in Shizuishan, Ningxia (Ningxia Shurang Jiyuan), with an annual output of 45,000 tons of fuel ethanol and 5,000 tons of protein powder, which has been put into operation and used for nearly 1 year. In September 2022, Ningxia Binze completed an industrial project of fermentation of ferroalloy tail gas, with an annual output of 60,000 tons of fuel ethanol and 6,600 tons of protein powder. In 2023, Guizhou Jinze is building an integrated project of industrial tail gas bioconversion with an annual output of 60,000 tons of fuel ethanol and 6,600 tonnes of protein powder.

4.2 Process description

4.2.1 LDG-ethanol production process

The LDG-ethanol technology route is illustrated in **Figure 19**. The LDG gas piped from the steeling industry is firstly pre-treated to remove the dust, oil, naphthalene and sulphur compounds, which harm the biological fermentation process. After pressurized, the purified LDG is fed into the fermentation unit. CO composition gas is biologically transformed into ethanol, which is generally followed by **equation (26)**.

In this process, proprietary microbes consume waste gases to make alcohol, much like yeast consuming sugars to make beer in a brewery. Therefore, an extra expenditure of chemicals and energy is needed to keep stable pH and temperature conditions. Then, the fermentation liquid is roughly separated into the crude ethanol solution and protein biomass. After deep distillation dehydration, the ethanol product is obtained from the solution, with a small amount of butanol co-produced. For the crude protein biomass, after high-temperature drying, a high-value protein product is obtained. Due to the great amount of wastewater from distillation and drying, additional wastewater treatment is needed and the obtained fresh water is recycled into the fermentation and cooling system. The wastewater is treated with anaerobic treatment to remove most of the chemical oxygen demand, and the remaining organic pollutants are converted to biogas as a by-product, which is stored in a natural gas tank. As shown in Figure 19, the red boxes indicate the main by-products produced by the process. In addition, the tail gas from the fermentation unit (containing a small amount of CO) is completely combusted to produce steam and recycled for use.

$$6CO+3H_2O \xrightarrow{\text{Microbes}} C_2H_5OH+4CO_2 \quad (26)$$

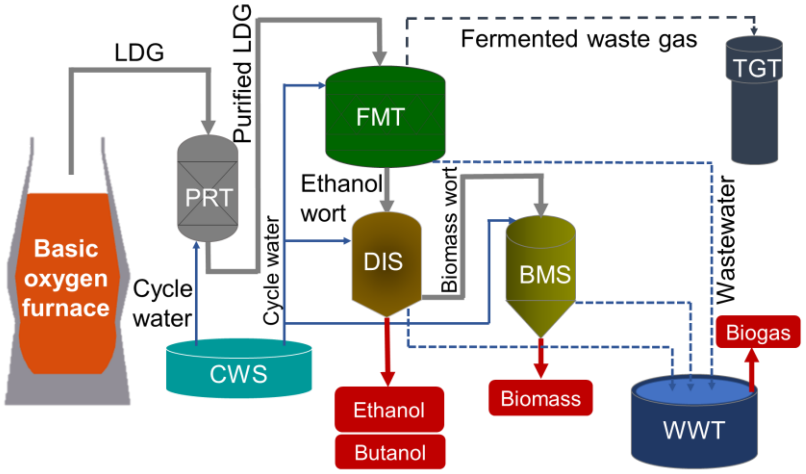

Figure 19. Process flow diagram of LDG-ethanol by bio-fermentation from steel industry tail-gas. Note: PRT (Pre-treatment unit), FMT (Fermentation unit), DIS (Distillation dehydration unit), WWT (Wastewater treatment unit), TGT (Tail-gas treatment), CWS (Cycle water system), BMS (Biomass unit).

4.2.2 Coal-ethanol and Corn-ethanol production process

In comparison, ethanol from biomass- and coal- routes are also investigated in this work. According to the technological situation in China, these two routes are roughly described.

For the Coal-ethanol route (**Figure 20(a)**), a two-stage process was employed. After mining and washing, the hard coal was gasified into crude syngas (a mixture gas of CO and H_2). In order to obtain appropriate H/C ratios (~2.1–2.2), part crude syngas reacts with steam

via a water-gas shift reaction to generate a crude shift gas. After purification, part clean shift syngas was converted into methanol. The remaining crude syngas were purified and separated into carbon monoxide and hydrogen-rich gas. The obtained methanol, hydrogen, and carbon monoxide further reacted together to generate fuel ethanol, ethyl acetate, and other heavy components.

For the Corn-ethanol route (**Figure 20(b)**), the corn is firstly processed and the left corn starch is converted to slurry. After enzymatic liquefaction and saccharification, the starch slurry is converted to mash. Then the mash is continuously fermented for 55–60 h. The mash in the fermentation gas is recovered by scrubbing and transferred to the distillation process. Ethanol vapour is dehydrated via molecular sieve adsorption to generate ethanol product. Distillers' waste is used to produce distillers dried grains with soluble via centrifugation, evaporation, and drying.

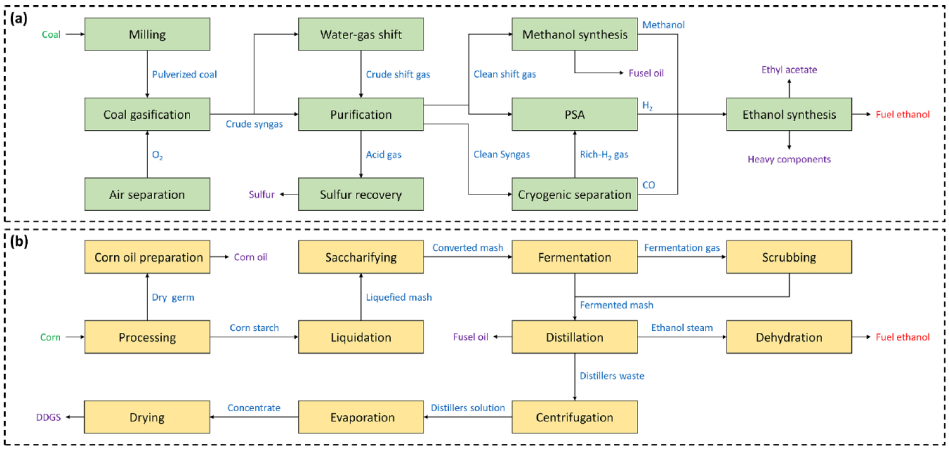

Figure 20. Process flow diagram of Coal-ethanol and Corn-ethanol (cited from [48]).

4.3 Methodology

4.3.1 Goal and scope definition

System boundaries and functional unit

This study conducted a comprehensive environmental impact by life cycle assessment (LCA) on the LDG-ethanol technology to fill the gap of environmental impact awareness and reveal the pros and cons of its competitors. The “cradle-to-gate” system boundaries (**Figure 21**) are proposed, covering the raw materials exploitation, intermediate upstream and ethanol production process. To fairly compare different ethanol production routes, the functional unit of the investigated system

was defined as 1 ton of ethanol produced by the selected technical routes.

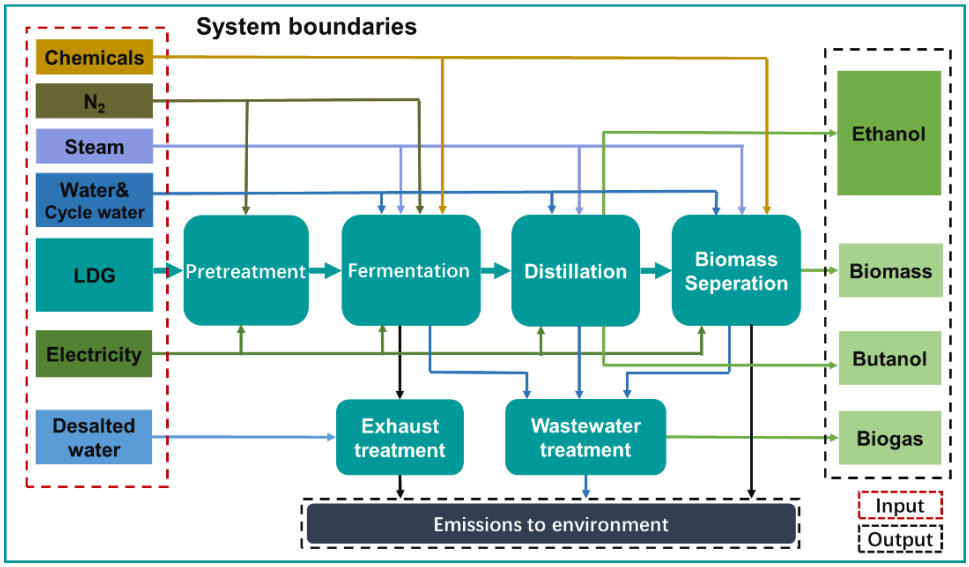

Figure 21. System boundaries of LDG-ethanol technology.

Cut-off criteria

To eliminate the uncertainty caused by unknown or complicated factors, the major limitations and assumptions in our analysis are emphasized here. According to the cut-off criteria of ISO 14044, any life cycle stages, processes, inputs or outputs that do not significantly affect the overall conclusions can be neglected from the analysis. For the LDG impact during the steel process, it is supposed that 1 ton of steeling is produced with 81.7 Nm^3 LDG by-product [161]. The prices of steel and LDG are 4000 Yuan/t and 0.235 Yuan/Nm^3 [162, 163]. The economic allocation

factor refers to the economic proportion of LDG gas in steel production. The products in the steel production process mainly include the main products steel and LDG gas, and the by-products slag, sludge and dust. The economic allocation factor of LDG gas here refers to the proportion of the economic value of LDG gas in the cumulative value of the economic value of all main and by-products. In this study, the economic allocation factor of LDG in the steel-making process is low to ~0.5%. Thus, the LDG impact from upstream could be neglected by the cut-off principle. The impact of any materials or energy during transportation is also neglected according to previous studies [163, 164]. In addition, the impact during equipment manufacturing, factory construction and facility replacement is not included [165].

Allocation procedure

In the LDG-ethanol production process, multiple products make the environmental impact inevitable to allocate. Generally, the allocation procedure is performed according to the physical or economic relationships of different products [125, 166]. In this work, mass allocation is chosen here. In the LDG-ethanol route, except BMS, the material and energy consumption in PRT, FMT, DIS, WWT, TGT, and CWS units is all allocated by the mass of ethanol, butanol and protein

biomass (here the protein biomass is quantified by dry weight). The allocation factor for ethanol is 0.8, as shown in **Table 6**.

Table 6. Allocation factor of multiple products.

Product	Ethanol	Butanol	Biomass	Biogas
Allocation factor	0.8	0.02	0.1	0.08

4.3.2 Life cycle inventories (LCI)

4.3.2.1 LDG-ethanol production process inventory

The data inventory of the LDG-ethanol process, including the inputs and outputs of the entire technical chain, is listed in **Table 7**. These data are collected from the average values during the practical operation of Beijing Shougang LangzaTech New Energy & Technology Co., Ltd. in 2020, with an annual capacity of 0.04 Mt ethanol.

4.3.2.2 Coal-ethanol and Corn-ethanol production process inventories

As listed in **Table 8**, the inventory data of the Corn-ethanol and Coal-ethanol routes are extracted from the literature [48], based on the average operating data of typical plants in China in 2020, with an annual capacity of 0.6 Mt and 0.1 Mt, respectively.

Table 7. Data inventory for the LDG-ethanol process.

Process units	Inputs	Quantity	Unit	Outputs	Quantity	Unit
PRT	LDG	7110	Nm^3	LDG	7110	Nm^3
	Nitrogen	71	Nm^3			
	Power	763	kWh			
FMT	LDG	7110	Nm^3	Penetrants	14500	kg
	Phosphoric acid	6	kg	Microbial mash	5440	kg
	Sodium hydroxide	5	kg	Wastewater	107	kg
	Ammonia	154	kg	Tail-gas	6040	Nm^3
	Sodium hydrosulphide	9	kg			
	Potassium hydroxide	12	kg			
	Water	6000	kg			
	Power	562	kWh			
DIS	Penetrants	14500	kg	Ethanol	1	t
	Microbial mash	5440	kg	Butanol	22	kg
	Water	11	kg	Microbial distillate	5170	kg
	Power	66	kWh	Wastewater	3910	kg
BMS	Microbial distillate	5170	kg	Biomass	129	kg
	Sodium hydroxide	26	kg	Wastewater	4130	kg
	Power	186	kWh	Exhaust	28400	Nm^3
	Compressed air	190	Nm^3	Cleaning wastewater	2610	kg
	Water	2610	kg			
WWT	Wastewater	10800	kg	Biogas	72	Nm^3
	Polymerized ferrous sulphate	22	kg	Wastewater	2390	kg
	Power	117	kWh	Waste residue	74	kg
TGT	Fermentation tail-gas	6040	Nm^3	CO_2	3580	Nm^3
	Desalinated water	120	kg	Nitrogen	5370	Nm^3
	Air	3670	Nm^3	O_2	471	Nm^3
	Power	81	kWh	Steam	11800	MJ
CWS	Process water	3560	kg			
	Power	182	kWh			

Table 8. Data inventory for Corn-ethanol and Coal-ethanol.

Corn-ethanol			Coal-ethanol		
Input	Quantity	Unit	**Input**	Quantity	Unit
Corn	3.33E+03	kg	Coal (feedstock)	1.89E+03	kg
Water	1.11E+04	kg	Water	7.60E+03	kg
Amylase	1.82E+01	kg	Catalyst	7.35E-01	kg
Limestone	1.01E+01	kg	Limestone	8.25E+01	kg
Liquid ammonia	2.63	kg	Liquid ammonia	6.55	kg
Sodium Hydroxide	4.98	kg	Sodium Hydroxide	5.24E-01	kg
Sulfuric acid	1.20E+01	kg	Coal (energy)	8.87E+02	kg
Urea	2.23	kg	Electricity	6.51E+02	kWh
Yeast	7.50E-01	kg	**Output**		
Coal	8.00E+02	kg	Ethanol	1	t
Electricity	2.37E+02	kWh	Ammonium sulphate	3.84E+01	kg
Output			Ethyl acetate	1.58E+01	kg
Ethanol	1	t	Butanol	1.24E+01	kg
Corn oil	5.63E+01	kg	Heavy components	3.09	kg
DDGS	9.00E+02	kg	Sodium chloride	2.33	kg
Fusel oil	3.13	kg	Sodium sulphate	4.65	kg
Emission to air		kg	Sulphur	8.69	kg
Ammonia	1.63E-03	kg	**Emission to air**		
Arsenic	1.68E-04	kg	Ammonia	8.17E-02	kg
Carbon dioxide	2.43E+03	kg	Arsenic	1.87E-04	kg
Chromium	3.98E-06	kg	Carbon dioxide	5.36E+03	kg
Lead	1.75E-06	kg	Chromium	5.61E-06	kg
Mercury	2.67E-05	kg	Lead	2.47E-06	kg
Methane	4.50E-02	kg	Mercury	1.45E-06	kg
Nitrogen oxide	2.60E-01	kg	Methane	1.57E-02	kg
Dinitrogen monoxide	9.70E-01	kg	Nitrogen oxide	4.70E-01	kg
Particulates	8.23E-02	kg	Dinitrogen monoxide	3.15E-02	kg
sulphur dioxide	1.98E-01	kg	Particulates	1.00E-01	kg
Volatile organic compounds	3.98E-01	kg	Sulphur dioxide	2.71E-01	kg
Zinc	5.88E-06	kg	Volatile organic compounds	1.44	kg
Emission to water			Zinc	8.30E-06	kg
Ammonia	4.27E-02	kg	**Emission to water**		
Total nitrogen	8.00E-02	kg	General solid waste	4.53E+02	kg
Total phosphorous	2.67E-03	kg	Hazardous solid waste	1.80	kg
General solid waste	1.98E+02	kg			

4.3.2.3 Dataset source in GaBi

To realise the LCIA analysis, several tools, such as GREET model, GaBi, SimaPro, and OpenLCA are developed and well applied in LCA research work [15, 36, 38, 42]. GaBi software, with a powerful database and diversified evaluation indicators, is popularly used [10-12, 15, 18, 42, 43, 113, 167]. In this work, the GaBi software (version 10.0) was applied to model the ethanol production routes. The gate-to-gate foreground data were collected via the on-site plant (Shougang Lanze took the lead in December 2016 to build the world's first 45,000 tonnes/year industrialised plant for bio-fermentation of steel industry tail gas to fuel ethanol in the yard of Shougang Jingtang United Steel Co., Ltd. in Caofeidian Industrial Zone of Hebei Province, which was approved by the Development and Reform Commission of Hebei Province for energy and was put into production in May 2018. The project is designed to produce 45,000 tonnes of fuel ethanol and 5,000 tonnes of protein feed annually. The fuel ethanol products meet the requirements of the National Standard for Denatured Fuel Ethanol (GB 18350-2013)) and literature support; the cradle-to-gate background data for the related upstream processes were directly derived from GaBi or the ecoinvent database, which was also built into the GaBi software. The referenced

dataset information in GaBi is described in **Table 9**. For the materials and energy flow, the background datasets in the database were selected in the following order: (1) China's localized data, (2) global average values, European Union (EU) and US average values, and (3) if part of individual chemicals were not available in the GaBi database, data reported in the literature [168] were used for modelling.

Table 9. Description of dataset source in GaBi.

Item	Data source	Technical description
LDG-ethanol		
Electricity	China electricity council 2020 average [169]	Electricity grid mix
Nitrogen	GaBi database (CN)	Cryogenic air separation
Phosphoric acid (75% solution)	GaBi database (US)	Phosphate wet process phosphoric acid
Sodium hydroxide (32% solution)	GaBi database (EU-28), concentration corrected	Technology mix
Ammonia water (25% solution)	GaBi database（US）	Ammonium mixed with water
Sodium hydrosulfide (35% solution)	GaBi modelling is based on the absorption of hydrogen sulphide by sodium hydroxide [170]	Sodium hydroxide absorption method
Potassium hydroxide (48% solution)	GaBi database (US)	Electrolysis of sodium hydroxide and potassium chloride
Process water	GaBi database（CN）	Surface water purification
Compressed air	GaBi database（EU-28）	Air compression
Polymerized ferrous sulphate	GaBi modelling is based on the catalytic oxidation of ferrous sulphate with sulphuric acid [171]	Catalytic oxidation
Desalinated water	GaBi database (CN)	Ion exchange method
Corn-ethanol		
Corn	GaBi modelling [172]	Cropping corn
Process water	GaBi database (CN)	Surface water purification
Amylase	GaBi database (RER)	Alpha-amylase
Limestone	GaBi database (US)	Limestone mining and grinding
Liquid ammonia	GaBi database (CN)	Haber-bosch process
Sodium hydroxide	GaBi database (EU-28)	Technology mix
Sulfuric acid	GaBi database (RNA)	Evaporating oleum
Urea	GaBi database (US)	Technology mix
Yeast	GaBi database (EU-28)	Sugarcane fermentation and distillation
Coal	GaBi database (CN)	Hard coal mix
Electricity	China electricity council 2020 average	Electricity grid mix
Coal-ethanol		
Coal (feedstock & energy)	GaBi database (CN)	Hard coal mix
Process water	GaBi database (CN)	Surface water purification
Limestone	GaBi database (US)	Limestone mining and grinding
Liquid ammonia	GaBi database (CN)	Haber-Bosch process
Sodium hydroxide	GaBi database (EU-28)	Technology mix
Electricity	China electricity council 2020 average	Electricity grid mix

Note: CN (China), EU-28 (EU 28), RER (Europe), RNA (North America).

4.3.3 Life cycle impact assessment (LCIA)

4.3.3.1 CML midpoint analysis method

CML (Corner Middle Layer) 2016 developed by the environmental research centre of Leiden University, is the mainstream midpoint analysis method based on traditional life cycle inventory analysis features and a standardised approach for classifying and describing environmental impacts [173]. At present, it is the most accepted and widely used analysis method due to its comprehensive evaluation indicators and the continuous updating of characterisation and standardisation factors. In this study, eleven indicators were selected: Global Warming Potential (GWP), Acidification Potential (AP), Eutrophication Potential (EP), Human Toxicity Potential (HTP), Abiotic Depletion elements (ADP-e), Abiotic Depletion fossil (ADP-f), Photochemical Ozone Creation Potential (POCP), Freshwater Aquatic Ecotoxicity Potential (FAETP), Marine Aquatic Ecotoxicity Potential (MAETP), Terrestrial Ecotoxicity Potential (TETP), are used to quantify environmental performance (**Table 10**) based on CML 2016 method. and the feature of these indicators is explained in **Table 10**.

The eleven environmental indicators of ethanol routes are calculated by **equation (27)**:

$$LEP_{ij} = \sum_k S_{kj} \times EF_{kj} \times AF_i \quad (27)$$

where LEP_{ij} is the j-th life cycle environmental performance indicator of the i-th ethanol route; S_k is the amount of the k-th emission substances; EF_{kj} is the equivalent factor of the k-th emission substances relative to the j-th environmental indicator; AF_i is the allocation factor of the i-th ethanol route.

Table 10. Environmental impact categories in CML.

Environmental impact categories	Unit	Introduction
GWP (Global Warming potential)	kg CO_2 eq.	Greenhouse gas (GHG) impacts global climate, including CO_2, CH_4, N_2O, SF_6, HFCs, PFCs, etc.
AP (Acidification Potential)	kg SO_2 eq.	The emission of acid gases such as SO_2, NO_x, and other pollutants causes acid rain.
EP (Eutrophication Potential)	kg Phosphate eq.	The potential for water pollution is caused by total nitrogen, phosphorus, and other substances in water.
HTP (Human Toxicity Potential)	kg DCB eq.	Toxic substances potentially attack humans in the environment (dioxins, polycyclic aromatic hydrocarbons, heavy metals, etc.)
ADP-e (Abiotic Depletion elements)	kg Sb eq.	Uranium also has other applications besides “energy carrier” the extraction of uranium is classified under the impact category of “abiotic resource depletion-elements” and not together with fossil fuels [174].
ADP-f (Abiotic Depletion fossil)	MJ	The resources in the impact category of fossil fuels are fuels like oil, natural gas, and coal, all energy carriers.
POCP (Photochemical Ozone Creation Potential)	kg Ethene eq.	The ratio of photochemical smog concentrations from primary pollutants such as HC and NO_X to those from ethylene.
ODP (Ozone layer Depletion Potential)	kg R11 eq.	Assessment of the capacity of different gases to deplete the ozone layer, including HCFCs and ozone-depleting substances.
FAETP (Freshwater Aquatic Ecotoxicity Potential)	kg DCB eq.	Potential for freshwater resources to be attacked by toxic substances in the environment.
MAETP (Marine Aquatic Ecotoxicity Potential)	kg DCB eq.	Potential of seawater resources to be exposed to toxic substances in the environment.
TETP (Terrestrial Ecotoxicity Potential)	kg DCB eq.	The potential of terrestrial ecosystems to be attacked by environmental toxic substances.

4.3.3.2 Entropy weight method

Based on the multi-index system by LCIA results, a unified comprehensive evaluation by the weight method is needed to achieve a semiquantitative comparison between different technologies. As an objective weighting method, the entropy weight (EW) method has the advantage of determining objective weights based on the magnitude of the variability of the indicators. It is a mature methodology for comprehensive evaluation under a multi-index system due to higher reliability and accuracy than subjective weighting [164, 165]. Therefore, the EW method is employed to calculate comprehensive environmental impact (EI) based on the LCA results of eleven environmental indicators. The calculation steps are described as follows:

(1) The eleven sub-indicators were normalised by the range normalisation method using **equation (28)**:

$$Y_{ij} = (1-\alpha) + \alpha \frac{LEP_{ij} - MinLEP_{ij}}{MaxLEP_{ij} - MinLEP_{ij}} \quad (28)$$

where Y_{ij} and LEP_{ij} are the normalized and original values of the j_{th} sub-indicator in the i_{th} ethanol routes, respectively; $MaxLEP_{ij}$ and $MinLEP_{ij}$ are the maximum and minimum values of the corresponding indicator, respectively, and α belongs to (0,1). Here, α is set to 0.9 according to the literature [164].

(2) The information entropy E_j of the eleven environmental sub-indicators were calculated by **equation (29)**:

$$E_j = -\frac{1}{lnm}\sum_{i=1}^{m}\frac{Y_{ij}}{\sum_i^m Y_{ij}} \times ln\frac{Y_{ij}}{\sum_i^m Y_{ij}} \quad (29)$$

where m is the overall number of ethanol routes and related scenarios, then $0 \leq E_j \leq 1$.

(3) The difference coefficient D_j of the j_{th} sub-indicator was calculated by **equation (30)**:

$$D_j = 1 - E_j \quad (30)$$

(4) The coefficients of the different indicators are normalized using **equation (31)** to obtain the weights W_j for each sub-indicator:

$$W_j = \frac{D_j}{\sum_{j=1}^{11} D_j} \quad (31)$$

(5) The comprehensive environmental impact EI of each ethanol route was calculated by **equation (32)**:

$$EI_i = \sum_{j=1}^{11} Y_{ij} \times W_j \quad (32)$$

4.3.3.3 LCIA modelling by GaBi software

The entire process of bio-fermentation to LDG-Ethanol technology and the sub-unit processes were modelled by GaBi software, and the modelling process is shown in **Figure 22**.

The entire process of Corn-ethanol technology and the sub-unit processes were modelled by GaBi software, and the modelling process is shown in **Figure 23**.

The entire process of Corn-ethanol technology and the sub-unit processes were modelled by GaBi software, and the modelling process is shown in **Figure 24**.

Figure 22. Process modelling of bio-fermentation to LDG-ethanol technology.

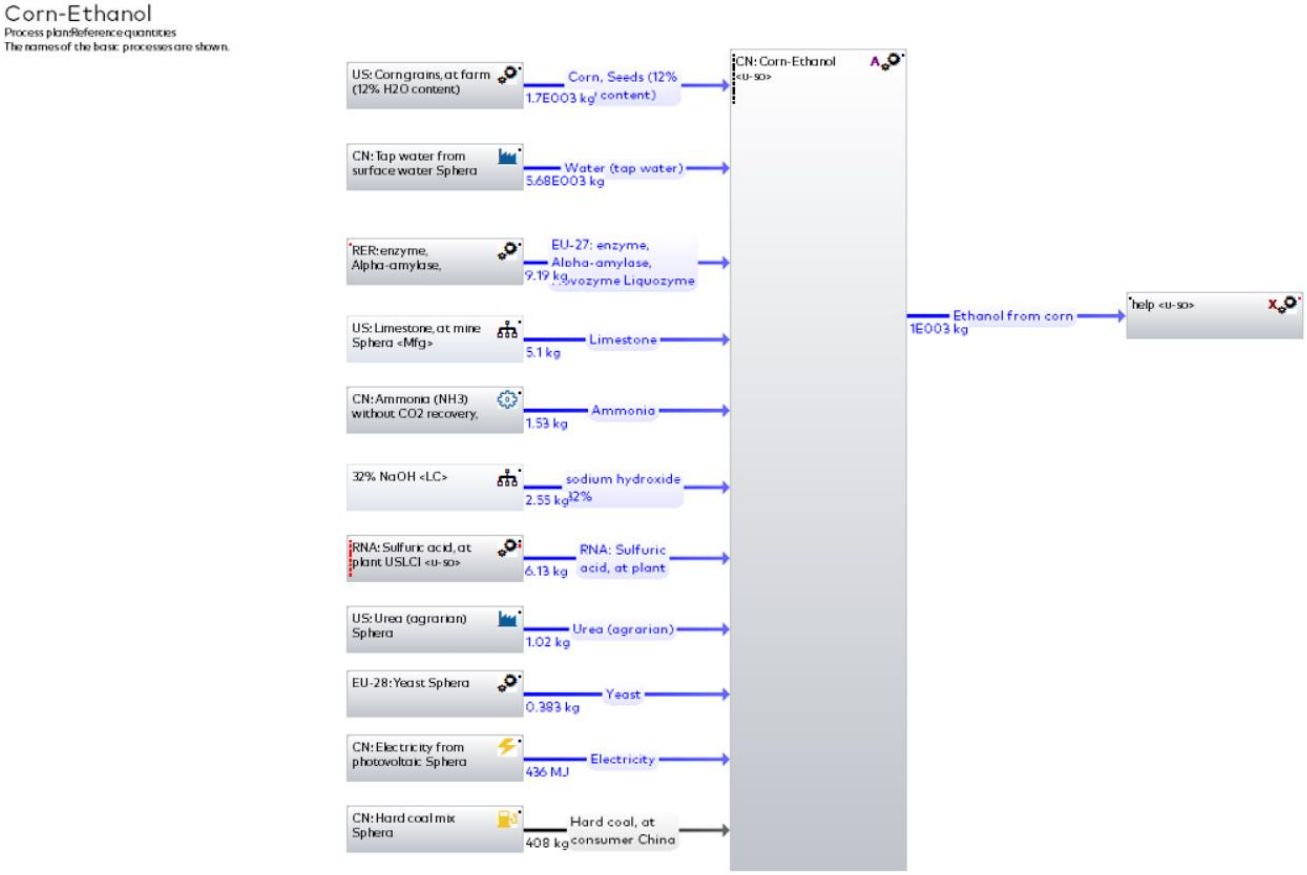

Figure 23. Process modelling of Corn-ethanol technology.

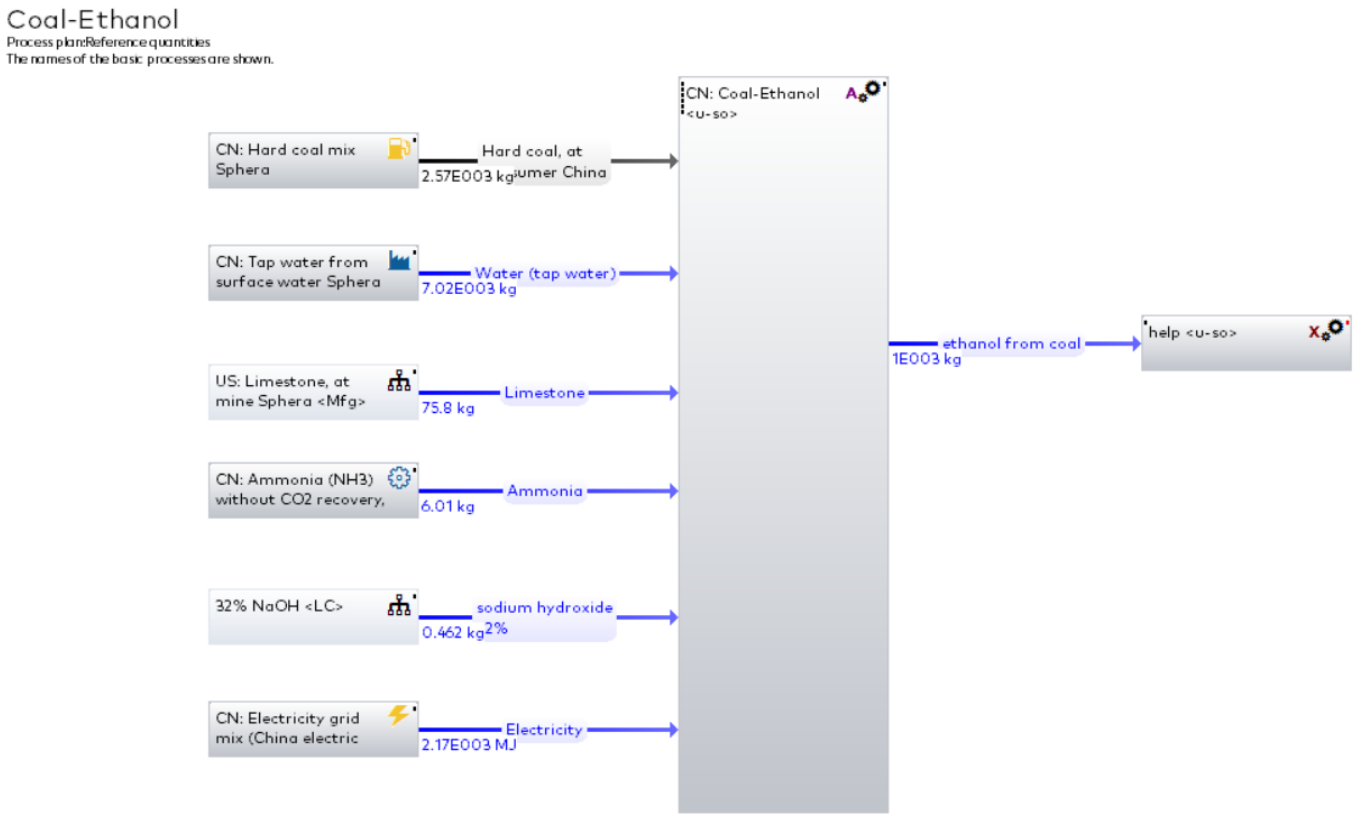

Figure 24. Process modelling of Coal-ethanol technology.

4.3.4 Sensitivity analysis

Sensitivity analysis refers to the influence degree to the change of the result by the change of input and output data. Based on the LCA results, sensitivity analysis is performed to reveal the sensitive factors to the environmental indicators. Generally, the sensitivity analysis could be expressed mathematically as **equation (33)**. That is, as specific parameters change according to a certain proportion, such as 5%, 10%, etc, the ratio of the change of the response result relative to the initial result. The greater the ratio, the more sensitive the factor is. The greater the ratio is, the more sensitive the factor is.

In this study, the sensitivity analysis was carried out according to **equation (33)** by adjusting influencing parameters with ± 10% fluctuation. The parameters with a sensitivity of less than 0.02% are ignored in this study.

$$Z = \frac{y_j - y_o}{y_o} \quad (33)$$

where y_i is the corresponding value with specific parameters fluctuating by ± 10% and y_0 is the original value.

4.3.5 Scenario assumption

To comprehensively reveal the investigated LDG-ethanol route,

prospective development scenarios are considered and described in **Table 11**.

Table 11. Scenario description.

Scenarios		Key features
Baseline scenario	LDG-ethanol (LE)	Existing technology
Energy-efficient scenario	LDG-ethanol-energy efficient (LEE)	Energy efficient equipment with electricity consumption decreased from 1956 kWh/t to 1422 kWh/t.
Green power scenario	LDG-ethanol-photovoltaic power (LEGP)	Photovoltaic power supply
	LDG-ethanol-wind power (LEGW)	Wind power supply
	LDG-ethanol-hydropower (LEGH)	Hydropower supply
Comprehensive optimisation scenario	LDG-ethanol-energy efficient + photovoltaic power (LEEGP)	Energy efficient equipment and photovoltaic power supply combination
	LDG-ethanol-energy efficient + wind power (LEEGW)	Energy efficient equipment and wind power supply combination
	LDG-ethanol-energy efficient + hydropower (LEEGH)	Energy efficient equipment and hydropower supply combination

Energy-efficient scenario: the current LDG production process, as the first-generation technology, still has plenty of potential for improvement via optimizing the operation equipment. Their energy consumption could be reduced by replacing advanced energy-efficient equipment, such as introducing variable frequency drives, centrifuges, and other low-power equipment. The space for energy efficiency improvement is estimated by advice provided by professional technicians in the LDG-ethanol plant (See **Table 12** for specific energy efficient schemes), denoted as LDG-ethanol energy efficient (LEE).

Table 12. Energy-efficient scenario data.

Unit	Power before optimisation		Optimisable power	
	Equipment number	Rated power (kW)	Optimised equipment power (kW)	Reduced Power (kW)
PRT	4	5820.7	4820.7	1000
FMT	63	4849.5	3646.5	1203
BMS	33	1443.55	900.55	543
WWT	69	937.99	684	254

Green power scenario: it is generally believed that a clean power structure is an inevitable trend in forthcoming China. Therefore, the environmental impact of the LDG-ethanol route with photovoltaic power (PV), wind power (WP) and hydropower (HP) are systematically investigated, which are denoted as LDG-ethanol-photovoltaic power (LEGP), LDG-ethanol-wind power (LEGW) and LDG-ethanol-hydropower (LEGH), respectively.

Comprehensive optimization scenario: the environmental impact of the LDG-ethanol route could be further improved by simultaneously employing energy-efficient and green power use as optimization means, which is denoted as LDG-ethanol-energy efficient + photovoltaic power (LEEGP), LDG-ethanol-energy efficient + wind power (LEEGW) and LDG-ethanol-energy efficient + hydropower (LEEGH).

4.4 Results and discussions

4.4.1 LCA results

4.4.1.1 Comprehensive comparisons of LCA results for the three ethanol routes

To begin with, LCIA based on the CML method was carried out for the LDG-ethanol, and the results are compared with that of Corn-ethanol and Coal-ethanol routes as listed in **Table 13**. LDG-ethanol route has the lowest values on the ADP-f, EP and FAETP indicators, which only account for 80%, 12%, and 4% of the Corn-ethanol route and 18%, 85%, and 70% of the Coal-ethanol route, respectively. The ADP-e, GWP, HTP, ODP, POCP and TETP indicators are calculated to be 1.94E-04, 5.11E+03, 1.08E+02, 1.02E-11, 0.41, 1.23, respectively. These are in between the values for Coal-ethanol and Corn-ethanol routes. For the left two indicators (AP and MAETP), the LDG-ethanol route has the highest impact, which is 2.10 and 2.18 times that of the Corn-ethanol route, and 1.27 and 1.76 times that of the Coal-ethanol route, respectively.

As carbon neutrality is becoming a commonly understood target to abate climate change, it is worth discussing the GWP indicator in more

detail because of its correlation to the emission of greenhouse gases. From **Table 13**, the GWP value of the LDG-ethanol route is 5.11 t CO_2eq/t, while for the Corn-ethanol and Coal-ethanol routes, they are -0.46 t CO_2eq/t and 6.21 t CO_2eq/t, respectively. There is no doubt that biomass, as a negative carbon raw material, has natural advantages in GHG emissions compared with traditional fossil raw materials. Therefore, it is unsurprising that the LDG-ethanol route has no advantage compared to the Corn-ethanol route on the GWP indicator. On the other hand, it is encouraging to find that the GHG emission of the LDG-ethanol route is 18% lower than the Coal-ethanol route, despite both processes using fossil energy as raw materials.

Table 13. LCA characterisation results.

Environmental indicator		LDG-ethanol	Corn-ethanol	Coal-ethanol	LDG/Corn ratio	LDG/Coal ratio
ADP-e	kg Sb eq. (E-04)	1.94	6.05	0.89	0.32	2.19
ADP-f	MJ (E+04)	1.36	1.69	7.38	0.80	0.18
AP	kg SO_2 eq.	3.59	1.71	2.82	2.10	1.27
EP	kg Phosphate eq.	0.37	0.31	0.43	0.12	0.85
FAETP	kg DCB eq.	1.71	46.60	2.43	0.04	0.70
GWP	kg CO_2 eq. (E+03)	5.11	-0.46	6.21	-11.18	0.82
HTP	kg DCB eq. (E+02)	1.08	0.64	1.28	1.68	0.84
MAETP	kg DCB eq. (E+04)	11.90	5.46	6.77	2.18	1.76
ODP	kg R11 eq. (E-11)	1.02	0.90	11.30	1.13	0.09
POCP	kg Ethene eq.	0.42	0.12	0.75	3.58	0.56
TETP	kg DCB eq.	1.23	1.03	1.31	1.19	0.94

Based on the 11 environmental indicators shown in **Figure 25(a)**, the comprehensive EI was calculated using the EW method [175]. Very interestingly, the LDG-ethanol route occurs to be the most environmentally benign option among the technologies investigated here. The obtained EI value is 0.41, i.e., 22.6% and 25.5% lower than that of Corn-ethanol (0.53) and Coal-ethanol (0.55), respectively. As presented in detail in **Figure 25(b)**, the highest EI for Coal-ethanol could be ascribed to its massive footprint in GWP, HTP, TETP, and particularly in ADP-f and POCP. These mainly result from the significant consumption of fossil resources and thus the generation of pollutants, including volatile organic chemicals, oxysulfide, oxynitride, etc. Similarly, the unexpectedly high EI for Corn-ethanol is mainly driven by the great demand for water, pesticides, and fertilizers during the corn growth process, which led to considerably higher EP and FAETP. As for the LDG-ethanol route, on the other hand, low-value tail gas is used as the main raw material, and a biological fermentation mechanism could generate high-value products. Meanwhile, the process is simply operated under mild conditions, which means less energy consumption. Taken together, it is believed that LDG-ethanol with low environmental impact, low land resource– occupancy and high economic benefit is

undoubtedly more attractive than other ethanol routes [176].

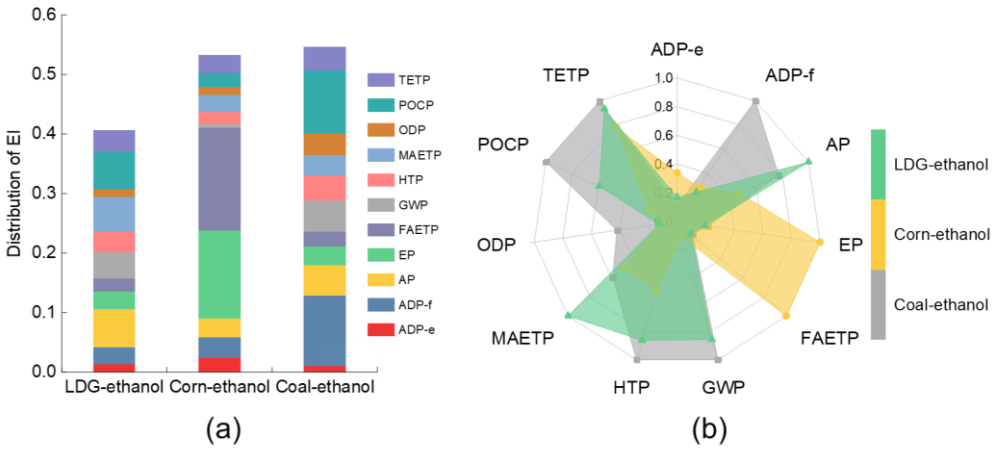

Figure 25. Comprehensive comparisons of the three ethanol routes. (a) EI comparison. (b) specific indicator comparison.

4.4.1.2 Contribution analysis of LCA results for LDG-ethanol

The above results encouraged us to identify further contributions of different units and input features of the LDG-ethanol process to the 11 indicators, which is of pivotal importance for future technological improvements. To this end, the 11 environmental indicators are decomposed according to the relative contribution from all the production units (**Figure 26(a)**). It can be observed that the PRT and FMT units dictate the environmental footprints of the LDG-ethanol process, with total contributions of over 75% to all the indicators. Generally, the PRT unit's contributions to ADP-f, AP, EP, FAETP, HTP,

MAETP, ODP, POCP and TETP indicators ranged between 35–42%, with a relatively lower contribution to GWP (9%) and ADP-e (22%). Similarly, the contributions from the FMT unit to ADP-e, AP, EP, FAETP, HTP, MAETP, ODP, POCP and TETP account for 32–41%, and its contributions to GWP and ADP-e indicators are even higher (65% and 54%). Apart from PRT and FMT, the contributions from other units decreased followed by WWT (6–11%) > CWS (5–9%) > TGT (3–4.5%) > DIS (0.8–3.6%). In fact, these results are expected as a large portion of feedstocks, chemicals and energy are consumed in the PRT and FMT units. Therefore, PRT and FMT should be placed in a central position during future technical improvement.

The contribution of different utility inputs (electricity, nitrogen, chemicals, water, etc.) to the 11 indicators is also analysed, and the results are shown in **Figure 26(b)**. It is found that electricity plays a determining role in the environmental footprint of the LDG-ethanol process, with over 80% contributions to 9 indicators (ADP-f, AP, EP, FAETP, HTP, MAETP, ODP, POCP and TETP), 52% to ADP-e, and 22% to GWP. It should be mentioned that although electricity contribution to GWP is relatively low, it still accounts for 89% of the indirect GHG emission, and the largest GWP source is direct process emission (75%).

The significant impact of electricity may result from China's dominant coal-fired power generation process. As well known, a great number of polluting gases (carbon dioxide, sulphur dioxide, nitrogen oxides, harmful particulate matter), heavy metals (Hg, Pb, As *et al*.) and wastewater are discharged during the coal mining and combustion process [177].

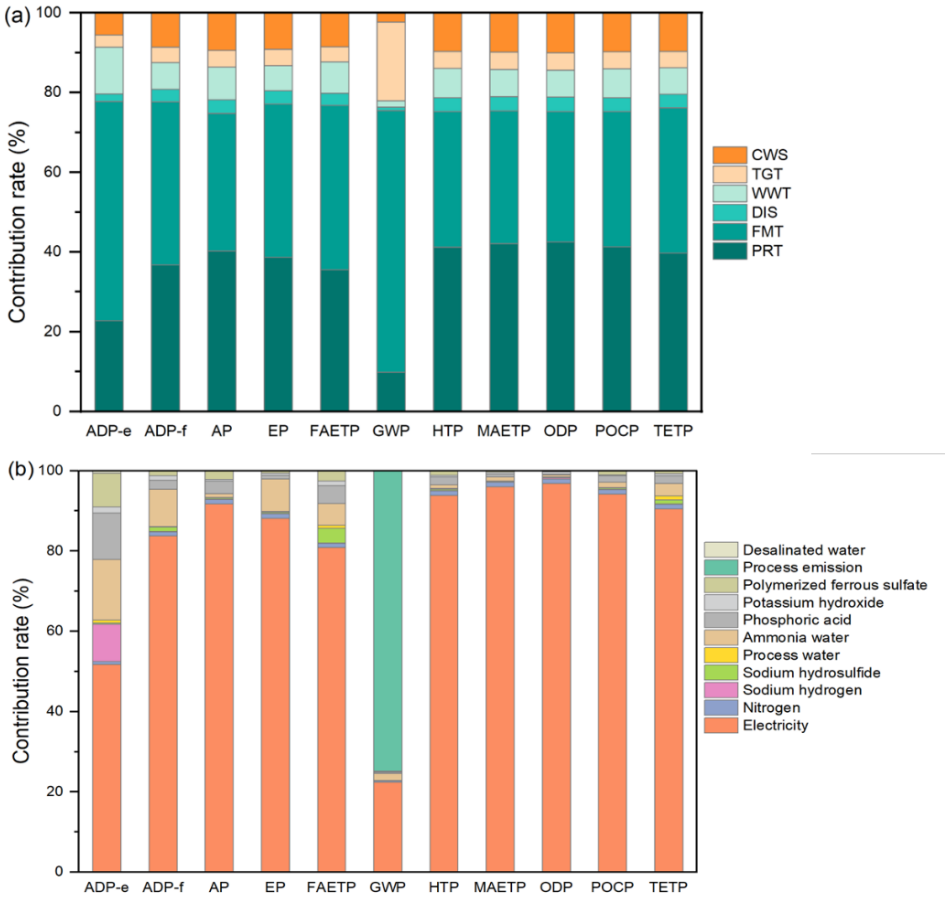

Figure 26. Contribution analysis of the LCA results for the LDG-ethanol. (a) contribution of the process unit. (b) contribution of energy and material consumption.

4.4.2 Carbon flow and energy flow

Based on the carbon balance of LDG bio-fermentation technology, the carbon flow diagram is shown in **Figure 27(a)**.

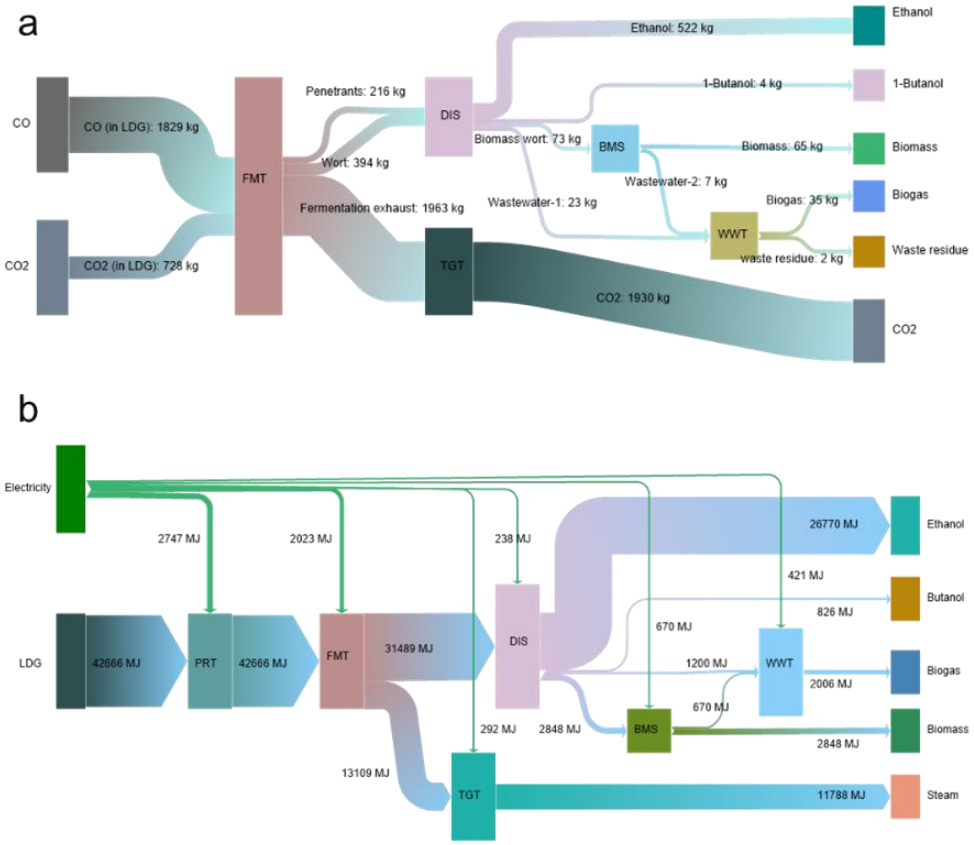

Figure 27. Carbon flow (a) and energy flow (b) diagram of LDG-ethanol.

For 1 ton ethanol as the FU, the fermentation tail-gas is the largest carbon flow ratio source, including CO_2 produced by the CO fermentation process, incompletely reacted CO, and CO_2 in LDG raw materials, with a proportion of 75%. On the input side, the proportion of effective carbon input (carbon mass of CO) is 72%, and the carbon

weight of CO_2 in LDG (which does not participate in the fermentation reaction and can be regarded as an inert gas) is 28%. On the output side, the total carbon mass of the product is 625 kg, and the carbon mass of the ethanol is 522 kg, accounting for 28%. In general, the carbon ratio of the product to the effective carbon input is about 34%; that is, 34% of the effective carbon is fixed in the product. It can be seen that most of the carbon after the FMT unit comes to the TGT unit in the form of fermentation tail gas. The fermentation tail gas includes the unreacted CO and the CO_2 produced by the fermentation reaction. If the carbon in CO and CO_2 can be used more efficiently, the carbon emission reduction will be greatly reduced. Therefore, the TGT unit has the biggest potential for carbon reduction. In **Figure 27(b)**, based on the energy conservation, the energy efficiency of the LDG-ethanol technology is 89%, the energy weight of ethanol is 54%, followed by steam energy weight (24%).

4.4.3 Sensitivity analysis

The sensitivity analysis quantitively proves the key factors for each environmental indicator, as shown in **Figure 28**. The top five key factors are almost related to electricity from different process units (PRT-electricity, FMT-electricity, CWS-electricity, TGT-electricity, DIS-

electricity). Specifically, PRT-electricity and FMT-electricity are the most important ones. For example, when PRT-electricity fluctuates by ±10%, the results of GWP, HTP, MAETP, ODP, POCP fluctuate > ±4%, ADP-f, AP, EP, FAETP, TETP fluctuate ±(3% – 4%), ADP-e fluctuate < ±3%. These results indicate that the electricity parameters are the most sensitive to the LCA results, compared to other parameters such as chemicals, water, etc. Therefore, optimising power in the LDG-ethanol process, especially FRT-electricity and FMT-electricity, is supposed to improve environmental performance effectively.

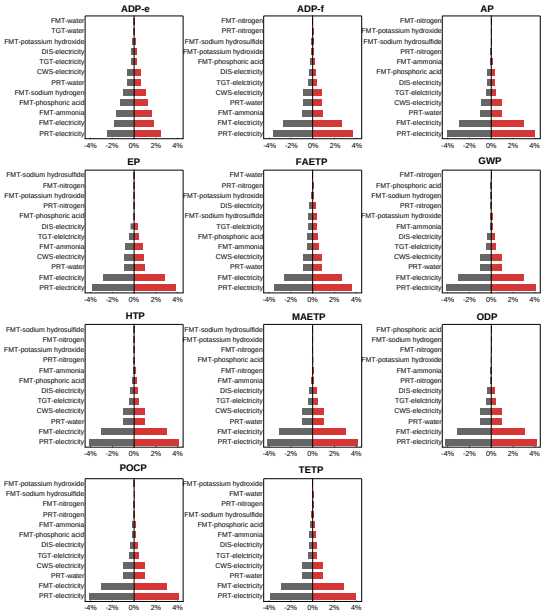

Figure 28. Sensitivity analysis of the key input features of LDG-ethanol (Note: when all the input parameters ranged ±10%, the resulted fluctuation for the specific indicator is shown).

4.4.4 Investigation of LDG-ethanol optimisation

4.4.4.1 LCA environmental impact of LDG-ethanol in different scenarios

Based on LCIA studies discussed in section 3.4.1, in this part, we focused on the effect when the involvement of electricity is altered. Three sets of scenarios, i.e., increased electricity efficiency and decarbonization of grid mix are investigated (see Section 3.3.5 for more details about scenario design). As observed in **Figure 29**, in the LEE scenario with higher electricity efficiency, most indicators drop by ~20% due to the decrease in electricity consumption, except ADP-e and GWP. As a result, the EI value is reduced to 0.34, 17% lower than the current situation (LE scenario). Most of the indicators decreased substantially when shifting the electricity source to a non-fossil type (PV, WP, HP for LEGP, LEGW, and LEGH scenarios, respectively). In the LEGP scenario, a significant reduction between 55%-88% is observed for ADP-f, AP, EP, FAETP, HTP, MAETP, and POCP indicators, and for the GWP indicator, the reduction space is narrowed to 21%. However, two exceptional indicators (ADP-e and ODP) are even more severe, which are fifteen-fold and forty-fold as large as the LE scenario. The LEGW scenario results are similar to the LEGP situation, with 64 – 95% reduction rates

in ADP-f, AP, EP, FAETP, HTP, MAETP, POCP, a 22% reduction rate in GWP and a 2% increase rate in TETP. As for the ADP-e and ODP indicators, the values are one to two times higher than the LE scenario.

In the LEGH scenario, all impact indicators are reduced with 82–97% reduction rates in ADP-f, AP, EP, FAETP, HTP, MAETP, ODP, POCP, TETP and 43%, 22% in ADP-e and GWP indicators, respectively. Therefore, from the results of the green power scenarios, it is proved that introducing green power in the LDG-ethanol route could effectively reduce the environmental footprint. However, it is worth noting that the utilization of photovoltaic and wind power adversely affects ADP-e and ODP, probably because of the production of the infrastructure materials. It is reported that wind power plant blades are mainly made of polymer materials [178], which is problematic during post-use management. The fabrication of photovoltaic cells also emits hazardous pollutants [179]. Nevertheless, employing green electricity can greatly lower the overall environmental impact, with EI values dropping to 0.35, 0.20, and 0.13 for LEGP, LEGW, and LEGH, respectively. All 11 environmental impacts can be further decreased in the LEEGP, LEEGW, and LEEGH scenarios, namely by increasing electricity efficiency and decarbonizing the grid mix simultaneously. (see **Table A1** for numerical results).

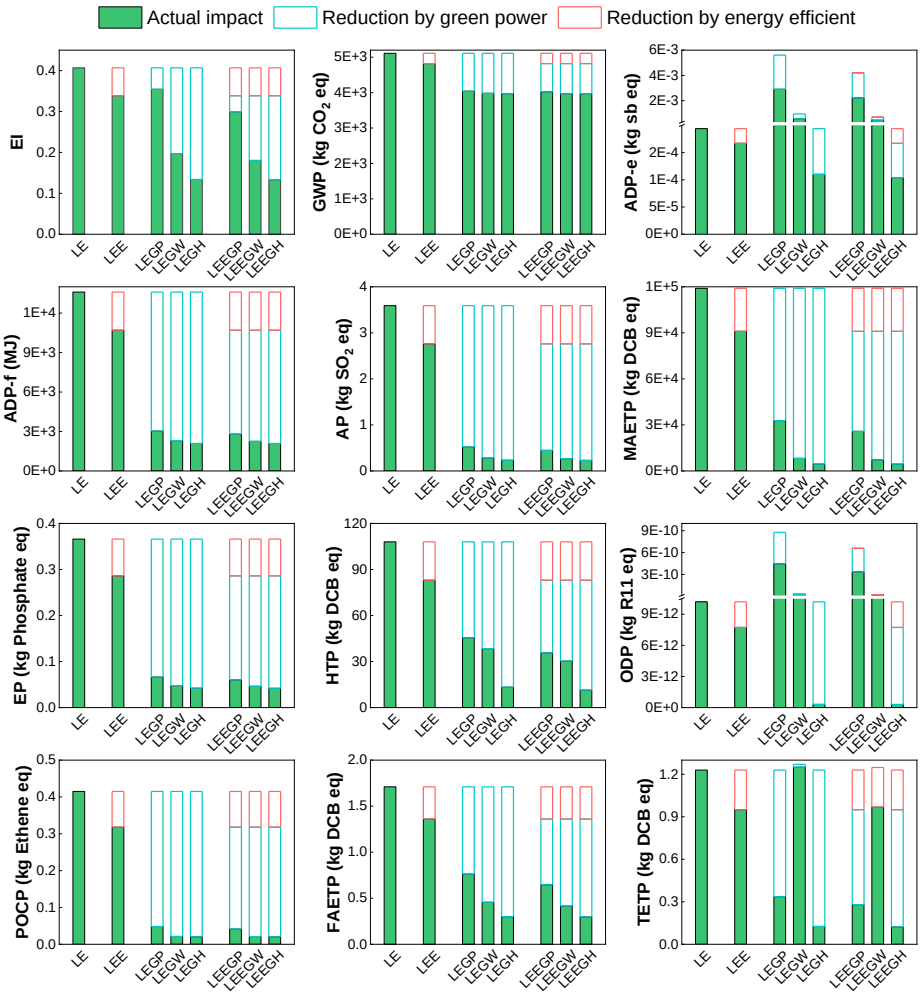

Figure 29. The environmental impact of LDG-ethanol in different scenarios.

4.4.4.2 Green electricity optimisation

Considering the decisive role of electricity on the environmental impact of the LDG-ethanol technology, its contributions under different scenarios are further analysed in **Figure 30** (see **Table A2** for numerical results). The electricity contribution is reduced by 0.6 – 7.0% for all indicators in the case of the LEE scenario. However, it is still the main

influencing factor among all the utility inputs. The situation is different after green power is introduced. In the LEGP scenario, only seven indicators (ADP-e, AP, FAETP, HTP, MAETP, ODP and TETP) are electricity-dominated (>50% contribution), which is further decreased to four indicators (ADP-e, HTP, ODP and TETP) and one (HTP) for LEGW and LEGH scenarios, respectively. The results trend of the comprehensive scenario is similar to the green power scenario. Therefore, from the above results, it is concluded that the decarbonization of the grid mix is surely conducive to reducing environmental impact. Relatively speaking, HP is the most environmentally friendly. For PV and WP, the issue of high ADP-e and ODP indicators needs more systematic and fundamental improvements in the future.

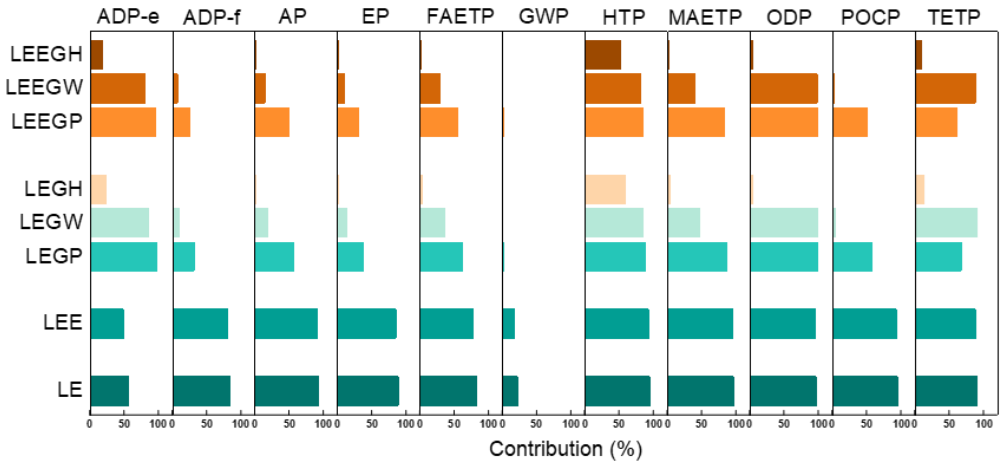

Figure 30. Electricity contribution under different scenario optimization.

Since the decarbonization of electricity offers an efficient means of lowering the environmental impact of the LDG-ethanol technology, further comparison to green electricity-powered Corn-ethanol and Coal-ethanol processes was made. From **Figure 31**, it is found that when coal-fired power is substituted by PV, WP, and HP, the LDG-ethanol route is still the most environmentally friendly technology. In the PV scenario (**Figure 31 (a)**), LDG-ethanol has higher ADP-e and ODP indicators than the other two routes, indicating higher abiotic resource depletion elements and ozone-depleting gases. Corn-ethanol has higher EP and FAETP, confirming its higher water consumption during the growth of corn feedstock. Coal-ethanol has a higher GWP, ADP-f and HTP, indicating a higher consumption of coal as a fossil resource and the emission of toxic substances (dioxins, polycyclic aromatic hydrocarbons (PAHs), heavy metals, etc.) that may harm human beings during the use of fossil fuels. In total, the EI values of Coal-ethanol-PV and Corn-ethanol-PV are both 0.53, which is 51% higher than that of LDG-ethanol (0.35). This difference is even more pronounced in the WP scenario, where the EI of LDG-ethanol decreases to 0.20, as compared to 0.52 and 0.46 for Corn-ethanol and Coal-ethanol, respectively. The sharpest contrast is observed in the HP scenario, with an EI value as low as 0.13

obtained for LDG-ethanol, whereas those for Corn-ethanol and Coal-ethanol can hardly change (0.51 and 0.40, respectively). We also noticed that for the Corn-ethanol and Coal-ethanol processes, the EI values in **Figure 25** and **Figure 31** are almost similar, suggesting that the environmental footprints of these technologies are less sensitive to the decarbonization of electricity. Clearly, this observation can be ascribed to the considerably higher contribution of electricity for the LDG-ethanol process, whereas the major influencing factors for the other two technologies are material-related. Consequently, we envision that the LDG-ethanol process is of great promise in terms of environmental perspective, particularly when decarbonization of electricity becomes a must in a holistic picture of carbon reduction, climate management, and sustainable development.

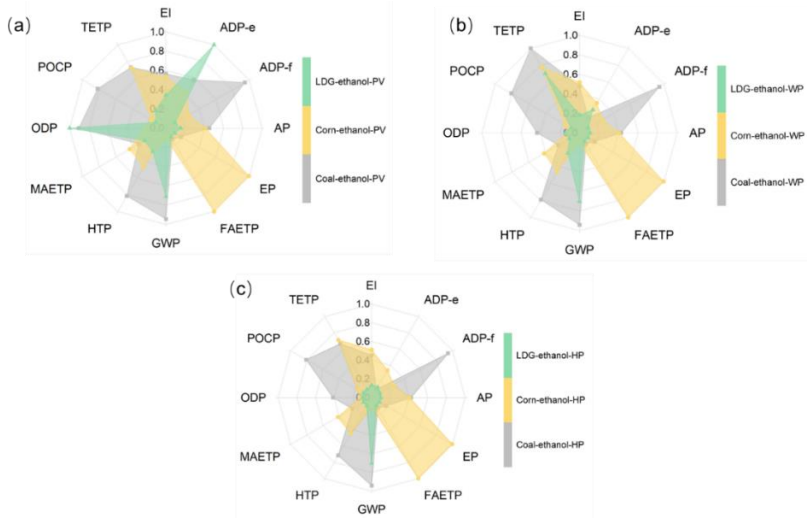

Figure 31. Comparisons of the LDG-ethanol and other routes under three scenarios. (a) PV scenario. (b) WP scenario. (c) HP scenario.

4.5 Summary

This chapter comprehensively evaluated the environmental performance of the LDG-ethanol route and its competitive routes by using the LCA and EW methods. Based on the CML method, the LDG-ethanol route has the best impact on ADP-f, EP and FAETP and the worst impact on the AP and MAETP indicators. Overall, in the Chinese scenario, the LDG-ethanol route is the most environmentally benign, with a comprehensive environmental impact >20% lower than the other two competitors. As electricity is a sensitive factor, with energy saving and green power introduction, the comprehensive environmental impact of the LDG-ethanol route could be further alleviated by 15–68%. It is interesting to find that with grid decarbonization, if coal-fired power is substituted by photovoltaic power, wind power and hydropower respectively, the EI values of the LDG-ethanol route will be low to 0.35, 0.20 and 0.13 and the advantage is further extended compared to the competitive routes. Consequently, the LDG-ethanol process is of great promise in terms of environmental perspective, particularly when the decarbonization of electricity becomes a must in a holistic picture of sustainable development.

The competitiveness of environmental impact over LDG-ethanol with traditional routes was revealed by taking China as a scenario, but its data and results could provide valuable knowledge and insights for the scientific development of the LDG-ethanol industry in other countries with strong fuel ethanol demands. The sensitivity and scenario analysis can also extend the assessment results to overcome the period and geographic limitations of the applications in this study. From this work result, it is believed that countries with ample clean power could gain larger profits if LDG-ethanol technology developed.

CHAPTER 5. Integrated life cycle assessment and techno-economic analysis of the low-carbon ethanol production intensified by electro-catalytic CO_2 reduction

Part of this Chapter's work has been published in "Lingyun Zhang, Qun Shen, Kien-Woh Kow, Wei Chen, Tao Wu, Edward Lester, Cheng Heng Pang, Wei Wei, et al. Potential solution to the sustainable ethanol production from industrial tail gas: An integrated life cycle and techno-economic analysis*, Chem. Eng. J.,* 2024 (487), 150493."

5.1 Overview

In Chapter 4, it was revealed that the LDG-ethanol technology has numerous advantages, such as greatly increased resource efficiency, mitigated carbon emissions, and significantly reduced energy consumption due to mild operation conditions, which make LDG-ethanol production a more promising viable alternative ethanol technology than biological and fossil ethanol production routes. Overall, the comprehensive environmental impact of LDG-ethanol is 22–25% lower than that of Corn-ethanol and coal- ethanol production. However, the global warming potential of the LDG-ethanol route was also found to be

far more than that of the Corn-ethanol route, indicating the low carbon conversion efficiency which led to a large amount of CO_2 being generated from the associated bio-fermentation process. Therefore, the use of enabling process intensification technologies to convert CO_2 to CO to achieve carbon recycling is essential to drastically improve the climate benefits of sustainable ethanol production.

Electro-catalytic CO_2 reduction (ECR) to CO is generally seen as a promising route [29] for CO_2 conversion and utilisation [30-32]. Chen *et al.* [33] recently found that the use of hierarchical micro/nanostructured silver hollow fibre electrodes in ECR can effectively reduce CO_2 to CO under ambient pressure and temperature. It has also been shown that the ECR process can be powered directly with low-grade renewable energy [180], which augurs well for low cost and high operation flexibility. All these benefits make ECR a viable technology [35, 181] for integration with the tail gas based-ethanol (TG-ethanol) process. Therefore, a novel TG-ethanol with integrated electro-catalytic CO_2 reduction technology (TGEE, **Figure 32**) for sustainable ethanol production is proposed for the first time to address the carbon efficiency issues associated with LDG-ethanol production technology. Whilst this coupling process is an

ideal solution from a technical point of view, its environmental sustainability and techno-economic viability are still unknown.

This chapter aims to investigate the integrated LCA and TEA performance of TGEE technology. Three typical industrial tail gases, sourced from steel, iron alloy, and calcium carbide production, serve as feedstocks for the TGEE process in the case study. The process was modularly modelled for different ECR integration scenarios for three typical industrial tail gas streams, and life cycle & techno-economic analysis based on Monte Carlo simulation were employed to assess the environmental and economic performance of the TGEE process. Results show that ethanol capacity can be increased by 1.3 – 2.9 times with carbon efficiency up to 36 – 82%. Life cycle carbon footprints of TGEE-ethanol were estimated to be 1.77 – 3.93 t CO_2eq/t ethanol, with a carbon reduction potential of 32 – 63% higher than the TG-ethanol. Minimum ethanol selling price has been estimated to be \$428 – 962/t ethanol, which is lower than the ethanol market price (\$900 – 1080t). Overall, the comprehensive analysis suggests that the TGEE process could present a more economically and environmentally benign next-generation technology for producing ethanol from industrial tail gas. These results not only show the environmental, economic and energy

impacts but also provide valuable insights for researchers and stakeholders for the commercial deployment of TGEE technology.

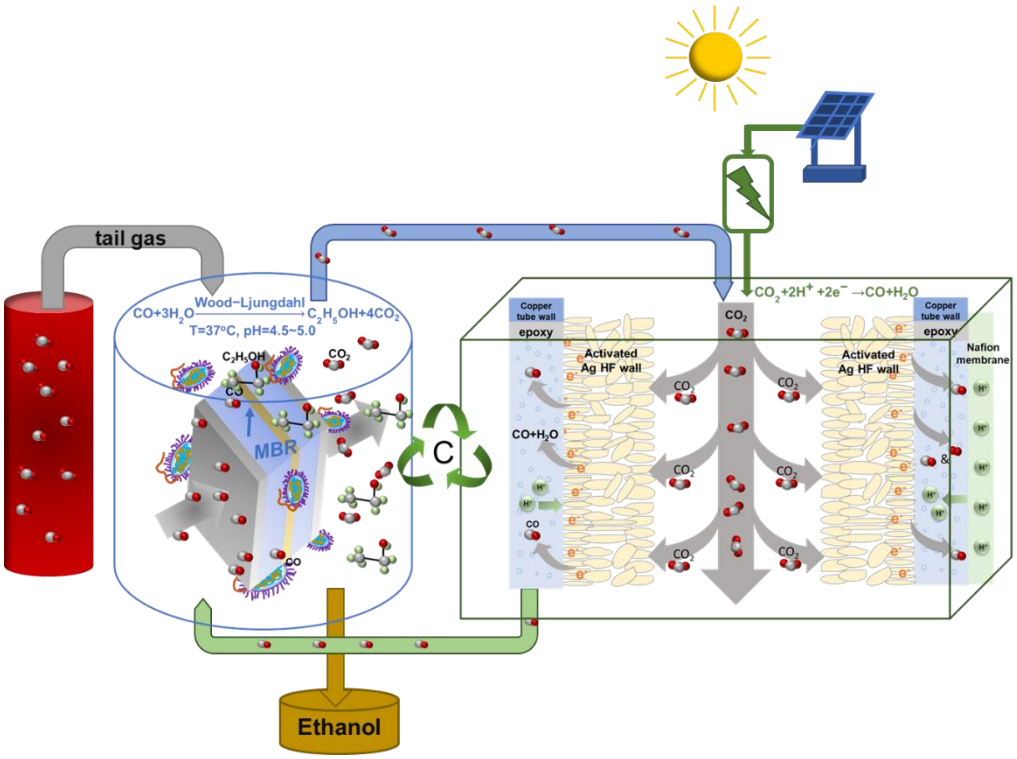

Figure 32. Graphical abstract of this chapter.

5.2 Methodology

5.2.1 System boundary

The system boundary of this TGEE process is shown in **Figure 33**, covering purchasing tail gas from a co-located factory, processing into ethanol and steam products, distribution of products, and CO_2 emissions. Generally, the ECR-integrated TGEE technology could be retrofitted to all types of tail-gas streams containing CO such as those from ammonia,

steel, iron alloy, calcium carbide, silicon carbide, phosphorous chemical and acetic acid industries. Henceforth, off-gas is used to mean the waste gas from the fermentation and tail gas is used to mean the industrial tail gas feedstock. Particularly, two different technical pathways of ECR coupling to the TG-ethanol process are considered: (i) pre-combustion ECR (PRE) where coupling the ECR process before the fermented off-gas is combusted, part of fermented off-gas (mix of CO and CO_2) from the bio-fermenter was direct transfer to ECR unit to convert the CO_2 in mix gas to CO and the reduced CO was recycled into tail gas feed stream, while the remaining fermented off-gas enters the TGT unit to be oxidation and combustion to CO_2 and then discharged; and (ii) post-combustion ECR (POE) where coupling the ECR process after the fermented off-gas was completely combusted, in which the fermented off-gas is first subjected to a TGT combustion unit to convert the residual CO to CO_2, and then part of CO_2 is recycled to the ECR unit for CO_2 to CO conversion and remaining non-recycled CO_2 is directly emitted. The commercial Aspen Plus© software was used to simulate the PRE and POE pathways, and the obtained mass and energy balance data were used in LCA [182] and TEA [183].

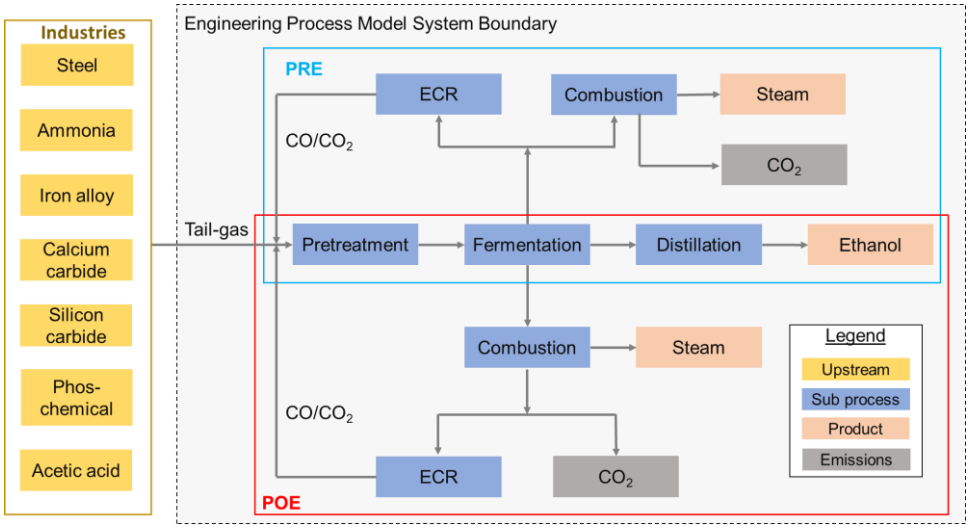

Figure 33. Process system and boundary conditions for the TGEE process, which shows the two scenarios of ECR coupling i.e. pre-combustion ECR (PRE) and post-combustion ECR (POE) coupling to the fermented off-gas.

5.2.2 Process model and scenario design

5.2.2.1 Process description and modelling

Firstly, the feed tail gas is subjected to a pre-treatment unit (PRT) to be pressurised and fed into the fermentation unit (FMT) where the tail gas-contained CO is converted into ethanol and other products through **equation (34)**. The biological fermentation is conducted under a constant pH and temperature, thus requiring energy input and the addition of chemicals (i.e., pH conditioners, phosphoric acid, and sodium hydroxide) into the fermenter. To produce the ethanol product, the raw

ethanol-containing aqueous stream from FMT is processed in a distillation unit (DIS) coupled with adsorption and dehydration treatment using molecular sieves. The off-gas stream from the bio-fermenter, which contains unreacted CO, is combusted in a tail-gas combustion treatment unit (TGT) to provide the heat required to operate the fermentation and distillation units. ECR is an electrically driven catalytic conversion process of CO_2 to CO, i.e., the waste gas CO_2 emitted from FMT or TGC units can be converted into CO through ECR as shown in **equation (35)**, with the CO recycled to synthesize ethanol. According to Li *et al.* [180], the use of hierarchical micro/nanostructured silver hollow fibre electrodes with the catalyst of activated Ag HF can effectively facilitate the efficient electro-reduction of CO_2 to CO, at a conversion rate of 50% with a faradaic efficiency of 93% under ambient conditions [33]. The ECR process described in this thesis is not yet commercially available and is still at a laboratory scale. In the Aspen simulation of this study, we calculated the number of electrons required to convert CO_2 into CO. The number of electrons contained in 1 kWh of electricity is related to both the line voltage and the power factor. Assuming the power factor is 1, the power consumption of 1 ton of CO at different voltages can be calculated. Therefore, the ECR process operates at a voltage of

3V with renewably generated power, such as wind power, photovoltaic (PV), or hydropower. Given the readily available local solar resources, PV is selected to power the ECR process. It has been revealed that the electrical energy required in the ECR process is 5763 kWh per ton of CO from CO_2 conversion [184]. In this study, the original TG-ethanol process remains powered by existing grid power.

In summary, **equation (34)-(35)** are the core reactions for ethanol produced by the TGEE process, and the ethanol capacity refers to the amount of ethanol produced from industrial tail gas through the TGEE process, which is calculated by **equation (36)**.

$$6CO + 3H_2O \rightarrow C_2H_5OH + 4CO_2 \quad \Delta G=28.7 \text{ kcal/mol} \tag{34}$$

$$CO_2 + 2H^+ + 2e^- \rightarrow CO\uparrow + H_2O \quad E^o = -0.52v \text{ at pH } 7 \tag{35}$$

$$\text{Annual ethanol capacity} = \frac{m_{eth,S19} \times 8000}{1000} \tag{36}$$

where $m_{eth,s19}$ is the mass flow rate (kg/h) of ethanol in stream S19ETH, and the annual operating time is 8000 h to get the ethanol capacity (t/year).

The modular TGEE-ethanol process and related mass and energy flow were simulated by using Aspen Plus©, as shown in **Figure 34**. The whole process model can be decomposed into several modular sub-process models, which have their attributes for different process

components while maintaining a consistent system boundary. A feed stream flowing at a volume rate of 40000 Nm^3/h with an annual operating time of 8000 h was selected, and the NRTL model was employed to simulate the physical properties of the inputs in the TGEE-ethanol process [185]. The TG-ethanol subprocess model was validated based on industrial-scale operating data, as reported in our previous work [104] while the ECR process modelling was based on the datasets obtained from bench experiments [33]. The model assumes that the TGEE process is co-located with the source of a tail gas stream to reduce the costs and eliminate the energy consumption for capture, storage and transportation of the tail gas [186], which aligns with the practices of the existing operating factory. A more detailed modelling description is listed in **Table 14**.

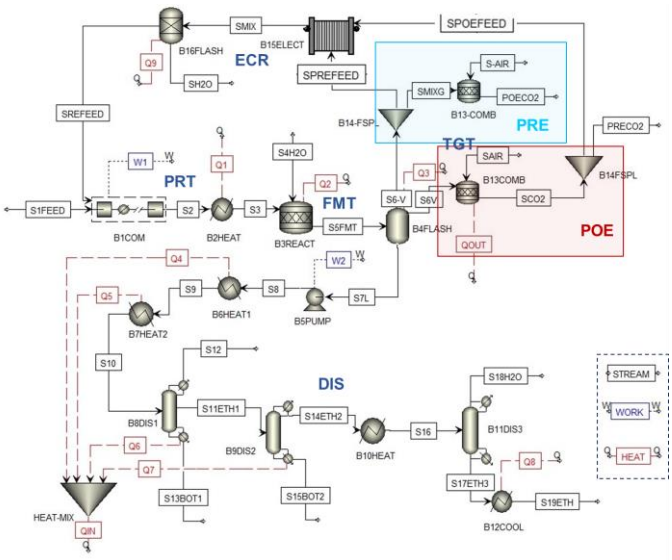

Figure 34. Process flow diagram of the TGEE process.

Table 14. Model Inputs.

Feed Conditions			
	Feed rate	40000	Nm^3/h
	Feed temperature	50	℃
	Feed Pressure	1.1	atm
Composition			
	CO	45-80	wt%
	CO_2	5-20	wt%
	N_2	10-35	wt%
Pretreatment			
Compressor-B1			
	Compressor model	Isentropic	
	Number of stages	3	stages
	Discharge pressure-stage 1	1.8	atm
	Discharge pressure-stage 2	3.1	atm
	Discharge pressure-stage 3	5.2	atm
	Cooler outlet temperature	25	℃
HeatX-B2			
	Inlet temperature	25	℃
	Outlet temperature	37	℃
Fermentation			
B3 Bio-fermentation reactor			
	Temperature	37	℃
	Pressure	0.52	atm
	Fermentation time	22	sec
	Ethanol yield	88	%
	Ethanol concentration	5	%
Material loadings			
	Phosphoric acid	0.64	% by mass of product
	Sodium hydroxide	0.40	% by mass of product
	Ammonia	17.10	% by mass of product
	Sodium hydrosulfide	0.86	% by mass of product
	Potassium hydroxide	1.18	% by mass of product
	Nitrogen	13.33	% by mass of product
	Water	8.6	Times of feedstock
Distillation			
First column-B9			
	Number of stages	18	Stages
	Feed stream	5	Above-stage
	Reflux ratio	3	
	Pressure	1.86	atm
	Ethanol concentration	>55	wt% by mass in distillate
Second column-B10			
	Number of stages	20	Stages
	Feed stream	7	Above-stage
	Reflux ratio	2.2	
	Pressure	2	atm
	Ethanol concentration	>95	wt% by mass in distillate
Dehydration-B12			
	Type	molecular sieves adsorption	
	Ethanol concentration	>99.5	wt% by mass in distillate
Tail-gas combustion			
Combustion-B7			
	Temperature	40	℃
	Pressure	1.1	atm
	Oxygenation efficiency	>99	%
ECR			
Electrolyzer-B8			
	Temperature	25	℃
	Pressure	1.3	atm
	CO_2 conversion rate	50	%
Separators			
	Type	Sep	
	Efficiency	>99.9	%

5.2.2.2 Scenario design

To aid the TGEE process scenario design and analysis, a tail gas composition survey was first conducted for different process industries, including steel, ammonia, iron alloy, calcium carbide, silicon carbide, phos-chemical, and acetic acid production [7, 8], and the results are provided in **Table A3**, which provides a reference for the scenario setting in this study. Among the tail gas streams surveyed, three typical industrial tail gas streams (steel, iron alloy, and calcium carbide production) were selected for the case studies in this work, with a total of 25 scenarios examined, as shown in **Table 15**. In particular, ECR0.1/0.2/0.3, etc. denote the ECR recycle ratio, which refers to the proportion of tail gas recycled to the ECR unit to the total amount of fermented off-gas from the FMT unit, as shown in **equation (37)**.

$$\text{Recycle ratio} = \frac{\text{Gas recycled to ECR unit}}{\text{Fermented off-gas}} = \frac{\text{SPREFEED or SPOEFEED}}{\text{S6V}} \quad (37)$$

where the SPREFEED, SPOEFEED and S6V are the gas mass flow rates, as shown in **Figure 35**.

Table 15. Scenarios design for the TGEE-ethanol production.

	Scenarios	Key features
Baseline scenario (BAS)	BAS-Steel (BASS) (CO-45%/CO_2-20%/N_2-35%) BAS-Iron alloy (BASI) (CO-70%/CO_2-20%/N_2-10%) BAS-Calcium carbide (BASC) (CO-80%/CO_2-5%/N_2-15%)	i. Three typical tail gases were selected as the feedstock stream and modelled as baseline scenarios. ii. All three BAS include PRT, FMT, DIS and TGT processes, and their simulation data were verified by the data of an actual operating TG-ethanol factory.
PRE and POE selection scenarios	PRE/POE-Steel-ECR0.1 (PRSE0.1/POSE0.1) PRE/POE-Steel-ECR0.2 (PRSE0.2/POSE0.2) PRE/POE-Steel-ECR0.3 (PRSE0.3/POSE0.3) PRE/POE-Steel-ECR0.4 (PRSE0.4/POSE0.4)	Compare the PRE and POE performance of upgraded TGEE technology: i. Same tail gas composition from the steel industry as the feedstock stream, with different ECR recycle ratios in PRE and POE processes.
	PRE/POE-Steel-ECR0.3 (PRSE0.3/POSE0.3) PRE/POE-Iron alloy-ECR0.3 (PRIE0.3/POIE0.3) PRE/POE-Calcium carbide-ECR0.3 (PRCE0.3/POCE0.3)	ii. Different tail gas feed streams (steel, iron alloy and calcium carbide) with the same ECR recycle ratio (fixed as 0.3) to ethanol production in PRE and POE processes.
Sequence scenarios for optimised processes	POE-Steel-ECR0.1/0.2/0.3/0.4 (POSE0.1/0.2/0.3/0.4) POE-Iron alloy-ECR0.1/0.3/0.5/0.7/0.9 (POIE0.1/0.3/0.5/0.7/0.9) POE-Calcium carbide-ECR0.1/0.3/0.5/0.7/0.9 (POCE0.1/0.3/0.5/0.7/0.9)	In the optimal POE process, the maximum ECR recycle ratio was determined according to the requirement of CO content in the mixed feed stream for fermentation, which should be ≥40% v/v.

5.2.3 Life cycle assessment

5.2.3.1 Life cycle carbon footprints

A “Cradle-to-gate” LCA of TGEE-ethanol was performed according to ISO 14040 & 14044 standards [187], covering the raw materials exploitation, upstream intermediate, ethanol production, and ECR process. The full life cycle carbon footprints for all scenarios in this study were calculated by using the mass and energy balances from the engineering process model. Estimates for the LCA carbon footprints associated with energy production, upstream utility and manufacture of chemicals were taken from the GaBi database [104], which includes six typical greenhouse gases (CO_2, CH_4, N_2O, HFCs, PFCs, SF_6), and their CO_2 equivalence (CO_2eq) were combined based on the100-year GWP [188]. The functional unit of this system was defined as the 1 ton of ethanol product [189]. LCA carbon footprints per ton of ethanol production from the TGEE process for different scenarios were calculated by **equation (38)**.

$$CF=\left(\begin{matrix}\text{Process carbon emission}+\sum_{n=1}^{N}\text{feedstock consumption}\times EF_n+\\ \sum_{k=1}^{K}\text{utilities consumption}\times EF_k\end{matrix}\right)-SC_{credit} \quad (38)$$

where CF is the net life cycle carbon footprints, EF is the emission factor of feedstock, n=1, …, N (total number of feedstocks), k=1, …, K (total number of utilities), SC_{credit} is the embodied credit of the steam.

According to the cut-off criteria of ISO 14044, any life cycle stages, processes, inputs or outputs that do not significantly affect the overall conclusions can be neglected from the analysis. Accordingly, this study excludes three complications: (i) background emission of the feedstock tail gas because of its low value to the original main-product process; (ii) transportation of any materials or energy as suggested by previous studies [190]; and (iii) equipment manufacturing, factory construction and facility replacement etc., due to their low impact to the overall analysis (<1%) [168]. Furthermore, this process produces excess steam by burning the unreacted CO from the fermented gas to recycle the heat for system use. If more steam is produced than the initial input, some carbon credits will be deducted because of possible steam resale to the upstream plant.

5.2.3.2 Data Inventories

Life cycle inventories of a series of scenarios for TGEE-ethanol production from tail gas in the steel, iron ally and calcium carbide industries are listed in the following **Table 16-18.**

Table 16. Life cycle inventory of tail gas from steel for ethanol production.

Inputs	Quantities									Unit (Per year)
	BASE	**PRSE0.1**	**POSE0.1**	**PRSE0.2**	**POSE0.2**	**PRSE0.3**	**POSE0.3**	**PRSE0.4**	**POSE0.4**	
CO					144					Mm^3
CO_2					64					Mm^3
N_2					112					Mm^3
Phosphoric acid	266	280	279	301	298	321	324	343	343	t
Sodium hydroxide	167	175	174	188	186	201	203	214	214	t
Ammonia	7118	7489	7451	8037	7962	8578	8666	9152	9166	t
Sodium hydrosulfide	358	377	375	404	400	431	436	460	461	t
Potassium hydroxide	491	517	514	555	549	592	598	632	632	t
Nitrogen	5549	5838	5809	6265	6207	6687	6755	7134	7145	t
Water	0.248	0.249	0.249	0.254	0.254	0.255	0.255	0.256	0.256	Mt
Grid power	55.01	57.92	57.82	63.08	62.88	68.98	69.52	76.38	76.49	GWh
PV	0	54	61	119	136	197	229	297	339	GWh
Steam	249091	322519	240041	332817	246617	338305	267258	364195	260604	GJ

Table 17. Life cycle inventory of tail gas from iron alloy for ethanol production.

Inputs	BASI	POIE0.1	POIE0.3	POIE0.5	POIE0.7	POIE0.9	Unit (Per year)
CO				224			Mm^3
CO_2				64			Mm^3
N_2				32			Mm^3
Phosphoric acid	415	439	498	567	728	1205	t
Sodium hydroxide	260	275	311	354	455	753	t
Ammonia	11099	11742	13294	15138	19443	32187	t
Sodium hydrosulfide	558	591	669	761	978	1619	t
Potassium hydroxide	766	810	917	1045	1342	2221	t
Nitrogen	8652	9153	10363	11801	15157	25091	t
Water	0.342	0.343	0.348	0.348	0.349	0.350	Mt
Grid power	68	71	82	99	141	268	GWh
PV	0	78	291	621	1318	3495	GWh
Steam	354001	373587	378731	415306	449567	657957	GJ

Table 18. Life cycle inventory of tail gas from carbide calcium for ethanol production.

Inputs	BASC	POCE0.1	POCE0.3	POCE0.5	POCE0.7	POCE0.9	Unit (Per year)
CO				256			Mm^3
CO_2				16			Mm^3
N_2				48			Mm^3
Phosphoric acid	479	483	543	617	748	1305	t
Sodium hydroxide	300	302	340	386	467	816	t
Ammonia	12805	12915	14517	16499	19981	34865	t
Sodium hydrosulfide	644	650	730	830	1005	1753	t
Potassium hydroxide	884	891	1002	1139	1379	2406	t
Nitrogen	9982	10068	11317	12861	15576	27178	t
Water	0.384	0.385	0.386	0.388	0.389	0.390	Mt
Grid power	74	75	86	104	138	286	GWh
PV	0	69	253	555	1078	3533	GWh
Steam	396580	391413	412302	431413	468449	641051	GJ

5.2.4 Techno-economic analysis

Discounted Cash Flow (DCF) [165] model, which aims to estimate the economic performance of an investment by using future cash flow predictions and discounting them to present value, is popularly used to evaluate the profitability of a project investment. In fact, capturing the time dependency of cashflows during the project is very important for investors. An investment is worth undertaking if it creates more value than it costs, considering the time value of money (discounted cash in-flows and out-flows). Therefore, in consideration of the time value of capital investment i.e., the DCF model assumes that money to be received or paid in the future is lower than the equivalent amount received or paid today [191]. To make an investment decision, the foreseen profit from an investment must be evaluated relative to some economic criteria, i.e., the quantitative measurement of profit concerning the investment necessary to generate that profit. The main indicators of DCF analysis are the net present value (NPV) and minimum selling price (MSP). A project with a positive NPV is regarded as being profitable whereas a project with a negative NPV results in a net loss. This means that, for a process to be economically viable, it must have an NPV above

zero (NPV=0 means break-even point, value created is equal to costs). Also, at this break-even point, the MSP can be estimated.

In this work, economic metrics such as NPV and minimum ethanol selling price (MESP) are selected as TEA indicators to perform the comparative analysis. It's assumed that the project lifetime is 20 years, discount rate is 8%, residual rate is 5%, and tax rate is 13%. A brief description of the economic model used in this study is presented as follows:

(1) The NPV is estimated as the sum of yearly cash flows discounted to the present year [192] at a specific interest rate, using **equation (39)**:

$$NPV=\sum_{t=1}^{T}\frac{C_t}{(1+\omega)^t}-C_0=\sum_{t=1}^{T}\frac{1}{(1+\omega)^t}\times[TAR-TPC-INT]-C_0=\sum_{t=1}^{T}\frac{1}{(1+\omega)^t}\times[TAR-FOC-VOC-INT]-(TEI+EEI) \quad (39)$$

where t (plant lifetime) =1, …, T, ω is the discount rate, C_t is net cash inflow during the plant's lifetime, C_0 is the total initial capital investment, TAR is the total annual revenue, TPC is the total production cost, INT is the cost-income tax, FOC is the fixed operating cost, VOC is the variable operating cost, TEI is the TG-ethanol plant investment and EEI is the ECR equipment investment.

Finally, the NPV is fully given by **equation (40)**:

$$NPV = \sum_{t=1}^{T} \frac{1}{(1+\omega)^t} \times \Big[(\text{ethanol revenue} + \text{carbon tax} + \text{residual value}) - \Big(\begin{matrix}\text{operating and maintenance costs} + \text{administrative costs} + \text{distribution and selling costs} \\ + \text{labour cost}\end{matrix}\Big) - \Big(\sum_{n=1}^{N} \text{feedstock consumption} \times \text{price} + \sum_{k=1}^{K} \text{utilities} \times \text{price}\Big) - \text{income taxes}\Big] - \Big(\begin{matrix}\text{TG-ethanol plant costs} + \text{electrolytic cell costs} + \text{PEM costs} + \text{electrode costs} \\ + \text{KOH electrolyte costs}\end{matrix}\Big) \quad (40)$$

where n=1, …, N (total number of raw materials), k=1, …, K (total number of utilities), PEM is the proton exchange membrane, and the carbon tax is extracted from literature [193].

(2) When NPV=0, MESP (sum of all costs) could be estimated for which the project would break even (by rearranging **equation (39)**) using the goal-seek function and setting the NPV to zero [190] while maintaining all the other variables constant.

5.2.5 Monte Carlo simulation and sensitivity analysis

Monte Carlo simulation forecasts possible outcomes by repeatedly generating random values within defined probability distributions for independent variables. This crucial tool for risk and uncertainty assessment provides a more nuanced and reliable explanation compared to traditional single LCA and TEA results. The process involves establishing a predictive model, identifying the dependent and independent variables, specifying probability distributions for input

variables, and running iterative simulations to obtain representative results [194, 195]. In this study, a Monte Carlo simulation with 10000 iterations was implemented. Distributions of parameters are assigned to investigate how input uncertainty propagates through the model.

In the LCA carbon footprints of the Monte Carlo simulation, the probability distribution and data sources of the involved key parameters (feedstocks, materials and utilities) are summarised in **Table 19**. A triangular distribution, widely employed in previous studies [168, 192, 195, 196], was assigned to these variables. The probability results of LCA carbon footprints can be estimated according to **equation (38)**.

The TEA analysis examines uncertainties in NPV and MESP associated with market price fluctuations, capital investment, operating costs, discount and tax rates. The key economic variables used in the Monte Carlo simulation are summarised in **Table 20**. A triangular distribution is assigned to the cost of feedstocks for which there is some confidence in the mode and range of possible values [190], and normal distribution is employed for ethanol price. It is worth noting that the model is quite flexible, and other distribution functions can be considered if more appropriate distribution curves can be found.

Table 19. Summary of key life cycle GHG emissions parameters in the Monte Carlo simulation.

Parameter	Distribution	Value*	Units	Data source	Technical description
Water	Triangular	(0.00016, 0.0002, 0.00024)	$kgCO_2eq/kg$	GaBi database（CN）	Surface water purification
Grid power	Triangular	(0.456, 0.570, 0.684)	$kgCO_2eq/kWh$	China electricity council 2020 average [169]	Electricity grid mix
PV	Triangular	(0.043, 0.054, 0.065)	$kgCO_2eq/kWh$	GaBi database（CN）	Electricity from Photovoltaic
Coal to steam	Triangular	(0.09, 0.112, 0.134)	$kgCO_2eq/MJ$	GaBi database（CN）	Hard coal 90%
Phosphoric acid	Triangular	(1.64, 2.05, 2.46)	$kgCO_2eq/kg$	GaBi database (US)	Phosphate wet process phosphoric acid
Sodium hydroxide	Triangular	(0.23, 0.287, 0.344)	$kgCO_2eq/kg$	GaBi database (EU-28), concentration corrected	Technology mix
Ammonia	Triangular	(0.53, 0.67, 0.80)	$kgCO_2eq/kg$	GaBi database（US）	Ammonium mixed with water
Sodium hydrosulfide	Triangular	(0.407, 0.509, 0.611)	$kgCO_2eq/kg$	GaBi modelling is based on the absorption of hydrogen sulphide by sodium hydroxide [170]	Sodium hydroxide absorption method
Potassium hydroxide	Triangular	(0.848, 1.272, 1.060)	$kgCO_2eq/kg$	GaBi database (EU-28), concentration corrected	Technology mix
Nitrogen	Triangular	(0.097, 0.145, 0.121)	$kgCO_2eq/kg$	GaBi database (CN)	Cryogenic air separation

Distributions are written as: Triangular (lower, mode, upper),

Note: CN (China), US (United States), EU-28 (EU 28).

Table 20. Summary of key economic parameters in the Monte Carlo analysis.

Parameter	Value or Distribution	Units	Remarks
Plant lifetime	20	years	
Discount rate	Triangular (6, 8, 10)	%	Straight-line depreciation
Income tax rate	Triangular (10, 13, 16)	%	State taxation administration
Carbon tax	Triangular (7, 30, 50)	$/t$CO_2$	[68]
Residual rate	Triangular (4, 5, 6)	%	[48]
Total capital investment			
Ethanol plant	58571429	$	
ECR equipment			
electrolytic cell	Triangular (130, 163, 195)	$/t ECR-CO	
PEM (proton exchange membrane)	Triangular (6.51, 8.13, 9.76)	$/t ECR-CO	[33]
electrode	Triangular (5.31, 6.64, 7.96)	$/t ECR-CO	
KOH electrolyte	Triangular (3.50, 4.37, 5.25)	$/t ECR-CO	
Fixed operating costs			
Operating and maintenance cost	2% of total capital investment		
Administrative cost	1% of total capital investment		[39, 47]
Distribution and selling cost	1% of total capital investment		
Labor cost	1% of total capital investment		
Variable operating costs			
Water	Triangular (0.34, 0.43, 0.51)	$/t	
Grid power	Triangular (0.043, 0.086, 0.114)	$/kWh	
PV (photovoltaic)	Triangular (0.014, 0.036, 0.050)	$/kWh	
steam	Triangular (0.009, 0.011, 0.013)	$/MJ	
Tail-gas	Triangular (0.024, 0.034, 0.40)	$/$m^3$	*
Phosphoric acid (75%)	Triangular (514, 643, 771)	$/t	
Sodium hydroxide (32%)	Triangular (114, 143, 173)	$/t	
Ammonia (25%)	Triangular (91, 114, 137)	$/t	
Sodium hydrosulfide (38%)	Triangular (126, 157, 189)	$/t	
Potassium hydroxide	Triangular (549, 686, 823)	$/t	
Product			
Steam	Triangular (0.009, 0.011, 0.013)	$/MJ	
Ethanol price	Normal (1071, 90)	$/t	*

Distributions are written as Triangular (lower, mode, upper) and Normal (mean, standard deviation).

* Average price in 2010-2022.

A sensitivity analysis was further performed to identify the high-impact variables which focused on the reduction potential of LCA carbon footprints and NPV. For the sensitivity analysis method, variance components analysis [197] was employed to estimate the effect of each random effect's distribution on the variance of the dependent variable. Then, the results were used in an Anderson-Darling (*AD*) test to determine the *AD* value for the varied variable [182], with the *AD* value falling outside the two-tail 95% confidence interval indicating high-impact variables.

5.2.6 Comprehensive analysis of entropy weight method

Given the multi-dimensional assessment in this study, the use of a unified comprehensive evaluation method is necessary for semi-quantitative comparisons of different scenarios. To ensure the reliability and accuracy of LCA & TEA analyses in a multi-index system like the TGEE plant system, the entropy weight (EW) method [47], an objective weighting technique, is chosen for calculating the comprehensive performance index (CP) of the TGEE process using five indicators: CF, NPV, MESP, carbon efficiency (CE), and energy demand (ED). To be clear, CE is the effective carbon conversion rate of CO to ethanol, the

formula is shown in **equation (41)**. ED is the net energy demand of electricity and steam consumption, and electricity consumption is normalised to MJ through 3.6 MJ/kWh, as shown in **equation (42)**.

$$\text{Carbon efficiency}=\frac{\text{Carbon mass in ethanol}}{\text{Carbon mass of CO in S1FEED}} \quad (41)$$

$$\text{Energy demand} = \text{PV} + \text{Grid power} + \text{Input steam} - \text{Output steam} \quad (42)$$

The EW procedure is as follows:

(1) The five indicators are normalised via a range normalisation method. CE and NPV are positive performance indicators for which **equation (43)** should be used for normalisation. CF, MESP and ED are considered as being negative indicators where **equation (44)** should be used for normalisation.

$$Y_{ij} = (1-\alpha) + \alpha \frac{PI_{ij} - MinPI_{ij}}{MaxPI_{ij} - MinPI_{ij}} \quad (43)$$

$$Y_{ij} = (1-\alpha) + \alpha \frac{MaxPI_{ij} - PI_{ij}}{MaxPI_{ij} - MinPI_{ij}} \quad (44)$$

where Y_{ij} and PI_{ij} are the normalised and original values of the j_{th} sub-indicator in the i_{th} scenarios, respectively, and α belongs to (0,1), which is set to 0.9 according to the literature [47].

(2) The information entropy E_j of the five selected indicators were calculated with **equation (45)**. A lower information entropy results in a higher indicator dispersion, exerting a greater influence on CP.

$$E_j = -\frac{1}{lnm}\sum_{i=1}^{m}\frac{Y_{ij}}{\sum_i^m Y_{ij}} \times ln\frac{Y_{ij}}{\sum_i^m Y_{ij}} \quad (45)$$

where *m* is the overall number of scenarios, $0 \leq E_j \leq 1$.

(3) The difference coefficient (D_j), induced by the j_{th} sub-indicator was evaluated by using **equation (46)**:

$$D_j = 1 - E_j \tag{46}$$

(4) The weights W_j for each sub-indicator are calculated by normalising the coefficients of the different indicators using **equation. (47)**:

$$W_j = \frac{D_j}{\sum_{j=1}^{m} D_j} \tag{47}$$

(5) Then, the resultant comprehensive performance index (CP) of each TGEE process scenario can be obtained by using **equation (48)**:

$$CP_i = \sum_{j=1}^{m} Y_{ij} \times W_j \tag{48}$$

5.3 Results and discussion

5.3.1 PRE VS POE performance for TGEE-ethanol production

As shown in **Figure 34**, there are two options to configure the ECR as a process intensification technology for the TG-ethanol process: pre-combustion ECR (PRE) and post-combustion ECR (POE). The difference is that in PRE, part of the CO in the original tail gas surviving the fermentation process is recycled back to the fermenter, together with the CO from the CO_2 conversion in ECR, whereas in POE all the CO is from the ECR conversion of CO_2 because the CO surviving the

fermentation was completely combusted to CO_2 before ECR. As a result, the energy demand of ECR for producing the same amount of ethanol could vary for the two different ECR configurations. Therefore, the overall TGEE performance is evaluated in different conditions by (i) varying the fermented off-gas recycle ratio for ECR (ECR=0.1, 0.2, 0.3, 0.4) for a given tail gas stream from the steel industry and (ii) varying the tail gas streams with different composition at a selected ECR recycle ratio of ECR=0.3. This has led to a total of 18 sub-scenarios examined for ECR process integration as defined in **Table 15**, and **Table 21-22** presents the full set of numerical results obtained on ethanol capacity, carbon efficiency, energy demand and carbon footprints with the same amount of tail gas feed stream (40000 Nm^3/h).

In scenario (i), the results demonstrate that the ethanol capacity and carbon efficiency were found to be almost identical for both PRE and POE processes, as shown in **Table 21.** In the case of the process intensification with the PRE process for steel tail gas (PRSE), an increase in ECR recycle ratio from 0.1 to 0.4 (PRSE0.1 to PRSE 0.4) led to an increase in ethanol capacity by 5–28% compared with the baseline scenario (BASS) (41625 t/year), and the carbon efficiency is 2–12% higher than BASS (28%). Clearly, increasing the ECR recycle

ratio is beneficial for both ethanol capacity and carbon efficiency. Similar ethanol capacity and carbon efficiency results were also obtained for ethanol production with the POE process for steel tail gas (POSE). However, the overall energy demand and carbon footprints were found to differ considerably between the two different ECR configuration scenarios, as shown in **Figure 35(a, b).** It can be seen that the electrical energy demand of ECR for CO_2-to-CO conversion increased almost linearly with increasing tail gas recycle ratio for both PRSE and POSE, with little difference obtained between the PRSE and POSE at the same tail gas recycle ratios. Furthermore, compared to PRSE, POSE was found to give rise to considerably lower net energy demand and carbon footprints, because of its lower steam consumption, resulting in energy and carbon credits. For instance, the energy demand of POSE0.4 was reduced by 9% with a 10% reduction in the carbon footprints compared with PRSE0.4.

In scenario (ii), the results show that regardless of the retrofit modes for TGEE-ethanol production from all three different tail gas streams, the introduction of ECR (PRE or POE) boosted the ethanol capacity by 20% with up to 5% improvement in carbon efficiency **(Table 22).** However, the POE process shows persistently higher energy efficiency and lower

carbon footprints than the PRE process, as shown in **Figure 35(c, d)**. In the case of ethanol production from steel tail gas, the energy demand and carbon footprints of POSE0.3 were reduced by 12% and 7%, respectively, compared to PRSE0.3. A similar trend can be observed in the other two series of cases (PRIE0.3 & POIE0.3, PRCE0.3 & POCE0.3). The results also demonstrate that due to the source of tail gas, different initial CO concentrations also had a considerable effect on the energy demand and associated carbon footprints of the ECR-intensified ethanol production, with the order of energy demand and carbon footprints per ton of ethanol being POSE0.3 > POIE0.3 > POCE0.3. Among the tail gas streams examined, calcium carbide tail gas has the highest initial CO concentration, showing the best overall performance (POCE0.3).

Based on the above analysis, the POE process generally has better performance than PRE for all tail gas streams examined, making it more appealing for medium to long-term carbon neutrality targets. Consequently, the optimal POE process will dominate in the subsequent analysis.

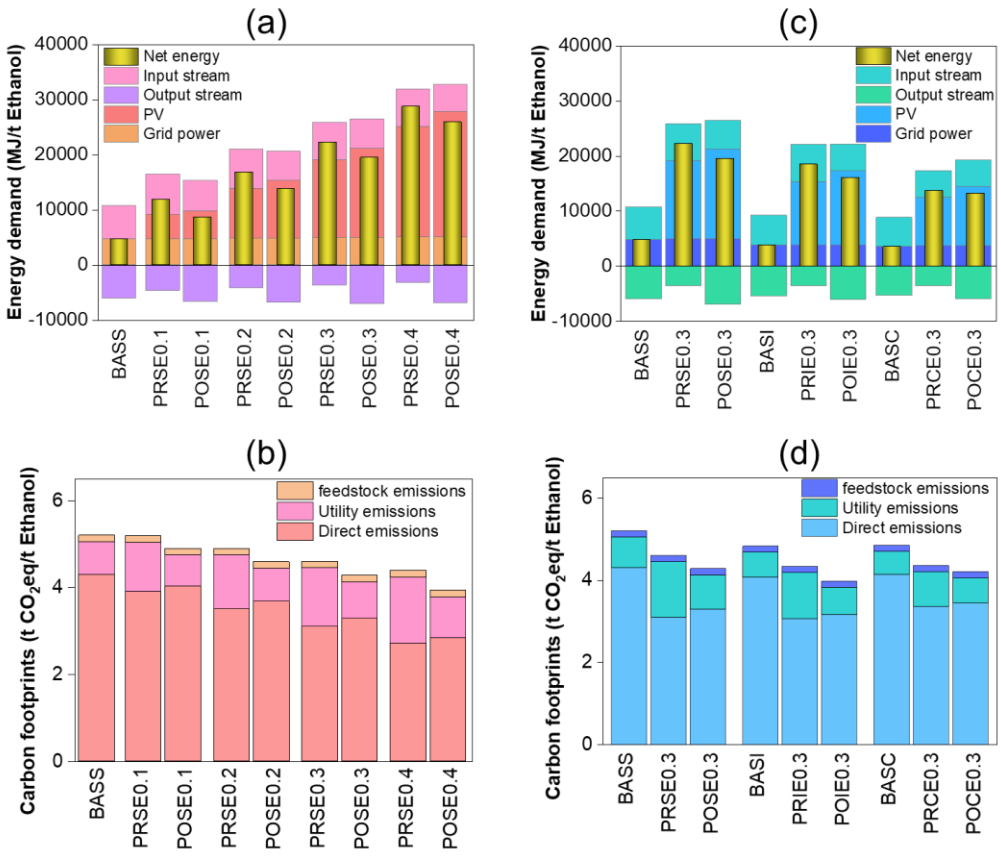

Figure 35. Performance comparison for POE and PRE. (a), (b) the energy demand and carbon footprints of different ECR recycle ratios for a given tail gas composition; (c), (d) the energy demand and carbon footprints of different tail gas streams with the same ECR recycle ratio.

Table 21. PRE and POE performance comparison for ethanol production from steel tail gas.

Items	BASE	PRSE0.1	POSE0.1	PRSE0.2	POSE0.2	PRSE0.3	POSE0.3	PRSE0.4	POSE0.4	Unit
Capacity	41625	43795	43576	46998	46563	50163	50678	53522	53601	t/year
Carbon efficiency	28	29	29	32	31	33	34	36	36	%
Water	248000	248800	248800	254400	250400	255200	255200	256000	256000	t/year
Electricity										
Total	1322	2548	2731	3866	4264	5310	5891	6977	7743	kWh/t
Grid power	1322	1323	1327	1342	1350	1375	1372	1427	1427	kWh/t
PV	0	1225	1404	2524	2913	3935	4519	5550	6316	kWh/t
Steam										
Net steam	−7	2759	−1104	2974	−1487	3132	−1708	3631	−1906	MJ/t
Output steam	−5991	−4605	−6612	−4108	−6784	−3612	−6982	−3174	−6788	MJ/t
Input steam	5984	7364	5509	7081	5296	6744	5274	6805	4862	MJ/t
Carbon footprints										
Net emissions	5.20	5.19	4.9	4.9	4.59	4.6	4.28	4.39	3.93	t CO_2eq/t
Direct emissions	4.300	3.905	4.037	3.513	3.681	3.102	3.294	2.720	2.843	t CO_2eq/t
Grid power emissions	0.753	0.754	0.756	0.765	0.770	0.784	0.782	0.813	0.813	t CO_2eq/t
PV emissions	0.000	0.066	0.076	0.136	0.157	0.212	0.244	0.300	0.341	t CO_2eq/t
Steam emissions	−0.001	0.309	−0.124	0.333	−0.167	0.351	−0.191	0.407	−0.216	t CO_2eq/t
Water emissions	0.001	0.00103	0.00103	0.00098	0.00097	0.00092	0.00091	0.00087	0.00086	t CO_2eq/t
Feedstock emission	0.15	0.15	0.15	0.15	0.15	0.15	0.15	0.15	0.15	t CO_2eq/t

Table 22. PRE and POE performance comparison for ethanol production from three industrial tail gas.

Items	BASS	PRSE0.3	POSE0.3	BASI	PRIE0.3	PRCE0.3	BASC	PRCE0.3	POCE0.3	Unit
Capacity	41625	50163	50678	64906	78263	77742	74883	85458	84897	t/year
Carbon efficiency	28	33	34	28	34	33	28	32	32	%
Water	248000	255200	255200	342400	348000	348000	384000	386400	386400	t/year
Electricity										
Total	1322	5310	5891	1049	4260	4802	986	3482	4003	kWh/t
Grid power	1322	1375	1372	1049	1056	1058	986	1013	1019	kWh/t
PV	0	3935	4519	0	3204	3744	0	2468	2985	kWh/t
Steam										
Net steam	−7	3132	−1708	−9	3172	−1255	−20	1196	−1132	MJ/t
Output steam	−5991	−3612	−6982	−5463	−3578	−6126	−5316	−3612	−5988	MJ/t
Input steam	5984	6744	5274	5454	6750	4872	5296	4809	4857	MJ/t
Carbon footprints										
Net emissions	5.20	4.6	4.28	4.83	4.34	3.98	4.85	4.35	4.21	t CO_2eq/t
Direct emissions	4.300	3.102	3.294	3.06	3.21	3.17	4.14	3.36	3.44	t CO_2eq/t
Grid power emissions	0.753	0.784	0.782	0.598	0.602	0.603	0.56	0.58	0.58	t CO_2eq/t
PV emissions	0.000	0.212	0.244	0	0.32	0.20	0	0.13	0.16	t CO_2eq/t
Steam emissions	−0.001	0.351	−0.191	−0.001	0.51	−0.14	−0.002	0.13	−0.13	t CO_2eq/t
Water emissions	0.001	0.00092	0.00091	0.001	0.0008	0.0006	0.001	0.0008	0.0008	t CO_2eq/t
Feedstock emission	0.15	0.15	0.15	0.15	0.15	0.15	0.15	0.15	0.15	t CO_2eq/t

5.3.2 Technical analysis of intensified ethanol production with POE

The POE performance of the TGEE-ethanol process corresponding to different ECR recycle ratios, which govern the composition of the mixed feed streams for bio-fermentation, was evaluated in detail for different industrial tail gas streams. The maximum ECR recycle ratio was determined according to the requirement of CO content in the mixed feed stream for fermentation, which should be ≥40% v/v. Because proprietary microbes are involved in bio-fermentation, the special microbes consume industrial tail gas to make ethanol, much like yeast consuming sugars to make beer in a brewery, which requires a suitable range of gas concentrations. If the recycle ratio is greater than current values, the CO content in the mixed feedstock stream will be less than 40%, which will result in the bio-fermentation reaction being inefficient or even stopping the reaction.

Table 23 shows the key technical indicators across all scenarios simulated by Aspen Plus modelling. Apparently, the coupling of the ECR unit has a positive effect on the ethanol capacity, as evidenced by the volume flow of CO in the SREFEED stream and ethanol capacity, where

more CO is recycled by the ECR process with the ECR recycle ratio increasing, and thus more CO is reused as feedstock to produce ethanol. From the steel tail gas for TGEE-ethanol production, it is shown that the ethanol capacity of POSE0.1 to POSE0.4 is increased by 5% to 29% compared to the BASS (41625 t/year). Simultaneously, the ECR unit also has a positive impact on the steam demand. With the ECR recycle ratio increasing, the amount of self-produced steam from CO combustion in the TGT is enhanced, allowing for the resale of surplus steam to upstream factories in addition to supplying self-use. Since the ECR unit is an electricity-driven process, the total electricity demand is sharply increased. The electricity demand of POSE0.4 (7743 kWh/t) has increased 4.8 times compared to BASS (1322 kWh/t), with the share of ECR electricity up to 82%.

A similar trend could be observed in the other two series of cases, as the higher CO initial concentration in the tail gas of iron alloy and calcium carbide industries compared to steel, their ECR recycle ratio can be larger, reaching 0.9, resulting in a larger ethanol capacity, electricity demand and steam surplus. When comparing the indicators of cases with their maximum ECR recycle ratio (POSE0.4, POIE0.9, POCE0.9), the ethanol capacity and surplus steam of POIE0.9 and POCE0.9 are

more than 3 times that of POSE0.4, and electricity demand is more than 2 times, with the ECR electricity share increases to about 90%. Remarkably, the ECR process can be supplied by the low-voltage power generated by the photovoltaic panel instead of coming from the national grid system. Therefore, electricity from renewable energy not only meets the great demand for the ECR process but also reduces carbon emissions.

In particular, carbon efficiency is considerably improved due to the ECR integration. In steel tail gas for TGEE-ethanol production, the carbon efficiency can be improved from 28% to 36% (BASS to POSE0.4), while a higher carbon efficiency is achieved in the iron alloy and calcium carbide tail gas to ethanol cases, that is 28% to 82% (BASI to POIE0.9) and 28% to 78% (BASC to POCE0.9). **Figure 36** illustrates the carbon flow diagrams for baseline and their potential maximum carbon efficiency cases to visually compare the carbon content changes in the process involved. With the same carbon mass input (77123 t) in BASS and POSE0.4 **(Figure 36(a)),** the carbon mass in ethanol increases from 21718 t to 27966 t (29% increase) with an 8% increase in carbon efficiency, and the carbon mass in final carbon dioxide decreases from 83084 t to 76282 t with 8% decrease in direct emissions. It’s worth noting

that the final carbon dioxide emissions (including raw material CO_2) here are different from the net carbon footprints in the subsequent LCA analysis, where the CO_2 in the feedstock is deducted to calculate the life cycle carbon footprints. Due to the larger carbon mass input in the iron alloy (119970 t in BASI and POSE0.9) and calcium carbide (137108 t in BASC and POCE0.9) tail gas, matched with a higher ECR recycle ratio, leading to a larger ethanol capacity with carbon efficiency improvement up to 82% and 78% **(Figure 36(b, c)),** respectively. In addition, further optimisation methods to enhance carbon efficiency can be taken from two aspects: 1) Improve the conversion rate of ethanol produced by bio-fermentation, which can be achieved by optimising the gas component and pressure, cultivating more robust and durable proprietary microbes, precisely controlling the pH & temperature and strengthen the gas-liquid mass transfer effect of the bioreactor [198]. 2) Improve the reduction rate of CO_2 to CO in the ECR reaction, which can be achieved by developing efficient catalysts, electrodes and electrolytes, optimising current density and reaction interface, enhance the molecular understanding of CO_2 electroreduction [199].

Table 23. Key technical indicators across all scenarios.

Scenarios	Volume flow in streams (Nm^3/h)			Ethanol capacity (t/year)	Electricity (kWh/t)	Grid power (kWh/t)	ECR electricity (PV) (kWh/t)	Net steam (MJ/t)	Carbon efficiency (%)
	S1FEED	CO in S1FEED	CO in SREFEED						
BASS	40000	18000	/	41625	1322	1322	0	−7	28
POSE0.1			1082	43576	2731	1327	1404	−1104	29
POSE0.2			2492	46563	4264	1350	2913	−1487	32
POSE0.3			4433	50678	5891	1372	4519	−1708	34
POSE0.4			5907	53601	7743	1427	6316	−1926	36
BASI	40000	28000	/	64906	1049	1049	0	−9	28
POIE0.1			1423	68668	2179	1038	1141	−478	30
POIE0.3			5517	77742	4802	1058	3744	−1255	34
POIE0.5			10532	88527	8134	1123	7011	−1757	39
POIE0.7			22523	113704	12826	1237	11589	−3160	50
POIE0.9			26384	188231	19991	1426	18565	−5859	82
BASC	40000	32000	/	74883	986	986	0	−20	28
POCE0.1			1244	75526	1896	993	903	−787	29
POCE0.3			4445	84897	4003	1019	2985	−1132	32
POCE0.5			9827	96484	6827	1079	5748	−1614	37
POCE0.7			19467	116847	10407	1182	9224	−2850	45
POCE0.9			25152	203889	18733	1405	17329	−6420	78

Note: Carbon efficiency = (carbon mass in ethanol) / (carbon mass in CO).

S1FEED (shown in Figure 2) represents the feedstock stream, and the tail gas composition is $CO/CO_2/N_2$.

SREFEED (shown in Figure 2) represents the recycled stream from the ECR process (CO_2 converted into CO with a 50% conversion rate), mixed into S1FEED as the feedstock stream.

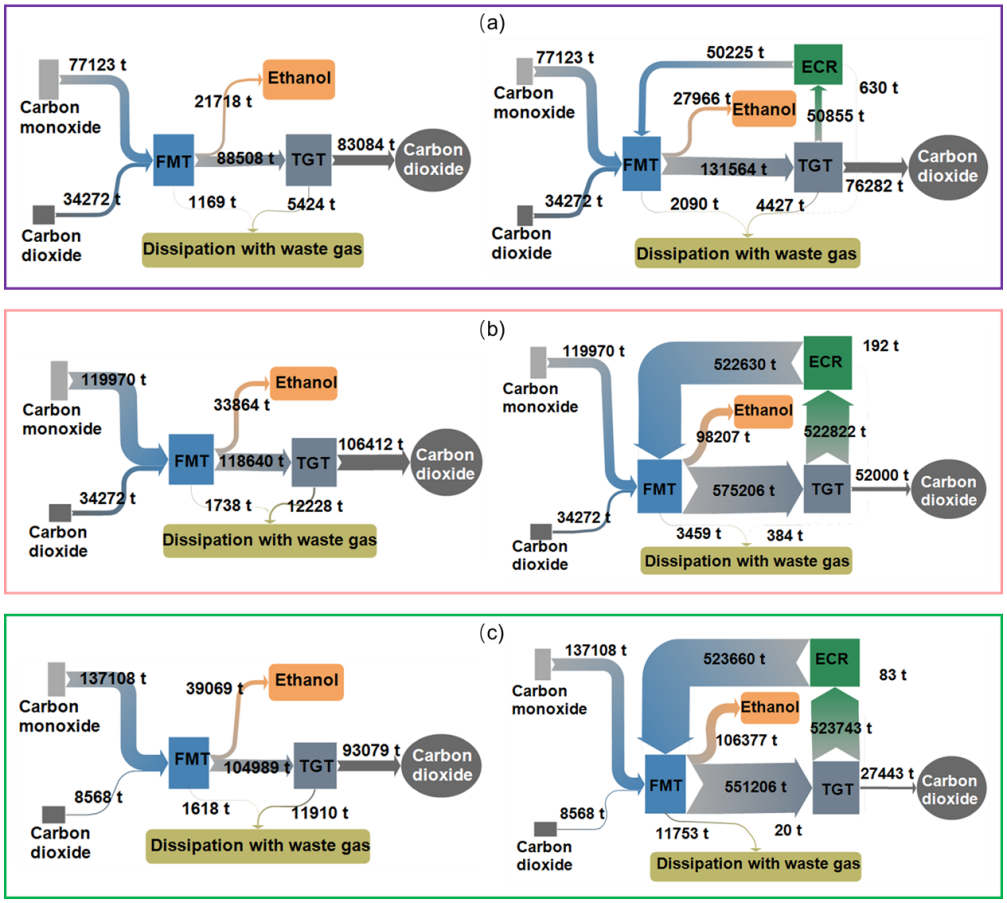

Figure 36. Carbon flow diagrams for the BAS scenario and their potential maximum carbon efficiency scenario. (a) steel tail gas to ethanol (BASS/POSE0.4), (b) iron alloy tail gas to ethanol (BASI/POIE0.9), and (c) calcium carbide tail gas to ethanol (BASC/POCE0.9). The numbers in the figure represent the annualized carbon mass flow.

5.3.3 Life cycle assessment

Figure 37(a)-(c) show the life cycle carbon footprints contribution of TGEE-ethanol production from three industrial tail gases, including direct

emissions, feedstock emissions (nitrogen, potassium hydroxide, sodium hydrosulphide, ammonia, sodium hydroxide and phosphoric acid emissions), utility emissions (grid power, PV, water) and steam carbon credits. In most scenarios (except POIE0.9 and POCE0.9 scenarios), it clearly shows that direct emissions account for the largest share in the entire life cycle carbon footprints, followed by utility emissions, with feedstock emissions being the smallest contributions. For POIE0.9 and POCE0.9 scenarios, utility emissions become the primary contributor due to the extensive electricity demand by the ECR process, while direct emissions sharply decrease benefiting from the maximum ECR intensification recycle ratio. In detail, from BASS to POSE0.4, the life cycle carbon footprints reduced from 5.20 t CO_2eq/t to 3.93 t CO_2eq/t (32% decrease), and the proportion of direct emissions decreased from 83% to 72%, utility emissions increased from 14% to 24%, negative emissions from steam credits increased from 0.1% to 5.5%. Similar results were observed in the iron alloy and calcium carbide tail gas to ethanol production cases, with more significant changes due to the higher maximum ECR recycle ratio. For instance, from BASI to POIE0.9, life cycle carbon footprints decreased from 4.83 t CO_2eq/t to 1.77 t CO_2eq/t (63% decrease), benefiting from a reduction in direct emissions

from 84% to 26% and an increase in negative steam emissions from 0.1% to 37%, respectively. Overall, as the ECR recycle ratio increases, direct emissions decrease, electricity emissions increase, and negative emissions from steam carbon credits also increase, leading to a decrease in net life cycle carbon footprints. See **Table A4** for numerical details.

Figure 37(d)-(f) displays the estimated life cycle carbon footprints probable range based on Monte Carlo simulation to discuss the uncertainty of life cycle inventory. For the probability density function of life cycle carbon footprints, it is seen that with the ECR ratio increasing, the uncertainty will expand, which should result from the great amount of electricity consumption. However, most curve distributions of probability density function between different ECR ratios are almost not overlapped, which could confirm that the data regularity about carbon footprints between each other is credible. Notably, higher CO concentration in the feed stream and ECR recycle ratio operating conditions result in a wider range of life cycle carbon footprints. In detail, POSE0.4 has a wider life cycle carbon footprint range (3.71 – 4.18 t CO_2eq/t) than BASS (5.05 – 5.38 t CO_2eq/t). As for the iron alloy and calcium carbide tail gas in ethanol production, the uncertainties in the

case of their maximum ECR recycle ratio are further expanded, i.e., the range of life cycle carbon footprints was expanded to 1.41 – 2.25 t CO_2eq/t (POIE0.9), 1.65 – 2.46 t CO_2eq/t (POCE0.9), respectively, which all wider than POSE0.4 cases.

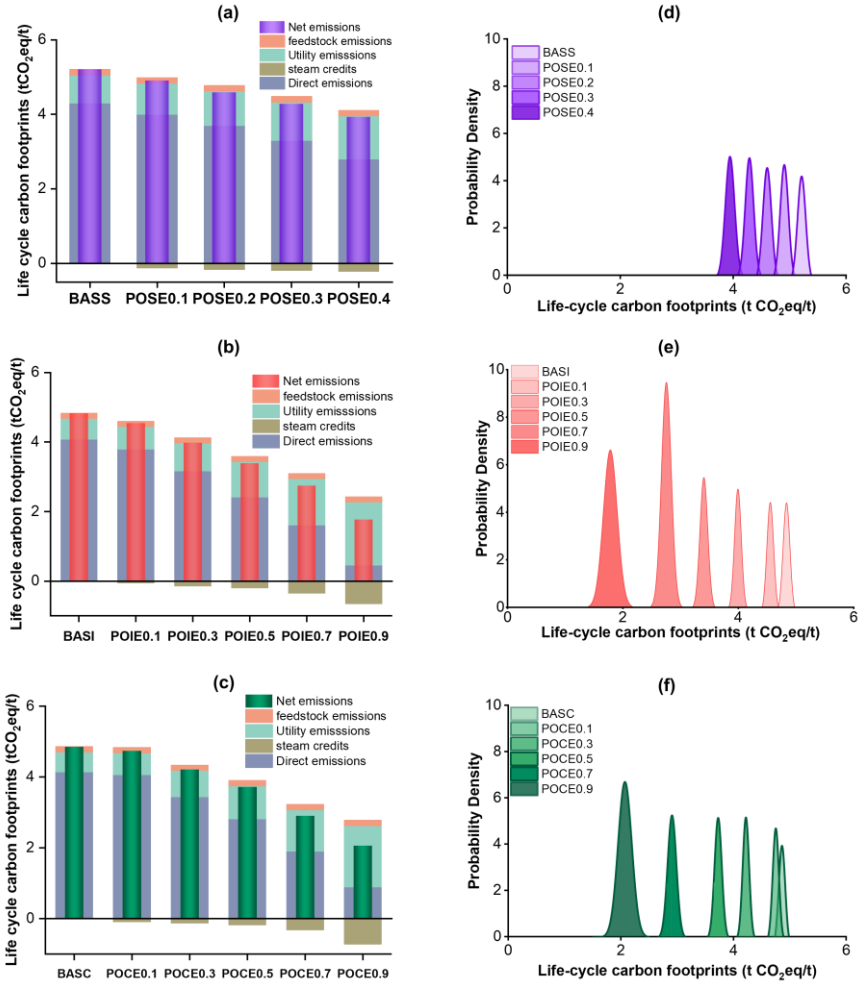

Figure 37. Life cycle carbon footprints and possible range estimated by Monte Carlo simulation for TGEE-ethanol production from three industrial tail gas streams, the left column shows the life cycle carbon footprints contribution and the right column shows the corresponding range, “probability density” as a relative proportion of modelled results. (a), (d) steel tail gas as feed stream; (b), (e) iron alloy tail gas as feed stream; (c), (f) calcium carbide tail gas as feed stream.

In addition, this work also estimated the carbon reduction potential range between the BAS and its different ECR recycle ratio scenarios, as shown in **Figure 38,** with the largest reduction potential coming from iron alloy tail gas-based TGEE-ethanol (POIE0.9 of 55–70%), followed by the calcium carbide tail gas feedstock (POCE0.9 of 51–65%), and finally steel (POSE0.4 of 28–36%). Since the CO concentration of iron alloy (POIE0.9) is lower than calcium carbide tail gas (POCE0.9) but results in higher carbon efficiency and carbon reduction potential, this suggests that there is an optimal scale for the tail gas feedstock and not just a case of 'bigger is better'. As for the critical effect parameters affecting the carbon reduction potential, this will be discussed further in the sensitivity analysis. Overall, the reduction in life cycle carbon footprints highlights the substantial carbon reduction potential of ethanol production from TGEE technology, suggesting that this technology has a promising future if policies are targeted at mitigating climate change.

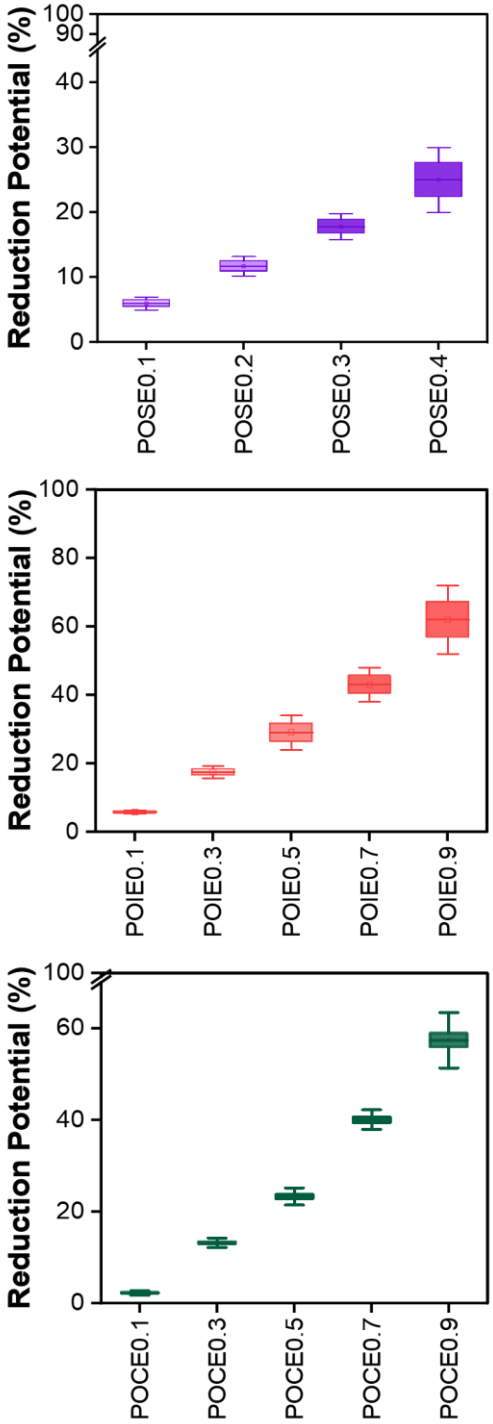

Figure 38. Carbon reduction potential and possible range estimated by Monte Carlo simulation.

5.3.4 Techno-economic analysis

NPV and MESP across all scenarios were estimated using the discount cash flow method to assess the techno-economic performance of TGEE-ethanol production. The key parameters considered for NPV and MESP include plant lifetime, discount and residual rate, total capital investment, fixed operating costs, variable operating costs, product revenue and tax costs, which can be found in **Table 19**.

The NPV probability results of all cases were illustrated with the cumulative distribution function curve in **Figure 39**. For TGEE-ethanol production from three typical tail gas cases, Monte Carlo simulation suggests that nearly all scenarios display about 100% probability of NPV>0, and POIE0.9 (P>78%) and POCE0.9 (P>93%) also show a positive NPV with a large probability. These results indicated that from an economic perspective, the investment in the project of tail gas for ethanol production is economically feasible within 20 years plant's lifetime, assuming that the ethanol price is between \$786–1071/t in Monte Carlo simulation.

When comparing the NPV range across three baseline cases, the probable NPV of BASS (M\$38–310) < BASI (M\$160–597) < BASC (M\$216–769). The reason is that higher CO concentration leads to

increased ethanol capacity and revenue, thereby augmenting NPV. After integrating ECR technology, the NPV growth rate slows down, which is mainly caused by the capital-intensive investment in the new ECR facility and more electricity demand, but the potential maximum NPV increases with the ECR recycle ratio, demonstrating the sustainable development prospects of the TGEE technology. As for the key effect parameters affecting NPV, this will be discussed further in Section 3.5 sensitivity analysis.

Figure 40(a) shows the MESP distribution of TGEE-ethanol, including fixed operating costs, materials costs, utility costs, tax costs and carbon tax credit (See numerical results in **Table A5**). The MESP for BASS is estimated to be $598/t, with materials costs (44%) accounting for the major portion, followed by fixed operating costs (23%) and utility costs (19%). From POSE0.1 to POSE0.4 cases, the MESP ($620/t to $743/t) increases as the ECR recycle ratio increases, and utility costs gradually become the dominant cost increasing from 25% to 45% with materials costs decreasing from 41% to 32%. Similar results were observed in the other two series of cases, where higher ECR recycle ratios led to higher MESP, with utility costs even higher than 75% in the POIE0.9 and POCE0.9 cases. At the same time, the MESP of BASI

($462/t) and BASC ($428/t) are lower than BASS ($598/t) because their higher CO concentration leads to a larger ethanol capacity and lower cost per ton of ethanol. Deeply, **Figure 40(b)** displays the complete breakdown of the MESP for BASC and POCE0.9 as a case study, with the MESP increase from $428/t to $910/t, where the tail gas cost in materials costs and ECR electricity (PV) in utility costs were found as the primary driven factors. As the ethanol capacity of POCE0.9 increased 1.7 times over BASC, the tail gas cost per ton of ethanol decreased from $122/t to $45/t, while ECR electricity cost increased from 0 to $619/t. Considering the reduction of life cycle carbon footprints of 2.79 t CO_2eq/t ethanol from BASC to POCE0.9, the carbon reduction cost can be estimated at $173/t CO_2.

Carbon price is a form of taxation used by the government to change the cost-benefit comparison of enterprises, indirectly guiding enterprises to take measures to reduce emissions. Carbon tax is a “tax” that needs to be paid according to the carbon price, which has the basic characteristics of mandatory, fixed and gratuitous that are unique to tax, and it is difficult to be adjusted at any time according to the change of the situation, but the advantage is that the tax rate is stable, and the uncertainty of the market main body is small, and it has an incentive

effect for the long-term emission reduction. Carbon price uses price mechanism to guide the whole society to reduce carbon emissions, which is a specific means to promote low-carbon development of the economy and society and achieve the goals of “carbon peak and carbon neutrality”. Based on the current carbon price in China ($10/t CO_2), the cost-offsetting effect of the carbon tax credit is minimal. If the carbon price rises to equal the carbon reduction cost, the TGEE-ethanol will achieve a large amount of carbon reduction at no additional cost. However, due to the low feedstock cost and simple process, the MESP of TGEE-ethanol across all scenarios ($428 – 962/t) can be competitive with the cost of bio-based ethanol ($464 – 803/t) [127, 199] in China.

Figure 40(c) displays the probable range of MESP based on Monte Carlo simulation with probability distribution employed in some key parameters to model a more realistic materials’ market price, carbon tax, discount rate and tax rate (See **Table 19**). With higher ECR recycle ratios, the MESP probability curve becomes flatter and the potential range of MESP wider. This increased range of uncertainties is driven by feedstock consumption, utility consumption and market price, which further amplified the cost impacts of feedstock and energy consumption. The peak of the MESP curve indicates the most probable selling price of

ethanol with the highest probability density. Compared to the current fixed MESP for BASS to POSE0.4 scenarios, the simulated MESP ranges from $503 – 679/t to $516 – 829/t, respectively, with a variation of ± (14% – 27%). In BASI to POIE0.9 and BASC to POCE0.9 cases, the MESP ranges are further expanded (± (16% – 48%)) due to the higher ECR recycle ratios, more materials and energy involved. Overall, the Monte Carlo simulated that the MESP of most scenarios will be less than the ethanol market price ($900 – 1080/t in 2022 and 2023), suggesting that there are considerable economic benefits for TGEE-ethanol production.

Furthermore, it is believed that the MESP for TGEE-ethanol production will gradually decline as the carbon market develops and the cost reduction of sustainable energy. It is reported that the PV cost will continue to decrease and may be reduced to about $0.01/kWh in the foreseeable future [200]. With the development of the carbon market, the carbon price in China is expected to reach $20/t CO_2eq in 2030 and $350/t CO_2eq in 2030 [193], it is expected that the carbon credits will considerably contribute to reducing production costs. Scale-up factories to increase the ethanol capacity and then reduce the fixed operating costs are also available measures to reduce MESP. Meanwhile, it is

believed that governmental support, incentives, preferential tax policy and investments are crucial to reduce MESP.

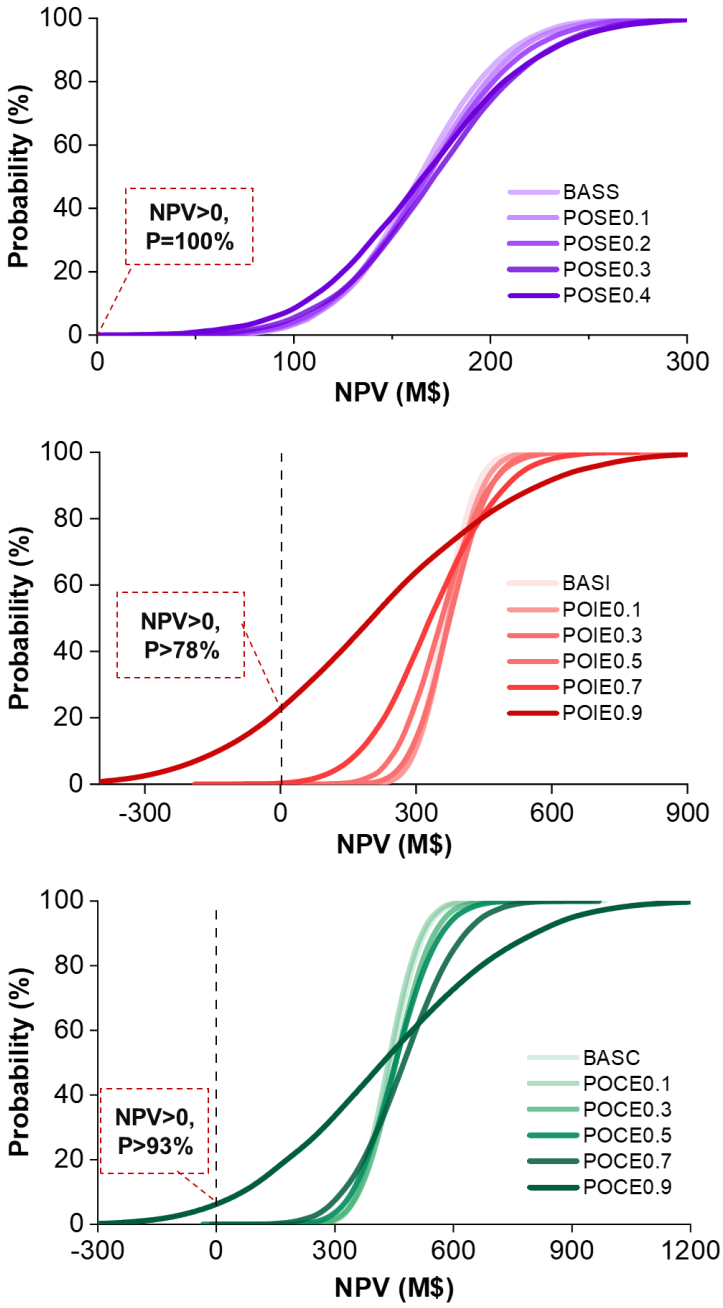

Figure 39. NPV performance based on Monte Carlo simulation for all scenarios, “P” means the probability.

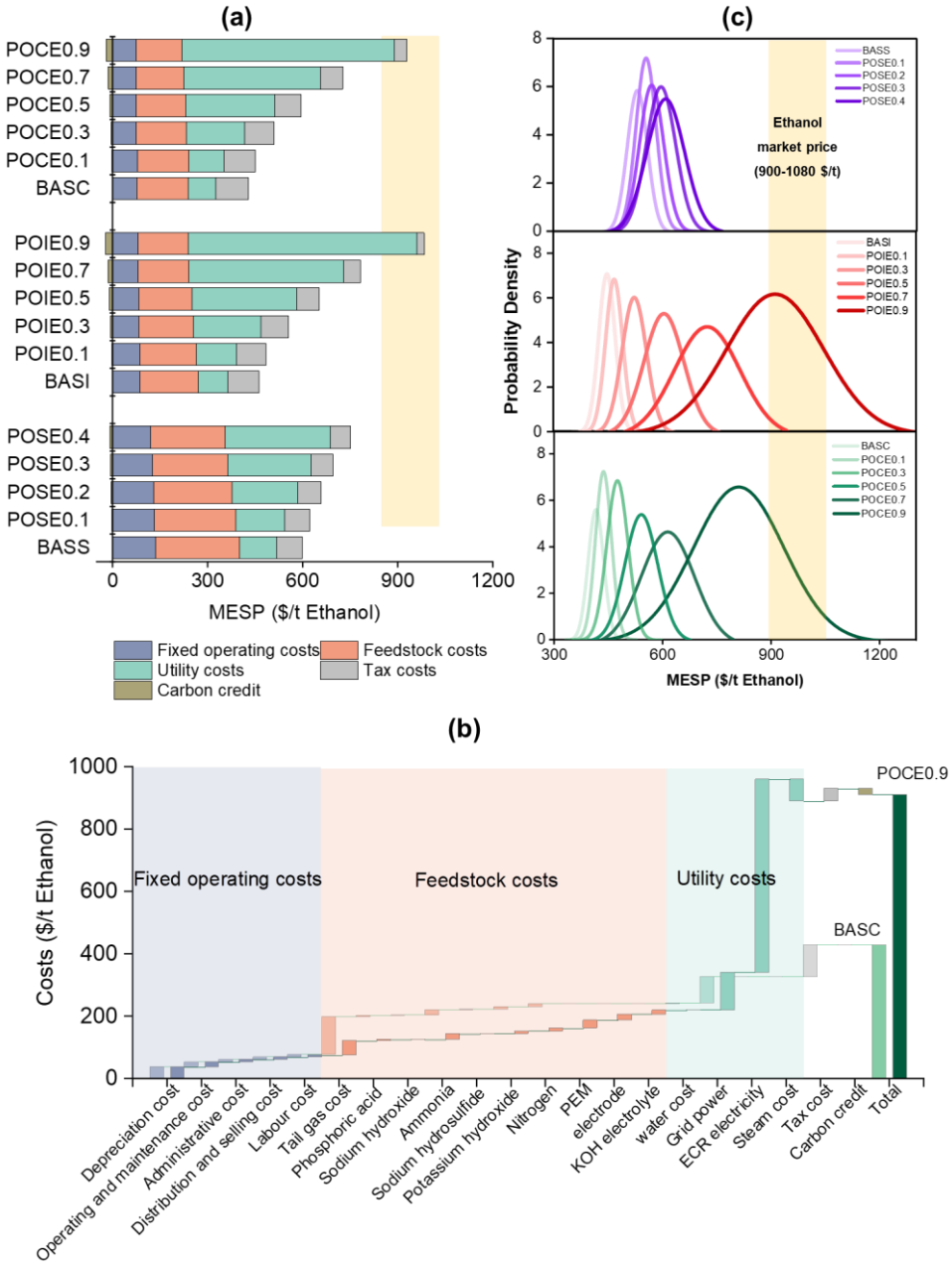

Figure 40. Minimum ethanol selling price (MESP) and probability results estimated by Monte Carlo simulation for TGEE-ethanol production from three industrial tail gas streams, (a) MESP distribution across all scenarios; (b) Breakdown of the MESP for BASC and POCE0.9 cases; (c) the probable MESP range with variables change (materials price, discount rate, tax rate and carbon tax) based on Monte Carlo simulation.

5.3.5 Sensitivity analysis

A sensitivity analysis was performed on NPV and carbon reduction potential to identify the high-impact variables in a series of scenarios for TGEE-ethanol production from tail gas in the steel, iron ally and calcium carbide industries (See numerical results in **Table 24-26**). For NPV, the results for the top 5 model input parameters are presented in **Figure 41**. All scenarios showed a trend that ethanol price and PV cost are the key factors affecting NPV, indicating that these two parameters need further data investigation and refinement in future work. When the initial ECR recycle ratio is relatively low, ethanol price is a positive factor that promotes the increase of NPV. With the increase of the ECR recycle ratio, the promoting effect [187, 201] of ethanol price weakens, and the negative inhibitory effect of PV cost on NPV strengths. In detail, for the TGEE-ethanol from steel tail gas cases **(Figure 41(a))**, from BASS to POSE0.4, the positive sensitivity range of ethanol price is 89% to 68% and the negative sensitivity range of PV cost is 2% to -26%, respectively; for the TGEE-ethanol from iron alloy and calcium carbide tail gas cases (**Figure 41(b) and (c)**), the sensitivity range is further expanded: ethanol price (90% to 20%) and PV cost (−1% to −77%), respectively.

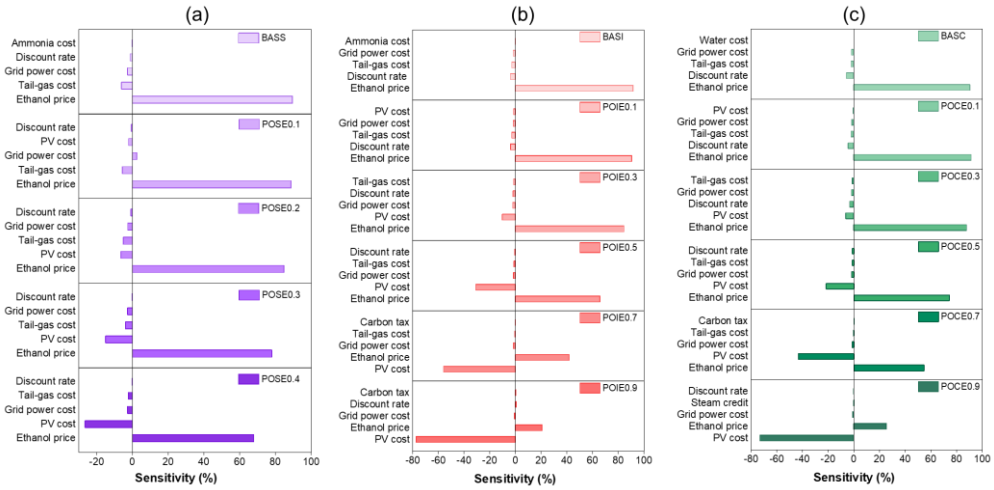

Figure 41. Sensitivity analysis for the NPV of three series scenarios. (a), (b) and (c) display the sensitivity results for the top 5 inputs on the NPV model for TGEE-ethanol production from steel, iron ally and calcium carbide tail gas, respectively.

A sensitivity analysis was also performed on the carbon reduction potential, as shown in **Figure 42**. All scenarios show that coal to steam, PV and grid power emissions are the critical factors affecting carbon reduction potential, indicating more investigation work should be focused on these indicators in future studies. Specifically, with the increase of the ECR recycle ratio, the promoting effect of coal to steam emission decreases (steam credit), and the negative inhibitory effect of PV and grid power emission increases. For the TGEE-ethanol from steel tail gas cases shown in **Figure 42(a)**, the sensitivity results order and range are coal to steam (68% to 18%), PV (−22% to −52%) and grid power (−8%

to −27%)), respectively; for the TGEE-ethanol from iron alloy and calcium carbide tail gas cases (**Figure 42(b) and (c)**), the sensitivity results order are changed to PV (−20% to −66%,), coal to steam (76% to 12%) and grid power (−3% to −23%).

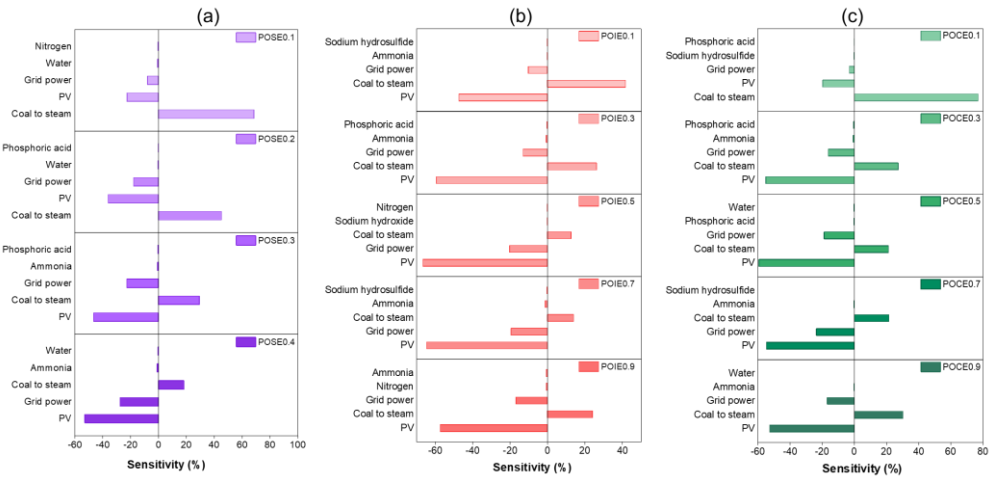

Figure 42. Sensitivity analysis for the carbon reduction potential of three series scenarios. (a), (b) and (c) display the sensitivity results for the top 5 inputs on the carbon reduction potential model for TGEE-ethanol production from steel, iron ally and calcium carbide tail gas, respectively.

Table 24. Sensitivity analysis of TGEE-ethanol from steel tail gas.

NPV		Carbon reduction potential	
BASS			
Ethanol	89.60%		
Tail-gas	-6.10%		
Grid power	-2.80%		
Discount rate	-1.30%		
Ammonia	-0.10%		
POSE0.1			
Ethanol	88.80%	Coal to steam	68.50%
Tail-gas	-5.60%	PV	-22.50%
Grid power	2.50%	Grid power	-7.90%
PV	-2.10%	Water	-0.60%
Discount rate	-0.70%	Nitrogen	-0.40%
POSE0.2			
Ethanol	84.80%	Coal to steam	45.20%
PV	-6.40%	PV	-36.10%
Tail-gas	-5.10%	Grid power	-17.80%
Grid power	-2.60%	Water	-0.40%
Discount rate	-0.90%	Phosphoric acid	-0.20%
POSE0.3			
Ethanol	78.00%	PV	-46.50%
PV	-15.00%	Coal to steam	29.40%
Tail-gas	-3.80%	Grid power	-22.70%
Grid power	-2.70%	Ammonia	-0.70%
Discount rate	-0.20%	Phosphoric acid	-0.40%
POSE0.4			
Ethanol	68.00%	PV	-52.80%
PV	-26.50%	Grid power	-27.50%
Grid power	-2.80%	Coal to steam	18.40%
Tail-gas	-2.20%	Ammonia	-0.90%
Discount rate	-0.10%	Water	-0.30%

Table 25. Sensitivity analysis of TGEE-ethanol from iron alloy tail gas.

NPV		Carbon reduction potential	
BASI			
Ethanol price	91.60%		
Discount rate	-3.80%		
Tail-gas cost	-2.70%		
Grid power cost	-1.60%		
Ammonia cost	-0.10%		
POIE0.1			
Ethanol price	90.50%	PV	-47.40%
Discount rate	-3.70%	Coal to steam	41.70%
Tail-gas cost	-2.70%	Grid power	-10.20%
Grid power cost	-1.70%	Ammonia	-0.20%
PV cost	-1.30%	Sodium hydrosulfide	-0.20%
POIE0.3			
Ethanol price	84.50%	PV	-59.40%
PV cost	-10.20%	Coal to steam	26.20%
Grid power cost	-2.00%	Grid power	-13.00%
Discount rate	-1.80%	Ammonia	-0.80%
Tail-gas cost	-1.30%	Phosphoric acid	-0.40%
POIE0.5			
Ethanol price	65.80%	PV	-66.60%
PV cost	-30.70%	Grid power	-20.20%
Grid power cost	-1.50%	Coal to steam	12.60%
Tail-gas cost	-1.10%	Sodium hydroxide	-0.20%
Discount rate	-0.40%	Nitrogen	-0.10%
POIE0.7			
PV cost	-55.80%	PV	-64.70%
Ethanol price	41.80%	Grid power	-19.50%
Grid power cost	-1.50%	Coal to steam	14.00%
Tail-gas cost	-0.50%	Ammonia	-1.30%
Carbon tax	0.20%	Sodium hydrosulfide	-0.30%
POIE0.9			
PV cost	-77.20%	PV	-57.30%
Ethanol price	20.70%	Coal to steam	24.10%
Grid power cost	-0.80%	Grid power	-16.80%
Discount rate	0.60%	Nitrogen	-0.60%
Carbon tax	0.30%	Ammonia	-0.60%

Table 26. Sensitivity analysis of TGEE-ethanol from calcium carbide tail gas.

NPV		Carbon reduction potential	
BASC			
Ethanol price	90.40%		
Discount rate	-5.70%		
Tail-gas cost	-2.00%		
Grid power cost	-1.70%		
Water cost	0.00%		
POCE0.1			
Ethanol price	91.40%	Coal to steam	76.90%
Discount rate	-4.30%	PV	-19.70%
Tail-gas cost	-2.00%	Grid power	-3.10%
Grid power cost	-1.50%	Sodium hydrosulfide	-0.20%
PV cost	-0.40%	Phosphoric acid	-0.10%
POCE0.3			
Ethanol price	87.80%	PV	-55.00%
PV cost	-6.20%	Coal to steam	27.20%
Discount rate	-3.10%	Grid power	-16.20%
Grid power cost	-1.60%	Ammonia	-0.70%
Tail-gas cost	-1.20%	Phosphoric acid	-0.50%
POCE0.5			
Ethanol price	74.30%	PV	-59.30%
PV cost	-21.50%	Coal to steam	21.20%
Grid power cost	-1.70%	Grid power	-18.80%
Tail-gas cost	-1.10%	Phosphoric acid	-0.30%
Discount rate	-1.10%	Water	-0.20%
POCE0.7			
Ethanol price	54.60%	PV	-54.60%
PV cost	-43.10%	Grid power	-23.60%
Grid power cost	-1.40%	Coal to steam	21.40%
Tail-gas cost	-0.30%	Ammonia	-0.30%
Carbon tax	0.30%	Sodium hydrosulfide	0.00%
POCE0.9			
PV cost	-73.00%	PV	-52.60%
Ethanol price	25.40%	Coal to steam	30.20%
Grid power cost	-0.80%	Grid power	-16.80%
Steam credit	0.30%	Ammonia	-0.30%
Discount rate	0.20%	Water	0.00%

5.3.6 Comprehensive analysis and comparison with other studies

This section performed a comprehensive performance analysis of all scenarios in terms of environmental, economic and energy aspects using the entropy weight method. **Figure 43(a)** illustrates the baseline and the maximum carbon efficiency scenario for TGEE-ethanol production from three tail gas streams. CP and five individual normalised indicators were employed and the highest value for each indicator is represented as 1, indicating the best performance. The results reveal that POCE0.9 achieves the highest CP (0.79), followed by POIE0.9 (0.66), while BASS exhibits the lowest CP (0.25). This difference is primarily due to the substantial impact of low information entropy and high dispersion in CE and CF on CP. However, NPV, MESP, and ED have higher information entropy and lower variability, resulting in a relatively minor impact on CP. As the ECR recycle ratios increase, CE and CF show more significant changes than NPV, MESP and ED on CP. Therefore, the steel tail gas to ethanol series performs relatively poorly overall compared to the other two series cases due to limited improvement in CE and CF.

In terms of individual indicators performance, POE outperforms BAS in CE and CF but fails behind BAS in NPV, MESP and ED. This trend is also evident in **Figure 43(b)-(d)**, indicating that adopting the TGEE technology certainly enhances environmental performance but results in economic losses and energy consumption. Nevertheless, POSE0.4, POIE0.9 and POCE0.9 scenarios in their series achieve the highest CP values, implying the superiority of the upgraded TGEE process. Therefore, ethanol production from these three scenarios is the recommended investment case from a comprehensive perspective. See supplementary material **Table A6** for numerical details.

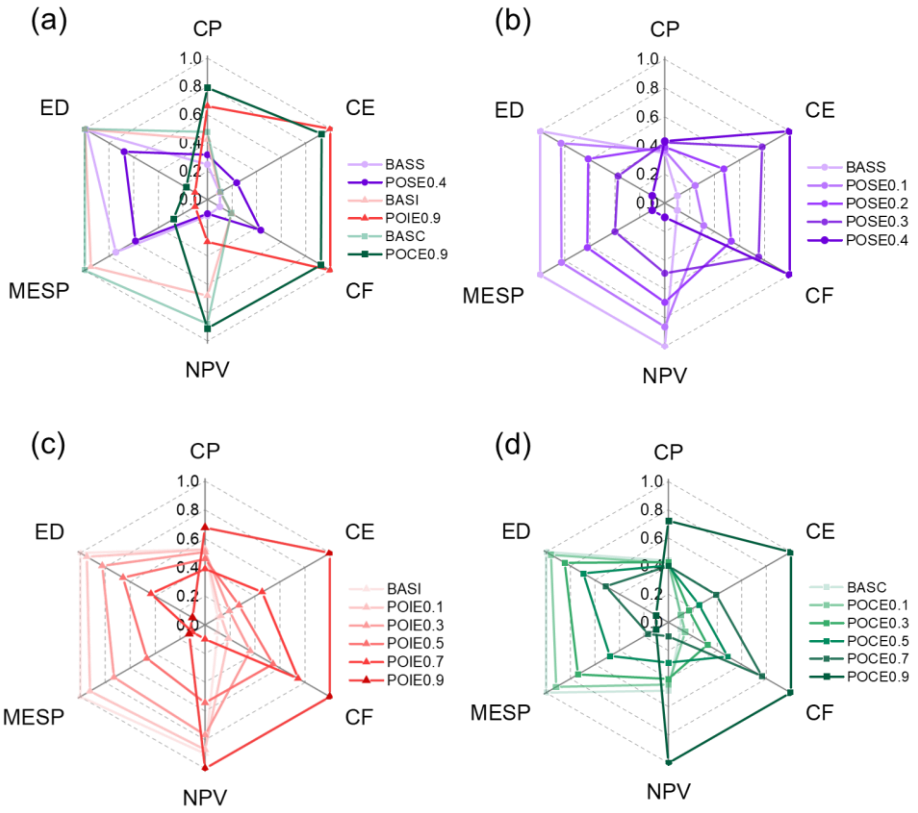

Figure 43. Comprehensive comparison of considered scenarios.

Table 27 shows the results of this study compared with earlier bio-based and fossil-based ethanol studies. The estimated energy demand and carbon footprints in the current study can compete with the performance in the previous research. i.e., the energy demand of BASS, BASI and BASC (3530 – 4750 MJ/t) are lower than bio-based (7968 – 146400 MJ/t) and fossil-based ethanol (48400 – 93687 MJ/t) pathways, and the POSE0.4, POIE0.9 and POCE0.9 (25950 – 66108 MJ/t) are between bio-based and fossil-based pathways, whereas the energy concern could be solved by renewable energy. For the carbon footprints, the value of the BASS, BASI and BASC (4.71 – 5.38 t CO_2eq/t) cases are between bio-based ethanol (−3.12 – 3.9 t CO_2eq/t) and fossil-based ethanol (1.14 – 8.37 t CO_2eq/t). However, the carbon footprints of POSE0.4, POIE0.9 and POCE0.9 (1.41 – 3.71 t CO_2eq/t) cases are relatively close to bio-based ethanol. The carbon footprints of bio-fermentation with ECR technology (if electricity from renewables) will be continuously reduced and potentially be comparable to bio-based ethanol. The lower MESP estimated by Monte Carlo simulation in this study ranged between $348 – 535/t is quite competitive with other bio-based ethanol ($464 – 1088/t) and fossil-based ethanol ($431/t) production pathways in China, also the price range depends on their

feedstock cost and energy source. In regional comparisons, energy demand and MESP of TGEE-ethanol in this study are competitive with Corn-ethanol in the U.S. and China, and sugar beet-ethanol in Europe. Additionally, the carbon footprints are significantly lower than China's coal-ethanol pathway, and the energy demand is less than Brazilian sugarcane-ethanol. The variations in energy demand, carbon footprints, and MESP of Corn-ethanol and Coal-ethanol across different studies can be attributed to varying assumptions and system boundaries [202].

In practice, the TGEE process can also be combined with other industrial technologies for syngas production, such as gasification of some carbon-rich wastes (municipal solid wastes [203], forestry and agricultural residues and other biomass resources [204]) to produce syngas containing mainly CO and H_2, which can be used as a substrate for bio-fermentation to further enhance the high-value and efficient utilisation of waste resources. Meanwhile, the energy supply of the TGEE process is not only the PV energy employed in this study but also other renewable energy sources such as wind power, hydropower, biomass power generation, etc., which can be combined with the smart grid and digital power to realise the efficient utilisation of clean energy. Furthermore, the TGEE process can be further coupled with its

downstream industries, such as sustainable aviation fuel, olefins, and acetic ether.

Certainly, the early-stage modelling design of processes is significantly affected by uncertainties due to the scarcity and variability of input parameters. Nevertheless, if reasonable approximations and distributions are used to describe the reliability of TEA & LCA, the results are still a reasonable reference point for screening out the feasible pathways, thereby increasing the effectiveness of investment decision-making. From the perspective of a carbon-neutrality target, this study does provide a green and low-carbon ethanol production pathway and looks forward to contributing a significant share of the ethanol market and downstream application in the future.

5.4 Summary

In this chapter, a novel TG-ethanol & ECR coupling technology (TGEE) has been simulated for ethanol production from low-value industrial tail gas. The feedstock of TGEE-ethanol is sourced widely, any industrial tail gas rich in CO and CO_2 can be used to produce ethanol via a bio-fermentation process. This study selected three typical industrial tail gases (steel, iron alloy and calcium carbide) as feedstock for ethanol

production, and the post-combustion ECR (POE) coupling process was examined as the optimal technology, which can increase ethanol capacity by 1.3 – 2.9 times with carbon efficiency up to 36 – 82% as the ECR recycle ratio increases. From the life cycle assessment, the carbon footprints of TGEE-ethanol were estimated to be 1.77 – 3.93 t CO_2eq/t ethanol, with a carbon reduction potential of up to 32 – 63%, much better than previously reported TG-ethanol. From the techno-economic analysis, the minimum ethanol selling price (MESP) has been estimated to be $428 – 962/t ethanol, which is lower than the ethanol market price ($900 – 1080/t). Uncertainty analysis using Monte Carlo simulation provided more reliable probabilistic results for the environmental and economic impacts. As for the comprehensive performance (CP) analysis in terms of environmental, economic and energy aspects, the POSE0.4, POIE0.9 and POCE0.9 scenarios in their series achieved the highest CP and made a comparison with previous studies of bio- and fossil-based ethanol, which could provide valuable insights for researchers and stakeholders for the commercial deployment of TGEE technology. Overall, the findings suggest that TGEE-ethanol production as a “waste-to-energy” technology helps the efficient and clean utilisation of industrial

tail gas with excellent economic and environmental performance, promoting the circular economy and sustainable development.

Table 27. Summary and comparison of the performance of ethanol production from the current study and previous studies.

Feedstock pathways		Region	Energy demand (MJ/t)	Carbon footprints (t CO_2eq/t)	MESP ($/t)
Bio-based ethanol	Corn [39]	US	8840	1.05	/
	Corn [48]	China	/	−1.34	/
	Corn [104]	China	24053	−0.46	600
	Corn [205]	US	8679	2.13	625–1088
	Sugarcane [39]	Brazil	13965	0.61	/
	Sugarcane [206]	Brazil	17121	0.33	300–525
	Cassava [47]	China	146400	3.9	697
	Corn stover [48]	China	/	−3.12	/
	Corn stover [a] [127]	China	19800	0.94	803
	Corn stover [b] [127]	China	18600	0.89	464
	Lignocellulosic [68]	Europe	119160	/	260
	Sugar beet [206]	Europe	1648	0.51	575–963
	Municipal solid waste [207]	UK	29748	−0.34	
Fossil-based ethanol	Coal [47]	China	80600	7.60	431
	Coal [48]	China	/	8.37	/
	Coal [104]	China	93687	6.21	/
	Petroleum [208]	China	48400	1.14	/
This study	BASS	China	4750	5.05–5.38	503–679
	BASI		3769	4.71–4.97	363–536
	BASC		3530	4.73–4.98	348–489
	POSE0.4		25950	3.71–4.18	516–829
	POIE0.9		66108	1.41–2.25	535–1229
	POCE0.9		61019	1.65–2.46	469–1102

[a] Direct fermentation

[b] Indirect fermentation

CHAPTER 6. Impact evaluation on upstream and downstream industries

6.1 Impact of LDG-ethanol on the Chinese steel-making industry

Part of this Chapter's work has been published in "Lingyun Zhang, Jumoke Oladejo, Ayotunde Dawodu, et al. Sustainable Jet Fuel from Municipal Solid Waste–Investigation of Carbon Negativity and Affordability Claims, *Resour. Conserve. Recycl.,* 2024 (210), 107819."

6.1.1 Comparison of LDG-Ethanol and LDG-power

The typical use of the steel industry tail-gas is burning for electricity, where all the CO in the LDG is converted into CO_2 and emitted into the atmosphere, and the combustion process also produces a large amount of SO_2 and NO_x causing serious air pollution. However, the LDG-ethanol production by bio-fermentation from steel industry tail-gas not only achieves the high-value utilisation of tail-gas but also dramatically reduces CO_2. In addition, there are no SO_2 and NO_x released during the fermentation process of LDG, which significantly reduces the polluting gas emission from the steel industry. **Figure 44** is the diagram of LDG-Ethanol and LDG-power, and **Table 28** compares the carbon footprint

results and economic benefits between LDG-Ethanol and LDG-power. For the 10000 Nm^3 LDG feedstock, the LDG-Ethanol process can produce ethanol 1.4 t, biomass 0.18 t, butanol 0.03 t, and LDG-power can generate 7000 kWh electricity by combustion. In comparison, the product value of LDG-Ethanol is $1250 higher than LDG-power, the CO_2 emission is 1310 kg CO_2eq lower, and the carbon intensity is 60% lower. Therefore, LDG-Ethanol bio-fermentation from steel industry tail-gas technology organically combines the steel industry with the new energy source of ethanol, providing a creative path for the high-value use of tail-gas in the steel industry, and strongly promoting energy conservation and emission reduction and the circular economy in steel enterprises.

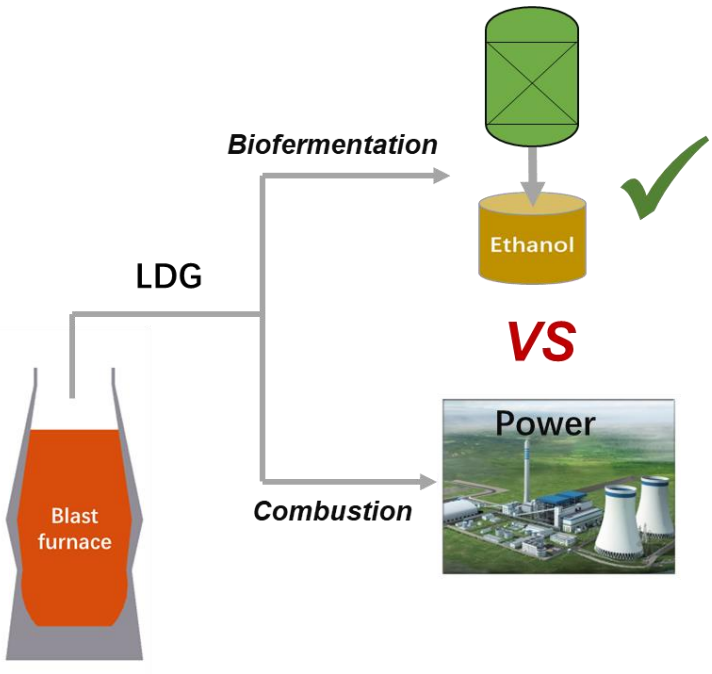

Figure 44. Diagram of LDG-ethanol and LDG-power.

Table 28. Comparison of LDG-ethanol and LDG-power.

Item	LDG-ethanol	LDG-power
LDG feedstock	10000 Nm^3	
Output	Ethanol-1.4 t, Biomass-0.18t, Butanol-0.03t.	7000 kWh
Energy	53279 MJ	25200 MJ
Price	Ethanol-$930/t, Biomass-$977/t, Butanol-$57/t.	$0.086/kWh
Product value	$1852	$602
Carbon footprint	8120 kg CO_2eq	9430 kg CO_2eq
Carbon intensity	$4.39/kg CO_2eq	$15.67/kg CO_2eq

6.1.2 Forecast of carbon reduction potential and economic benefits projections in 2025-2060

China is the largest steel manufacturer globally, contributing over 15% of the country's total carbon emissions. Furnace-Basic Oxygen Furnace (BF-BOF) is the dominant technology used in China, and generally, LDG from the BF-BOF process is directly combusted for electricity generation. Based on the above analysis, the LDG-ethanol technology can be regarded as a new LDG utilization option. Therefore, this section further estimates the carbon reduction potential and economic benefit to the context of the LDG-ethanol technology to the Chinese BF-BOF steeling production industry.

According to Wu *et al.* [209], with the upgrading of the steel-making structure and the increased production of steel scrap, the capacity of BF-BOF steel-making in China will decrease from 768 Mt in 2025 to 229 Mt by 2060. Based on the quantified GWP value of LDG-ethanol under different scenarios, the overall carbon reduction potential can be estimated as shown in **Figure 45(a)**. In general, a downtrend was observed due to the decrease in LDG production over the years. However, it should be mentioned that the prediction only reflects the upper bound of the reduction capacity, and the practical situation will be highly related to the level of technology deployment. Therefore, the downward trend does not necessarily indicate a diminished effect of the LDG-ethanol process in carbon reduction. In 2025, the carbon reduction potential of the technology widely ranges between 9.8 – 18.6 $MtCO_2$, ranked as electricity of predicted grid mix < PV < WP < HP. The cleaner the power, the greater the carbon reduction potential. With the decarbonization of electricity in the middle and long term (insert of Figure 9(a)), the estimated carbon reduction potential is narrowed to 6.6 – 7.0 $MtCO_2$ in 2050 and 5.3 – 5.6 $MtCO_2$ in 2060.

The economic benefit of LDG-ethanol is evaluated by considering both product margin and carbon tax. Herein, the ethanol price was

assumed to increase with a similar trend to that of oil, as predicted by Tan *et al.* [210], and a profit ratio of 15 – 25% was used for the estimation. As shown in **Figure 45(b)**, when fixing the carbon tax at the current level ($7/t) [201, 211], the overall profit ranges between $1.35 – 2.19 billion in 2025 and slightly decreases to $0.83 – 1.35 billion in 2060. If the carbon tax increased at a variable level reported by Zhang *et al*. [193], the overall economic benefit will range between $1.36 – 2.20 billion in 2025 and sharply increase to $2.97 – 3.49 billion in 2060. This is to say that the increase of carbon tax, will dominate the over-profit of the LDG-ethanol technology (insert of **Figure 45(b)**). Detailed numerical results of carbon reduction and economic benefits are available in **Table A7-A8**. In summary, developing LDG-ethanol from steel industry tail-gas can reduce air pollutant emissions, help to promote the transformation of steel enterprises, and cultivate new economic growth points.

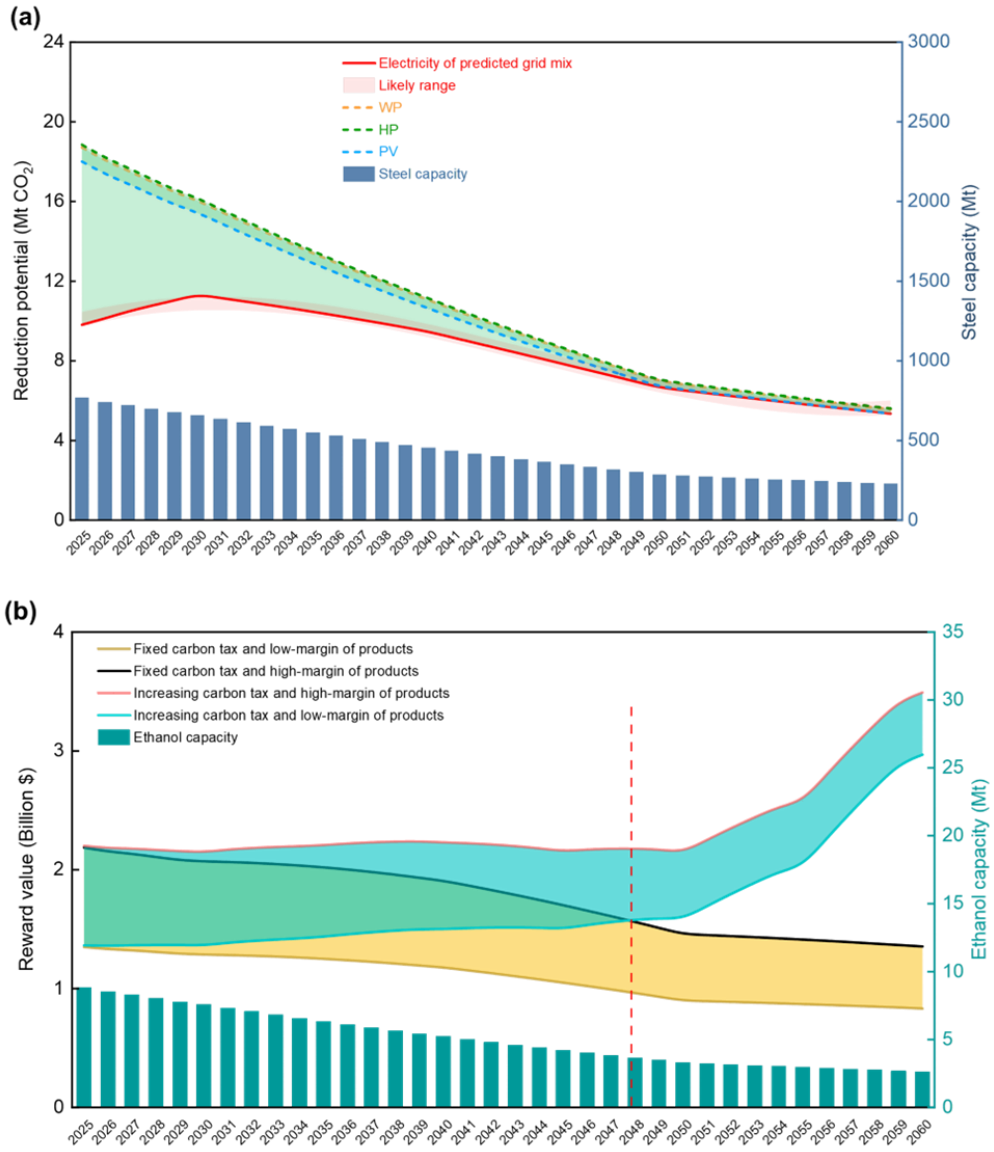

Figure 45. The positive effect of LDG-ethanol on China's BF-BOF steeling production industry: Carbon reduction (a) and economic benefits (b) of LDG-ethanol route compared with LDG-combustion route in the steeling industry.

6.1.3 Possible layout of the steeling-LDG-ethanol combined industry

As mentioned above, China has the largest steel-making industry as well as a massive shortage of fuel ethanol. As such, the LDG-ethanol technology may provide a new landscape to fill this gap and should be encouraged in the future. In this context, the geological matching of raw materials and renewable power is critical to maximize benefits. In China, the domestic iron ore resources are mainly distributed in Hebei, Liaoning, Sichuan, Shanxi, Inner Mongolia, Shandong and Xinjiang provinces. Whilst, imported iron ore resources are mainly in Shandong, Shanghai, Fujian, Jiangsu, and Zhejiang provinces [212]. Coke production [213] is mainly dominated in coal-rich areas, such as Shanxi, Shaanxi, Hebei, Inner Mongolia and Xinjiang *et al*. For renewable energy resources [214, 215], the photovoltaic resource is mainly distributed in Inner Mongolia, Xinjiang, Qinghai and Gansu *et al*. Wind power is mainly produced in Inner Mongolia, Xinjiang, Hebei, Yunnan, Gansu, Shanxi and Jiangsu. Hydropower is mainly in Sichuan, Yunnan, Hubei *et al*. From the overlapping analysis of the above resources (**Figure 46**, detailed numerical data can be found in **Table A9**), it can be observed that apart from southeast China, most regions in Southwest, Northwest, and South

China are suitable for the LDG-ethanol, and Inner Mongolia, Xinjiang, Qinghai, Sichuan, Guangxi may represent the early opportunities for deployment.

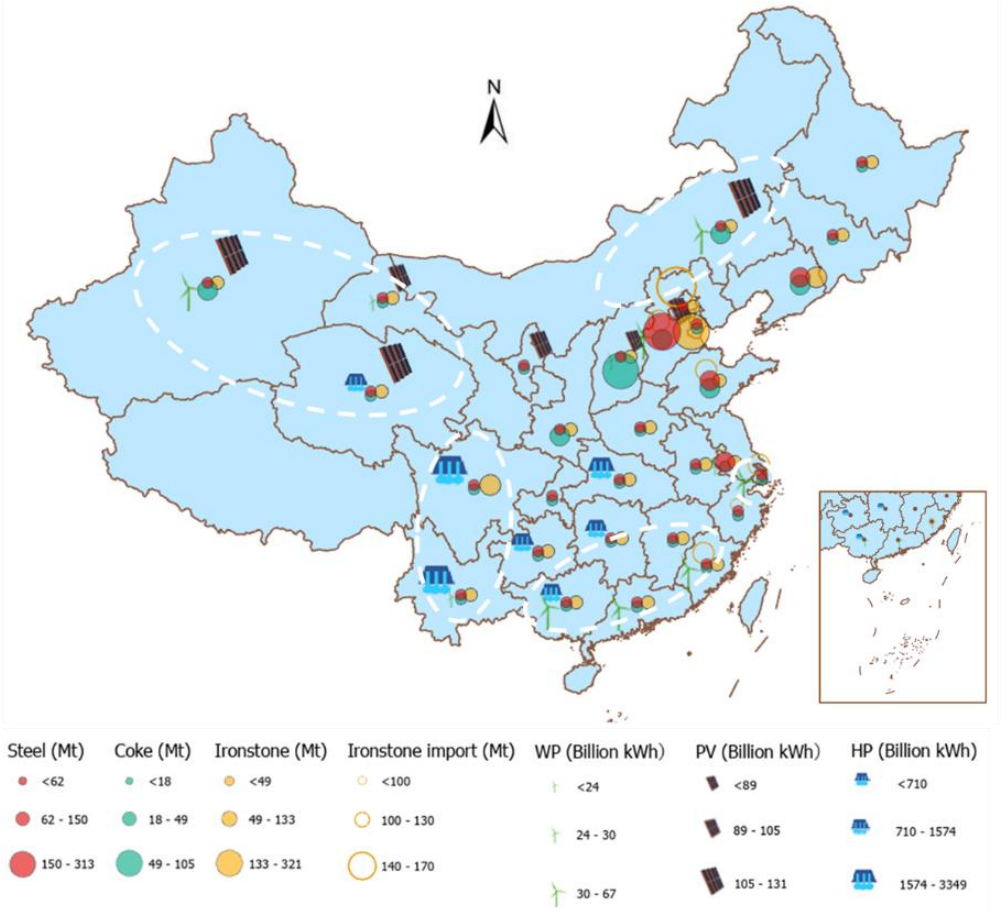

Figure 46. The layout of the steeling-LDG-ethanol combined industry in the future. (The white circle indicates the possible steel-LDG-ethanol plant location).

6.2 Impact of TGEE-ethanol on the Chinese sustainable aviation fuel industries

6.2.1 Sustainable aviation fuel (SAF) pathways

The aviation sector contributes $3.5 trillion (4.1%) to global GDP and 3% (about 10 billion tonnes) of global CO_2 emissions, but by 2050 it may account for 22% of CO_2 emissions as other industries decarbonize [216]. Achieving net-zero emissions is therefore critical to the sustainability of the aviation sector. China is currently the second-largest aviation market behind the United States. Aviation carbon emissions account for about 1% of China's overall carbon emissions, but the overall aviation industry is in a sustained growth phase of future emissions should not be underestimated [217]. However, the aviation sector is recognized as a "difficult to reduce emissions" sector, and aircraft fuel mainly uses aviation kerosene produced from traditional fossil fuels at present [69]. The aviation sector in particular has recognized that sustainable alternative jet fuels are essential to reduce the environmental impact and dependence of aviation on foreign sources of oil, improving the sustainability of transportation [218]. According to the prediction by the International Air Transport Association (IATA), 65% of emissions will be

reduced through the use of SAF by 2050 [219]. In order to reduce the carbon footprint of the aviation sector, sustainable aviation fuel will be the most important measure for aviation to achieve net-zero.

SAFs are liquid fuels currently used in commercial aviation, which can be produced from a number of sources (feedstock) including waste fats, oils and greases, municipal solid waste, agricultural and forestry residues, sugar and starch-based biomass, as well as the industrial tail gas [220, 221]. SAFs can be considered ‘sustainable’, as their feedstocks do not compete with food crops or output, nor require incremental resource usage such as water or land clearing, and more broadly, do not promote environmental challenges such as deforestation, soil productivity loss or biodiversity loss. Whereas fossil fuels add to the overall level of CO_2 by emitting carbon that had been previously locked away, SAF recycles the CO_2, which has been absorbed by the biomass used in the feedstock during its life. There are some SAF practice [222, 223]: in 2008, the first test flight with bio-jet fuel was performed by Virgin Atlantic; in 2016, US became the first airline to introduce SAF into normal business operations by commencing daily flights from Los Angeles Airport (LAX), supplied by Altair; in 2011-2020, commercial SAF flights exceed 250000 and more than 45 airlines gain experience using SAF,

which blends of up to 50% bio-jet fuel from feedstock including used cooking oil, jatropha, camelina, and algae; in 2022, SAF production reached to 300 million litres [224].

By 2023, the American Society for Testing Materials (ASTM) has approved 9 kinds of SAF production technology, among which 4 types of technical routes are now generally recognized by the aviation industry as highly promising routes [203, 225]. In contrast to the fossil jet fuel and these four SAF pathways: (1) Fischer-Tropsch (F-T); (2) hydroprocessed esters and fatty acids (HEFA); (3) Synthetic iso-paraffin (SIP); (4) Alcohol-to-jet (ATJ) or Ethanol-to-jet (ETJ), the diagram of fossil jet fuel and four SAF routes is shown in **Figure 47**. The F-T and HEFA processes have become commercial technologies for converting different feedstocks into liquid fuels [226]. The F-T process produces jet fuels from coal, natural gas, and municipal solid waste through reforming, cracking, and hydrotreating. HEFA process uses oil feedstocks from palm, algae, edible oil, vegetable oil and grease as feedstocks, go through hydrocracking of the large molecules, hydrodeoxygenation, and hydrogenation to obtain paraffinic hydrocarbons [227]. The SIP process obtains farnesane from sugars by fermentation, hydrogenation and distillation. The ATJ or ETJ process uses alcohol or ethanol as feedstock

and goes through dehydration, oligomerization, hydrogenation and fractionation to obtain paraffin [228]. The F-T and HEFA processes, as well as most of the ATJ/ETJ processes are further investigated, as shown in **Table 29** below. In terms of development stage, except for the HEFA route, which has been commercialized, both the FT and ETJ routes are only at laboratory scale. In terms of development potential, the HEFA route has the highest technological maturity and abundant raw materials, followed by the FT route, and the ETJ route has a very limited source of feedstock. However, the ETJ route has the lowest carbon footprint and the highest ethanol yield. In terms of production cost, the ETJ route has the highest production cost, followed by the FT route and the HEFA route has the lowest cost. In addition, I have adjusted the table within one page.

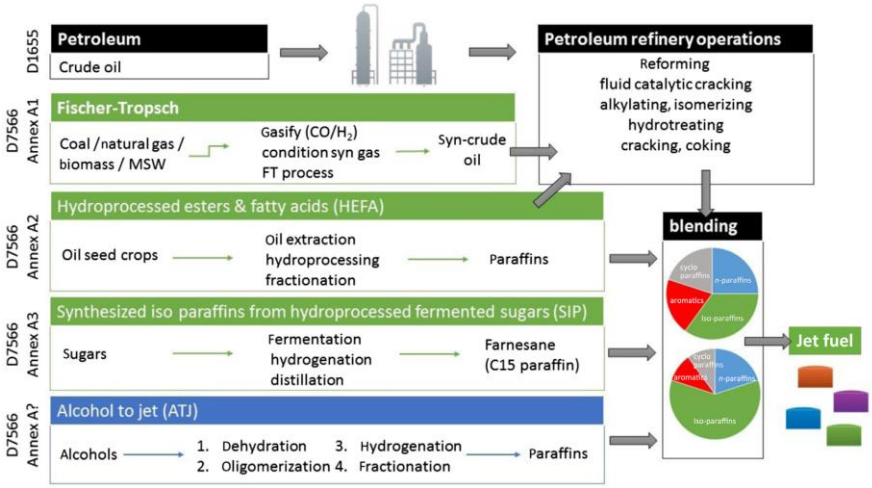

Figure 47. Diagram of fossil jet fuel and SAF routes (cited from [229]).

Table 29. Comparison of SAF pathways.

Items	HEFA	FT	ETJ
Development stage	Commercial	Lab-scale	Lab-scale
Feedstock	Algae, edible oil, vegetable oil, grease	forestry and agricultural residues, municipal solid waste,	Corn, sugarcane, industrial tail gas
Potential	Abundant raw materials, high technical maturity	Abundant raw materials	Raw material availability
Challenge	Collection costs	technical obstacle	technical obstacle
Carbon footprints (gCO_2eq/MJ)	22-66	32-63	18-61
Production costs ($/t)	1100-1600	1800-2300	2100-2900
SAF yield	40%	10%	50%
SAF potential capacity (Mt/year)	1.36	21.275	23.775

6.2.2 Carbon footprints and production cost of ethanol to jet fuel

In this study, we assessed the process of tail gas-based ethanol as feedstock to produce jet fuel, that is, industrial tail gas to ethanol by bio-fermentation, and then the ethanol will be converted to SAF through a series of catalytic steps in the Ethanol-to-Jet fuel (ETJ) pathway. This magic process starts with a waste gas, produced as a co-product of steel, iron alloy, calcium carbide etc, and using a combination of biotechnology and catalysis converts that gas into a liquid fuel that exceeds the standards required for jet aircraft. The core of the ETJ process is a concept developed to bridge the gap between alcohols that can be easily produced from renewable resources and the high-quality hydrocarbon

fuels necessary for jet fuels. This process is based on three catalytic reactions displayed in **Figure 48**, the transformation of ethanol into jet fuel occurs through ethanol dehydration, olefin oligomerization and hydrogenation, followed by fractionation of the synthetic jet fuel product. According to the data of UChicago Argonne and previous study, 0.042 kg ethanol, 0.007 kWh electricity, 0.001 kg hydrogen and 0.043 kg water were consumed per MJ jet fuel, while 0.212 MJ gasoline and 0.115 MJ diesel were produced as co-products. The allocation factor for ethanol is 0.75 based on energy content, as shown in **Table 30**.

Table 30. Allocation factor of the jet fuel process.

Product	Jet fuel	Gasoline	Diesel
Allocation factor	0.75	0.1	0.15

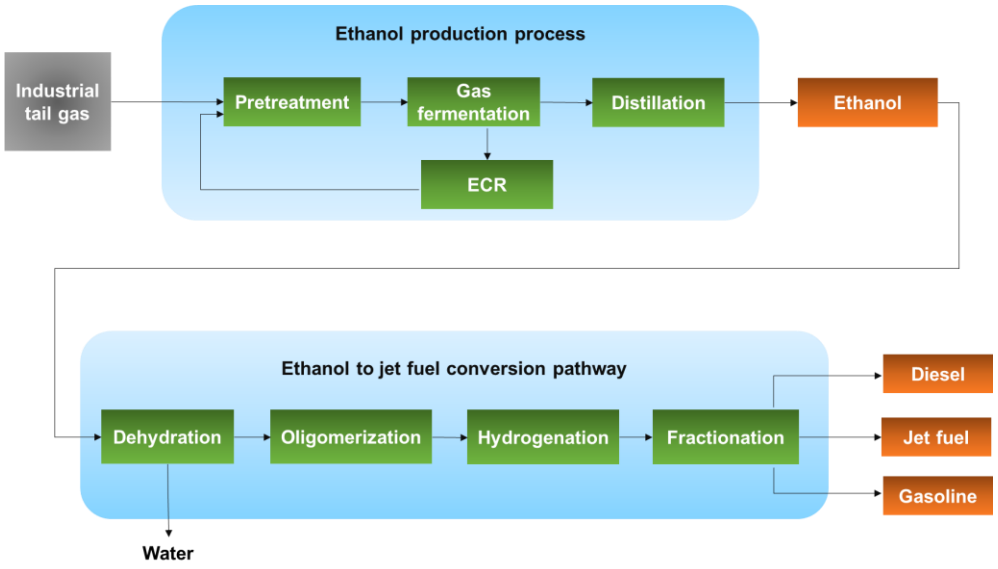

Figure 48. TGEE-ethanol to synthetic jet fuel.

6.2.2.1 Carbon footprints and production cost

Based on the above process, “cradle to gate” system boundaries were defined to conduct the life cycle assessment of the jet fuel production from TGEE-ethanol. Life cycle carbon footprints and total production cost are shown in **Figure 49** to illustrate the parameters of TGEE-ethanol to jet fuel compared to traditional fossil-based jet fuel after the allocation of emissions between final fuel products was performed based on energy content. **Figure 49 (a)** shows that compared to fossil jet fuel, jet fuel from POIE0.9-ethanol and POCE0.9 ethanol pathways reduced the carbon footprints by 28% and 18% respectively, while the other pathways are higher than fossil-based. The stage-by-stage results for the three TGEE-ethanol to jet fuel pathways (**Table 30**) show that the ethanol production stage is the primary contributor, while the ethanol to jet fuel stage has a relatively small carbon footprint due to lower utility and material consumption. However, in terms of total production costs (**Figure 49 (b)**), POIE0.9-ethanol and POCE0.9 ethanol to jet fuel are much higher than that of fossil jet fuel, only BASI and BASC ethanol to jet fuel pathways are lower cost. By breaking down its cost distribution, it can be seen that materials costs and utility costs are the main contributors, as it has been analysed in Chapter 4 that the coupling of

the ECR process results in a large amount of electricity consumption, and when added to the consumption of electricity in the ethanol to jet fuel production stage, the total cost of electricity accounts for about 68% of the total cost.

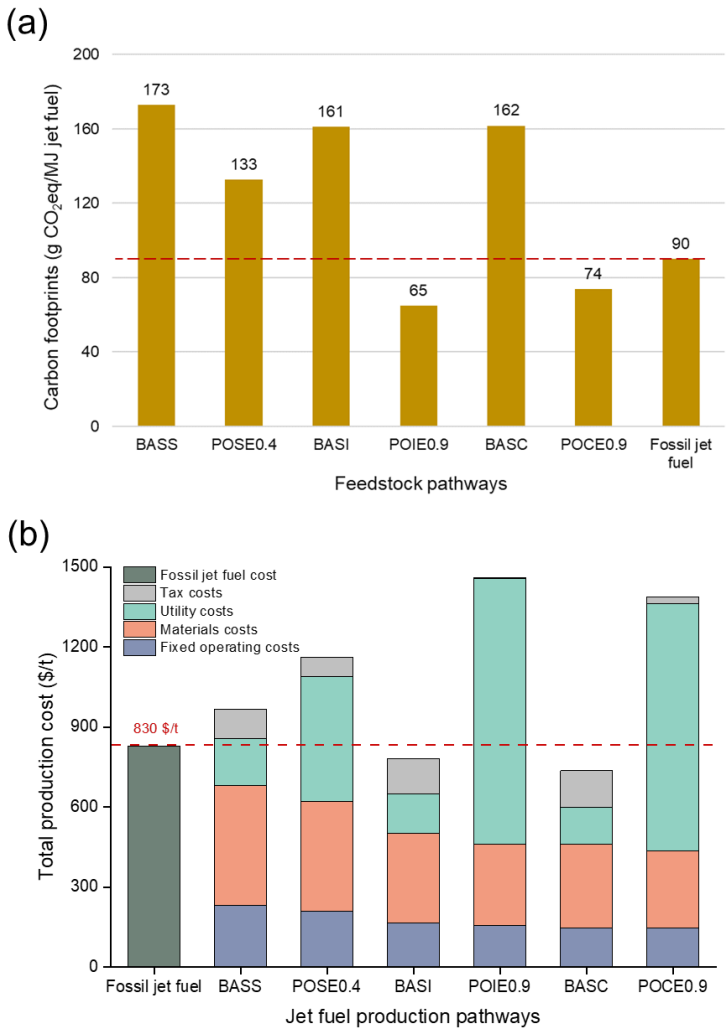

Figure 49. Life cycle carbon footprints and total production cost of jet fuel pathways, (a) Carbon footprints of TGEE-ethanol to jet fuel; (b) Production costs analysis of TGEE-ethanol to jet fuel.

Table 31 provides a comprehensive comparison of the environmental and economic performance at each stage of the three TGEE-ethanol to jet fuel pathways. Here, we assume that the carbon footprints and the cost of the ethanol-to-jet fuel stage are the same for all three pathways, and all units are normalized per ton of product in order to calculate the carbon footprint reduction cost. The carbon footprint reduction cost is the cost increase divided by the carbon footprint reduction of TGEE-ethanol to jet fuel relative to fossil fuel jet fuel. Current results show the reduction cost of TGEE-ethanol to jet fuel up to \$578 – 811/t CO_2, assuming the use of carbon price to offset the carbon reduction cost, it may increase to \$500 by 2050. In addition, compared with our previous investigation on the HEFA and FT pathways, the carbon footprints of TGEE-ethanol to jet fuel are almost higher than that of HEFA and FT, while the production cost is lower than FT and comparable to HEFA. The above results show a big challenge to its environmental sustainability and economic viability. However, in the long term, with the full penetration of sustainable electricity and increased carbon efficiency of this technology, combined with some carbon credits supplemented by carbon price, the carbon footprints and production cost of TGEE--ethanol to jet fuel will continue to decrease, and TGEE-

ethanol-based jet fuel will become a more promising SAF in terms of both low carbon and low cost.

Table 31. Life cycle carbon footprints and total production cost of jet fuel from TGEE-ethanol.

Items		Jet fuel from POIE0.9-ethanol	Jet fuel from POCE0.9-ethanol	Jet fuel from POSE0.4-ethanol
Ethanol production	GHG ($t CO_2eq/t$ ethanol)	1.77	2.06	3.93
	Cost ($/t ethanol)	962	910	743
Jet fuel production from ethanol [a]	GHG ($t CO_2eq/t$ jet fuel)	0.5	0.5	0.5
	Cost ($/t jet fuel)	210	210	210
Jet fuel production, life cycle [b]	GHG ($t CO_2eq/t$ jet fuel)	2.78	3.18	5.71
	Cost ($/t jet fuel)	1460	1390	1164
Jet fuel carbon footprint reduction over fossil jet fuel [c]		28%	18%	-48%
Jet fuel carbon footprint reduction cost over fossil jet fuel ($/t CO_2eq)		**578**	**811**	/

[a] 1.81 t ethanol was consumed to produce 1 t jet fuel, and the heat value of jet fuel is 43 MJ/kg jet fuel.

[b] Jet fuel from ethanol is a multiple-product process (jet fuel, diesel and gasoline), and the allocation factor of jet fuel is 0.75.

[c] The investigated carbon footprint of fossil jet fuel is 90 g CO_2eq/MJ jet fuel (3.87 t CO_2eq/t jet fuel).

6.2.2.2 Project of carbon footprints and production cost in 2020-2060

Given the technology innovation and market change, this section forecasted the carbon footprints and production cost potential of TGEE-ethanol to jet fuel pathways in 2020-2060. The carbon footprint–reduction potential of three tail gas-based ethanol to jet fuel was predicted, as in **Figure 50(a)**. In 2020–2060, the carbon footprints of

steel tail gas-based ethanol to jet fuel pathways (SEJ) decreased from 132 g CO_2eq/MJ to 101 g CO_2eq/MJ (23% decrease), which is still higher than that of fossil jet fuel. However, the calcium carbide tail gas-based ethanol to jet fuel (CEJ) and iron alloy tail gas-based ethanol to jet fuel (IEJ) decreased by 42% and 50% from 2020 to 2060, respectively. Based on the fossil jet fuel baseline, by 2060, the carbon footprints of the CEJ route will be reduced by up to 53%, while the carbon reduction of the IEJ route will be even more significant, up to 64%. As shown in **Figure 50(b)**, considering that electricity and hydrogen are the main factors affecting carbon footprint, we focused on considering the emission factor changes of these two factors at the time scale. Electricity is gradually transitioning from grid power to renewable electricity, while hydrogen production is estimated as an average value based on the future hydrogen supply structure in China **(Figure 51).** According to the data of literature and GaBi, the electricity emission factor considers the electricity supply structure from current grid power to renewable power, which was estimated from 0.57 kg CO_2eq/kWh to 0.05 kg CO_2eq/kWh. Considering the hydrogen production from fossil energy, industrial by-products, water electrolysis by renewable energy water and other

technologies, the estimated hydrogen emission factor in 2020 – 2060 will decrease from 7.72 kg CO_2eq/kg H_2 to 0.04 kg CO_2eq/kg H_2.

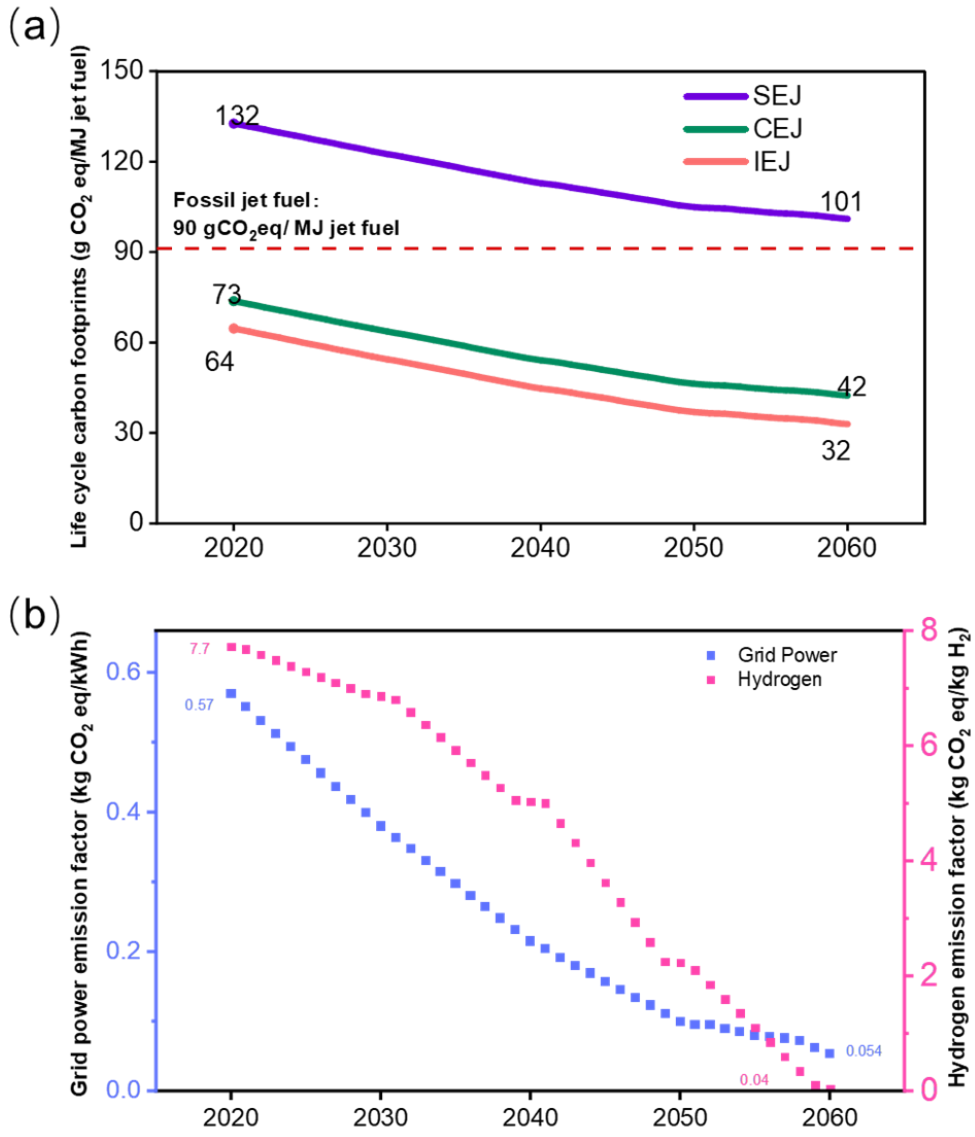

Figure 50. Carbon footprints forecast of TGEE-ethanol to jet fuel. SEJ, steel tail gas-based ethanol (POSE0.4) to jet fuel; CEJ, calcium carbide tail gas-based ethanol (POCE0.9) to jet fuel; IEJ, iron alloy tail gas-based ethanol (POIE0.9) to jet fuel.

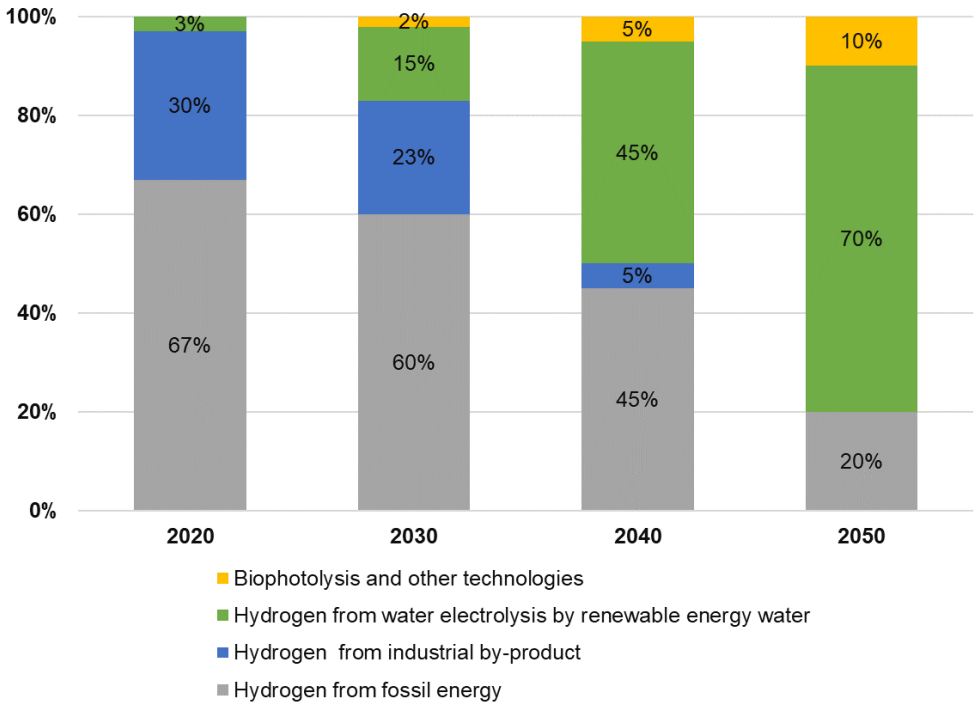

Figure 51. Hydrogen supply structure in China from 2020 to 2050 (cited from [230]).

Similarly, production cost projections for three tail gas-based ethanol to jet fuel are shown in **Figure 52**. Given that electricity and hydrogen prices are the main factors affecting production costs, this study assumes a gradual transition from current grid electricity prices to renewable electricity prices, with electricity prices falling 4% per year and hydrogen production costs falling 2% per year, according to EIA projections. Therefore, in 2020-2060, the price of grid power decreased from \$0.086/kWh to \$0.017/kWh, the PV price decreased from \$0.036/kWh to \$0.016/kWh, and the cost of hydrogen decreased from

$2.85/kg H_2 to $1.27/kg H_2. On this basis, the production cost of the SEJ route decreased from $1164/t to $793/t (32% decrease), while the cost reduction of CEJ and IEJ routes was even greater, reaching 48%. If the current cost of fossil jet fuel ($830/t) is used as a benchmark, the cost of these three routes will decrease to be equivalent to fossil jet fuel in approximately 2050, which corresponds to a price range of grid power ($0.027 – 0.023/kWh), for electricity from the blend, PV ($0.021 to 0.019/kWh) for photovoltaics, and hydrogen ($1.62 to 1.49/kg H_2).

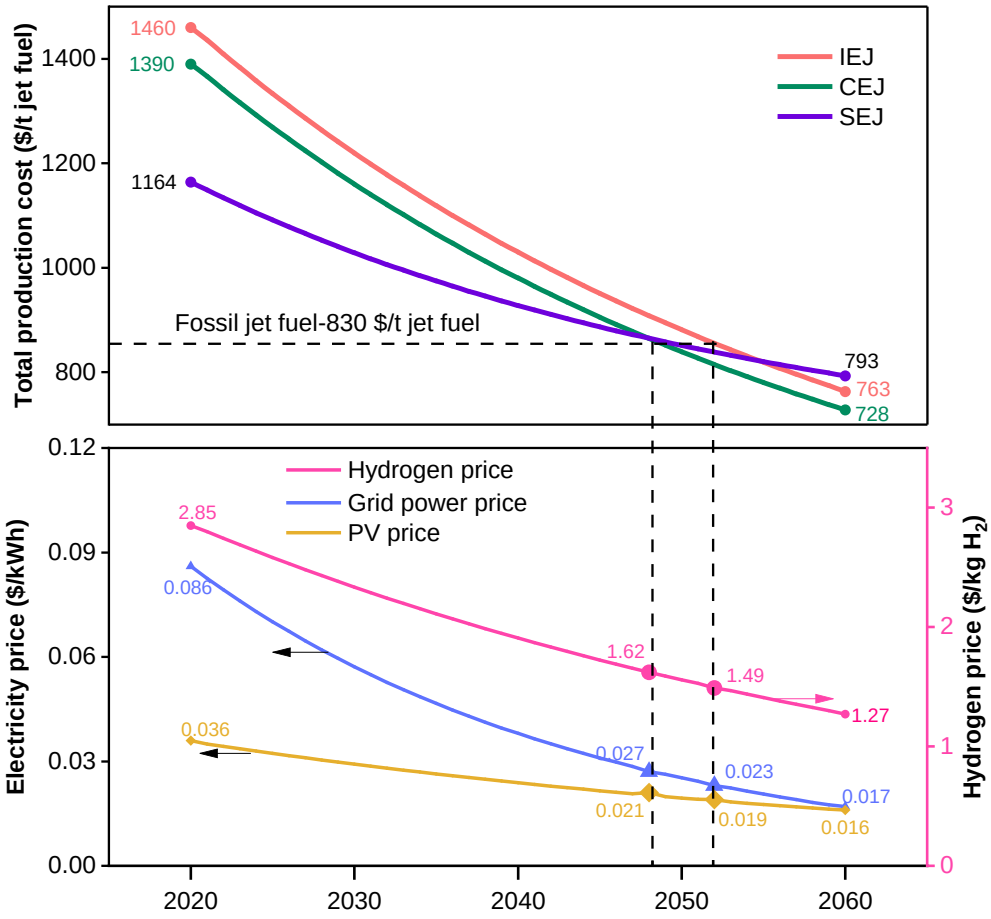

Figure 52. Hydrogen supply structure in China from 2020 to 2050.

With the booming development of the global carbon market, the carbon tax has become a non-negligible economic factor. Carbon assets derived by carbon reduction from low-carbon technology and clean energy will benefit from reducing the production cost of products. Based on the above cost projections that do not take into account the carbon tax scenario, this section further considers the cost change of jet fuel production from tail gas-based ethanol under different carbon tax prices, as shown in **Figure 53**. Four scenarios (carbon tax of $0, $10, $50, $100) were designed to investigate the effect of the carbon tax on the cost reduction of tail gas-based ethanol to jet fuel.

In **Figure 53(a)**, The results show that the SEJ route has a small inverse increase in its production cost under the carbon tax scenario because it has no carbon reduction effect compared to fossil-based routes. When the carbon tax is $10, $50, and $100, the production cost of the SEJ route will increase by 1%, 7%, and 14% in 2030 and increase by 0.6%, 3% and 6% in 2060, respectively. Compared to the above analysed time of ~2050 for the cost of SEJ without carbon tax reaches parity with fossil jet fuel, there is a delay of 5 to 10 years due to the cost-increasing effect of the carbon tax.

For the IEJ and CEJ routes (**Figure 53(b)-(c)**), there is a significant decrease in their production costs when the carbon tax is taken into account. When the carbon tax is $10, $50, and $100, respectively, the cost reduction by 2030 is IEJ (1%, 6%, 13%) and CEJ (1%, 5%, 10%). As for by 2060, the cost reduction benefits from the carbon tax are even more significant for IEJ (3%, 16%, 32%) and CEJ (3%, 14%, 28%). Compared to the above analysed time of ~2050 for the cost of tail gas-based ethanol to jet fuel to reach parity with fossil jet fuel, the time can be advanced by 2 to 10 years due to the cost reduction effect of the carbon tax.

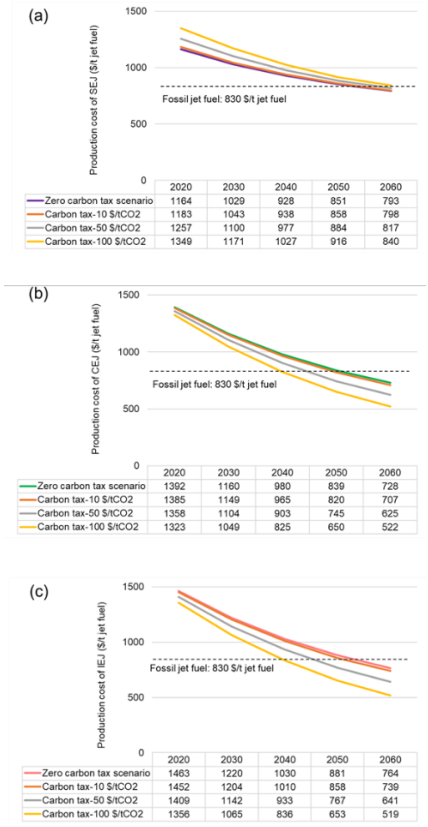

Figure 53. Carbon tax impact on production costs.

6.2.3 Forecast of carbon reduction potential to jet fuel industries in 2020-2060

This section investigates the aviation fuel demand and SAF demand in China, and then comprehensively evaluates and predicts the carbon reduction effect of using this TGEE-ethanol technology to produce jet fuel on the entire jet fuel industry.

According to data from the Peking University Energy Research Institute and IATA, China's aviation fuel consumption in 2020 was approximately 25 Mt/year, it is expected that the consumption will reach 60 Mt by 2030, with an annual growth rate of 9.2% from 2020 to 2030. If the Chinese aviation industry aligns with IATA's 5.2% share in global SAF demand should be achievable, it is expected that the SAF demand in China will reach 3 Mt/year by 2030. By 2050, it is expected that the total consumption of aviation fuel will reach 132.5 Mt, with an annual growth rate of 4% from 2031 to 2050, and the SAF demand will reach 86 Mt according to IATA's 65% SAF usage ratio. From 2050 to 2060, the annual growth rate of jet fuel consumption will be 4%, and the proportion of SAF use will reach 100% in 2060. Based on the above description, China's aviation fuel consumption and SAF demand in 2020-2060 are shown in **Figure 54**.

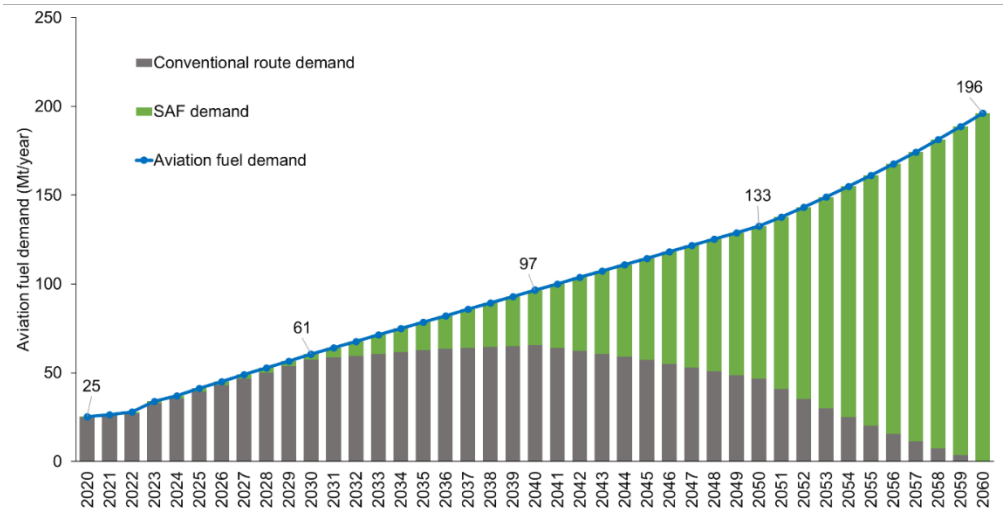

Figure 54. China's aviation fuel consumption and SAF demand in 2020-2060.

Figure 55 shows the carbon reduction potential of jet fuel production from TGEE-ethanol, where carbon reduction refers to the current routes compared to fossil jet fuel routes. Assuming that China's jet fuel is produced entirely from fossil-based routes, its emissions are shown by the black lines. Furthermore, assuming that the SAF capacity all comes from the TGEE-ethanol to jet fuel route, where the solid red line represents the average carbon emissions of industrial tail gas-based ethanol for jet fuel production (due to the wide gas component range of the three tail gas-based ethanol for jet fuel production, it's average carbon emissions can represent the general different industrial tail gas as feedstock to produce jet fuel), and where the red dashed line represents the IEJ route with the lowest carbon emission as the

representative route to simulate its maximum carbon reduction potential. The results show that the carbon emissions of fossil jet fuel will increase from 230 Mt/year in 2030 to 759 Mt/year in 2060, with an annual growth rate of 4%. During 2020–2040, due to the small consumption proportion of SAF, the average carbon emissions and minimum carbon emissions of jet fuel production from TGEE-ethanol with not much different compared with fossil fuels. By 2050, the average carbon emission will decrease to 411 Mt/year (20% carbon reduction), and the maximum carbon emission will decrease to 316 Mt/year (38% carbon reduction). By 2060, the great carbon reduction potential brought by this low-carbon technology is evident, with an average carbon reduction of 35% and a maximum carbon reduction of 63%. In particular, the red dashed line representing the optimal carbon emissions gradually decreases with the increasing SAF demand, indicating the environmental sustainability of this jet fuel from the TGEE-ethanol route.

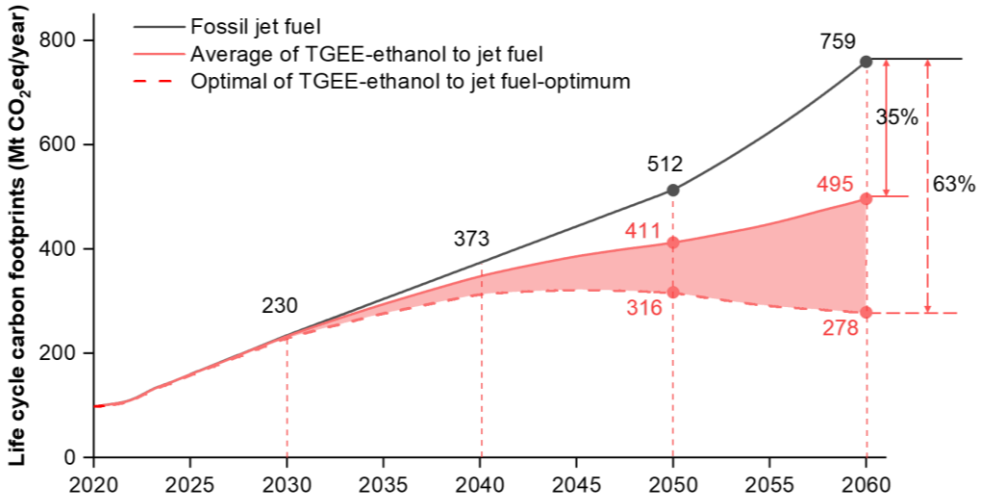

Figure 55. Carbon reduction potential for jet fuel production from TGEE-ethanol in 2020–2060.

6.2.4 Drivers and implications for ethanol to jet fuel

There is significant interest from both government and aviation sectors to displace fossil-based jet fuel in favour of affordable, high-quality alternative jet fuels. High fuel prices, fuel price volatility, the desire to reduce GHG emissions, and the fact that some governments are considering or implementing carbon emissions penalties for aviation make using low-carbon fuels attractive and beneficial [74]. There are three primary reasons that aviation has a strong need for non-petroleum-based jet fuel: cost, climate change, and national security [229]. Also, some other drivers should taken into account, such as energy density, green consumer market, and renewable fuel credits [231]. **Table 32**

identifies potential drivers for renewable ethanol to jet fuel. This table identifies potential drivers for considering jet fuel production from low-cost renewable ethanol rather than selling ethanol directly as a commodity chemical. To make this comparison, the value of ethanol relative to jet fuel in terms of its properties, price, and market size are evaluated. Changes to the market that make ethanol-derived jet fuel blend stocks more attractive to produce than petroleum-based fuels are discussed. The influence of government taxes and incentives both within the countries and abroad is also addressed. Based on the EIA's Annual Energy Outlook reference case, comparing the cost and market size of ethanol and jet fuel, ATJ appears to be economical if the cost of production of intermediate alcohol is substantially lower than the wholesale price and the cost of the alcohol conversion step is not prohibitive. Given sufficiently low production cost, ethanol availability and existing infrastructure suggest that it is a viable intermediate for the production of alternative jet fuel components.

Table 32. Drivers for ethanol to jet fuel.

Driver	Challenge	Solution
Cost	Crude oil has historically been susceptible to price fluctuations, seriously affecting airlines' fuel costs (40% total).	Domestically produced jet fuel from abundant industrial tail gas feedstock is less likely to experience such extreme fluctuations.
Price difference	There must be an adequate price difference between the wholesale jet fuel and intermediate ethanol.	EIA forecasts indicate positive spreads in most cases except for low oil price areas.
Climate change	The aviation sector has maximized the improvement of engine efficiency and limitations on renewable options compared to land transportation.	SAF is currently the best alternative fuel option, offering up to or even more than 80% reduction in carbon emissions.
National security	Over-reliance on foreign oil is believed to make China face the risk of supply interruption.	Domestically produced advanced "drop-in" fuels are expected to help the broader national security objectives.
Other air pollutions	Particles and SO_x are emitted from the combustion of petroleum-based fuels.	ATJ has low sulfur content and can be used for containing low aromatic hydrocarbons.
Energy density	Ethanol has a low energy density compared to fossil fuels.	Ethanol to jet fuel leads to a 60% increase in energy density.
Green consumer market	Consumers prefer to pay for green alternative fuels.	Sustainable jet fuel meets the "lifestyles of health and sustainability" (LOHAS) market.
Renewable fuel credits	Carbon taxes could be imposed on airlines in the future.	SAF reduces the cost impact of the carbon tax by about 30% when blended 50% with fossil jet fuel.
Flexibility to produce paraffin or Cyclic components	Not all alternative fuel routes allow for the production of paraffin or cyclic hydrocarbons.	Ethanol-to-jet has a lower hydrogen demand and greater flexibility to produce isoparaffins or cyclic components.

The aerospace industry has strict requirements for alternative fuels due to their extreme usage conditions and their safety implications, therefore it is not surprising that alternative fuels are meant to be drop-in and must exactly meet the standards of current jet fuels [232, 233]. This makes it rather disturbing how such technologies can be implemented on larger scales for creating high-valued jet fuel of suitable

quality [234]. This is considerably more difficult due to the lack of data on these waste-to-energy conversion technologies at appropriate scale [204, 235]. To accurately model such technologies (process, emissions and costs), it is crucial to have access to real data from scaled-up systems, but this is not feasible due to the intellectual property loophole in favour of private companies who own them. The available published data is limited to lab/pilot scale set-ups that may not provide appropriate insight into scaled-up systems. As the ethanol-to-jet fuel process data used for this study is extracted from various published literature, hence the limitations associated with this data must be noted.

It is important to note the implication of the life cycle carbon footprint under the carbon-neutrality target. This study has seen no evidence of carbon negativity in all the pathways investigated, and it should be noted that there are other products from the jet fuel production process e.g. gasoline, whose usage will increase the carbon footprint declared. Hence, determining the long-term environmental sustainability of such alternative jet fuels, how they can achieve zero carbon future, and the costs of this remains a concern. Furthermore, the affordability of the fuels, its impact on the cost of air travel and customer tolerance for higher travel costs will be another important consideration. Currently, the cost

of such alternative jet fuel is predictably at least two times more expensive than conventional jet fuels. This makes governmental support, incentives, and investments crucial to its uptake, as seen recently in the United States. Therefore, more work is needed in the future in terms of social acceptance and policy implications to comprehensively evaluate the sustainability of jet fuel production from ethanol feedstock.

Sustainability and decarbonisation of the aviation industry is a challenging long-term mission which might require intense technological transition and it is becoming increasingly vital that appropriate, proven and practical data must be used for viability and sustainability assessment of sustainable alternatives [236]. This would be useful to prevent churnalism and unsupported claims that deter the goal of finding suitable long-term solutions in favour of short-term alterations and strategies that allow the extension of business-as-usual. Overall, this brings up ‘transitional technologies’ which might be better than the conventional fossil technologies but not good enough as a long-term sustainable option [237]. Now, how much time, resources and money should be invested in those? How do they compete with research and development funding and resources for potentially better solutions? and how soon will the better solution need to be implemented? We are in a

race to a sustainable 2060 with net-zero emissions, with such a short time left, the efficacy of decision-making and investment is crucial. Considering the limited scope of this paper in establishing the carbon neutrality and affordability of jet fuel derived from ethanol, some of the practical questions, challenges they pose and potential strategies for tackling them will be further explored in future works.

6.3 Summary

This chapter evaluates the impact of ethanol production from tail gas on upstream and downstream industries. The upstream industry by taking the Chinese steel industry as a typical case study, examined the environmental, energy and economic differences between ethanol production and electricity generation from LDG gas, and projected the carbon reduction potential and economic benefits by 2060, as well as the possible layout of the steeling-LDG-ethanol in the future. The downstream industry investigated the impact of ethanol production of jet fuel on the aviation industry, calculated the carbon footprints and production cost of current ethanol to jet fuel technology, and projected the carbon reduction potential of ethanol-based jet fuel in the aviation industry.

By taking the Chinese steel industry as an example, it is found that if LDG-ethanol technology is applied, the carbon reduction potential can achieve 5.6 Mt CO_2/a by 2060, with \$2.97 – 3.49 billion economic profits compared with LDG-originated power route. Currently, the steel industry needs to be orientated towards collaborative carbon reduction, and driving the upgrade of ultra-low emission technology is an urgent need. Optimisation of ultra-low emission technologies, low carbon smelting and carbon reduction in the production process, optimisation of the production structure, low carbon production technologies and carbon dioxide capture and storage (CCS) utilisation are important ways to reduce pollution and carbon emissions in the iron and steel industry. In the future, the steel industry needs to complete four “comprehensive” tasks, namely, comprehensive upgrading of ultra-low emission technologies, comprehensive coverage of pollutant types, comprehensive construction of pollution reduction and carbon reduction standard system, and integration of carbon capture, utilization, storage and production, so as to achieve comprehensive pollution and carbon reduction in the steel industry.

We believe that huge environmental and economic benefits will promote the rapid development of LDG-ethanol technology in the steel-

making industry. Also, through the geographical analysis of raw material resources and renewable power, it is suggested Southwest, Northwest, and South China are suitable for the LDG-ethanol deployment. In fact, all the prediction is based on the theoretical maximum, there are many constraints to the realization of the ideal situation. For example, LDG gas steel plants are unlikely to have only one way to use them. In addition, due to the limitation of green power resources, it is impossible to fully consider the steel industry in practice. Meanwhile, the economic benefit prediction and the uncertainty are also inevitable. However, what we can confirm is that the conclusions are reasonable. Therefore, this work results provide valuable guidelines for the future planning of the LDG-ethanol industry in China.

When investigating the impact of TGEE-ethanol on aviation fuel, the carbon footprints show that iron alloy (IEJ, 65 g CO_2eq/MJ) and calcium carbide (CEJ, 74 g CO_2eq/MJ) tail gas ethanol-based to jet fuel routes had lower carbon footprints than fossil jet fuel (90 g CO_2eq/MJ) while their production cost is much higher than that of fossil jet fuel. From 2020 to 2060, the projected carbon footprints of the CEJ and IEJ routes are reduced by 42% and 50%, respectively. The production cost of the SEJ route decreased from $1164/t to $793/t (32% decrease), while the cost

reduction of CEJ and IEJ routes decreased by an even greater 48%, and all of them will be lower than the cost of fossil jet fuel route. Carbon taxes of $10, $50, and $100 could reduce costs by 3–32%, achieving cost parity with fossil fuels 2–10 years earlier than previously estimated around 2050. The carbon reduction potential of this TGEE-ethanol to jet fuel route in the Chinese aviation sector is estimated to be up to 63% by 2060, and the carbon emissions gradually decrease with the increasing SAF demand, indicating the environmental sustainability of this route. In addition, cost, climate change, and national security were identified as the three main drivers of strong demand for non-fossil fuel-based jet fuel. The pathway of TGEE-ethanol to aviation fuel may offer a low-carbon option for sustainability and decarbonization in the aviation industry.

CHAPTER 7. Conclusions

Ethanol is widely used in the chemical, pharmaceuticals, food and fuel industries as an essential bulk chemical and energy substitute. With the increasing global emphasis on climate change and environmental protection, the production of sustainable ethanol has garnered more attention. Converting industrial tail gas into ethanol can effectively reduce carbon dioxide emissions and achieve value-added utilization of waste gas. This not only contributes to carbon reduction and decarbonization goals but also improves environmental impact, promoting a circular economy and sustainable development. Therefore, it is essential to comprehensively and systematically analyse the environmental impact and techno-economic performance of tail gas ethanol from a life cycle perspective.

This thesis provides a comprehensive life cycle assessment (LCA) of ethanol production from industrial tail gas. It includes an environmental impact assessment of the production of renewable ethanol by biological fermentation of tailpipe from the steel industry (11 environmental indicators and comparison with competitive routes) and an analysis of the environmental potential of an optimized scenario through gradual decarbonization of the electricity supply. To further

enhance carbon efficiency and reduce carbon emissions, a novel technology combining tail gas ethanol production with electro-catalytic CO_2 reduction was proposed, followed by a life cycle and techno-economic analysis based on Monte Carlo simulation. Finally, the thesis evaluates the environmental and economic performance of TG-ethanol in upstream and downstream industries.

Chapter 4 presents a life cycle environmental impact assessment of ethanol production from Linz-Donawitz Gas (LDG) in the iron and steel industry via bio-fermentation technology, quantifies the results of 11 environmental impact indicators, different power supply structure scenarios, and environmental impact potential compared with competitive routes to answer the overall research question: **1)** What is the life cycle environmental impact of TG-ethanol throughout the cradle-to-gate production process, and how do they compare to biomass-based and fossil fuel-based ethanol? What are the contributions of each production unit, energy and material consumption to the environmental impact? **2)** What is the potential for reducing the environmental impacts of the three ethanol production pathways through the application of different renewable electricity sources? Results and discussion focus on the competitiveness of environmental impact over LDG-ethanol with

traditional routes revealed by taking China as a scenario, but its data and results could provide valuable knowledge and insights for the scientific development of the LDG-ethanol industry in other countries with strong fuel ethanol demands. The sensitivity and scenario analysis can also extend the assessment results to overcome the period and geographic limitations of the applications in this study. From this work result, it is believed that countries with ample clean power could gain larger profits if LDG-ethanol technology developed.

Regarding **research question 1**, the assessment results show that the LDG-ethanol route is the most environmentally benign option, whose environmental impact value is 22–25% lower than that of Corn-ethanol and Coal-ethanol routes. Based on the CML method, the LDG-ethanol route has the best impact on ADP-f, EP and FAETP and the worst impact on the AP and MAETP indicators. Additionally, the GWP value of the LDG-ethanol route is 5.11 t CO_2eq/t, while for the Corn-ethanol and Coal-ethanol routes, they are -0.46 t CO_2eq/t and 6.21 t CO_2eq/t, respectively. The 11 environmental indicators are decomposed according to the relative contribution from all the production units, the PRT and FMT units dictate the environmental footprints of the LDG-ethanol process, with total contributions of over 75% to all the indicators, and the contributions

from other units decrease following by WWT (6 – 11%) > CWS (5 – 9%) > TGT (3 – 4.5%) > DIS (0.8 – 3.6%). The contribution of different utility inputs (electricity, nitrogen, chemicals, water etc.) to the 11 indicators is also analysed and results show that electricity plays a determining role in the environmental footprint of the LDG-ethanol process, with over 80% contributions to 9 indicators (ADP-f, AP, EP, FAETP, HTP, MAETP, ODP, POCP and TETP), 52% to ADP-e, and 22% to GWP. The significant impact of electricity may result from China's dominant coal-fired power generation process.

Regarding **research question 2,** since electricity is identified as a sensitive factor by sensitive analysis, with the energy saving and green power introduction, the comprehensive environmental impact of the LDG-ethanol route could be further alleviated by 15 – 68%. In the LEE scenario with higher electricity efficiency, most indicators drop by ~20% due to the decrease in electricity consumption, except ADP-e and GWP. Most of the indicators decreased substantially when shifting the electricity source to a non-fossil type (PV, WP, HP for LEGP, LEGW, and LEGH scenarios, respectively). In the LEGP scenario, a significant reduction between 55 – 88% is observed for ADP-f, AP, EP, FAETP, HTP, MAETP, and POCP indicators, and for the GWP indicator, the reduction

space is narrowed to 21%. Nevertheless, employing green electricity can greatly lower the overall environmental impact, with EI values dropping to 0.35, 0.20 and 0.13 for LEGP, LEGW, and LEGH, respectively. All 11 environmental impacts can be further decreased in the LEEGP, LEEGW, and LEEGH scenarios, namely by increasing electricity efficiency and decarbonizing the grid mix simultaneously.

Chapter 5 proposes a novel ethanol production technology integrating tail gas-based ethanol (TG-ethanol) with electro-catalytic CO_2 reduction (ECR), called TGEE technology, which was first proposed to address the energy and carbon efficiency issues associated with the state-of-the-art TG-ethanol technologies. The process was modularly modelled to accommodate different ECR integration scenarios for three typical industrial tail gas streams (steel, iron alloy and calcium carbide). Life cycle & techno-economic analysis based on Monte Carlo simulation were employed to evaluate the environmental and economic performance of the TGEE process to answer the overall research question: **3)** What are the two process feasibility of TG-ethanol production intensified by electro-catalytic CO_2 technology (TGEE)? What are the technical performance indicators of the optimal process and the analysis of carbon flow? **4)** What are the results of the life cycle

carbon footprint and economic performance of TGEE technology? What is the more reliable probability range of sensitivity analysis and Monte Carlo simulation to evaluate the LCA and TEA results of TGEE technology? The results and discussion focus on the life cycle carbon footprints and economic affordability of TGEE-ethanol production, which could provide valuable insights for researchers and stakeholders regarding the commercial deployment of TGEE technology, thereby promoting the circular economy and sustainable development.

Regarding **research question 3**, three typical industrial tail gases (steel, iron alloy and calcium carbide) were selected as feedstock for ethanol production, and the POE process generally outperforms the PRE process, making it more appealing for medium to long-term carbon neutrality targets. Across the three series of cases, ethanol capacity can increase by 1.3–2.9 times, with carbon efficiency reaching up to 36–82%. For steel tail gas in TGEE-ethanol production, carbon efficiency can be improved from 28% to 36% (BASS to POSE0.4), while a higher carbon efficiency is achieved in the iron alloy and calcium carbide tail gas to ethanol cases, that is 28% to 82% (BASI to POIE0.9) and 28% to 78% (BASC to POCE0.9). When comparing the indicators of cases with their maximum ECR recycle ratio (POSE0.4, POIE0.9, POCE0.9), the

ethanol capacity and surplus steam of POIE0.9 and POCE0.9 are more than 3 times that of POSE0.4, and electricity demand is more than 2 times, with the ECR electricity share increases to about 90%. Remarkably, the ECR process can be powered by low-voltage electricity generated by photovoltaic panels instead of the national grid. Therefore, renewable energy not only meets the high demand for the ECR process but also reduces carbon emissions.

Regarding **research question 4**, from the life cycle assessment, the carbon footprints of TGEE-ethanol were estimated to be 1.77 – 3.93 t CO_2eq/t ethanol, with a carbon reduction potential of up to 32 – 63%, much better than previously reported TG-ethanol. In most scenarios, the life cycle carbon footprint contribution of TGEE-ethanol indicated that direct emissions account for the largest share in the entire life cycle carbon footprints, followed by utility emissions, with feedstock emissions being the smallest contributions. From the techno-economic analysis, the minimum ethanol selling price (MESP) has been estimated to be \$428 – 962/t ethanol, which is lower than the ethanol market price (\$900 – 1080/t). The MESP contribution of TGEE-ethanol suggested that materials costs accounted for the major portion, followed by fixed operating costs and utility costs. Uncertainty analysis using Monte Carlo

simulation provided more reliable probabilistic results for the environmental and economic impacts. For the probability density function of life cycle carbon footprints, it is seen that higher CO concentration in the feed stream and ECR recycle ratio operating conditions result in a wider range of life cycle carbon footprints, the simulated LCA carbon footprints range from 1.41 – 4.18 t CO_2eq/t ethanol, with a variation of (± (5% – 27%)). As for the NPV results, nearly all scenarios display about 100% probability of NPV>0, and POIE0.9 (P>78%) and POCE0.9 (P>93%) also show a positive NPV with a large probability. The simulated MESP ranges from $348 – 1229/t, with a variation of (± (14% – 48%)). As for the comprehensive performance (CP) analysis in terms of environmental, economic and energy aspects, the POSE0.4, POIE0.9 and POCE0.9 scenarios in their series achieved the highest CP and made a comparison with previous studies of bio- and fossil-based ethanol. Overall, the comprehensive analysis suggests that the TGEE process could present a more economically and environmentally benign next-generation technology for producing ethanol from industrial tail gas.

Chapter 6 answers **research question 5** by evaluating and projecting the impact of LDG-ethanol production on upstream and

downstream industries. The upstream industry by taking the Chinese steel industry as a typical case study, examined the environmental, energy, and economic differences between ethanol production and electricity generation from LDG gas, and projected the carbon reduction potential and economic benefits by 2060, as well as the possible layout of the steeling-LDG-ethanol in the future. Comparatively, the product value of LDG-ethanol is $1250 higher than LDG-power, with a 1310 kg CO_2 equivalent reduction and 60% lower carbon intensity. With the decarbonization of electricity in the middle and long term, the estimated carbon reduction potential is narrowed to 9.8–18.6 $MtCO_2$ in 2025 and 5.3–5.6 $MtCO_2$ in 2060, and the overall economic benefit will range between $1.36–2.20 billion in 2025 and sharply increase to $2.97–3.49 billion in 2060. Furthermore, through the geographical analysis of raw material and renewable power resources, it is suggested Southwest, Northwest, and South China are suitable for the LDG-ethanol deployment. Therefore, the integration of LDG-ethanol bio-fermentation technology with the steel industry provides an innovative path for the high-value utilization of steel industry tail gas, effectively promoting energy conservation, emissions reduction, and circular economy in steel enterprises.

The downstream industry investigated the impact of ethanol production of jet fuel on the aviation industry, calculated the carbon footprints and production cost of current ethanol to jet fuel technology, and projected the carbon reduction potential of ethanol-based jet fuel in the aviation industry. Results show that the carbon footprints of tail gas ethanol production from iron alloy (IEJ, 65 g CO_2eq/MJ) and calcium carbide (CEJ, 74 g CO_2eq/MJ) routes had lower carbon footprints than fossil jet fuel (90 g CO_2eq/MJ) while their production cost is much higher than that of fossil jet fuel. From 2020 to 2060, the projected carbon footprints of the CEJ and IEJ routes are reduced by 42% and 50%, respectively. The production cost of the SEJ route decreases from $1164/t to $793/t (a 32% decrease), while CEJ and IEJ routes see a larger cost decrease of 48%, both lower than the fossil jet fuel route costs. Carbon taxes of $10, $50, and $100 could reduce costs by 3–32%, achieving cost parity with fossil fuels 2–10 years earlier than previously estimated around 2050. By 2060, the carbon reduction potential of this TGEE-ethanol to jet fuel route in the Chinese aviation sector is estimated to be up to 63%. The pathway for converting TGEE-ethanol into jet fuel may provide a low-carbon option for the sustainability and decarbonization of the aviation industry.

7.1 Implications of this thesis to stakeholders

The latest breakthroughs in the production of renewable ethanol from industrial tail gas could have significant implications for stakeholders in the ethanol industry and its upstream and downstream sectors, particularly regarding greenhouse gas emissions and economic feasibility. TG-ethanol, as an emerging technology, demonstrates a better overall environmental impact compared to bio-based and fossil-based ethanol, although its greenhouse gas emissions are higher than those of bio-based ethanol. TGEE-ethanol shows great potential for greenhouse gas reduction, but its environmental impact and economic viability largely depend on feedstock sources, resource consumption, energy supply, and supply chain management. Therefore, stakeholders should focus on energy supply, supply chain management, and technological innovation when considering the development and application of tail gas ethanol technology.

- **Key Role of Energy Supply and Renewable Energy.** The structure of electricity supply significantly affects environmental impact, especially in China, where coal-fired power is dominant. Thus, the introduction of clean energy and the decarbonization of the grid are crucial for further reducing environmental impact. By

improving electricity efficiency and introducing green power sources such as photovoltaic, wind, and hydroelectric power, the environmental impact of LDG-ethanol production can be reduced by 15–68%, greatly enhancing the technology's environmental performance.

- **Supply Chain Management and Industrial Integration.** Studies indicate that LDG-ethanol technology performs well in both environmental and economic terms. Countries and regions with abundant clean energy can better leverage its advantages. Stakeholders in carbon-rich tail gas industries like steel, calcium carbide, and ferroalloy can integrate TGEE-ethanol bio-fermentation technology to achieve high-value utilization of tail gas, promoting energy conservation, emission reduction, and a circular economy. Economic benefits are expected to significantly increase, and carbon reduction potential will greatly expand by 2060. Downstream industries such as aviation and ethylene production can benefit from tail gas ethanol-derived products with lower carbon footprints than traditional fossil fuels, and production costs are expected to significantly decrease in the future. By 2060,

carbon neutrality and economic affordability are projected to reach optimal levels.

- **Technological Innovation.** This study introduces a novel technology combining tail gas ethanol production with electro-catalytic CO_2 reduction (ECR), known as TGEE, which shows great potential for improving carbon efficiency and reducing carbon emissions. TGEE technology also demonstrates competitive economic performance, with the minimum ethanol selling price (MESP) ranging from $428/t to $962/t, lower than the market price ($900/t to $1080/t). With ongoing improvements in bio-fermentation efficiency and CO_2 conversion technologies, similar innovative concepts will be the focus of future research.

In summary, stakeholders should continuously monitor the ongoing development of tail gas ethanol technology, integrating advanced technologies and renewable energy sources to contribute significantly to global carbon reduction goals and sustainable development.

7.2 Main limitations and uncertainties

It should be pointed out that there are still some limitations in this work. Although LCA is an essential tool for assessing environmental

impacts, some uncertainties related to ethanol production were encountered during this analysis, such as limited data availability, rapid technological progress, regional and supply chain variability.

- **Limited data availability.** LCA relies on accurate and traceable data to assess the environmental impacts at various stages of ethanol production. However, data availability may be limited. While the data on TG-ethanol in Chapter 4 comes from reliable plant operation data, data for other competing routes and process modelling routes still require ongoing validation and optimisation, which brings uncertainty and affects the accuracy of the assessment.
- **Future technological progress.** The LCA results of TG-ethanol technology may change significantly with future technological progress. The continuous development of new feedstocks, new microbes and manufacturing processes will have a significant impact on the environmental performance of TG-ethanol. For example, if the fermentation efficiency of the microbes of the next generation of TG-ethanol technology is greatly improved, the ethanol yield will double, or the industrial tail gas feedstocks become more diverse and current results might become outdated.

- **Regional and supply chain variability.** The environmental impacts associated with TG-ethanol production will vary greatly depending on the geographical location and the energy mix supplied. Different plant locations and the types of energy used in production significantly influence environmental impacts. The energy source, whether fossil fuels or renewable energy, affects the overall carbon footprint and other environmental indicators.

In particular, in Chapter 4, the upstream steel process is not included in the system boundary. If the system boundary is expanded, there will be a more comprehensive understanding of the impact and benefits of the bio-fermentation ethanol technology. Therefore, in order to evaluate the reduction benefit, a technical system for coupling steel and bio-fermented ethanol before and after application is encouraged to be investigated, which is ongoing research.

In Chapter 5, the early-stage modelling design of processes is significantly affected by uncertainties due to the scarcity and variability of input parameters. This means that during the initial phase of model development, there may be a lack of sufficient accurate data, or these data may exhibit substantial volatility, leading to uncertainty in model predictions. For instance, factors such as the supply and cost of raw

materials, energy prices, technological efficiency, and environmental impacts can vary significantly by region and over time, affecting the accuracy and reliability of the model. Nevertheless, if reasonable approximations and distributions are used to describe the reliability of TEA & LCA, the results still provide a reasonable reference point for identifying feasible pathways, thereby increasing the effectiveness of investment decision-making.

In Chapter 6, for the final part of the influence on the steel industry, all the prediction is based on the theoretical maximum. In fact, there are many constraints to the realization of the ideal situation. For example, LDG gas steel plants are unlikely to have only one way to use them. In addition, due to the limitation of green power resources, it is impossible to fully consider the steel industry in practice. Meanwhile, the economic benefit prediction and the uncertainty are also inevitable. However, what we can confirm is that the conclusions are reasonable.

7.3 Future work

This section discusses recommendations for future work in the following research areas: ethanol production, ethanol supply chain, and upstream-downstream industry integration.

- **Ethanol Production.** This study evaluates the environmental impact of tail gas ethanol production by considering national grid data and simulating lower-carbon technologies through the coupling of electrocatalytic technology. Analysis indicates that decarbonization in the power sector reduces the overall GHG emissions from TG-ethanol production. Over time, tail gas ethanol could potentially become a zero-carbon or even negative-carbon technology. Future work should assess the role of other decarbonization measures involving non-electric energy inputs, such as thermal energy supply and carbon efficiency improvements at different stages of the ethanol lifecycle. Optimizing carbon efficiency can be approached from two angles: 1) Enhancing the conversion rate of ethanol production via bio-fermentation: This can be achieved by optimizing gas composition and pressure, cultivating more robust and durable proprietary microorganisms, precisely controlling pH and temperature, and enhancing gas-liquid mass transfer in bioreactors. 2) Increasing the rate of CO_2 reduction to CO in the electrocatalytic reaction: This can be accomplished by developing efficient catalysts, electrodes, and electrolytes, optimizing current

density and reaction interfaces, and enhancing the molecular understanding of CO_2 electroreduction. Furthermore, Chapter 5 of this study focuses primarily on three indicators: Global Warming Potential (GWP), Net Present Value (NPV), and Minimum Ethanol Selling Price (MESP). Future research could include other relevant indicators, such as water consumption and land use, as these are scarce resources with sometimes limited availability.

- **Ethanol Supply Chain.** The primary advantage of tail gas ethanol technology is that the raw materials are derived from industrial tail gas, turning waste into valuable resources. This study emphasizes using industrial tail gas rich in CO from typical industries as feedstock and the minimum percentage of CO content in the tail gas should be 40% v/v. Future work could also consider integrating other syngas production industrial technologies, such as gasification of carbon-rich wastes (e.g., municipal solid waste, forestry and agricultural residues, and other biomass resources), producing syngas primarily composed of CO and H_2, which can serve as substrates for bio-fermentation, thereby enhancing the efficient utilization of waste resources.

Additionally, energy supply is not limited to photovoltaic energy used in this study; it could also include wind power, hydropower, biomass power generation, and other renewable energy sources. These can be integrated with smart grids and digital power systems to achieve efficient utilization of clean energy. As the market grows, optimizing the tail gas ethanol supply chain and ensuring the sustainable supply of raw materials and energy is essential to avoid potential supply bottlenecks.

- **Upstream-Downstream Industry Integration.** Enterprises producing industrial tail gas for tail gas ethanol can consider extending their industrial chains by collecting other industrial waste gases from their plants as raw materials for bio-fermentation. The production process can be divided into three stages: 1) Bio-fermentation and centrifugation to produce ethanol; 2) Production of protein feed; 3) Using part of the ethanol as raw material to produce ethylene, aviation fuel, and other downstream products. By comprehensively considering and extending the industrial chain, the overall environmental and economic performance of enterprises from cradle to grave can be improved.

Implementing these optimization measures can lead to more efficient and sustainable ethanol production and supply chain operations, maximizing economic and environmental benefits through upstream-downstream industry integration.

Appendix

Table A1. LCIA results of all ethanol routes.

Scenarios	EI	ADP-e	ADP-f	AP	EP	FAETP	GWP	HTP	MAETP	ODP	POCP	TETP
	—	kg Sb eq.	MJ	kg SO_2 eq.	kg Phosphate eq.	kg DCB eq.	kg CO_2 eq.	kg DCB eq.	kg DCB eq.	kg R11 eq.	kg Ethene eq.	kg DCB eq.
LE	0.41	1.94E-04	1.36E+04	3.59E+00	3.70E-01	1.71E+00	5.11E+03	1.08E+02	1.19E+05	1.02E-11	4.20E-01	1.23E+00
LEE	0.34	1.67E-04	1.07E+04	2.76E+00	2.90E-01	1.36E+00	4.82E+03	8.30E+01	9.10E+04	7.73E-12	3.20E-01	9.50E-01
LEGP	0.35	2.90E-03	3.03E+03	5.20E-01	7.00E-02	7.60E-01	4.04E+03	4.60E+01	3.28E+04	4.44E-10	5.00E-02	3.40E-01
LEGW	0.20	5.73E-04	2.31E+03	2.80E-01	5.00E-02	4.60E-01	3.98E+03	3.80E+01	8.20E+03	2.23E-11	2.00E-02	1.25E+00
LEGH	0.13	1.10E-04	2.09E+03	2.30E-01	4.00E-02	3.00E-01	3.97E+03	1.30E+01	4.50E+03	3.05E-13	2.00E-02	1.30E-01
LEEGP	0.30	2.21E-03	2.80E+03	4.50E-01	6.00E-02	6.50E-01	4.02E+03	3.60E+01	2.58E+04	3.35E-10	4.00E-02	2.80E-01
LEEGW	0.18	4.52E-04	2.25E+03	2.70E-01	5.00E-02	4.20E-01	3.97E+03	3.00E+01	7.24E+03	1.68E-11	2.00E-02	9.70E-01
LEEGH	0.13	1.04E-04	2.09E+03	2.30E-01	4.00E-02	3.00E-01	3.97E+03	1.10E+01	4.45E+03	3.01E-13	2.00E-02	1.20E-01
Corn-ethanol	0.53	6.05E-04	1.69E+04	1.71E+00	3.12E+00	4.66E+01	-4.57E+02	6.40E+01	5.46E+04	9.02E-12	1.20E-01	1.03E+00
Corn-ethanol-PV	0.53	8.17E-04	1.61E+04	1.47E+00	3.10E+00	4.66E+01	-5.36E+02	5.90E+01	4.78E+04	4.32E-11	9.00E-02	9.50E-01
Corn-ethanol-WP	0.52	6.33E-04	1.60E+04	1.45E+00	3.10E+00	4.65E+01	-5.41E+02	5.90E+01	4.58E+04	9.96E-12	8.00E-02	1.03E+00
Corn-ethanol-HP	0.51	5.97E-04	1.60E+04	1.45E+00	3.10E+00	4.65E+01	-5.41E+02	5.70E+01	4.55E+04	8.23E-12	8.00E-02	9.40E-01
Coal-ethanol	0.55	8.85E-05	7.38E+04	2.82E+00	4.30E-01	2.43E+00	6.21E+03	1.28E+02	6.77E+04	1.13E-10	7.50E-01	1.31E+00
Coal-ethanol-PV	0.53	1.15E-03	6.97E+04	1.62E+00	3.20E-01	2.06E+00	5.79E+03	1.04E+02	3.39E+04	2.83E-10	6.00E-01	9.60E-01
Coal-ethanol-WP	0.46	2.37E-04	6.94E+04	1.53E+00	3.10E-01	1.94E+00	5.77E+03	1.01E+02	2.43E+04	1.18E-10	5.90E-01	1.32E+00
Coal-ethanol-HP	0.44	5.58E-05	6.93E+04	1.51E+00	3.10E-01	1.88E+00	5.77E+03	9.10E+01	2.28E+04	1.10E-10	5.90E-01	8.80E-01

Table A2. Electricity contribution in different scenarios of LDG-ethanol routes.

Item	LE	LEE	LEGP	LEGW	LEGH	LEEGP	LEEGW	LEEGH
ADP-e	1.09E-04	8.25E-05	9.74E-01	8.51E-01	2.36E-01	9.61E-01	8.13E-01	1.88E-01
ADP-f	1.15E+04	8.66E+03	3.17E-01	1.00E-01	7.83E-03	2.58E-01	7.75E-02	5.90E-03
AP	3.37E+00	2.53E+00	5.64E-01	1.93E-01	2.29E-02	4.93E-01	1.53E-01	1.74E-02
EP	3.24E-01	2.44E-01	3.75E-01	1.32E-01	1.57E-02	3.11E-01	1.03E-01	1.19E-02
FAETP	1.42E+00	1.07E+00	6.20E-01	3.65E-01	3.36E-02	5.50E-01	3.02E-01	2.56E-02
GWP	1.15E+03	8.64E+02	2.06E-02	4.92E-03	2.88E-03	1.56E-02	3.72E-03	2.17E-03
HTP	1.03E+02	7.76E+01	8.78E-01	8.59E-01	5.92E-01	8.46E-01	8.19E-01	5.20E-01
MAETP	1.15E+05	8.67E+04	8.70E-01	4.75E-01	4.29E-02	8.32E-01	4.06E-01	3.26E-02
ODP	9.88E-12	7.44E-12	9.99E-01	9.85E-01	5.32E-02	9.99E-01	9.85E-01	4.06E-02
POCP	3.95E-01	2.98E-01	5.78E-01	4.05E-02	5.25E-03	5.08E-01	3.08E-02	3.95E-03
TETP	1.12E+00	8.41E-01	6.75E-01	9.12E-01	1.33E-01	6.11E-01	8.87E-01	1.03E-01

Table A3. Tail gas composition of typical industrial processes [8].

Industry		CO/%	CO_2/%	N_2/%	Others/%
Ammonia	Purge gas	25-45	/	41-64	H_2, 2.5-8
Steel	Linz-Dinowitz Gas (LDG)	45-55	15-20	25-30	/
Iron alloy	Tail gas	65-75	10-20	5-10	H_2, 5-10 CH_4, 0-2
Calcium carbide	Closed electric furnace flue gas	70-90	3	1-8	H_2, 2-7
Silicon carbide	Tail gas	70-90	2-3	1-3	H_2, 1-5 CH_4, 2-4
Phoschemical	Yellow phosphorus production	75-90	2-4	/	O_2, 0.5-1 H_2O, 3-5
Acetic acid	Tail gas	81	3	2	H_2, 12 CH_4, 1.5

Table A4. Life cycle carbon footprint contributions of all scenarios.

Scenarios	Net emissions	Direct emissions	steam	grid power	PV	Phosphoric acid	Sodium hydroxide	Ammonia	Sodium hydrosulfide	Potassium hydroxide	Nitrogen	water
BASS	5.20	4.30	–0.001	0.753	0.000	0.013	0.002	0.103	0.004	0.013	0.016	0.001
POSE0.1	4.90	4.00	–0.124	0.756	0.076	0.013	0.002	0.103	0.004	0.013	0.016	0.001
POSE0.2	4.59	3.70	–0.167	0.770	0.157	0.013	0.002	0.103	0.004	0.013	0.016	0.001
POSE0.3	4.28	3.30	–0.191	0.782	0.244	0.013	0.002	0.103	0.004	0.013	0.016	0.001
POSE0.4	3.93	2.80	–0.216	0.813	0.341	0.013	0.002	0.103	0.004	0.013	0.016	0.001
BASI	4.83	4.08	–0.001	0.598	0.000	0.013	0.002	0.103	0.004	0.013	0.016	0.001
POIE0.1	4.54	3.79	–0.053	0.592	0.062	0.013	0.002	0.103	0.004	0.013	0.016	0.001
POIE0.3	3.98	3.17	–0.141	0.603	0.202	0.013	0.002	0.103	0.004	0.013	0.016	0.001
POIE0.5	3.39	2.42	–0.197	0.640	0.379	0.013	0.002	0.103	0.004	0.013	0.016	0.001
POIE0.7	2.74	1.61	–0.354	0.705	0.626	0.013	0.002	0.103	0.004	0.013	0.016	0.001
POIE0.9	1.77	0.46	–0.656	0.813	1.003	0.013	0.002	0.103	0.004	0.013	0.016	0.001
BASC	4.85	4.14	–0.002	0.562	0.000	0.013	0.002	0.103	0.004	0.013	0.016	0.001
POCE0.1	4.74	4.06	–0.089	0.568	0.049	0.013	0.002	0.103	0.004	0.013	0.016	0.001
POCE0.3	4.21	3.44	–0.127	0.581	0.161	0.013	0.002	0.103	0.004	0.013	0.016	0.001
POCE0.5	3.72	2.82	–0.181	0.615	0.310	0.013	0.002	0.103	0.004	0.013	0.016	0.001
POCE0.7	2.90	1.90	–0.319	0.674	0.498	0.013	0.002	0.103	0.004	0.013	0.016	0.001
POCE0.9	2.06	0.89	–0.719	0.801	0.936	0.013	0.002	0.103	0.004	0.013	0.016	0.001

Table A5. Cost distributions of MESP ($/t).

	BASS	POSE0.1	POSE0.2	POSE0.3	POSE0.4	BASI	POIE0.1	POIE0.3	POIE0.5	POIE0.7	POIE0.9	BASC	POCE0.1	POCE0.3	POCE0.5	POCE0.7	POCE0.9
Fixed operating costs	137	133	131	127	121	88	86	84	84	81	82	76	78	76	75	74	76
Depreciation cost	67	64	64	62	62	43	42	41	41	39	40	37	38	37	37	36	37
Operating and maintenance cost	28	28	27	26	26	18	18	17	17	17	17	16	16	15	15	15	16
Administrative cost	14	14	13	13	13	9	9	9	9	8	8	8	8	8	8	8	8
Distribution and selling cost	14	14	13	13	13	9	9	9	9	8	8	8	8	8	8	8	8
Labor cost	14	14	13	13	13	9	9	9	9	8	8	8	8	8	8	8	8
Variable operating costs	380	410	453	499	567	265	324	388	525	672	934	250	277	343	438	552	814
Feedstock and material costs	264	256	247	237	236	182	178	172	168	160	158	163	162	158	155	150	144
Feedstock cost	223	210	196	180	173	141	133	118	103	80	57	122	118	108	95	78	45
Phosphoric acid	4	4	4	4	4	4	4	4	4	4	4	4	4	4	4	4	4
Sodium hydroxide	1	1	1	1	1	1	1	1	1	1	1	1	1	1	1	1	1
Ammonia	18	18	18	18	18	18	18	18	18	18	18	18	18	18	18	18	18
Sodium hydrosulfide	1	1	1	1	1	1	1	1	1	1	1	1	1	1	1	1	1
Potassium hydroxide	8	8	8	8	8	8	8	8	8	8	8	8	8	8	8	8	8
Nitrogen	10	10	10	10	10	10	10	10	10	10	10	10	10	10	10	10	10
PEM (proton exchange membrane)	0	2	4	6	9	0	2	5	10	16	25	0	1	4	8	13	25
electrode	0	2	3	5	7	0	1	4	8	13	21	0	1	3	7	11	20
KOH electrolyte	0	1	2	3	5	0	1	3	5	9	13	0	1	2	4	7	13
Utility costs	116	154	206	263	331	92	127	213	330	487	722	87	112	184	282	432	670
water cost	3	2	2	2	2	2	2	2	2	1	1	2	2	2	2	1	1
Grid power	113	114	116	118	122	90	89	91	97	106	122	85	86	88	93	102	120
ECR electricity	0	50	104	161	227	0	41	134	250	414	663	0	32	107	205	360	619
steam cost	0	–12	–16	–19	–21	0	–5	–14	–19	–34	–64	0	–9	–12	–18	–31	–70
Tax cost	81	79	74	70	64	99	93	87	71	55	22	102	99	92	82	70	39
Carbon credit	0	–2	–4	–6	–9	0	–2	–6	–10	–15	–21	0	–1	–5	–8	–14	–20
Total	598	620	654	689	743	462	482	549	643	769	962	428	450	505	587	714	910

Table A6. Comprehensive performance comparison of considered scenarios.

	BASS	POSE0.1	POSE0.2	POSE0.3	POSE0.4	BASI	POIE0.1	POIE0.3	POIE0.5	POIE0.7	POIE0.9	BASC	POCE0.1	POCE0.3	POCE0.5	POCE0.7	POCE0.9
CP	0.25	0.27	0.28	0.31	0.32	0.42	0.45	0.48	0.50	0.55	0.66	0.48	0.48	0.53	0.56	0.63	0.79
CE	0.10	0.12	0.16	0.20	0.24	0.10	0.13	0.20	0.27	0.46	1.00	0.11	0.11	0.17	0.24	0.37	0.93
CF	0.10	0.18	0.26	0.34	0.43	0.20	0.27	0.42	0.58	0.75	1.00	0.19	0.22	0.36	0.49	0.70	0.92
NPV	0.11	0.12	0.12	0.13	0.10	0.68	0.70	0.73	0.68	0.61	0.30	0.88	0.88	0.95	0.95	1.00	0.91
MSP	0.75	0.72	0.68	0.64	0.59	0.95	0.91	0.80	0.65	0.44	0.10	1.00	0.97	0.88	0.76	0.57	0.28
ED	0.98	0.93	0.85	0.77	0.68	1.00	0.94	0.82	0.65	0.43	0.10	1.00	0.96	0.86	0.72	0.55	0.17

Table A7. Carbon reduction of LDG-ethanol in China's BF-BOF steeling production industry.

Year	Steel capacity[209] (Mt)	GHG emissions in the current grid mix (Mt CO_2)	LDG-ethanol reduction potential in different electricity supplies (Mt CO_2)				
			Current grid mix	Predicted grid mix	PV	WP	HP
2025	768	1418	7.09	9.81	18.00	18.71	18.85
2026	742	1368	6.84	10.13	17.38	18.06	18.20
2027	721	1330	6.65	10.48	16.89	17.55	17.69
2028	698	1288	6.44	10.77	16.36	17.00	17.13
2029	676	1247	6.24	11.03	15.84	16.46	16.59
2030	659	1216	6.08	11.33	15.45	16.05	16.17
2031	636	1174	5.87	11.15	14.91	15.50	15.61
2032	614	1133	5.66	10.99	14.39	14.95	15.07
2033	592	1093	5.46	10.82	13.88	14.43	14.53
2034	571	1054	5.27	10.64	13.38	13.91	14.02
2035	550	1016	5.08	10.46	12.90	13.41	13.51
2036	530	978	4.89	10.27	12.43	12.91	13.01
2037	511	942	4.71	10.08	11.96	12.43	12.53
2038	491	906	4.53	9.88	11.51	11.96	12.05
2039	472	871	4.36	9.67	11.07	11.50	11.59
2040	454	837	4.19	9.46	10.63	11.05	11.13
2041	436	804	4.02	9.19	10.21	10.61	10.69
2042	418	771	3.85	8.91	9.79	10.17	10.25
2043	400	738	3.69	8.63	9.38	9.75	9.82
2044	383	707	3.53	8.35	8.98	9.33	9.40
2045	366	676	3.38	8.08	8.58	8.92	8.99
2046	350	645	3.23	7.79	8.19	8.52	8.58
2047	334	615	3.08	7.51	7.81	8.12	8.18
2048	318	586	2.93	7.23	7.44	7.73	7.79
2049	302	557	2.79	6.95	7.07	7.35	7.41
2050	287	529	2.64	6.66	6.71	6.98	7.03
2051	280	517	2.59	6.52	6.57	6.83	6.88
2052	274	506	2.53	6.38	6.43	6.68	6.73
2053	268	495	2.47	6.25	6.28	6.53	6.58
2054	262	484	2.42	6.12	6.15	6.39	6.44
2055	256	473	2.37	5.98	6.01	6.24	6.29
2056	251	462	2.31	5.86	5.87	6.10	6.15
2057	245	452	2.26	5.73	5.74	5.97	6.01
2058	239	442	2.21	5.60	5.61	5.83	5.88
2059	234	432	2.16	5.48	5.48	5.70	5.74
2060	229	422	2.11	5.36	5.36	5.57	5.61

Table A8. Economic benefits of LDG-ethanol to China's BF-BOF steeling production industry.

Year	Steel capacity (Mt)	GHG emissions (Mt CO_2)	Carbon Tax[193] ($/t)	Ethanol price[238] ($/t)	LDG-ethanol reward value (Billion $)			
					Fixed carbon tax and low-margin of products	Fixed carbon tax and high-margin of products	Increasing carbon tax and low-margin of products	Increasing carbon tax and low-margin of products
2025	768	1418	10	901	1.35	2.19	1.36	2.20
2026	742	1368	11	918	1.33	2.15	1.36	2.18
2027	721	1330	12	935	1.32	2.13	1.37	2.18
2028	698	1288	14	952	1.31	2.11	1.37	2.17
2029	676	1247	15	970	1.29	2.08	1.37	2.16
2030	659	1216	15	987	1.29	2.07	1.36	2.15
2031	636	1174	17	1020	1.28	2.07	1.39	2.17
2032	614	1133	19	1053	1.28	2.06	1.40	2.18
2033	592	1093	21	1087	1.27	2.05	1.41	2.19
2034	571	1054	23	1120	1.26	2.04	1.42	2.20
2035	550	1016	25	1153	1.25	2.02	1.44	2.21
2036	530	978	29	1187	1.24	2.00	1.46	2.22
2037	511	942	32	1220	1.22	1.98	1.47	2.23
2038	491	906	35	1253	1.21	1.96	1.49	2.24
2039	472	871	39	1287	1.19	1.93	1.50	2.24
2040	454	837	41	1322	1.18	1.91	1.50	2.23
2041	436	804	45	1350	1.15	1.87	1.51	2.22
2042	418	771	50	1379	1.13	1.83	1.51	2.21
2043	400	738	54	1408	1.10	1.79	1.51	2.20
2044	383	707	58	1436	1.08	1.75	1.51	2.18
2045	366	676	62	1465	1.05	1.70	1.50	2.16
2046	350	645	71	1493	1.02	1.66	1.54	2.17
2047	334	615	81	1522	0.99	1.61	1.56	2.18
2048	318	586	90	1550	0.96	1.56	1.58	2.18
2049	302	557	99	1579	0.93	1.51	1.59	2.17
2050	287	529	107	1607	0.90	1.46	1.59	2.15
2051	280	517	126	1634	0.89	1.45	1.69	2.25
2052	274	506	144	1662	0.89	1.44	1.80	2.35
2053	268	495	163	1690	0.88	1.43	1.89	2.44
2054	262	484	182	1717	0.88	1.42	1.98	2.53
2055	256	473	195	1745	0.87	1.41	2.03	2.58
2056	251	462	238	1772	0.86	1.40	2.26	2.80
2057	245	452	280	1800	0.85	1.39	2.48	3.02
2058	239	442	323	1828	0.85	1.38	2.69	3.22
2059	234	432	366	1855	0.84	1.37	2.89	3.41
2060	229	422	10	1881	0.83	1.35	1.36	3.49

Table A9. Relevant resource distribution in China.

Province	Steel capacity[212] (Mt)	Ironstone capacity[213] (Mt)	Ironstone import[213] (Mt)	Coke[213] (Mt)	PV[214, 215] (Billion kWh)	WP[214, 215] (Billion kWh)	HP[214, 215] (Billion kWh)
Hebei	313	321	129	48	99	34	5
Jiangsu	150	0.62	101	13	65	21	32
Shandong	112	31	121	32	56	19	8
Liaoning	76	133	49	23	24	17	33
Shanxi	62	49.8	8	105	89	21	44
Tianjin	57	-	18	2	4	1	-
Guangdong	49	5.93	46	6	30	9	155
Guangxi	47	0.07	27	8	9	9	556
Henan	42	6.01	12	19	45	9	134
Fujian	39	20.8	114	2	3	11	208
Zhejiang	38	-	96	2	43	3	152
Hubei	36	5.91	11	8	43	7	1575
Anhui	36	26.15	21	12	67	5	41
Sichuan	34	108	2	11	22	9	3349
Jiangxi	31	7.56	7	7	34	5	74
Inner Mongolia	29	42.72	13	42	132	67	48
Hunan	27	1.09	26	6	12	9	539
Yunnan	26	21.7	5	11	30	25	2763
Shaanxi	20	13.55	7	49	67	8	121
Shanghai	19	-	119	5	1	1	-
Jilin	17	6.08	-	4	23	10	74
Xinjiang	14	30.77	2	23	-	42	226
Chongqing	13	-	5	3	4	1	223
Gansu	11	9.7	-	5	105	24	379
Heilongjiang	8.8	2.56	6	11	15	12	25
Guizhou	7.4	0.99	1	4	40	10	710
Ningxia	4.8	-	-	9	-	17	22
Qinghai	1.9	0.0089	-	2	-	6	572
Beijing	1.8	14.57	161	-	1	-	11
Hainan	-	-	-	-	4	1	5
Xizang	-	-	-	-	-	-	58

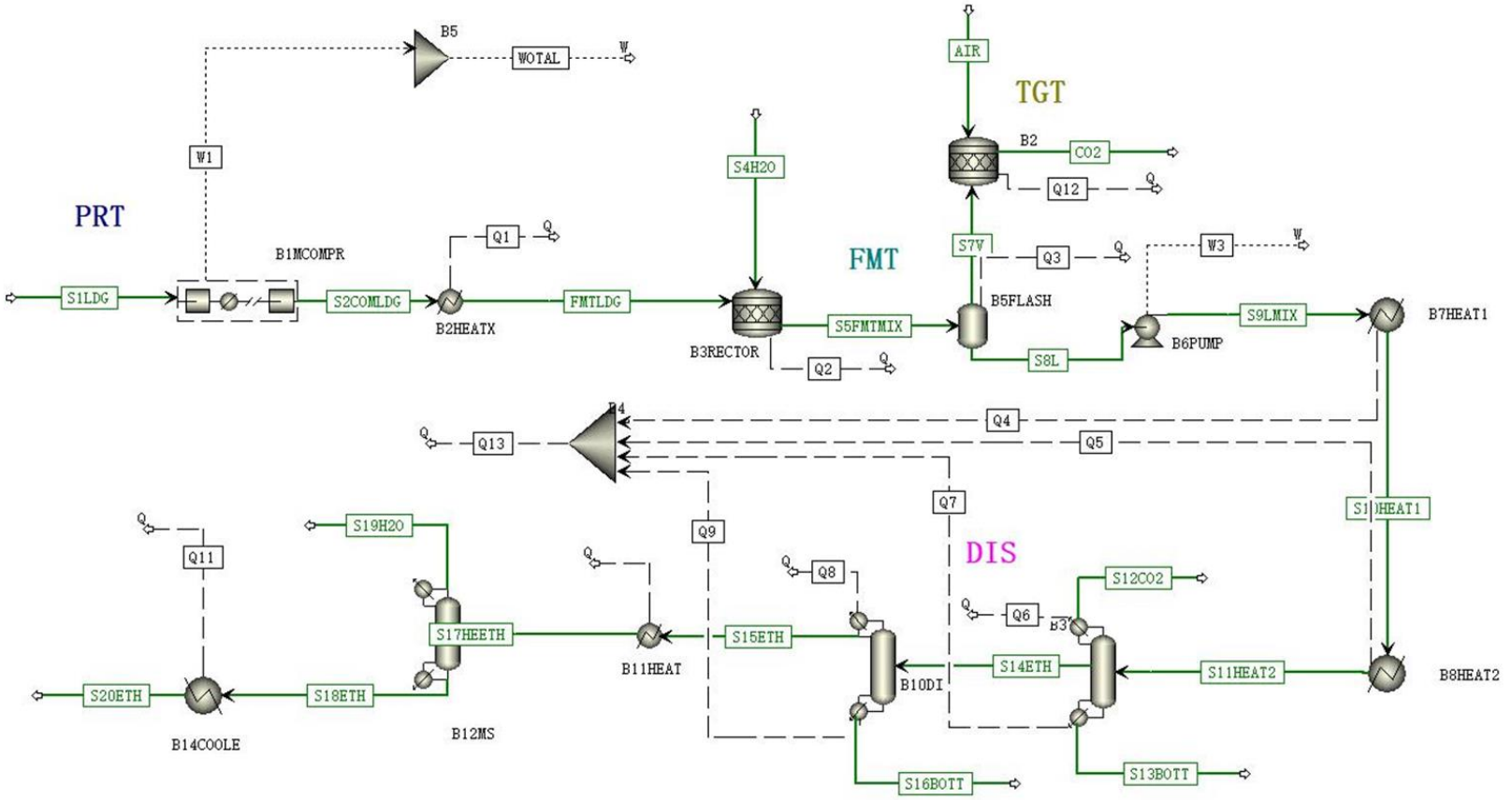

Figure A1. Aspen Plus modelling diagram of the original process of TG-ethanol.

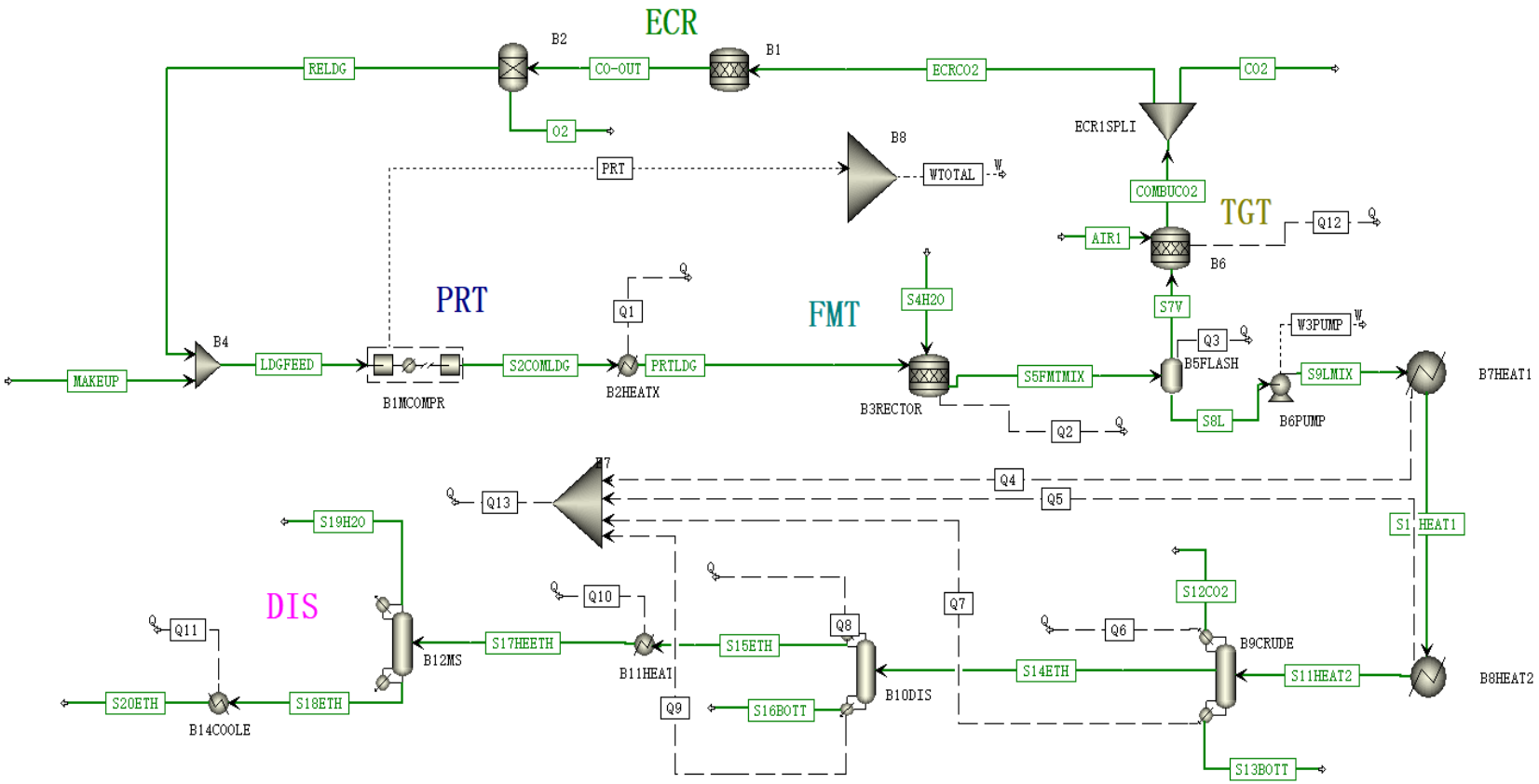

Figure A2. Aspen Plus modelling diagram of the Pre-combustion integrated with the TG-ethanol process.

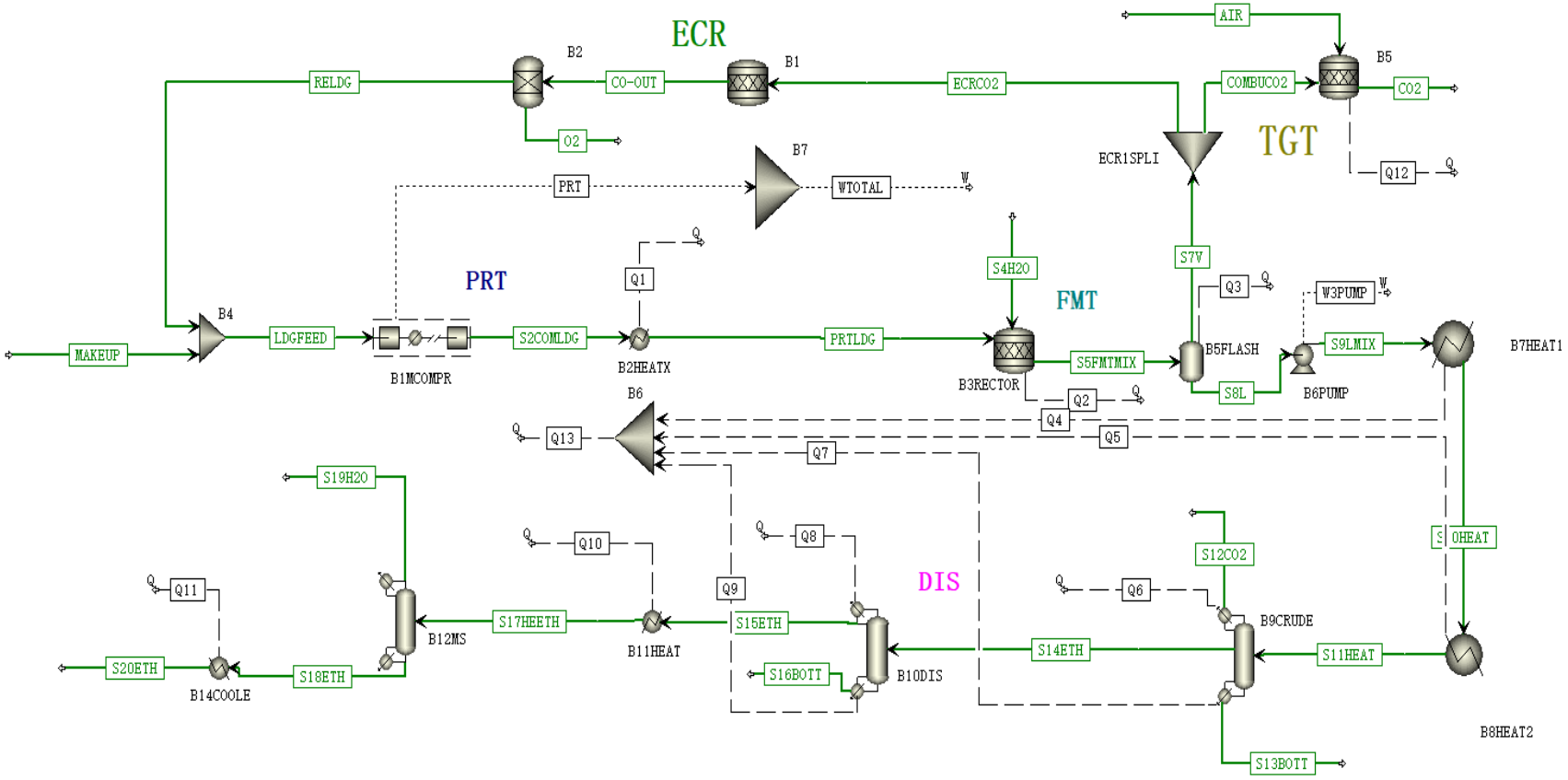

Figure A3. Aspen Plus modelling diagram of the Post-combustion integrated with the TG-ethanol process.

References

1. Wu, B., et al., *Current status and future prospective of bio-ethanol industry in China.* Renewable and Sustainable Energy Reviews, 2021. **145**: p. 111079.
2. *Securing Clean Energy Technology Supply Chains*. 2022, International Energy Agency.
3. *China energy statistic yearbook 2021*. 2021: National Bureau of Statistics.
4. *Ethanol Industry Outlook 2021*. 2021, Washington, US: Renewable Fuels Association.
5. Fu, J., et al., *Analysis of Yield Potential and Regional Distribution for Bioethanol in China.* Energies, 2021. **14**(15): p. 4554.
6. Li, Z., X. Hu, and Q. Zhang, *Development Status and Technical and Economic Analysis of Ethanol Gasoline for Automobile in China.* IOP Conference Series: Earth and Environmental Science, 2020. **558**(2): p. 022056.
7. Mo, Z., *Fuel ethanol production by biofermentation of steel industry tail-gas and its industrial application.* 2020 National Metallurgical Energy and Environmental Protection Technology Exchange Conference, 2020. p. 306-310

8. WANG Yuelin, C.W., LAN Xiaocheng, MO Zhipeng, TONG Shuhuan, WANG Tiefeng, *Review of ethanol production via biological syngas fermentation.* CIESC Journal, 2022. **73**(8): p. 3448-3460.

9. van der Werf, H.M.G., M.T. Knudsen, and C. Cederberg, *Towards better representation of organic agriculture in life cycle assessment.* Nature Sustainability, 2020. **3**(6): p. 419-425.

10. Li, C., et al., *Life-cycle assessment for coal-based methanol production in China.* Journal of Cleaner Production, 2018. **188**: p. 1004-1017.

11. Li, J., et al., *Life cycle assessment and economic analysis of methanol production from coke oven gas compared with coal and natural gas routes.* Journal of Cleaner Production, 2018. **185**: p. 299-308.

12. Bueno, C., et al., *Sensitivity analysis of the use of Life Cycle Impact Assessment methods: a case study on building materials.* Journal of Cleaner Production, 2016. **112**: p. 2208-2220.

13. Liu, B. and D. Rajagopal, *Life-cycle energy and climate benefits of energy recovery from wastes and biomass residues in the United States.* Nature Energy, 2019. **4**(8): p. 700-708.

14. Barjoveanu, G., et al., *Life cycle assessment of polyphenols extraction processes from waste biomass.* Scientific Reports, 2020. **10**(1): p. 13632.

15. Aziz, N.I.H.A., M.M. Hanafiah, and S.H. Gheewala, *A review on life cycle assessment of biogas production: Challenges and future perspectives in Malaysia.* Biomass and Bioenergy, 2019. **122**: p. 361-374.

16. Yu, S. and J. Tao, *Economic, energy and environmental evaluations of biomass-based fuel ethanol projects based on life cycle assessment and simulation.* Applied Energy, 2009. **86**: p. S178-S188.

17. Yu, S. and J. Tao, *Simulation based life cycle assessment of airborne emissions of biomass-based ethanol products from different feedstock planting areas in China.* Journal of Cleaner Production, 2009. **17**(5): p. 501-506.

18. Ou, X., et al., *Energy consumption and GHG emissions of six biofuel pathways by LCA in (the) People's Republic of China.* Applied Energy, 2009. **86**: p. S197-S208.

19. Lindahl, M., E. Sundin, and T. Sakao, *Environmental and economic benefits of Integrated Product Service Offerings*

quantified with real business cases. Journal of Cleaner Production, 2014. **64**: p. 288-296.

20. Zaman, K., et al., *Econometric applications for measuring the environmental impacts of biofuel production in the panel of worlds' largest region.* International Journal of Hydrogen Energy, 2016. **41**(7): p. 4305-4325.
21. Sakao, T. and M. Lindahl, *A method to improve integrated product service offerings based on life cycle costing.* CIRP Annals, 2015. **64**(1): p. 33-36.
22. Bressanin, J.M., et al., *Techno-Economic and Environmental Assessment of Biomass Gasification and Fischer–Tropsch Synthesis Integrated to Sugarcane Biorefineries.* Energies, 2020. **13**(17): p. 4576.
23. Atsonios, K., K.D. Panopoulos, and E. Kakaras, *Investigation of technical and economic aspects for methanol production through CO_2 hydrogenation.* International Journal of Hydrogen Energy, 2016. **41**(4): p. 2202-2214.
24. Qi, H., X. Wu, and H. Huan, *Simulation and comprehensive technical, economic, and environmental assessments of carbon dioxide capture for methanol production through flue gas of a*

combined cycle power plant. International Journal of Energy and Environmental Engineering, 2022. **14**: p. 405-429.

25. Harris, K., et al., *A comparative techno-economic analysis of renewable methanol synthesis from biomass and CO_2: Opportunities and barriers to commercialization.* Applied Energy, 2021. **303**: p. 117637.
26. *2022 China Ethanol Industry Analysis Report*. 2022, Insight and Info.
27. Sollai, S., et al., *Renewable methanol production from green hydrogen and captured CO_2: A techno-economic assessment.* Journal of CO_2 Utilization, 2023. **68**: p. 102345.
28. Khojasteh-Salkuyeh, Y., et al., *CO_2 utilization for methanol production; Part I: Process design and life cycle GHG assessment of different pathways.* Journal of CO_2 Utilization, 2021. **50**: p. 101608.
29. Zhang, X., et al., *Molecular engineering of dispersed nickel phthalocyanines on carbon nanotubes for selective CO_2 reduction.* Nature Energy, 2020. **5**(9): p. 684-692.

30. Kim, D., et al., *Selective CO_2 electrocatalysis at the pseudocapacitive nanoparticle/ordered-ligand interlayer.* Nature Energy, 2020. **5**(12): p. 1032-1042.

31. Jin, S., et al., *Advances and Challenges for the Electrochemical Reduction of CO_2 to CO: From Fundamentals to Industrialization.* Angewandte Chemie International Edition, 2021. **60**(38): p. 20627-20648.

32. Spurgeon, J.M. and B. Kumar, *A comparative technoeconomic analysis of pathways for commercial electrochemical CO_2 reduction to liquid products.* Energy & Environmental Science, 2018. **11**(6): p. 1536-1551.

33. Li, S., et al., *Hierarchical micro/nanostructured silver hollow fiber boosts electroreduction of carbon dioxide.* Nature Communications, 2022. **13**(1): p. 3080.

34. Li, S., et al., *Chloride Ion Adsorption Enables Ampere-Level CO_2 Electroreduction over Silver Hollow Fiber.* Angewandte Chemie International Edition, 2022. **61**(42): p. e202210432.

35. Moreno-Gonzalez, M., et al., *Carbon-neutral fuels and chemicals: Economic analysis of renewable syngas pathways via CO_2*

electrolysis. Energy Conversion and Management, 2021. **244**: p. 114452.

36. Yang, Q., et al., *Comparative study on life cycle assessment of gasoline with methyl tertiary-butyl ether and ethanol as additives.* Sci Total Environ, 2020. **724**: p. 138130.

37. Maga, D., et al., *Comparative life cycle assessment of first- and second-generation ethanol from sugarcane in Brazil.* The International Journal of Life Cycle Assessment, 2019. **24**(2): p. 266-280.

38. Scully, M.J., et al., *Carbon intensity of corn ethanol in the United States: state of the science.* Environmental Research Letters, 2021. **16**(4): p. 043001.

39. Mekonnen, M.M., et al., *Water, Energy, and Carbon Footprints of Bioethanol from the U.S. and Brazil.* Environmental science & technology, 2018. **52 24**: p. 14508-14518.

40. Yu, S. and J. Tao, *Simulation-based life cycle assessment of energy efficiency of biomass-based ethanol fuel from different feedstocks in China.* Energy, 2009. **34**(4): p. 476-484.

41. *2021 Ethanol Industry Outlook*. 2021, Renewable Fuels Association.

42. Zhang, Y. and A. Kendall, *Life Cycle Performance of Cellulosic Ethanol and Corn Ethanol from a Retrofitted Dry Mill Corn Ethanol Plant.* BioEnergy Research, 2017. **10**(1): p. 183-198.

43. Pang, B., et al., *Improved value and carbon footprint by complete utilization of corncob lignocellulose.* Chemical Engineering Journal, 2021. **419**: p. 129565.

44. Skolrud, T.D., et al., *The role of federal Renewable Fuel Standards and market structure on the growth of the cellulosic biofuel sector.* Energy Economics, 2016. **58**: p. 141-151.

45. Zhang, P.F., et al., *Cost Estimates of Cellulosic Ethanol Production: A Review.* Journal of Manufacturing Science and Engineering, 2013. **135**(2): p. 021005.

46. Zheng, X., et al., *Comprehensive Evaluation of Fuel Ethanol Production from Poplar Wood Fermentation and its Coupled Pathway with Lignin Gasification Based on Energy-Environment-Economy.* Waste and Biomass Valorization, 2024. 15: p. 5511-5526.

47. Li, J. and W. Cheng, *Comparison of life-cycle energy consumption, carbon emissions and economic costs of coal to ethanol and bioethanol.* Applied Energy, 2020. **277**: p. 115574.

48. Li, J., et al., *Life cycle assessment and techno-economic analysis of ethanol production via coal and its competitors: A comparative study.* Applied Energy, 2022. **312**: p. 118791.

49. Kang, J., et al., *Single-pass transformation of syngas into ethanol with high selectivity by triple tandem catalysis.* Nature Communications, 2020. **11**(1): p. 827.

50. Li, W., et al., *Perspective on the low-carbon transformation pathways of fossil energy under dual carbon goals.* Chinese Science Bulletin, 2024. **69**(8): p. 990-996.

51. Gupta, M., M.L. Smith, and J.J. Spivey, *Heterogeneous Catalytic Conversion of Dry Syngas to Ethanol and Higher Alcohols on Cu-Based Catalysts.* ACS Catalysis, 2011. **1**(6): p. 641-656.

52. Yoshimaru, S., et al., *Support Effect of Metal–Organic Frameworks on Ethanol Production through Acetic Acid Hydrogenation.* ACS Applied Materials & Interfaces, 2021. **13**(17): p. 19992-20001.

53. Wang, Z., et al., *Aqueous phase hydrogenation of acetic acid to ethanol over Ir-MoOx/SiO2 catalyst.* Catalysis Communications, 2014. **43**: p. 38-41.

54. Zhang, M., et al., *Insights into the mechanism of acetic acid hydrogenation to ethanol on Cu(111) surface.* Applied Surface Science, 2017. **412**: p. 342-349.

55. Zhou, M., et al., *Insight on mechanism of Sn modification in alumina supported RhSn catalysts for acetic acid hydrogenation to fuel-grade ethanol.* Fuel, 2017. **203**: p. 774-780.

56. Bergem, H., et al., *Low temperature aqueous phase hydrogenation of the light oxygenate fraction of bio-oil over supported ruthenium catalysts.* Green Chemistry, 2017. **19**(14): p. 3252-3262.

57. Zhao, Z., J. Jiang, and F. Wang, *An economic analysis of twenty light olefin production pathways.* Journal of Energy Chemistry, 2021. **56**: p. 193-202.

58. Phaiboonsilpa, N., et al., *Two-step Conversion of Acetic Acid to Bioethanol by Ethyl Esterification and Catalytic Hydrogenolysis.* Journal of the Japan Petroleum Institute, 2020. **63**(4): p. 196-203.

59. Santiago, M.A.N., et al., *Catalytic Reduction of Acetic Acid, Methyl Acetate, and Ethyl Acetate over Silica-Supported Copper.* Journal of Catalysis, 2000. **193**(1): p. 16-28.

60. Long, B. and Z. Yang, *Measurements of the solubilties of m-phthalic acid in acetone, ethanol and acetic ether.* Fluid Phase Equilibria, 2008. **266**(1): p. 38-41.

61. Chen, J., et al., *Experimental testing of a spatiotemporal metabolic model for carbon monoxide fermentation with Clostridium autoethanogenum.* Biochemical Engineering Journal, 2018. **129**: p. 64-73.

62. Zhan, E., Z. Xiong, and W. Shen, *Dimethyl ether carbonylation over zeolites.* Journal of Energy Chemistry, 2019. **36**: p. 51-63.

63. Li, S., et al., *Identifying the Active Silver Species in Carbonylation of Dimethyl Ether over Ag−HMOR.* ChemCatChem, 2020. **12**(12): p. 3290-3297.

64. Wei, Q., et al., *A facile ethanol fuel synthesis from dimethyl ether and syngas over tandem combination of Cu-doped HZSM35 with Cu-Zn-Al catalyst.* Chemical Engineering Journal, 2017. **316**: p. 832-841.

65. Li, X., et al., *Direct synthesis of ethanol from dimethyl ether and syngas over combined H-Mordenite and Cu/ZnO catalysts.* ChemSusChem, 2010. **3**(10): p. 1192-9.

66. Du, C., et al., *Developing Cu-MOR@SiO2 Core–Shell Catalyst Microcapsules for Two-Stage Ethanol Direct Synthesis from DME and Syngas.* Industrial & Engineering Chemistry Research, 2020. **59**(8): p. 3293-3300.

67. Chen, S., et al., *Integrated bioethanol production from mixtures of corn and corn stover.* Bioresource Technology, 2018. **258**: p. 18-25.

68. He, J. and W. Zhang, *Techno-economic evaluation of thermo-chemical biomass-to-ethanol.* Applied Energy, 2011. **88**(4): p. 1224-1232.

69. da Silva, C.R.U., et al., *Long-Term Prospects for the Environmental Profile of Advanced Sugar Cane Ethanol.* Environmental Science & Technology, 2014. **48**(20): p. 12394-12402.

70. Chen, S., et al., *Integrated bioethanol production from mixtures of corn and corn stover.* Bioresour Technol, 2018. **258**: p. 18-25.

71. Wu, L.X., J.P. Ji, and X.M. Ma, *Assessing the Impact of Corn-Ethanol Production on Global Corn Price Based on a VAR Model.* Advanced Materials Research, 2013. **616-618**: p. 1358-1362.

72. Haixia, W. and L. Shiping, *Volatility spillovers in China's crude oil, corn and fuel ethanol markets.* Energy Policy, 2013. **62**: p. 878-886.

73. Oladosu, G.A., K.L. Kline, and J.W.A. Langeveld, *Structural Break and Causal Analyses of U.S. Corn Use for Ethanol and Other Corn Market Variables.* Agriculture, 2021. **11**(3): p. 267.

74. Yu, J., et al., *Integration of corn ethanol and corn stover ethanol processes for improving xylose fermentation performance.* Biomass Conversion and Biorefinery, 2023. **13**(8): p. 6989-6999.

75. Yang, Q. and G.Q. Chen, *Nonrenewable energy cost of corn-ethanol in China.* Energy Policy, 2012. **41**: p. 340-347.

76. Li, X., et al., *Ethanol production from mixtures of Distiller's Dried Grains with Solubles (DDGS) and corn.* Industrial Crops and Products, 2019. **129**: p. 59-66.

77. Hong, J., J. Zhou, and J. Hong, *Comparative study of life cycle environmental and economic impact of corn- and corn stalk-based-ethanol production.* Journal of Renewable and Sustainable Energy, 2015. **7**(2): p. 023106.

78. Sica, P., et al., *Effects of Energy Cane (Saccharum spp.) Juice on Corn Ethanol (Zea mays) Fermentation Efficiency: Integration*

towards a More Sustainable Production. Fermentation, 2021. **7**(1). p. 1-30.

79. Kurambhatti, Kumar, and Singh, *Impact of Fractionation Process on the Technical and Economic Viability of Corn Dry Grind Ethanol Process.* Processes, 2019. **7**(9). p. 578.

80. Lewandrowski, J., et al., *The greenhouse gas benefits of corn ethanol – assessing recent evidence.* Biofuels, 2019. **11**(3): p. 361-375.

81. Nwufo, O.C., O.M.I. Nwafor, and J.O. Igbokwe, *Effects of blends on the physical properties of bioethanol produced from selected Nigerian crops.* International Journal of Ambient Energy, 2016. **37**: p. 10 - 15.

82. de Léis, C.M., et al., *Environmental and energy analysis of biopolymer film based on cassava starch in Brazil.* Journal of Cleaner Production, 2017. **143**: p. 76-89.

83. Crago, C.L., et al., *Competitiveness of Brazilian sugarcane ethanol compared to US corn ethanol.* Energy Policy, 2010. **38**(11): p. 7404-7415.

84. Papong, S., et al., *Environmental life cycle assessment and social impacts of bioethanol production in Thailand.* Journal of Cleaner Production, 2017. **157**: p. 254-266.

85. Vohra, M., et al., *Bioethanol production: Feedstock and current technologies.* Journal of Environmental Chemical Engineering, 2014. **2**(1): p. 573-584.

86. Pradyawong, S., et al., *Comparison of Cassava Starch with Corn as a Feedstock for Bioethanol Production.* Energies, 2018. **11**(12). p. 3476.

87. Mupondwa, E., et al., *Status of Canada's lignocellulosic ethanol: Part II: Hydrolysis and fermentation technologies.* Renewable and Sustainable Energy Reviews, 2017. **79**: p. 1535-1555.

88. Weng, Y., X. Wang, and Y. Zhang, *Cellulosic ethanol production with bio- and chemo-catalytic methods.* Trends in Chemistry, 2022. **4**(5): p. 374-377.

89. Schuenemann, F. and R. Delzeit, *Potentials, subsidies and tradeoffs of cellulosic ethanol in the European Union.* Ecological Economics, 2022. **195**: p. 107384.

90. Liu, Z.L. and B.S. Dien, *Cellulosic Ethanol Production Using a Dual Functional Novel Yeast.* International Journal of Microbiology, 2022. **2022**(1): p. 7853935.

91. Gao, X., Q. Gao, and J. Bao, *Improving cellulosic ethanol fermentability of Zymomonas mobilis by overexpression of sodium ion tolerance gene ZMO0119.* Journal of Biotechnology, 2018. **282**: p. 32-37.

92. Aui, A. and Y. Wang, *Cellulosic ethanol production: Assessment of the impacts of learning and plant capacity.* Technological Forecasting and Social Change, 2023. **197**: p. 122923.

93. Uden, D.R., et al., *The Feasibility of Producing Adequate Feedstock for Year-Round Cellulosic Ethanol Production in an Intensive Agricultural Fuelshed.* BioEnergy Research, 2013. **6**(3): p. 930-938.

94. Liu, C.G., et al., *Cellulosic ethanol production: Progress, challenges and strategies for solutions.* Biotechnol Adv, 2019. **37**(3): p. 491-504.

95. Padella, M., A. O'Connell, and M. Prussi, *What is still Limiting the Deployment of Cellulosic Ethanol? Analysis of the Current Status of the Sector.* Applied Sciences, 2019. **9**(21): p. 4523.

96. Shi, A., et al., *Production and evaluation of biodiesel and bioethanol from high oil corn using three processing routes.* Bioresour Technol, 2013. **128**: p. 100-6.

97. Luangthongkam, P., et al., *Addition of cellulolytic enzymes and phytase for improving ethanol fermentation performance and oil recovery in corn dry grind process.* Industrial Crops and Products, 2015. **77**: p. 803-808.

98. Basen, M., et al., *Single gene insertion drives bioalcohol production by a thermophilic archaeon.* Proceedings of the National Academy of Sciences, 2014. **111**(49): p. 17618-17623.

99. Liu, C.-G., et al., *Cellulosic ethanol production: Progress, challenges and strategies for solutions.* Biotechnology Advances, 2019. **37**(3): p. 491-504.

100. Wang, Y. and M.-H. Cheng, *Greenhouse gas emissions embedded in US-China fuel ethanol trade: A comparative well-to-wheel estimate.* Journal of Cleaner Production, 2018. **183**: p. 653-661.

101. Yang, Q., et al., *Comparative study on life cycle assessment of gasoline with methyl tertiary-butyl ether and ethanol as additives.* Science of The Total Environment, 2020. **724**: p. 138130.

102. Vasilakou, K., et al., *Geospatial environmental techno-economic assessment of pretreatment technologies for bioethanol production.* Renewable and Sustainable Energy Reviews, 2023. **187**: p. 113743.

103. Smith, J.P., et al., *Evaluating the sustainability of the 2017 US biofuel industry with an integrated techno-economic analysis and life cycle assessment.* Journal of Cleaner Production, 2023. **413**: p. 137364.

104. Zhang, L., et al., *Life cycle assessment of bio-fermentation ethanol production and its influence in China's steeling industry.* Journal of Cleaner Production, 2023. **397**: p. 136492.

105. Gerrior, D., et al., *Life cycle assessment and techno-economic analysis of a novel closed loop corn ethanol biorefinery.* Sustainable Production and Consumption, 2022. **30**: p. 359-376.

106. Leng, R., et al., *Life cycle inventory and energy analysis of cassava-based Fuel ethanol in China.* Journal of Cleaner Production, 2008. **16**(3): p. 374-384.

107. Jiao, J., J. Li, and Y. Bai, *Uncertainty analysis in the life cycle assessment of cassava ethanol in China.* Journal of Cleaner Production, 2019. **206**: p. 438-451.

108. Hiloidhari, M., et al., *Life cycle energy–carbon–water footprints of sugar, ethanol and electricity from sugarcane.* Bioresource Technology, 2021. **330**: p. 125012.

109. Silva Ortiz, P.A., F. Maréchal, and S. de Oliveira Junior, *Exergy assessment and techno-economic optimization of bioethanol production routes.* Fuel, 2020. **279**: p. 118327.

110. Nguyen, T.L.T. and S.H. Gheewala, *Life cycle assessment of fuel ethanol from cane molasses in Thailand.* The International Journal of Life Cycle Assessment, 2008. **13**(4): p. 301-311.

111. Nguyen, T.L.T. and S.H. Gheewala, *Life cycle assessment of fuel ethanol from cassava in Thailand.* The International Journal of Life Cycle Assessment, 2008. **13**(2): p. 147-154.

112. Cavalett, O., et al., *Comparative LCA of ethanol versus gasoline in Brazil using different LCIA methods.* The International Journal of Life Cycle Assessment, 2013. **18**(3): p. 647-658.

113. Murphy, C.W. and A. Kendall, *Life cycle analysis of biochemical cellulosic ethanol under multiple scenarios.* GCB Bioenergy, 2015. **7**(5): p. 1019-1033.

114. Kadhum, H.J., K. Rajendran, and G.S. Murthy, *Optimization of Surfactant Addition in Cellulosic Ethanol Process Using*

Integrated Techno-economic and Life Cycle Assessment for Bioprocess Design. ACS Sustainable Chemistry & Engineering, 2018. **6**(11): p. 13687-13695.

115. Pati, S., S. De, and R. Chowdhury, *Integrated techno-economic, investment risk and life cycle analysis of Indian lignocellulosic biomass valorisation via co-gasification and syngas fermentation.* Journal of Cleaner Production, 2023. **423**: p. 138744.

116. Murali, G. and Y.N. Shastri, *Life-cycle assessment-based comparison of different lignocellulosic ethanol production routes.* Biofuels, 2019. **13**: p. 237 - 247.

117. Olofsson, J., et al., *Integrating enzyme fermentation in lignocellulosic ethanol production: life-cycle assessment and techno-economic analysis.* Biotechnology for Biofuels, 2017. **10**(1): p. 51.

118. Ma, D., *Life cycle assessment of fuel ethanol based on SimaPro*, in *Environmental Science and Engineering*. 2019, Qingdao University of Science & Technology: Qingdao. p. 1-77.

119. Liu, H., *Study of Life Cycle Sustainability Assessment of Fuel Bioethanol*, in *Environmental Science and Engineering*. 2019, ShanDong University: ShanDong. p. 1-59.

120. Pieragostini, C., P. Aguirre, and M.C. Mussati, *Life cycle assessment of corn-based ethanol production in Argentina.* Science of The Total Environment, 2014. **472**: p. 212-225.

121. Börjesson, P., *Good or bad bioethanol from a greenhouse gas perspective – What determines this?* Applied Energy, 2009. **86**(5): p. 589-594.

122. Souza, A., et al., *Social life cycle assessment of first and second-generation ethanol production technologies in Brazil.* The International Journal of Life Cycle Assessment, 2018. **23**(3): p. 617-628.

123. Amores, M.J., et al., *Life cycle assessment of fuel ethanol from sugarcane in Argentina.* The International Journal of Life Cycle Assessment, 2013. **18**(7): p. 1344-1357.

124. Tsiropoulos, I., et al., *Life cycle assessment of sugarcane ethanol production in India in comparison to Brazil.* The International Journal of Life Cycle Assessment, 2014. **19**(5): p. 1049-1067.

125. Murphy, C.W. and A. Kendall, *Life cycle inventory development for corn and stover production systems under different allocation methods.* Biomass and Bioenergy, 2013. **58**: p. 67-75.

126. Zheng, X., et al., *Techno-economic analysis and life cycle assessment of hydrogenation upgrading and supercritical ethanol upgrading processes based on fast pyrolysis of cornstalk for biofuel.* Biomass Conversion and Biorefinery, 2023. 14: p. 17819-17835.

127. Zheng, J.-L., et al., *Life cycle assessment and techno-economic analysis of fuel ethanol production via bio-oil fermentation based on a centralized-distribution model.* Renewable and Sustainable Energy Reviews, 2022. **167**: p. 112714.

128. García-Velásquez, C.A. and C.A. Cardona, *Comparison of the biochemical and thermochemical routes for bioenergy production: A techno-economic (TEA), energetic and environmental assessment.* Energy, 2019. **172**: p. 232-242.

129. Roy, P. and A. Dutta, *Life cycle assessment of ethanol derived from sawdust.* Bioresource Technology, 2013. **150**: p. 407-411.

130. González-García, S., et al., *Life cycle assessment of hemp hurds use in second generation ethanol production.* Biomass and Bioenergy, 2012. **36**: p. 268-279.

131. Fasahati, P., et al., *Seaweeds as a sustainable source of bioenergy: Techno-economic and life cycle analyses of its*

biochemical conversion pathways. Renewable and Sustainable Energy Reviews, 2022. **157**: p. 112011.

132. Olukoya, I.A., et al., *Life cycle assessment of the production of ethanol from eastern redcedar.* Bioresource Technology, 2014. **173**: p. 239-244.

133. ISO14040:2006, *Environmental management - Life cycle assessment - Principles and framework*. 2006.

134. Pryshlakivsky, J. and C. Searcy, *Life Cycle Assessment as a decision-making tool: Practitioner and managerial considerations.* Journal of Cleaner Production, 2021. **309**: p. 127344.

135. Lei, H., et al., *An analytical review on application of life cycle assessment in circular economy for built environment.* Journal of Building Engineering, 2021. **44**: p. 103374.

136. Zhou, X., et al., *From full life cycle assessment to simplified life cycle assessment: A generic methodology applied to sludge treatment.* Science of The Total Environment, 2023. **904**: p. 167149.

137. Wang, Q., et al., *Life cycle assessment and the willingness to pay of waste polyester recycling.* Journal of Cleaner Production, 2019. **234**: p. 275-284.

138. Zschieschang, E., P. Pfeifer, and L. Schebek, *Life Cycle Assessment in Chemical and Micro Reaction Engineering.* Chemical Engineering & Technology, 2013. **36**(6): p. 911-920.

139. Kovačič Lukman, R., V. Omahne, and D. Krajnc, *Sustainability Assessment with Integrated Circular Economy Principles: A Toy Case Study.* Sustainability, 2021. **13**(7): p. 3856.

140. Omran, N., A.H. Sharaai, and A.H. Hashim, *Visualization of the Sustainability Level of Crude Palm Oil Production: A Life Cycle Approach.* Sustainability, 2021. **13**(4): p. 1607.

141. Institute, W.R., *Product life cycle accounting and reporting standard*. 2011.

142. Summerscales, J. and N.P.J. Dissanayake. *Allocation in the Life Cycle Assessment (LCA) of Flax Fibres for the Reinforcement of Composites*. in *Advances in Natural Fibre Composites*. 2018. p. 223-235. Cham: Springer International Publishing.

143. Standardization, I.O.f., *ISO14044: 2006 Environmental management — Life cycle assessment — Requirements and guidelines*. 2006.

144. Maga, D., et al., *How to account for plastic emissions in life cycle inventory analysis?* Resources, Conservation and Recycling, 2021. **168**: p. 105331.

145. Reijnders, L., *Life Cycle AssessmentLife cycle assessment (LCA) of BiofuelsBiofuels*, in *Biofuels and Biodiesel*, C. Basu, Editor. 2021, Springer US: New York, NY. p. 53-67.

146. Schenker, V., C. Oberschelp, and S. Pfister, *Regionalized life cycle assessment of present and future lithium production for Li-ion batteries.* Resources, Conservation and Recycling, 2022. **187**: p. 106611.

147. McAvoy, S., et al., *Combining Life Cycle Assessment and System Dynamics to improve impact assessment: A systematic review.* Journal of Cleaner Production, 2021. **315**: p. 128060.

148. Strunge, T., P. Renforth, and M. Van der Spek, *Uncertainty quantification in the techno-economic analysis of emission reduction technologies: a tutorial case study on CO_2 mineralization.* Frontiers in Energy Research, 2023. **11**: p. 3389.

149. Zimmermann, A.W., et al., *Techno-Economic Assessment Guidelines for CO_2 Utilization.* Frontiers in Energy Research, 2020. **8**: p. 00005.

150. Deng, S., et al., *A dynamic price model based on supply and demand with application to techno-economic assessments of rare earth element recovery technologies.* Sustainable Production and Consumption, 2021. **27**: p. 1718-1727.

151. Fu, R., et al., *Application and progress of techno-economic analysis and life cycle assessment in biomanufacturing of fuels and chemicals.* Green Chemical Engineering, 2023. **4**(2): p. 189-198.

152. Azzouz, A. and M. Hayyan, *Techno-economic feasibility analysis: The missing piece in the puzzle of deep eutectic solvents.* Sustainable Materials and Technologies, 2024. **39**: p. e00795.

153. Vazquez-Sanchez, H., et al., *A techno-economic analysis of a thermally regenerative ammonia-based battery.* Applied Energy, 2023. **347**: p. 121501.

154. Barahmand, Z. and M.S. Eikeland, *Techno-Economic and Life Cycle Cost Analysis through the Lens of Uncertainty: A Scoping Review.* Sustainability, 2022. **14**(19): p. 12191.

155. Asadi, L. and A.S. Nateri, *The use of Monte Carlo simulation to evaluate the optical properties of polyester fabric treated with*

titanium dioxide nanopigments. Coloration Technology, 2023. **139**(1): p. 28-44.

156. Yuan, R., et al., *Monte-Carlo Integration Models for Multiple Scattering Based Optical Wireless Communication.* IEEE Transactions on Communications, 2020. **68**(1): p. 334-348.

157. Benson, R. and D. Kellner. *Monte Carlo Simulation for Reliability*. in *2020 Annual Reliability and Maintainability Symposium (RAMS)*. 2020. p. 1-6.

158. Yuan, R., et al. *An Importance Sampling Method for Monte-Carlo Integration Model for Ultraviolet Communication*. in *2019 International Conference on Advanced Communication Technologies and Networking (CommNet)*. 2019. p. 1-6.

159. Diyang, Z. *The principle and application of Monte Carlo simulation in public health, finance, and physics*. in *Proc.SPIE*. 2022. p. 12259.

160. Shao, J., et al., *Monte Carlo simulation on kinetics of batch and semi-batch free radical polymerization.* Macromolecular Research, 2015. **23**(11): p. 1042-1050.

161. Chen, Q., et al., *Assessment of low-carbon iron and steel production with CO_2 recycling and utilization technologies: A case study in China.* Applied Energy, 2018. **220**: p. 192-207.

162. Ma, Y. and J. Wang, *Time-varying spillovers and dependencies between iron ore, scrap steel, carbon emission, seaborne transportation, and China's steel stock prices.* Resources Policy, 2021. **74**: p. 102254.

163. Hongtao, W., *The process research and implementation of producing fuel ethanol by bio-fermentation using gas from steel industry.* Energy for metallurgical industry, 2017. **36**: p. 31-33.

164. Zhang, Y., et al., *Life cycle assessment of ammonia synthesis in China.* The International Journal of Life Cycle Assessment, 2022. **27**(1): p. 50-61.

165. Li, J., et al., *High-resolution analysis of life-cycle carbon emissions from China's coal-fired power industry: A provincial perspective.* International Journal of Greenhouse Gas Control, 2020. **100**: p. 103110.

166. Hanes, R.J., et al., *Allocation Games: Addressing the Ill-Posed Nature of Allocation in Life-Cycle Inventories.* Environ Sci Technol, 2015. **49**(13): p. 7996-8003.

167. Chen, Z., et al., *Life cycle assessment of typical methanol production routes: The environmental impacts analysis and power optimization.* Journal of Cleaner Production, 2019. **220**: p. 408-416.

168. Zhang, Y., J. Li, and X. Yang, *Comprehensive competitiveness assessment of four coal-to-liquid routes and conventional oil refining route in China.* Energy, 2021. **235**: p. 121442.

169. *China Energy & Electricity Outlook 2021*. 2021: Global Energy Interconnection Research Institute Co. Ltd.

170. Rongju, L., *Development and application of sodium hydrosulphide device for desulfurization in small refinery.* Pertrochemical safety and environmental protection technology, 2011. **27**(20): p. 54-56.

171. Pan, L.T., et al., *The Preparation and Characterization of a New High Polymeric Flocculant-Polymeric Aluminum Ferric Sulfate Chloride.* Advanced Materials Research, 2012. **356-360**: p. 445-450.

172. Ma, D., *Life cycle assessment of fuel ethanol based on Simpro*. 2020, Qingdao University of Science & Technology. p. 1-77.

173. Imtiaz, L., et al., *Life Cycle Impact Assessment of Recycled Aggregate Concrete, Geopolymer Concrete, and Recycled Aggregate-Based Geopolymer Concrete.* Sustainability, 2021. **13**(24): p. 13515.

174. Van Oers, L. and J. Guinée, *The Abiotic Depletion Potential: Background, Updates, and Future.* Resources, 2016. **5**(1): p. 16.

175. Liu, X., et al., *Exploring the optimisation of mulching and irrigation management practices for mango production in a dry hot environment based on the entropy weight method.* Scientia Horticulturae, 2022. **291**: p. 110564.

176. *The Sustainable Development Goals Report 2021*. 2021: United Nations. Department of Economic and Social Affairs. p. 64.

177. Hu, Y., et al., *Characteristics and potential ecological risks of heavy metal pollution in surface soil around coal-fired power plant.* Environmental Earth Sciences, 2021. **80**(17): p. 566.

178. Piotrowska, K. and I. Piasecka, *Specification of Environmental Consequences of the Life Cycle of Selected Post-Production Waste of Wind Power Plants Blades.* Materials, 2021. **14**(17): p. 4975.

179. Fthenakis, V.M. and P.D. Moskowitz, *Photovoltaics: environmental, health and safety issues and perspectives.* Progress in Photovoltaics: Research and Applications, 2000. **8**(1): p. 27-38.

180. Li, S., et al., *Chloride Ion Adsorption Enables Ampere-Level CO(2) Electroreduction over Silver Hollow Fiber.* Angew Chem Int Ed Engl, 2022. **61**(42): p. e202210432.

181. Zhang, L., et al., *Frontiers of CO_2 Capture and Utilization (CCU) towards Carbon Neutrality.* Advances in Atmospheric Sciences, 2022. **39**(8): p. 1252-1270.

182. DeRose, K., et al., *Conversion of Distiller's Grains to Renewable Fuels and High Value Protein: Integrated Techno-Economic and Life Cycle Assessment.* Environ Sci Technol, 2019. **53**(17): p. 10525-10533.

183. Posen, I.D., et al., *Changing the renewable fuel standard to a renewable material standard: bioethylene case study.* Environ Sci Technol, 2015. **49**(1): p. 93-102.

184. Zhu, C., et al., *Ampere-level CO_2 reduction to multicarbon products over a copper gas penetration electrode.* Energy & Environmental Science, 2022. **15**(12): p. 5391-5404.

185. Liu, F., et al., *Process simulation and economic and environmental evaluation of a corncob-based biorefinery system.* Journal of Cleaner Production, 2021. **329**: p. 129707.

186. Liu, F., et al., *Exergy analysis of a new lignocellulosic biomass-based polygeneration system.* Energy, 2017. **140**: p. 1087-1095.

187. Zhang, L., et al., *Driving factors and predictions of CO_2 emission in China's coal chemical industry.* Journal of Cleaner Production, 2019. **210**: p. 1131-1140.

188. Ravi, S., D.B. Lobell, and C.B. Field, *Tradeoffs and Synergies between biofuel production and large solar infrastructure in deserts.* Environ Sci Technol, 2014. **48**(5): p. 3021-30.

189. Posen, I.D., P. Jaramillo, and W.M. Griffin, *Uncertainty in the Life Cycle Greenhouse Gas Emissions from U.S. Production of Three Biobased Polymer Families.* Environmental Science & Technology, 2016. **50**(6): p. 2846-2858.

190. Suresh, P., et al., *Life Cycle Greenhouse Gas Emissions and Costs of Production of Diesel and Jet Fuel from Municipal Solid Waste.* Environ Sci Technol, 2018. **52**(21): p. 12055-12065.

191. Dheskali, E., A.A. Koutinas, and I.K. Kookos, *Risk assessment modeling of bio-based chemicals economics based on Monte-*

Carlo simulations. Chemical Engineering Research & Design, 2020. **163**: p. 273-280.

192. Gargalo, C.L., et al., *Economic Risk Assessment of Early Stage Designs for Glycerol Valorization in Biorefinery Concepts.* Industrial & Engineering Chemistry Research, 2016. **55**: p. 6801-6814.

193. Zhang, X., et al., *Research on the Pathway and Policies for China's Energy and Economy Transformation toward Carbon Neutrality.* Management world, 2022. **38**(1): p. 19.

194. da Silva, C.R., et al., *Long-term prospects for the environmental profile of advanced sugar cane ethanol.* Environ Sci Technol, 2014. **48**(20): p. 12394-402.

195. Leow, S., et al., *A Unified Modeling Framework to Advance Biofuel Production from Microalgae.* Environ Sci Technol, 2018. **52**(22): p. 13591-13599.

196. Mullins, K.A., W.M. Griffin, and H.S. Matthews, *Policy Implications of Uncertainty in Modeled Life-Cycle Greenhouse Gas Emissions of Biofuels.* Environmental Science & Technology, 2011. **45**(1): p. 132-138.

197. Dornelles, L.B., R.M. Filho, and A.P. Mariano, *Organosolv fractionation of eucalyptus: Economics of cellulosic ethanol and chemicals versus lignin valorization to phenols and polyols.* Industrial Crops and Products, 2021. 173: p. 114097.

198. He, Y., et al., *Enhanced Ethanol Production From Carbon Monoxide by Enriched Clostridium Bacteria.* Frontiers in Microbiology, 2021. **12**: p. 754713.

199. Zhang, Z., et al., *Molecular understanding of the critical role of alkali metal cations in initiating CO_2 electroreduction on Cu(100) surface.* Nature Communications, 2024. **15**(1): p. 612.

200. Xin-gang, Z. and W. Zhen, *Technology, cost, economic performance of distributed photovoltaic industry in China.* Renewable and Sustainable Energy Reviews, 2019. **110**: p. 53-64.

201. Zhang, L., et al., *The integration of hydrogenation and carbon capture utilisation and storage technology: A potential low-carbon approach to chemical synthesis in China.* International Journal of Energy Research, 2021. **45**(14): p. 19789-19818.

202. Liska, A.J. and K.G. Cassman, *Towards Standardization of Life-Cycle Metrics for Biofuels: Greenhouse Gas Emissions Mitigation*

and Net Energy Yield. Journal of Biobased Materials and Bioenergy, 2008. **2**: p. 187-203.

203. Hussain, I., et al., *A state-of-the-art review on waste plastics-derived aviation fuel: Unveiling the heterogeneous catalytic systems and techno-economy feasibility of catalytic pyrolysis.* Energy Conversion and Management, 2022. **274**: p. 116433.

204. Valkenburt, C., et al. *Municipal Solid Waste (MSW) to Liquid Fuels Synthesis, Volume 1: Availability of Feedstock and Technology*. 2008. p. 18144.

205. Wang, M., et al., *Well-to-wheels energy use and greenhouse gas emissions of ethanol from corn, sugarcane and cellulosic biomass for US use.* Environmental Research Letters, 2012. **7**(4): p. 045905.

206. Manochio, C., et al., *Ethanol from biomass: A comparative overview.* Renewable & Sustainable Energy Reviews, 2017. **80**: p. 743-755.

207. Meng, F., et al., *Process simulation and life cycle assessment of converting autoclaved municipal solid waste into butanol and ethanol as transport fuels.* Waste Management, 2019. **89**: p. 177-189.

208. Xiang, D., et al., *Techno-economic analysis of the coal-to-olefins process in comparison with the oil-to-olefins process.* Applied Energy, 2014. **113**: p. 639-647.

209. Wu, Y., et al., *Forecast analysis of steel-coke-coking coal demand based on China's GDP development.* Coal economic research, 2019. **39**(11): p. 15-22.

210. Tan, X., et al., *Energy-saving and emission-reduction technology selection and CO_2 emission reduction potential of China's iron and steel industry under energy substitution policy.* Journal of Cleaner Production, 2019. 222: p. 823-834.

211. Gu, Y., et al., *Comparative techno-economic study of solar energy integrated hydrogen supply pathways for hydrogen refueling stations in China.* Energy Conversion and Management, 2020. **223**: p. 113240.

212. *China Iron and Steel Industry Yearbook*. 2021: China Iron and Steel Association.

213. *China Energy Statistical Yearbook 2021*. 2021, Beijing, China: National Bureau of Statistics.

214. Petroleum, B., *BP Statistical Review of World Energy*. 2022, UK.

215. *China's renewable energy generation*. 2022: China Business Industry Research Institute.

216. Dray, L., et al., *Cost and emissions pathways towards net-zero climate impacts in aviation.* Nature Climate Change, 2022. **12**(10): p. 956-962.

217. Sacchi, R., et al., *How to make climate-neutral aviation fly.* Nature Communications, 2023. **14**(1): p. 3989.

218. Geleynse, S., et al., *The Alcohol-to-Jet Conversion Pathway for Drop-In Biofuels: Techno-Economic Evaluation.* ChemSusChem, 2018. **11**(21): p. 3728-3741.

219. Stratton, R.W., P.J. Wolfe, and J.I. Hileman, *Impact of Aviation Non-CO_2 Combustion Effects on the Environmental Feasibility of Alternative Jet Fuels.* Environmental Science & Technology, 2011. **45**(24): p. 10736-10743.

220. Emmanouilidou, E., et al., *Solid waste biomass as a potential feedstock for producing sustainable aviation fuel: A systematic review.* Renewable Energy, 2023. **206**: p. 897-907.

221. Shahabuddin, M., et al., *A review on the production of renewable aviation fuels from the gasification of biomass and residual wastes.* Bioresource Technology, 2020. **312**: p. 123596.

222. Doliente, S.S., et al., *Bio-aviation Fuel: A Comprehensive Review and Analysis of the Supply Chain Components.* Frontiers in Energy Research, 2020. **8**: p. 00110.

223. Wang, Z.J., et al., *Quantitative Policy Analysis for Sustainable Aviation Fuel Production Technologies.* Frontiers in Energy Research, 2021. **9**: p. 751-772

224. Ravi, S., D.B. Lobell, and C.B. Field, *Tradeoffs and Synergies between Biofuel Production and Large Solar Infrastructure in Deserts.* Environmental Science & Technology, 2014. **48**(5): p. 3021-3030.

225. Pressley, P.N., et al., *Municipal solid waste conversion to transportation fuels: a life-cycle estimation of global warming potential and energy consumption.* Journal of Cleaner Production, 2014. **70**: p. 145-153.

226. Seber, G., et al., *Environmental and economic assessment of producing hydroprocessed jet and diesel fuel from waste oils and tallow.* Biomass and Bioenergy, 2014. **67**: p. 108-118.

227. Wang, W.-C. and L. Tao, *Bio-jet fuel conversion technologies.* Renewable and Sustainable Energy Reviews, 2016. **53**: p. 801-822.

228. Staples, M.D., et al., *Aviation CO_2 emissions reductions from the use of alternative jet fuels.* Energy Policy, 2018. **114**: p. 342-354.

229. Brooks, K.P., et al., *Chapter 6 - Low-Carbon Aviation Fuel Through the Alcohol to Jet Pathway*, in *Biofuels for Aviation*, C.J. Chuck, Editor. 2016, Academic Press. p. 109-150.

230. *Towards 2060 Carbon Neutrality-White Paper on Low Carbon Development in the Petrochemical Industry*. 2022: SINOPEC research institute of petroleum processing.

231. Prussi, M., A. O'Connell, and L. Lonza, *Analysis of current aviation biofuel technical production potential in EU28.* Biomass and Bioenergy, 2019. **130**: p. 105371.

232. Cronin, D.J., et al., *Sustainable Aviation Fuel from Hydrothermal Liquefaction of Wet Wastes.* Energies, 2022. **15**(4): p. 1306.

233. Beal, C.M., A.D. Cuellar, and T.J. Wagner, *Sustainability assessment of alternative jet fuel for the U.S. Department of Defense.* Biomass and Bioenergy, 2021. **144**: p. 105881.

234. Bergthorson, J.M. and M.J. Thomson, *A review of the combustion and emissions properties of advanced transportation biofuels and their impact on existing and future engines.* Renewable and Sustainable Energy Reviews, 2015. **42**: p. 1393-1417.

235. Park, C., et al., *COVID-19 mask waste to energy via thermochemical pathway: Effect of Co-Feeding food waste.* Energy, 2021. **230**: p. 120876.

236. Liu, S., et al., *Plastic waste to fuels by hydrocracking at mild conditions.* Science Advances, 2021. **7**(17): p. eabf8283.

237. Rollinson, A.N. and J.M. Oladejo, *'Patented blunderings', efficiency awareness, and self-sustainability claims in the pyrolysis energy from waste sector.* Resources, Conservation and Recycling, 2019. **141**: p. 233-242.

238. Tan, X., et al., *Energy-saving and emission-reduction technology selection and CO_2 emission reduction potential of China's iron and steel industry under energy substitution policy.* Journal of Cleaner Production, 2019. **222**: p. 823-834.